Western Graduate&PostdoctoralStudies

Western University
Scholarship@Western

Electronic Thesis and Dissertation Repository

7-14-2014 12:00 AM

Options Pricing and Hedging in a Regime-Switching Volatility Model

Melissa A. Mielkie, *The University of Western Ontario*

Supervisor: Dr. Matt Davison, *The University of Western Ontario*

A thesis submitted in partial fulfillment of the requirements for the Doctor of Philosophy degree in Applied Mathematics

© Melissa A. Mielkie 2014

Follow this and additional works at: https://ir.lib.uwo.ca/etd

Part of the Finance Commons, Numerical Analysis and Computation Commons, Other Applied Mathematics Commons, and the Partial Differential Equations Commons

Recommended Citation

Mielkie, Melissa A., "Options Pricing and Hedging in a Regime-Switching Volatility Model" (2014). *Electronic Thesis and Dissertation Repository*. 2160.
https://ir.lib.uwo.ca/etd/2160

This Dissertation/Thesis is brought to you for free and open access by Scholarship@Western. It has been accepted for inclusion in Electronic Thesis and Dissertation Repository by an authorized administrator of Scholarship@Western. For more information, please contact wlswadmin@uwo.ca.

OPTIONS PRICING AND HEDGING IN A REGIME-SWITCHING VOLATILITY MODEL

(Thesis format: Monograph)

by

Melissa Anne Mielkie

Graduate Program in Applied Mathematics

A thesis submitted in partial fulfillment
of the requirements for the degree of
Doctor of Philosophy

The School of Graduate and Postdoctoral Studies
The University of Western Ontario
London, Ontario, Canada

© Melissa Anne Mielkie 2014

Abstract

Both deterministic and stochastic volatility models have been used to price and hedge options. Observation of real market data suggests that volatility, while stochastic, is well modelled as alternating between two states. Under this two-state regime-switching framework, we derive coupled pricing partial differential equations (PDEs) with the inclusion of a state-dependent market price of volatility risk (MPVR) term.

Since there is no closed-form solution for this pricing problem, we apply and compare two approaches to solving the coupled PDEs, assuming constant Poisson intensities. First we solve the problem using numerical solution techniques, through the application of the Crank-Nicolson numerical scheme. We also obtain approximate solutions in terms of known Black-Scholes formulae by reformulating our problem and applying the Cauchy-Kowalevski PDE theorem. Both our pricing equations and our approximate solutions give way to the analysis of the impact of our state-dependent MPVR on theoretical option prices. Using financially intuitive constraints on our option prices and Deltas, we prove the necessity of a negative MPVR. An exploration of the regime-switching option prices and their implied volatilities is given, as well as numerical results and intuition supporting our mathematical proofs.

Given our regime-switching framework, there are several different hedging strategies to investigate. We consider using an option to hedge against a potential regime shift. Some practical problems arise with this approach, which lead us to set up portfolios containing a basket of two hedging options. To be more precise, we consider the effects of an option going too far in- and out-of-the-money on our hedging strategy, and introduce limits on the magnitude of such hedging option positions. A complementary approach, where constant volatility is assumed and investor's risk preferences are taken into account, is also analysed.

Analysis of empirical data supports the hypothesis that volatility levels are affected by upcoming financial events. Finally, we present an extension of our regime-switching framework with deterministic Poisson intensities. In particular, we investigate the impact of time and stock varying Poisson intensities on option prices and their corresponding implied volatilities, using numerical solution techniques. A discussion of some event-driven hedging strategies is given.

Keywords: Analytic Approximation; Coupled Partial Differential Equations; European Option; Hedging; Implied Volatility; Option Pricing; Quantitative Finance; Regime-Switching; Risk Premia

Acknowlegements

First and foremost, I would like to thank my supervisor, Dr. Matt Davison, who was instrumental in first sparking my interest in financial mathematics back during my undergraduate thesis. Your constant support and guidance has been invaluable throughout my years as a graduate student. As well, your insight has helped me develop my mathematical and financial intuition, both of which have contributed to my success throughout my education.

I would also like to thank Dr. Adam Metzler and Dr. Mark Reesor, both members of my supervisory committee and of our financial mathematics research group. I have appreciated your insightful feedback of my research over the years.

The financial mathematics Power Hour group was an integral part of why I chose to complete my graduate studies in applied mathematics. I would like to thank each and every member of our group. I will always deeply cherish the friendships we have formed and the discussions we have had over the years. I wish you all the best in your future endeavours.

I would like to thank all the students, faculty, and staff from the Department of Applied Mathematics. As a whole, the department has provided a very welcoming and supportive environment which I have greatly appreciated over the years. Whether it be the friendly hellos in the hallway or the fun we have all had at the various social events, I will never forget my time in the department.

My parents, Barbara and Ken, have provided me with their unconditional love and support throughout my education. You have always supported me no matter what path I have chosen and for that I will be forever grateful.

Finally, I would like to thank my fiancé, Michael, for the love and encouragement you have given me. Without you, I do not think I would have accomplished what I have to date.

Contents

Abstract **ii**

Acknowlegements **iii**

List of Figures **vii**

List of Tables **xi**

List of Appendices **xii**

List of Abbreviations and Symbols **xiii**

1 Introduction **1**

2 Regime-Switching Framework **7**
- 2.1 Market Assumptions 7
- 2.2 Geometric Brownian Motion 7
- 2.3 N-State Case 8
  - 2.3.1 Regime-Switching Volatility 8
  - 2.3.2 Regime-Switching Option Dynamics 9
  - 2.3.3 Pricing Equation Derivation 10
- 2.4 Two-State Case 15

3 Numerical Solution **18**
- 3.1 Overview of Crank-Nicolson Numerical Scheme 19
- 3.2 Application to the One-Dimensional Heat Equation 20
- 3.3 Application to the Black-Scholes PDE 22
- 3.4 Application to Coupled One-Dimensional Heat Equations 25
- 3.5 Application to Regime-Switching PDEs 31

4 Approximate Solution **36**
- 4.1 Review of Cauchy-Kowalevski Theorem 36
- 4.2 Reformulating our Regime-Switching Pricing Model 37
  - 4.2.1 Applying Cauchy-Kowalevski to the One-Dimensional Black-Scholes Problem 39
  - 4.2.2 Applying Cauchy-Kowalevski to the Regime-Switching Problem 42
- 4.3 Error Introduced by Approximate Solution 49

4.4 Discussion 53
4.5 Summary 62

5 Impact of Market Price of Volatility Risk 63
5.1 Restrictions Derived Directly from Coupled Pricing Equations 64
5.2 Restrictions Derived from Approximate Solutions 66
5.2.1 Behaviour of $g(t, T)$ 68
5.2.2 Case 1: $f_{HL} \in \mathbb{R}$, $f_{HL} + f_{LH} < 0$ 69
5.2.3 Case 2: $f_{LH} \in \mathbb{R}$, $f_{HL} + f_{LH} < 0$ 70
5.3 Implied Volatility Smiles 74
5.4 Summary 80

6 Hedging Strategies 82
6.1 Simulation Framework 83
6.1.1 Simulating Regime-Switching Volatility 83
6.1.2 Simulating Geometric Brownian Motion 83
6.2 Simulating Hedging Strategies 83
6.3 Black-Scholes Hedging 85
6.4 Overview of Hedging Strategies 87
6.4.1 Portfolio I: Hedging with One Option 87
Hedging with $C_2^i(S, t)$ 90
Hedging with $C_3^i(S, t)$ 90
Issues with Portfolio I 91
6.4.2 Portfolio II: Hedging with Two Options 92
Minimum Variance Hedging Approach 95
Hedging with a Limit 99
6.4.3 Hedging with Constant Volatility 102
Unconditional Volatility 103
Hedging Given Investor's Risk Preferences 103
6.5 Hedging Strategies Analysis 105
6.5.1 Effect of Stock Price Drift 107
6.5.2 Effect of Delta Limit 111
6.5.3 Effect of Transaction Costs 114
6.6 Summary 117

7 Deterministic Poisson Intensities 119
7.1 Motivation 121
7.1.1 5-Day Moving Average Volatility 122
7.1.2 5-Day Moving Average Trading Volume 124
7.2 Earnings Release Framework 126
7.2.1 Time Varying Poisson Intensities 126
7.2.2 Time and Stock Varying Poisson Intensities 129
7.3 Effect of the Time Intensity Parameter, κ 133
7.4 Discussion 134
7.4.1 Case 1: Time Varying, Maturity Event Poisson Intensities 135

7.4.2 Case 2: Time Varying, Non-Maturity Event Poisson Intensities 138
7.4.3 Case 3: Time and Stock Varying, Maturity Event Poisson Intensities . . 140
7.4.4 Case 4: Time and Stock Varying, Non-Maturity Event Poisson Intensities 143
7.5 Hedging Strategies 145
7.6 Summary 146

8 Concluding Remarks 148
8.1 Summary 148
8.2 Future Work 150

Bibliography 151

A Additional Deterministic Intensity Analysis 155

Curriculum Vitae 158

List of Figures

1.1 Historical daily close prices for the S&P/TSX Composite Index. Ticker symbol: GSPTSE on the Toronto Stock Exchange. Data obtained from Yahoo Canada Finance [51], covering from April 23, 1984 to March 25, 2014. 2
1.2 Distribution of historical daily log returns for close prices of the S&P/TSX Composite Index. Data obtained from Yahoo Canada Finance [51], covering from April 23, 1984 to March 25, 2014. 2
1.3 S&P/TSX Composite Index historical daily log returns. Data obtained from Yahoo Canada Finance [51], covering from April 23, 1984 to March 25, 2014. . 3

3.1 Comparison of the numerical and true solution for one-dimensional heat equation at time $t = 1$. All parameters as given in Table 3.1. 22
3.2 Comparison of the numerical and true solution for the Black-Scholes PDE at time $t = 0$. All parameters as given in Table 3.2. 24
3.3 Visualization of coupled numerical grids interacting simultaneously to solve coupled PDEs for a single set of points (U_M^2, V_M^2). 25
3.4 Comparison of the numerical and true solution for the coupled one-dimensional heat equation, $U(x,t)$, at time $t = 1$. All parameters as given in Table 3.3. 30
3.5 Comparison of the numerical and true solution for the coupled one-dimensional heat equation, $V(x,t)$, at time $t = 1$. All parameters as given in Table 3.3. 31
3.6 Crank-Nicolson numerical solution for the regime-switching coupled pricing PDEs at time $t = 0$. All parameters as given in Table 3.4. 35

4.1 Comparison of the error estimate for various values of τ. $\varepsilon = 0.005$, all other parameters as given in Table 4.1. 42
4.2 Comparison of the error estimate for various sizes of ε. $\tau = 1$, all other parameters as given in Table 4.1. 43
4.3 Comparison of the numerical and approximate solution of the high state regime-switching risk-neutral call option at $t = 0$. Parameters as given in Table 4.2. . . 57
4.4 Comparison of the numerical and approximate solution of the low state regime-switching risk-neutral call option at $t = 0$. Parameters as given in Table 4.2. . . 58
4.5 Comparison of the backward error associated with solving the state-dependent Black-Scholes PDEs at $t = 0$ using the Crank-Nicolson numerical scheme. Parameters as given in Table 4.2. 59
4.6 Comparison of the backward error associated with solving the coupled regime-switching risk-neutral PDEs at $t = 0$ using the Crank-Nicolson numerical scheme. Parameters as given in Table 4.2. 59

4.7 Comparison of the backward error associated with our approximate regime-switching risk-neutral solution at $t = 0$. Parameters as given in Table 4.2. 60
4.8 Effect of time on the L^2 norm associated with the difference between the approximate and numerical solutions for the regime-switching risk-neutral coupled PDEs. Parameters as given in Table 4.2. 60
4.9 Effect of varying the time increments, dt, on the L^2 norm associated with the difference between the approximate and numerical solutions at $t = 0$ for the regime-switching risk-neutral coupled PDEs. Parameters as given in Table 4.2 . 61

5.1 Crank-Nicolson numerical solutions for the coupled pricing PDEs. $m_{HL} = -1, m_{LH} = 4$, all other parameters as given in Table 5.1. 72
5.2 Comparison of the numerical and approximate solution of the high state pricing PDE. $m_{HL} = m_{LH} = -2$, all other parameters as given in Table 5.1. 73
5.3 Comparison of the numerical and approximation solution of the low state pricing PDE. $m_{HL} = m_{LH} = -2$, all other parameters as given in Table 5.1. 74
5.4 Implied volatility smile corresponding to high and low state risk-neutral regime-switching options prices. $m_{HL} = m_{LH} = 0$ and $S = \$100$, all other parameters as given in Table 5.1. 75
5.5 State-dependent implied volatility smiles resulting from varying the market prices of volatility risk. $m_{HL} = \{0, -1\}$, $m_{LH} = \{0, -1\}$, $S = \$100$, all other parameters as given in Table 5.1. 76

6.1 Example of Portfolio II set-up when $S_T < K_3$. 93
6.2 Example of Portfolio II set-up when $S_T > K_2$. 94
6.3 Effect of Δ_2 limit on mean % of trading days with limit breaches. $\mu = 0\%$, all other parameters as given in Table 6.1. 111
6.4 Effect of Δ_3 limit on mean % of trading days with limit breaches. $\mu = 0\%$, all other parameters as given in Table 6.1. 112
6.5 Effect of Δ_2 limit on profit/loss of Portfolio II. $\mu = 0\%$, all other parameters as given in Table 6.1. 113
6.6 Effect of Δ_3 limit on profit/loss of Portfolio II. $\mu = 0\%$, all other parameters as given in Table 6.1. 114
6.7 Effect of stock price drift, μ, on the mean profit/loss of differing portfolios. $N_{lim} = 1$, $TC_{stock} = 0$ bps and $TC_{option} = 0$ bps, all other parameters as given in Table 6.1. 115
6.8 Effect of stock price drift, μ, on the mean profit/loss of differing portfolios. $N_{lim} = 1$, $TC_{stock} = 0$ bps and $TC_{option} = 10$ bps, all other parameters as given in Table 6.1. 116
6.9 Effect of stock price drift, μ, on the mean profit/loss of differing portfolios. $N_{lim} = 1$, $TC_{stock} = 1$ bps and $TC_{option} = 100$ bps, all other parameters as given in Table 6.1. 117

7.1 Two types of event studies: discontinuous stock price movement and volatility regime change. 120

7.2 5-day moving average volatility for TD Bank for fiscal year 2013. Data obtained from Yahoo Canada Finance [52]. 123
7.3 5-day moving average volatility for Apple for fiscal year 2013. Data obtained from Yahoo Canada Finance [50]. 123
7.4 5-day moving average of daily trading volume for TD Bank for fiscal year 2013. Data obtained from Yahoo Canada Finance [52]. 124
7.5 5-day moving average of daily trading volume for Apple for fiscal year 2013. Data obtained from Yahoo Canada Finance [50]. 125
7.6 Time varying Poisson intensity assuming the financial event occurs at maturity. $\kappa = 1$, $\lambda^\star = 10\%$ (daily), and $T = 1$ year. 128
7.7 Time varying Poisson intensity assuming the financial event occurs before maturity. $\kappa = 1$, $\lambda^\star = 10\%$ (daily), $\tau^\star = 9$ months, and $T = 1$ year. 129
7.8 Time and stock varying Poisson intensity assuming the financial event occurs at maturity. Parameters as given in Table 7.3. 131
7.9 Time and stock varying Poisson intensity assuming the financial event occurs before maturity. Parameters as given in Table 7.3. 132
7.10 Impact of κ on the time-dependent Poisson intensity assuming the event occurs at option maturity. $\lambda^\star = 10\%$ (daily) and $T = 1$ year. 133
7.11 Impact of κ on the time-dependent Poisson intensity assuming the event occurs before option maturity. $\lambda^\star = 10\%$ (daily), $\tau^\star = 9$ months, and $T = 1$ year. . . . 134
7.12 Comparison of numerical regime-switching option prices between the benchmark case and Case 1 at $t = 0$. Parameters as given in Table 7.4. 136
7.13 Difference between the benchmark case and Case 1 numerical option prices at $t = 0$. Parameters as given in Table 7.4. 137
7.14 Implied volatility smiles corresponding to option prices for the benchmark case and Case 1. $S = \$100$, all other parameters as given in Table 7.4. 137
7.15 Comparison of regime-switching option prices between the benchmark case and Case 2 at $t = 0$. Parameters as given in Table 7.4. 138
7.16 Difference between the benchmark case and Case 2 numerical option prices at $t = 0$. Parameters as given in Table 7.4. 139
7.17 Implied volatility smiles corresponding to option prices for the benchmark case and Case 2. $S = \$100$, all other parameters as given in Table 7.4. 140
7.18 Comparison of regime-switching option prices between the benchmark case and Case 3 at $t = 0$. Parameters as given in Table 7.4. 141
7.19 Difference between the benchmark case and Case 3 numerical option prices at $t = 0$. Parameters as given in Table 7.4. 142
7.20 Implied volatility smiles corresponding to option prices for the benchmark case and Case 3. $S = \$100$, all other parameters as given in Table 7.4. 142
7.21 Comparison of regime-switching option prices between the benchmark case and Case 4 at $t = 0$. Parameters as given in Table 7.4. 143
7.22 Difference between the benchmark case and Case 4 numerical option prices at $t = 0$. Parameters as given in Table 7.4. 144
7.23 Implied volatility smiles corresponding to option prices for the benchmark case and Case 4. $S = \$100$, all other parameters as given in Table 7.4. 145

A.1 Comparison of benchmark case and Case 1 numerical regime-switching option prices, zoomed about the strike $K = \$100$. Parameters as given in Table 7.4. Original plot depicted in Figure 7.12. 155
A.2 Comparison of benchmark case and Case 2 numerical regime-switching option prices, zoomed about the strike $K = \$100$. Parameters as given in Table 7.4. Figure 7.15 depicts original, non-zoomed plot. 156
A.3 Comparison of benchmark case and Case 3 numerical regime-switching option prices, zoomed about the strike $K = \$100$. Parameters as given in Table 7.4. Figure 7.18 depicts original, non-zoomed plot. 156
A.4 Comparison of benchmark case and Case 4 numerical regime-switching option prices, zoomed about the strike $K = \$100$. Parameters as given in Table 7.4. Figure 7.21 depicts original, non-zoomed plot. 157

List of Tables

3.1 Parameters used in the implementation of the Crank-Nicolson numerical scheme for the one-dimensional heat equation. 21
3.2 Parameters used in the implementation of the Crank-Nicolson numerical scheme for the Black-Scholes PDE. 24
3.3 Parameters used in the implementation of the Crank-Nicolson numerical scheme for the coupled one-dimensional heat equations. 29
3.4 Parameters used in the implementation of the Crank-Nicolson numerical scheme for the regime-switching coupled PDEs. 34

4.1 Parameters used in investigation of error estimate. 41
4.2 Parameters used in the implementation of the Crank-Nicolson numerical scheme. 56

5.1 Parameters used in the implementation of the Crank-Nicolson numerical scheme. 72

6.1 Parameters used in the analysis of hedging strategies for varying stock price path drifts. 106
6.2 Summary of total state occupations and total state transitions for price paths used in hedging analysis. 107
6.3 Hedging analysis for varying stock price path drifts using numerical option prices. Parameters as given in Table 6.1. 108
6.4 Hedging analysis for varying stock price path drifts using approximate option prices. Parameters as given in Table 6.1. 110

7.1 Quarter end and earnings release dates for Toronto Dominion bank for fiscal year 2013. Ticker symbol TD.TO on TSX. Data obtained from [42], [43], [44], and [45]. 121
7.2 Quarter end and earnings release dates for Apple for fiscal year 2013. Ticker symbol APPL on Nasdaq. Data obtained from [1], [2], [3], and [4]. 122
7.3 Parameters used in the analysis of time and stock varying Poisson intensities. . 131
7.4 Parameters used in the analysis of option pricing for deterministic Poisson intensities. Note: † This event date is only used for Case 2 and Case 4 where it is assumed that the event occurs before the maturity date of our regime-switching call option. 135
7.5 Summary of results for the time varying and time and stock varying Poisson intensity cases. 147

List of Appendices

Appendix A Additional Deterministic Intensity Analysis 155

List of Abbreviations and Symbols

List of Abbreviations

- CDF – cumulative distribution function
- GBM – geometric Brownian motion
- MPVR – market price of volatility risk
- PDE – partial differential equation
- SDE – stochastic differential equation
- TC – transaction cost

List of Symbols

- i, j – volatility states
- t – time
- $C^i(S,t)$ – state-dependent regime-switching call option value, conditional on volatility state i
- $C^i_{BS}(S,t)$ – Black-Scholes call option value, conditional on volatility state i
- $S(t)$ – price underlying asset at time t
- r – risk-free rate of interest
- μ – drift of underlying asset
- σ_i – state-dependent volatility of underlying asset
- K – strike price of an option
- T – maturity date of an option
- $W(t)$ – Brownian motion
- $\lambda_{ij}(S,t)$ – state-dependent Poisson intensity, driving the switch from volatility state i to volatility state j
- $dq_{ij}(t)$ – independent Poisson process with probability $\lambda_{ij}(S,t)dt$
- $f_{ij}(S,t)$ – PDE source term coefficient
- $m_{ij}(S,t)$ – state-dependent market price of volatility risk
- $X(S,t)$ – difference between low volatility state Black-Scholes and regime-switching call option values
- $Y(S,t)$ – difference between high volatility state Black-Scholes and regime-switching call option values
- $\Pi^i(S,t)$ – state-dependent hedge portfolio, conditional on volatility state i
- Δ^i – hedge ratio of a hedging instrument, conditional on volatility state i
- N_{lim} – limit on hedge ratio for hedging option
- TC_{stock} – transaction cost for underlying asset
- TC_{option} – transaction cost for hedging options
- $\sigma_{i,imp}$ – state-dependent implied volatility
- $P_{i,unconditional}$ – unconditional probability of occupying state i

- $\sigma_{i^\star}$ – volatility estimate used for constant volatility hedging strategies
- κ – time intensity parameter
- $\tau^\star$ – time of financial event
- $\lambda_{ij}^\star$ – maximum state-dependent constant Poisson intensity
- N – number of volatility regimes; number of hedging options
- dx, dS, dt – space, stock price and time increment, respectively
- m, l – space/stock and time index, respectively
- $M, \tilde{L}$ – number space/stock price and time increments, respectively
- $n, n^\star$ – hedging option and additional hedging option index, respectively

Chapter 1

Introduction

Both practitioners and academics have focused for decades on characterizing the randomness of stock prices and on the underlying market conditions which affect their evolution. One of the factors affecting stock price evolution is volatility: the degree to which prices fluctuate. Volatility has long been known to vary over time in an essentially unpredictable way. Studying empirical equity data can provide a way to formulate reasonable and tractable volatility models. This thesis is based on the assumption that volatility is stochastic in a very particular way; it fluctuates between a finite number of regimes. Our focus is on formulating financially appropriate mathematical models to describe the evolution of volatility over time. This thesis does not consider the important and interesting problem of volatility prediction. We will first motivate the existence of stochastic volatility by studying empirical equity data.

Consider a price path such as that for the S&P/TSX Composite Index which is currently composed of 244 of the largest public companies, by market capitalization, trading on the Toronto Stock Exchange (TSX). One can observe an overall trend in the price path which covers from 1984 to 2014, as illustrated in Figure 1.1 for the S&P/TSX Composite Index. It is also immediately evident that daily prices move randomly and it is easy to see how they could be hard to predict.

A common mathematical finance technique for studying stock price paths is to consider the log returns of the asset prices. This allows for us to study the distribution of the returns and to analyse their magnitude. Higher magnitude stock returns are associated with higher volatility in the underlying stock price path. It is commonly thought that stock returns follow, at least approximately, a lognormal distribution and as such this distribution is used as a benchmark model in finance. In general, stock price returns are computed as follows:

$$u(t+1) = \ln\left(\frac{S(t+1)}{S(t)}\right), \tag{1.1}$$

where $S(t)$ is the price of the underlying asset at time t.

First, we plot a histogram containing the stock returns associated with the daily close prices, which are illustrated in Figure 1.2.

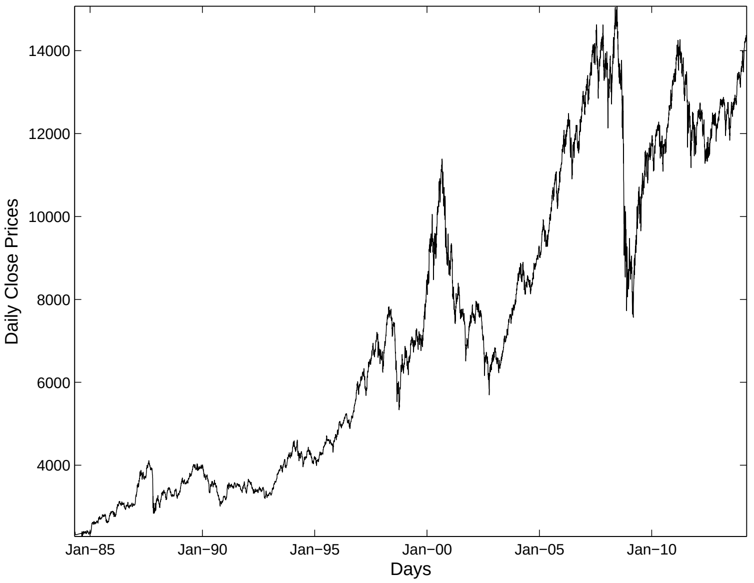

Figure 1.1: Historical daily close prices for the S&P/TSX Composite Index. Ticker symbol: GSPTSE on the Toronto Stock Exchange. Data obtained from Yahoo Canada Finance [51], covering from April 23, 1984 to March 25, 2014.

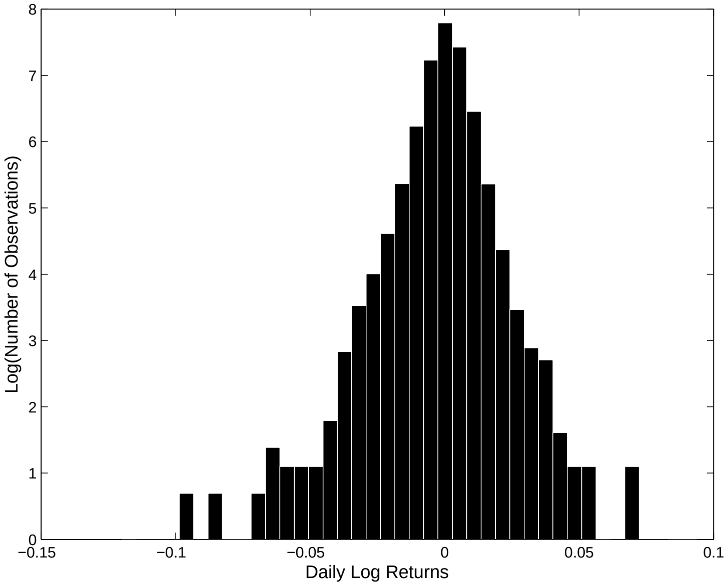

Figure 1.2: Distribution of historical daily log returns for close prices of the S&P/TSX Composite Index. Data obtained from Yahoo Canada Finance [51], covering from April 23, 1984 to March 25, 2014.

The histogram shown in Figure 1.2 seems to indicates two magnitudes of stock returns, visible in the separation in the data. It can also be observed that the data do not appear to follow a lognormal distribution. Instead the data appears fat-tailed with outliers on either side of the main data peak. Another way to analyze the data, in order to determine if there are changes in the volatility, is to consider the log returns plotted against time.

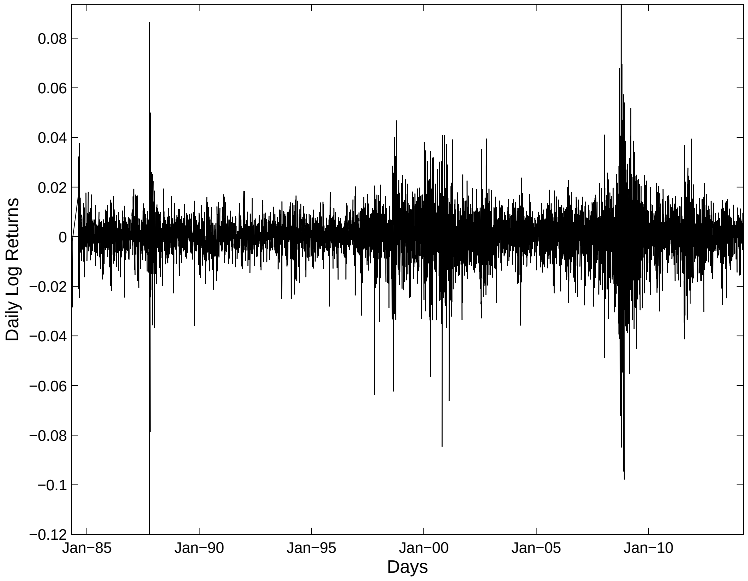

Figure 1.3: S&P/TSX Composite Index historical daily log returns. Data obtained from Yahoo Canada Finance [51], covering from April 23, 1984 to March 25, 2014.

Looking at Figure 1.3, which depicts a time series of the daily log returns for the S&P/TSX Composite index from 1984 to 2014 allows us to easily identify periods of abnormal volatility levels. There are several "bursts" observed in the daily log returns. These bursts, which refer to the observable increases in the magnitude of the daily log returns, are associated with increased volatility. After these bursts are observed in the market, they can sometimes be associated with known economic and financial events in history. High magnitude returns in 1987 can be attributed to the stock market crash, known as Black Monday, on October 19, 1987. Around the year 2001, increases in volatility levels can be explained by the Dot-Com Bubble and more recently in the years 2007-2008, increases in volatility can be associated with the Subprime Mortgage Crisis. This empirical data indicates that volatility is in fact stochastic and is influenced by economic events. Interestingly enough, different economic and financial events could also in return be a trigger for shifts in volatility levels. One part of this thesis involves exploring the relationship between increases in volatility levels and the arrival of upcoming financial events.

Although we can now observe that volatility is stochastic, there are several fundamental frameworks which form the basis of options pricing in mathematical finance. Black and Scholes [6] created the well known options pricing model in which a European option was priced on an underlying asset following geometric Brownian motion (GBM) with constant drift and constant volatility. Although the constant volatility assumption has now been disproven, their closed-form solution for European options and associated hedging arguments provide for a nice benchmark model for comparison with subsequent options pricing frameworks.

There has been much recent interest on pricing and hedging options written on stocks following diffusion processes with random volatility coefficients. Heston [27] was a pioneer in modelling volatility uncertainty, pricing a European option written on an underlying asset, the price of which followed geometric Brownian motion (GBM) with stochastic volatility. He chose his volatility process to incorporate mean reversion which allowed for the process to revert to a long run average volatility level over time at a specified speed. Another popular stochastic volatility model is the Generalized Autoregressive Conditional Heteroskedasticity (GARCH) model. Hansen and Lunde [24] compared 330 volatility models, including variations of GARCH and ARCH (Autoregressive Conditional Heteroskedasticity) to forecast out-of-sample intraday volatility for US equity data. Using a variety of statistical tests, they showed that for small time intervals, a Markov regime-switching GARCH with two states outperformed GARCH in forecasting volatility. Although this thesis does not consider parameter estimation for Markov models, much progress has been made in this area, including work by Xi and Mamon [53], [55], and Xi, Rodrigo, and Mamon [54].

Economists have long considered that the business cycle fluctuates between different stages, such as expansion and contraction. Hamilton [22], [23] studied US post-war gross national product (GNP) data and found that growth rates for specific regimes of a Markov process were associated with different business cycles. More recently financial literature has proposed that volatility can be well modelled by shifts between a finite number of regimes. The consideration of the business cycle, as well as observation of market data, suggests that volatility is well modelled by random moves between low and high regimes. Hardy [25] showed that a two-regime lognormal model was sufficient to model equity data, in particular the Canadian Toronto Stock Exchange (TSX), and was preferable over other statistical approaches used in volatility modelling. Furthermore, Filardo [19] used a Markov model with time-varying transitional probabilities to model business cycles, in particular two phases: expansion and contraction.

For simplicity and tractability, as well as for realism, we will consider a two-regime model in which the volatility can switch between high and low regimes. Similarly to Merton's [32] model, which included Poisson jumps in the stock price dynamics, we model the shifts between regimes by Poisson processes with deterministic intensities. We begin our study of this model with constant Poisson intensities driving the switches between regimes. Later on, the intensities are allowed to vary with time and stock price levels. We set up a hedge portfolio where we take simultaneous positions in an asset and in an option, as suggested by Naik [35], to hedge against our risk exposure. Using Black and Scholes type hedging and standard arbitrage arguments, we derive a system of coupled partial differential equations (PDEs) representing state-dependent option prices in a regime-switching market. Our generalized N-state pricing PDEs have a similar form to those previously derived by Boyle and Draviam [9], Buffington and Elliott [11], Di Masi et al. [15], and Naik [35], with the additional inclusion of a market price of volatility risk term.

Assuming that volatility risk was not priced, Boyle and Draviam solved their PDE to obtain prices in the risk-neutral measure. They considered the option price as a conditional expectation and took a Taylor series expansion approach to derive their pricing equations. Buffington and Elliott derived their regime-switching PDE using standard stochastic calculus techniques involving expectations and martingales. On the other hand, Di Masi et al. derived their PDEs using a hedging approach where they assumed that volatility could not be perfectly hedged and thus they hedge by locally minimizing the associated risk. Under the risk-neutral measure, Mamon and Rodrigo [31] derived an integral-type solution in terms of the Black-Scholes option prices. Furthermore, Naik reduced the solution for a European call option on a regime switching asset, assuming zero market price of volatility risk, to a quadrature. Bollen [7] priced both European and American options, written on underlying assets with regime-switching returns, using a pentanomial lattice.

As a benchmark for our volatility framework and pricing problem, we will consistently consider pricing and hedging a European call option throughout this thesis. We will solve our regime-switching pricing problem both numerically and by using approximation solution techniques. Both methods lead to further analysis of parameters such as the volatility risk premium. It also allows for us to directly compare our model to the constant volatility Black-Scholes model which allows for useful financial intuition of our switching framework.

Several key words arise frequently throughout our investigation of this framework. They are defined below for ease of reading.

- Financial option: Contract which gives its owner the right but not the obligation to buy or sell the underlying asset at a predetermined price (strike price) on or before a predetermined date (maturity date).
- European call option: Contract which gives its owner the right but not the obligation to buy the underlying asset at the strike price on the maturity date.
- Option premium: Price charged for the option at contract initiation (time $t = 0$).
- Moneyness: Relationship between the underlying asset's price and the strike price. It describes the option's intrinsic value (i.e. the value if the option were to expire today). Options can be in-the-money, at-the-money, or out-of-the-money.
- Hedging: Trading strategy that aims to reduce or eliminate the risk associated with financial instruments in our portfolio.
- Short position: Position in which an investor has sold a financial instrument to a counterparty.

It should be noted that on actual options exchanges such as the Chicago Board Options Exchange, options are usually exchanged for 100 units of the underlying asset [46]. For simplicity, we will just assume our option is exercised for one unit of the stock.

A summary of the remainder of the thesis is now given. Chapter 2 provides an introduction to the regime-switching volatility model upon which all subsequent work is based. An outline of the stochastic equations governing this framework is given as well as a detailed discussion surrounding the derivation of the corresponding options pricing equations. Chapters 3 through 6 will focus on a two-state volatility switching framework where the intensity of jumping between regimes is constant and known. Chapter 3 gives an overview of the Crank-Nicolson numerical scheme as well as a generalized application to the one dimensional heat equation.

A general application to financial pricing problems including our regime-switching model is also given. Chapter 4 focuses on the derivation of the approximate solution via the Cauchy-Kovalewski Theorem of PDEs and the intuition that results from this approximate solution. Chapter 5 focuses on the effect of the volatility risk premium on option prices as well as further investigation into its effect on implied volatility and investor risk preferences. Chapter 6 provides a detailed analysis of naive hedging strategies and those tailored to hedge specifically against all risks present in a volatility switching model. A mathematical discussion of each hedging strategy is included as well as a numerical study. Chapter 7 considers deterministic switching intensities and the resulting hedging insight that can arise from this altered switching model. Concluding remarks and a discussion of future work is given in Chapter 8.

Chapter 2

Regime-Switching Framework

We start with an introduction to regime-switching models in which the notation used in the subsequent chapters will be introduced. We will consistently consider throughout a European call option with payoff $(S(T)-K)^{+}$ [28], in which we assume the investor takes a short position. An overview of the market in which we are hedging and pricing is given as well as a description of geometric Brownian motion. A detailed discussion of the regime-switching framework follows, first for the generalized N-state, and then for the economically reasonable two-state case.

2.1 Market Assumptions

In order to derive the option pricing and hedge ratio relations in the subsequent sections, certain assumptions about the general market in which we are hedging and pricing options must hold. Many of these assumptions are the same as under the Black-Scholes constant volatility option pricing model [6].

First, we assume our financial market is such that the volatility can switch between a finite number of volatility regimes. The stock price follows geometric Brownian motion while independent Poisson processes are used to model the jumps between regimes. The expected return will be independent of state and it is assumed that the state-dependent volatilities have constant fixed values. The risk-free rate of interest is also assumed to be constant. Furthermore, it is assumed that we can hedge continuously and buy any quantity of the hedging instruments in our portfolio. This includes both the underlying asset and any hedging options. Finally, in the absence of transaction costs, there exists no arbitrage opportunities. In other words, there is no way for an investor to earn a riskless profit.

2.2 Geometric Brownian Motion

We assume the dynamics of our stock price (i.e. underlying asset) follow a widely used and well known stochastic differential equation (SDE) in mathematical finance, otherwise known as geometric Brownian motion (GBM). The stock price dynamics are as follows under the real world measure $\mathbb{P}$:

$$dS(t) = \mu S(t) + \sigma(t)S(t)dW(t), \tag{2.1}$$

where $dW(t)$ is an increment of a Wiener process (i.e. $W(t)$ is Brownian motion). The four properties of a Wiener process are as follows:

- $W(0) = 0$,
- $W(t + dt) - W(t) \sim N(0, dt)$ for all $t > 0$ and $dt > 0$,
- all increments are independent,
- $W(t)$ is continuous everywhere but differentiable nowhere.

Recall that in our model the expected return (i.e. drift) of the stock price, μ, is constant and independent of state, while the volatility, $\sigma(t)$, can switch between a finite number of regimes.

The first term in the SDE represents the deterministic growth of the stock price where the drift dictates the overall direction in which the stock price evolves. The second term incorporates randomness into the model, allowing fluctuations in the stock price to vary with the level of risk (i.e. volatility).

2.3 *N*-State Case

2.3.1 Regime-Switching Volatility

Given a finite number of volatility regimes, N, assuming volatility occupies volatility state i at time t, there are $N - 1$ possible regimes to which the market can transition to at time $t + dt$. Therefore at every time point we are exposed to the risk of $N - 1$ volatility jumps of differing magnitude and direction. It is possible to remain in the currently occupied regime, however there is no inherent risk associated with constant volatility, so no hedging option would be needed in our portfolio if we knew volatility was constant.

Under the real world measure $\mathbb{P}$, the volatility's stochastic differential equation (SDE) is governed by:

$$d\sigma(t) = \sigma(t) \sum_{\substack{j=1 \\ j \neq i}}^{N} \Big(J_{ij} - 1\Big) dq_{ij}(t), \tag{2.2}$$

where

$$J_{ij} = \frac{\sigma_j - \sigma(t)}{\sigma(t)} + 1, \tag{2.3}$$

and $\sigma(t) = \sigma_i$ for $i = 1, \ldots, N$. J_{ij} represents the relative magnitude of the volatility jump from regime i to regime j such that $i \neq j$ where σ_i is the fixed volatility value for regime i.

$$dq_{ij}(t) = \begin{cases} 1 \text{ with probability } \lambda_{ij}(S, t)dt \\ 0 \text{ with probability } 1 - \lambda_{ij}(S, t)dt \end{cases} \tag{2.4}$$

where $0 \leq \lambda_{ij}dt \leq 1$ must old. The independent Poisson processes, $q_{ij}(t)$, are also independent of the Brownian motion $W(t)$ embedded in the stock price dynamics. The Poisson intensity, $\lambda_{ij}(S,t)$ controls the likelihood of the jump from volatility state i at time t to volatility state j at time $t + dt$.

2.3.2 Regime-Switching Option Dynamics

We want to consider the dynamics of an option, $C(S,\sigma_i,t)$, written on an underlying asset, $S(t)$ with regime-switching volatility, $\sigma(t)$. There are $N-1$ possible regime shifts from each regime i. This does not include the possibility of remaining in the presently occupied regime.

Using the Itô-Doeblin formula for jump processes [39], we derive an expression for the dynamics of our regime-switching option. For simplicity of notation, $C^i(S,t) \equiv C(S,\sigma_i,t)$ and $S \equiv S(t)$.

Under the assumption that the time increment dt is very small:

$$dW(t) \approx \sqrt{dt} \Rightarrow (dW(t))^2 \approx dt, \tag{2.5}$$

$$dW(t)dt \approx 0, \tag{2.6}$$

$$(dt)^2 \approx 0. \tag{2.7}$$

We utilize the above results to obtain:

$$(dS)^2 = \mu^2 S^2 (dt)^2 + 2\mu\sigma_i S^2 dt dW(t) + \sigma_i^2 S^2 (dW(t))^2 = \sigma_i^2 S^2 dt, \tag{2.8}$$

and as a result:

$$\begin{aligned} dC^i(S,t) &= \frac{\partial C^i}{\partial S}(S,t)dS + \frac{\partial C^i}{\partial t}(S,t)dt + \frac{1}{2}\frac{\partial^2 C^i}{\partial S^2}(S,t)(dS)^2 \\ &\quad + \sum_{\substack{j=1 \\ j\neq i}}^{N} \left[C^j(S,t) - C^i(S,t)\right] dq_{ij}(t), \qquad (2.9) \\ \Rightarrow dC^i(S,t) &= \left(\frac{\partial C^i}{\partial t}(S,t) + \frac{1}{2}\sigma_i^2 S^2 \frac{\partial^2 C^i}{\partial S^2}(S,t)\right)dt + \frac{\partial C^i}{\partial S}(S,t)dS \\ &\quad + \sum_{\substack{j=1 \\ j\neq i}}^{N} \left[C^j(S,t) - C^i(S,t)\right] dq_{ij}(t). \qquad (2.10) \end{aligned}$$

In the generalized N-state case, the regime-switching option is exposed to the risk of the movements in the underlying asset, denoted by the term with dS. This option is also exposed to all possible $N-1$ jumps between volatility regimes, since the dynamics depend on terms containing $dq_{ij}(t)$.

It should be noted that any type of option contract, written in a regime-switching volatility market on an underlying asset following GBM, will be exposed to these same risks and as a result, possess the same option dynamics.

2.3.3 Pricing Equation Derivation

Here we present a detailed derivation of the equations for the value of an option contract written on an asset with regime-switching volatility. The contract price depends, as usual, on the stock price and time, but also on what state the volatility occupies. The result is a system of coupled pricing equations, one for each volatility state. These equations may be developed using standing hedging arguments dating back to Black and Scholes [6], as summarized in Wilmott [49]. These arguments are shown in detail in the succeeding sections for completeness.

For simplicity, suppose we are hedging against a position in a plain vanilla option. In particular, we consider an investor who takes a short position in a European call option. We can hedge against the stock price movements by taking a position in the underlying asset. Since the call option with price $C^i(S,t)$ is written on an underlying asset with regime-switching volatility, we need $N-1$ hedging options to hedge against all $N-1$ possible volatility switches. This is under the assumption that there are no available instruments that directly hedge volatility risk.

Our portfolio, $\Pi^i(S,t)$, consists of a short position in a European call option $C_1^i(S,t)$ struck at K_1 with maturity date T_1. We can minimize and in some cases offset such risk by dynamically hedging, where we readjust our hedge position in a portfolio as desired. As a result a position is taken in the underlying asset S and $N-1$ hedge positions in other call options $C_n^i(S,t)$ where $n = 2,\dots,N$, written on the same underlying asset but with different contract specifications. In particular, we require that $T_n > T_1$ for all $n = 2,\dots,N$.s In order for the hedging strategy to be non-redundant, we require that at least one of the strike price or the maturity date of our hedging options differs from the initial shorted call option.

Basic hedging and arbitrage arguments are utilized under our framework to derive the coupled pricing equations. This derivation is shown in complete detail below.

Our portfolio can be represented mathematically as:

$$\Pi^i(S,t) = -C_1^i(S,t) + \Delta_1^i S + \sum_{n=2}^{N} \Delta_n^i C_n^i(S,t). \tag{2.11}$$

We are interested in how the randomness inherent in our portfolio affects the actual change in the value of the hedge portfolio.

$$d\Pi^i(S,t) = -dC_1^i(S,t) + \Delta_1^i dS + \sum_{n=2}^{N} \Delta_n^i dC_n^i(S,t). \tag{2.12}$$

The dynamics of all options are the same since they are all written on the same underlying asset with volatility following a regime-switching process. Thus we can apply our result given by equation (2.10) for $dC_n^i(S,t)$ for all $n = 1,\dots,N$. The change in the portfolio value is now:

$$d\Pi^i(S,t) = -\left\{\left(\frac{\partial C_1^i}{\partial t}(S,t) + \frac{1}{2}\sigma_i^2 S^2 \frac{\partial^2 C_1^i}{\partial S^2}(S,t)\right)dt + \frac{\partial C_1^i}{\partial S}(S,t) + \sum_{\substack{j=1\\ j\neq i}}^{N} \left[C_1^j(S,t) - C_1^i(S,t)\right]\right\}$$

$$+ \Delta_1^i dS + \sum_{n=2}^{N} \Delta_n^i \left\{\left(\frac{\partial C_n^i}{\partial t}(S,t) + \frac{1}{2}\sigma^i S^2 \frac{\partial^2 C_n^i}{\partial S^2}(S,t)\right)dt + \frac{\partial C_n^i}{\partial S}(S,t)dS\right.$$

$$+ \sum_{\substack{j=1 \\ j\neq i}}^{N} \Big[C_n^j(S,t) - C_n^i(S,t)\Big] dq_{ij}(t) \Bigg\}, \tag{2.13}$$

$$\Rightarrow d\Pi^i(S,t) = \Bigg\{ -\left(\frac{\partial C_1^i}{\partial t}(S,t) + \frac{1}{2}\sigma_i^2 S^2 \frac{\partial^2 C_1^i}{\partial S^2}(S,t)\right) + \sum_{n=2}^{N} \Delta_n^i \left(\frac{\partial C_n^i}{\partial t}(S,t) + \frac{1}{2}\sigma_i^2 S^2 \frac{\partial^2 C_n^i}{\partial S^2}(S,t)\right)\Bigg\} dt$$

$$+ \left\{\Delta_1^i - \frac{\partial C_n^i}{\partial S}(S,t) + \sum_{n=2}^{N} \Delta_n^i \frac{\partial C_n^i}{\partial S}(S,t)\right\} dS$$

$$+ \sum_{\substack{j=1 \\ j\neq i}}^{N} \left\{ \sum_{n=2}^{N} \Delta_n^i \Big[C_n^j(S,t) - C_n^i(S,t)\Big] - \Big[C_1^j(S,t) - C_1^i(S,t)\Big]\right\} dq_{ij}(t). \tag{2.14}$$

We want to choose our hedge ratios, Δ_n^i, in such a way that the randomness associated with the stock price movements and the volatility switching is eliminated. This is done by setting the hedge ratios so that the groups of terms associated with dS and with all $dq_{ij}(t)$ vanish.

Thus, to hedge against movements in the underlying asset, choose:

$$\Delta_1^i = \frac{\partial C_1^i}{\partial S}(S,t) - \sum_{n=2}^{N} \Delta_n^i \frac{\partial C_n^i}{\partial S}(S,t). \tag{2.15}$$

To hedge against all possible $N-1$ volatility jumps at time t,

$$\sum_{n=2}^{N} \Delta_n^i \Big[C_n^j(S,t) - C_n^i(S,t)\Big] - \Big[C_1^j(S,t) - C_1^i(S,t)\Big] = 0, \tag{2.16}$$

for all $j = 1, \ldots, N, j \neq i$. ($N-1$ equations)

Since we hedged out all the risk associated with movements in the underlying asset and with jumps in volatility, the value of our portfolio only depends on the deterministic change in time. Therefore we can set the change in portfolio value equal to the risk-free return on the portfolio.

$$d\Pi^i(S,t) = r\Pi^i(S,t)dt, \tag{2.17}$$

$$\Bigg\{ -\left(\frac{\partial C_1^i}{\partial t}(S,t) + \frac{1}{2}\sigma_i^2 S^2 \frac{\partial^2 C_1^i}{\partial S^2}(S,t)\right) + \sum_{n=2}^{N} \Delta_n^i \left(\frac{\partial C_n^i}{\partial t}(S,t) + \frac{1}{2}\sigma_i^2 S^2 \frac{\partial C_n^i}{\partial S^2}(S,t)\right)\Bigg\} dt$$

$$= r\left\{ - C_1^i(S,t) + \Delta_1^i S + \sum_{n=2}^{N} \Delta_n^i C_n^i(S,t)\right\} dt, \tag{2.18}$$

$$-\left(\frac{\partial C_1^i}{\partial t}(S,t) + \frac{1}{2}\sigma_i^2 S^2 \frac{\partial^2 C_1^i}{\partial S^2}(S,t)\right) + \sum_{n=2}^{N} \Delta_n^i \left(\frac{\partial C_n^i}{\partial t}(S,t) + \frac{1}{2}\sigma_i^2 S^2 \frac{\partial C_n^i}{\partial S^2}(S,t)\right)$$

$$= -rC_1^i(S,t) + rS\left(\frac{\partial C_1^i}{\partial S} dS - \sum_{n=2}^{N} \Delta_n^i \frac{\partial C_n^i}{\partial S}(S,t)\right) + \sum_{n=2}^{N} \Delta_n^i r C_n^i(S,t), \tag{2.19}$$

$$\Rightarrow -\left(\frac{\partial C_1^i}{\partial t}(S,t) + \frac{1}{2}\sigma_i^2 S^2 \frac{\partial^2 C_1^i}{\partial S^2}(S,t) + rS\frac{\partial C_1^i}{\partial S}(S,t) - rC_1^i(S,t)\right)$$

$$+\sum_{n=2}^{N}\Delta_n^i\left(\frac{\partial C_n^i}{\partial t}(S,t)+\frac{1}{2}\sigma_i^2S^2\frac{\partial^2 C_n^i}{\partial S^2}(S,t)+rS\frac{\partial C_n^i}{\partial S}(S,t)-rC_n^i(S,t)\right)=0. \tag{2.20}$$

Defining the Black-Scholes type operator:

$$\mathcal{L}_{BS}(C(S,t))=\frac{\partial C}{\partial t}(S,t)+\frac{1}{2}\sigma^2S^2\frac{\partial^2 C}{\partial S^2}(S,t)+rS\frac{\partial C}{\partial S}(S,t)-rC(S,t), \tag{2.21}$$

we can rewrite our equation as follows:

$$-\mathcal{L}_{BS}(C_1^i(S,t))+\sum_{n=2}^{N}\Delta_n^i\mathcal{L}_{BS}(C_n^i(S,t))=0 \tag{2.22}$$

The values of $\Delta_n^i, n=2,\dots,N$ are still unknown, however using the following equations their value can be determined.

$$\sum_{n=2}^{N}\Delta_n^i\Big[C_n^j(S,t)-C_n^i(S,t)\Big]-\Big[C_1^j(S,t)-C_1^i(S,t)\Big]=0,\ (N-1\text{ equations}) \tag{2.23}$$

$$-\mathcal{L}_{BS}(C_1^i(S,t))+\sum_{n=2}^{N}\Delta_n^i\mathcal{L}_{BS}(C_n^i(S,t))=0, \tag{2.24}$$

for $j=1,\dots,N$ where $j\neq i$.

We have an overdetermined system of equations, since we have N equations for $N-1$ unknown variables. For such a system to be consistent (i.e. to have a solution), in matrix form we must have $\det(A)=0$ where A is an $N\times N$ matrix. A general version of this matrix, A, for our system is defined below.

$$A=\begin{bmatrix}\mathcal{L}_{BS}(C_1^i(S,t)) & \mathcal{L}_{BS}(C_2^i(S,t)) & \mathcal{L}_{BS}(C_3^i(S,t)) & \dots & \mathcal{L}_{BS}(C_N^i(S,t))\\ C_1^1(S,t)-C_1^i(S,t) & C_2^1(S,t)-C_2^i(S,t) & C_3^1(S,t)-C_3^i(S,t) & \dots & C_N^1(S,t)-C_N^i(S,t)\\ C_1^2(S,t)-C_1^i(S,t) & C_2^2(S,t)-C_2^i(S,t) & C_3^2(S,t)-C_3^i(S,t) & \dots & C^2_{N(S,t)}-C_N^i(S,t)\\ \vdots & \vdots & \vdots & \ddots & \vdots\\ C_1^N(S,t)-C_1^i(S,t) & C_2^N(S,t)-C_2^i(S,t) & C_3^N(S,t)-C_3^i(S,t) & \dots & C_N^N(S,t)-C_N^i(S,t)\end{bmatrix}.$$

It is important to note that this matrix does not include the case where the volatility does not switch regimes. This means that the row where the entries are as follows $C_n^i(S,t)-C_n^i(S,t)$ for any $i,n=1,\dots,N$ is removed from the matrix.

Given that we occupy a certain volatility regime i at time t, one of the rows in matrix A defined above will only consist of zeros. In order to determine our hedge ratios and our pricing equations, conditional on volatility state i, we remove this row from the matrix in order to define our matrix A and find what conditions are necessary such that $\det(A)=0$.

Following methods shown by Wilmott [49] for multi-factor interest rate models, we know that the only way $\det(A)=0$ can hold is if the first row of the matrix is a linear combination of the other $N-1$ rows in the matrix. This implies that:

$$\mathcal{L}_{BS}(C^i(S,t)) = \sum_{\substack{j=1 \\ j\neq i}}^{N} f(S,t,\sigma_i,\sigma_j)\Big[C^j(S,t) - C^i(S,t)\Big], \tag{2.25}$$

holds for all options in the portfolio. Now reduce the notation for $f_{ij}(S,t) \equiv f(S,t,\sigma_i,\sigma_j)$.

Following previous stochastic volatility techniques [27], we allow this function to be in terms of the intensity of the Poisson process, $\lambda_{ij}(S,t)$, (i.e. the drift of our volatility process) and the state-dependent market price of volatility risk, $m(S,t,\sigma_i,\sigma_j)$. Under our framework, the market price of volatility risk (MPVR) is the market's view of the reward that should be attached to the risk one takes on by taking a short or long position in a particular hedging instrument, in our case a European call option. The MPVR for our problem is state-dependent, as one does not expect to take on the same amount of risk in one volatility state with a fixed risk level compared to another state with a risk level of differing magnitude. Let $m_{ij}(S,t) \equiv m(S,t,\sigma_i,\sigma_j)$ to reduce the notation.

$$f_{ij}(S,t) = -\Big(\lambda_{ij}(S,t) - m_{ij}(S,t)\Big). \tag{2.26}$$

Thus,

$$\mathcal{L}_{BS}(C^i(S,t)) = \sum_{\substack{j=1 \\ j\neq i}}^{N} f_{ij}(S,t)\Big[C^j(S,t) - C^i(S,t)\Big], \tag{2.27}$$

$$\begin{aligned} &\frac{\partial C^i}{\partial t}(S,t) + \frac{1}{2}\sigma_i^2 S^2 \frac{\partial^2 C^i}{\partial S^2}(S,t) + rS\frac{\partial C^i}{\partial S}(S,t) - rC^i(S,t) \\ &\qquad = \sum_{\substack{j=1 \\ j\neq i}}^{N} f_{ij}(S,t)\Big[C^j(S,t) - C^i(S,t)\Big], \end{aligned} \tag{2.28}$$

$$\begin{aligned} \Rightarrow &\frac{\partial C^i}{\partial t}(S,t) + \frac{1}{2}\sigma_i^2 S^2 \frac{\partial^2 C^i}{\partial S^2}(S,t) + rS\frac{\partial C^i}{\partial S} - rC^i(S,t) \\ &\qquad - \sum_{\substack{j=1 \\ j\neq i}}^{N} f_{ij}(S,t)\Big[C^j(S,t) - C^i(S,t)\Big] = 0. \end{aligned} \tag{2.29}$$

Our regime-switching system of option pricing partial differential equations (PDEs) are:

$$\begin{aligned} &\frac{\partial C^i}{\partial t}(S,t) + \frac{1}{2}\sigma_i^2 S^2 \frac{\partial^2 C^i}{\partial S^2}(S,t) + rS\frac{\partial C^i}{\partial S}(S,t) - rC^i(S,t) \\ &\qquad - \sum_{\substack{j=1 \\ j\neq i}}^{N} f_{ij}(S,t)\Big[C^j(S,t) - C^i(S,t)\Big] = 0, \end{aligned} \tag{2.30}$$

subject to:

$$C^i(S,T) = C^j(S,T) = (S(T) - K)^+, \tag{2.31}$$

$$C^i(0,t) = C^j(0,t) = 0, \tag{2.32}$$

$$\lim_{S\to\infty} \frac{\partial C^i}{\partial S}(S,t) = \lim_{S\to\infty} \frac{\partial C^j}{\partial S}(S,t) = 1, \tag{2.33}$$

where:

$$f_{ij}(S,t) = -\Big(\lambda_{ij}(S,t) - m_{ij}(S,t)\Big), \tag{2.34}$$

for all $i = 1, \dots, N$ where $i \neq j$.

One special, if not particularly realistic, market contains investors who are indifferent to the risk inherent in the fluctuations between volatility states. Considering investors of this type allows us to neglect the risk premium in our pricing equation by assuming $m_{ij}(S,t) = 0$ for all $i = 1, \dots, N$ where $i \neq j$. Such investors are not necessarily indifferent to the risk of stock price fluctuations, however it is rather that the Delta hedging argument removes this type of risk from their portfolios. Thus our coupled system of PDEs reduces to:

$$\frac{\partial C^i}{\partial t}(S,t) + \frac{1}{2}\sigma_i^2 S^2 \frac{\partial^2 C^i}{\partial S^2}(S,t) + rS\frac{\partial C^i}{\partial S}(S,t) - rC^i(S,t) + \sum_{\substack{j=1\\ j\neq i}}^{N} \lambda_{ij}(S,t)\Big[C^j(S,t) - C^i(S,t)\Big] = 0. \tag{2.35}$$

The above result is consistent with Boyle and Draviam's [9] result, which was derived using a Taylor series expansion of a European call option under the risk-neutral measure. If there is no chance of switching from the initial volatility state i (i.e. $\lambda_{ij}(S,t) = 0$ for all $i \neq j$), this result reduces to the standard Black-Scholes options pricing PDE [6].

$$\frac{\partial C^i}{\partial t}(S,t) + \frac{1}{2}\sigma_i^2 S^2 \frac{\partial^2 C^i}{\partial S^2}(S,t) + rS\frac{\partial C^i}{\partial S}(S,t) - rC^i(S,t) = 0. \tag{2.36}$$

Although we have derived pricing equations for options under our regime-switching framework, the hedge ratios for all $N-1$ hedging options used in our portfolio still need to be determined. To determine their values, we will solve $\det(A) = 0$ by using co-factor expansion along the first row of the matrix A.

$$\det(A) = \sum_{n=1}^{N} (-1)^{1+n} a_{1n} M_{1n} = 0, \tag{2.37}$$

where M_{1n} is the minor of the matrix A and a_{1n} is the n^{th} entry along the first row of the matrix.

$$\sum_{n=1}^{N} (-1)^{1+n} a_{1n} M_{1n} = 0. \tag{2.38}$$

Since, $a_{1n} = \mathcal{L}_{BS}(C_n^i(S,t))$ for all n,

$$\sum_{n=1}^{N} (-1)^{1+n} \mathcal{L}_{BS}(C_n^i(S,t)) M_{1n} = 0, \tag{2.39}$$

$$\Rightarrow \mathcal{L}_{BS}(C_1^i(S,t))M_{11} + \sum_{n=2}^{N}(-1)^{1+n}\mathcal{L}_{BS}(C_n^i(S,t))M_{1n} = 0. \tag{2.40}$$

Making use of equation (2.24),

$$M_{11}\sum_{n=2}^{N}\Delta_N^i\mathcal{L}_{BS}(C_n^i(S,t)) + \sum_{n=2}^{N}(-1)^{1+n}\mathcal{L}_{BS}(C_n^i(S,t))M_{1n} = 0, \tag{2.41}$$

$$\sum_{n=2}^{N}\mathcal{L}_{BS}(C_n^i(S,t))\Big(\Delta_n^i M_{11} + (-1)^{1+n}M_{1n}\Big) = 0, \tag{2.42}$$

$$\sum_{n=2}^{N}\mathcal{L}_{BS}(C_n^i(S,t))\Big(\Delta_n^i M_{11} - (-1)^{n}M_{1n}\Big) = 0. \tag{2.43}$$

Since $C_n^i(S,t)$ is a regime-switching option with non-constant volatility it follows that $\mathcal{L}_{BS}(C_n^i(S,t)) \neq 0$. In order for equation (2.43) to hold, we must have:

$$\Delta_n^i = \frac{(-1)^n M_{1n}}{M_{11}}, \tag{2.44}$$

for all $n = 2, \dots, N$.

Although we chose to set up and hedge our portfolio for an investor taking a short position in a European call option, it is important to note that the same coupled pricing PDE can be derived from other option positions. For our purposes, these include any long position in a call option or short/long position in a put option. This PDE is not limited to European options as well. As long as the option is exposed to the risk of the same underlying asset and regime-switching volatility, the same pricing equations will be derived. It is the terminal condition (i.e. the payoff of the option) and the boundary conditions applying to the pricing equation which distinguish option type. The hedge ratios will take on the same form, however whether or not we choose to short or long our hedging instruments will change depending on our initial option position.

2.4 Two-State Case

The results from the N-state case can be specialized for a realistic two-state regime-switching volatility framework. It will be assumed that the volatility can switch between a high volatility regime and a low volatility regime with respective volatility levels σ_H and σ_L such that $\sigma_H \geq \sigma_L$.

Specializing equations (2.2) and (2.3) for two states, our regime-switching framework under the real world measure $\mathbb{P}$ is:

$$dS(t) = \mu S(t)dt + \sigma(t)S(t)dW(t), \tag{2.45}$$

$$d\sigma(t) = (\sigma_H - \sigma(t))dq_{LH}(t) + (\sigma_L - \sigma(t))dq_{HL}(t), \tag{2.46}$$

where:

$$dq_{ij}(t) = \begin{cases} 1 \text{ with probability } \lambda_{ij}(S,t)dt \\ 0 \text{ with probability } 1 - \lambda_{ij}(S,t)dt \end{cases} \tag{2.47}$$

for all $i \in \{H, L\}$ where $i \neq j$.

For the two regime case, our coupled system of pricing partial differential equations is:

$$\frac{\partial C^i}{\partial t}(S,t) + \frac{1}{2}\sigma_i^2 S^2 \frac{\partial^2 C^i}{\partial S^2}(S,t) + rS\frac{\partial C^i}{\partial S}(S,t) - rC^i(S,t) - f_{ij}(S,t)\Big[C^j(S,t) - C^i(S,t)\Big] = 0, \tag{2.48}$$

subject to:

$$C^i(S,T) = C^j(S,T) = (S(T) - K)^+, \tag{2.49}$$

$$C^i(0,t) = C^j(0,t) = 0, \tag{2.50}$$

$$\lim_{S\to\infty} \frac{\partial C^i}{\partial S}(S,t) = \lim_{S\to\infty} \frac{\partial C^j}{\partial S}(S,t) = 1, \tag{2.51}$$

where:

$$f_{ij}(S,t) = -\Big(\lambda_{ij}(S,t) - m_{ij}(S,t)\Big), \tag{2.52}$$

for all $i \in \{H, L\}$ where $i \neq j$.

Our hedge ratios used to hedge against the risks of movements in the underlying asset and the switching between volatility regimes are given below.

$$\Delta_1^i = \frac{\partial C_1^i}{\partial S}(S,t) - \left(\frac{C_1^j(S,t) - C_1^i(S,t)}{C_2^j(S,t) - C_2^i(S,t)}\right)\frac{\partial C_2^i}{\partial S}(S,t), \tag{2.53}$$

$$\Delta_2^i = \frac{C_1^j(S,t) - C_1^i(S,t)}{C_2^j(S,t) - C_2^i(S,t)}. \tag{2.54}$$

It should be noted that since we now only have the risk of switching to the opposing volatility regime, we only need one hedging option whose position is given by (2.54).

The prices that result from solving equation (2.48) are those priced under the risk neutral measure $\mathbb{Q}$. The dynamics of both our stock price path and volatility under this risk neutral measure are given below.

$$dS(t) = rS(t)dt + \sigma(t)S(t)d\tilde{W}(t), \tag{2.55}$$

$$d\sigma(t) = (\sigma_H - \sigma(t))d\tilde{q}_{LH}(t) + (\sigma_L - \sigma(t))d\tilde{q}_{HL}(t), \tag{2.56}$$

where:

$$d\tilde{q}_{ij}(t) = \begin{cases} 1 \text{ with probability } (\lambda_{ij}(S,t) - m_{ij}(S,t))dt \\ 0 \text{ with probability } 1 - (\lambda_{ij}(S,t) - m_{ij}(S,t))dt \end{cases} \tag{2.57}$$

and

$$dW(t) = d\tilde{W}(t) - \left(\frac{\mu - r}{\sigma}\right)dt \tag{2.58}$$

for all $i \in \{H, L\}$ where $i \neq j$. The market price of stock risk (i.e. $\frac{\mu - r}{\sigma}$) is taken into account as we change to the risk neutral measure.

Unless otherwise noted, for the remainder of the thesis both the Poisson intensities $\lambda_{ij}(S, t)$ and the state-dependent market price of volatility risk $m_{ij}(S, t)$ are assumed to take on constant values λ_{ij} and m_{ij} respectively.

Now that we have introduced our regime-switching framework, which provides the backbone for the remainder of this thesis, we must investigate numerical solution techniques for partial differential equations which can easily be extended to our coupled pricing problem.

Chapter 3

Numerical Solution

In Chapter 2 we introduced a regime-switching framework for volatility. We considered an investor with a short position in a European call option and derived partial differential equations to price options on a regime-switching underlying asset. Although we previously introduced both the generalized N-state case and the two-state case, for the remainder of this thesis we will focus primarily on the two-state case where the volatility can switch randomly between a high and a low volatility state. This case provides a nice balance between intuition and realism.

Our pricing problem has no closed-form solution and as such requires a solution via numerical methods. We will employ a finite difference method where derivatives in the equation in question are replaced by discrete approximations [38]. These discrete approximations are found by taking a Taylor series expansion of the function.

In general for initial value problems, when the equations are approximated by finite difference representations of the embedded derivatives, we must solve for the solution on a grid. Given some initial condition, we can work forward in time to determine the full solution set over the given time interval. All options pricing problems are considered terminal value problems as the known option payoff functions give rise to terminal data. Given that most numerical methods are generally applied to initial value problems, we will apply a time reversal to our problem to remove tedious discussion of the above mentioned point. Introducing a new variable $\tau = T - t$ transforms our terminal value pricing problem to an initial value problem, allowing us to apply the methods discussed in this chapter directly.

We choose to solve our coupled pricing problem using the Crank-Nicolson numerical scheme. This method will be discussed in detail in the next section. In this chapter, we will first show how to apply the Crank-Nicolson method to the classical one-dimensional heat equation. Our results will then be generalized to the Black-Scholes pricing equation, a well-known financial mathematics partial differential equation. Then we will apply our numerical method to a coupled system of one-dimensional heat equations, which produces a slightly more involved numerical problem than the uncoupled case. These results will then be generalized to our system of regime-switching pricing partial differential equations for the two-state case.

3.1 Overview of Crank-Nicolson Numerical Scheme

To numerically solve our pricing partial differential equations, we choose to use Crank-Nicolson over other numerical methods, such as an explicit finite difference scheme, due to its mathematical and computational benefits. We chose to implement Crank-Nicolson as it is unconditionally stable, has second order convergence, and provides increased accuracy in the solution [38]. These associated benefits have also been proven to hold when the numerical scheme is applied to coupled partial differential equations [47]. These results hold for all choices of space and time increment sizes as well as all constant and non-constant coefficients appearing within the equations.

In general, the Crank-Nicolson numerical scheme takes the average of the implicit and explicit finite difference methods applied to the space derivatives in the equation. The time derivative uses a backward difference equation. Consider a general problem for function $U(x,t)$,

$$\frac{\partial U}{\partial t}(x,t) = \mathcal{F}\left(U(x,t), x, t, \frac{\partial U}{\partial x}(x,t), \frac{\partial^2 U}{\partial x^2}(x,t)\right). \tag{3.1}$$

For all sections discussing the implementation of the Crank-Nicolson method, m will denote the space index while l denotes the time index. As a result, dx represents the space increment and dt represents the time increment. The above PDE is discretized where we denote $U(x,t) = U(mdx, ldt) \equiv U_m^l$ and $\mathcal{F}\left(U(x,t), x, t, \frac{\partial U}{\partial x}(x,t), \frac{\partial^2 U}{\partial x^2}(x,t)\right) \equiv \mathcal{F}_m^l$. The Crank-Nicolson numerical scheme implies we rewrite our discretized PDE as follows.

$$\frac{U_m^{l+1} - U_m^l}{dt} = \frac{1}{2}\left[\mathcal{F}_m^l + \mathcal{F}_m^{l+1}\right]. \tag{3.2}$$

In general, we use central differences for the partial derivatives in space:

$$\frac{\partial U}{\partial x}(x,t) = \frac{U_{m+1}^l - U_{m-1}^l}{2dx}, \tag{3.3}$$

$$\frac{\partial^2 U}{\partial x^2}(x,t) = \frac{U_{m+1}^l - 2U_m^l + U_{m-1}^l}{dx^2}. \tag{3.4}$$

After implementing the scheme, we end up with a matrix problem:

$$B^{l+1}\vec{U}^{l+1} = A^l\vec{U}^l, \tag{3.5}$$

where A and B are square tridiagonal matrices of size $M-1$. The above system is solved for every time step moving forward in time given an initial condition $\vec{U}^1$. Since the associated problem will have defined boundary conditions, for the solution vector $\vec{U}^{l+1}$ of size $M+1$, we only need to solve for the middle $M-1$ entries (i.e. U_1^{l+1} and U_{M+1}^{l+1} are given by the boundary conditions) at every time iteration. If the coefficients in the original PDE are time dependent, then both of the tridiagonal matrices must be redefined at every time point before solving for the solution vector. Given that we have a time vector of size $\tilde{L}+1$, we iterate through time $\tilde{L}$ times until we have a solution for the entire time interval defined in the original problem.

3.2 Application to the One-Dimensional Heat Equation

First, we apply the Crank-Nicolson numerical scheme to a classical applied mathematics partial differential equation. This equation is called the one-dimensional heat equation, otherwise known as the diffusion equation.

$$\frac{\partial U}{\partial t}(x,t) = D(x,t)\frac{\partial^2 U}{\partial x^2}(x,t). \tag{3.6}$$

Initial and boundary conditions are arbitrary, but we assume they are defined. We assume that the form of the boundary conditions are either Dirichlet or Neumann and homogeneous or non-homogeneous, or any mixture thereof.

Applying central differences to the space partial derivatives and backwards differences to the time partial derivative yields:

$$\frac{U_m^{l+1} - U_m^l}{dt} = \frac{1}{2}\left\{D_m^l\left(\frac{U_{m+1}^l - 2U_m^l + U_{m-1}^l}{dx^2}\right) + D_m^{l+1}\left(\frac{U_{m+1}^{l+1} - U_m^{l+1} + U_{m-1}^{l+1}}{dx^2}\right)\right\}, \tag{3.7}$$

$$U_m^{l+1} - U_m^l = \frac{1}{2}\frac{dt}{dx^2}D_m^l\left(U_{m+1}^l - 2U_m^l + U_{m-1}^l\right) + \frac{1}{2}\frac{dt}{dx^2}D_m^{l+1}\left(U_{m+1}^{l+1} - 2U_m^{l+1} + U_{m-1}^{l+1}\right). \tag{3.8}$$

Define:

$$a_m^l = \frac{1}{2}\frac{dt}{dx^2}D_m^l. \tag{3.9}$$

Then,

$$-a_m^{l+1}U_{m-1}^{l+1} + \left(1 + 2a_m^{l+1}\right)U_m^{l+1} - a_m^{l+1}U_{m+1}^{l+1} = a_m^l U_{m-1}^l + \left(1 - 2a_m^l\right)U_m^l + a_m^l U_{m+1}^l. \tag{3.10}$$

This results in a linear system that must be solved at every time point l:

$$B^{l+1}\vec{U}^{l+1} = A^l\vec{U}^l, \tag{3.11}$$

where:

$$B^{l+1} = \begin{bmatrix} 1 + 2a_2^{l+1} & -a_3^{l+1} & 0 & \dots & 0 \\ -a_2^{l+1} & 1 + 2a_3^{l+1} & -a_4^{l+1} & \ddots & \vdots \\ 0 & \ddots & \ddots & \ddots & 0 \\ \vdots & \ddots & \ddots & \ddots & -a_M^{l+1} \\ 0 & \dots & 0 & -a_{M-1}^{l+1} & 1 + 2a_M^{l+1} \end{bmatrix},$$

and

$$A^l = \begin{bmatrix} 1 - 2a_2^l & a_3^l & 0 & \dots & 0 \\ a_2^l & 1 - 2a_3^l & a_4^l & \ddots & \vdots \\ 0 & \ddots & \ddots & \ddots & 0 \\ \vdots & \ddots & \ddots & \ddots & a_M^l \\ 0 & \dots & 0 & a_{M-1}^l & 1 - 2a_M^l \end{bmatrix}.$$

Our tridiagonal matrices of size $M - 1$ defined above are redefined at every time iteration. We solve for the solution vector, $\vec{U}^{l+1}$, using the built-in left matrix division function in Matlab, iterating through for all $l = 2 \ldots \tilde{L} + 1$.

To analyse the effectiveness of this numerical method, we give a comparison of the numerical solution using Crank-Nicolson to the closed-form solution of the following problem with homogeneous Dirichlet boundary conditions.

$$\frac{\partial U}{\partial t}(x,t) = D\frac{\partial^2 U}{\partial x^2}(x,t), \tag{3.12}$$

subject to:

$$U(0,t) = U(\tilde{M},t) = 0, \tag{3.13}$$

$$U(x,0) = \sin\left(\frac{\pi x}{\tilde{M}}\right). \tag{3.14}$$

The above problem has the solution:

$$U(x,t) = e^{-\frac{D\pi^2 t}{\tilde{M}^2}} \sin\left(\frac{\pi x}{\tilde{M}}\right). \tag{3.15}$$

Diffusion Coefficient	D	$\frac{1}{2}$
Length of Space Interval	$\tilde{M}$	10
Length of Time Interval	T	1
Number of Time Increments	$\tilde{L}$	100

Table 3.1: Parameters used in the implementation of the Crank-Nicolson numerical scheme for the one-dimensional heat equation.

In the left hand plot given in Figure 3.1, we can observe that it is difficult to observe the discrepancies between the true solution of the PDE and the numerical solution provided by the Crank-Nicolson method. The plot of the absolute error between the two solutions shows that, although there is some difference between the solutions, this difference has a magnitude of 10^{-6} which is negligible given that the actual solution is of magnitude 10^{-1}. This motivates us to apply the Crank-Nicolson numerical scheme to the Black-Scholes pricing problem which has a well-known closed-form solution.

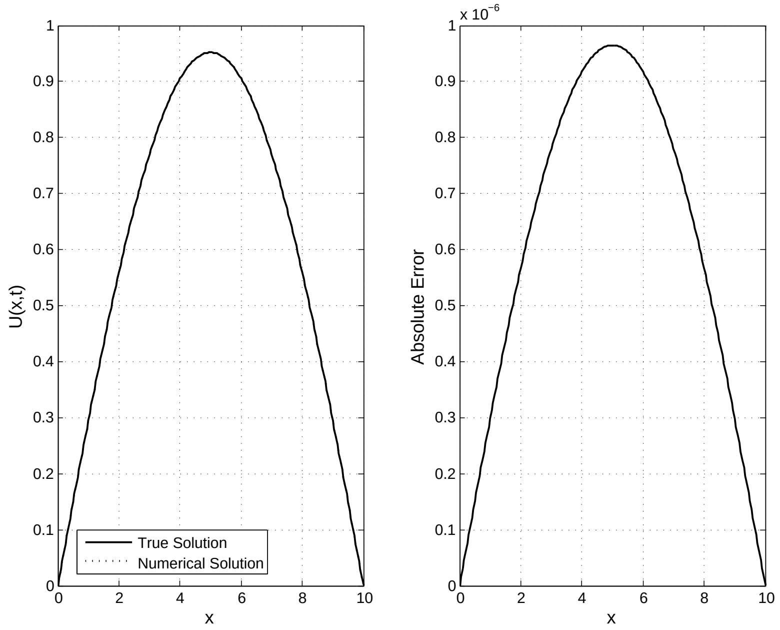

Figure 3.1: Comparison of the numerical and true solution for one-dimensional heat equation at time $t = 1$. All parameters as given in Table 3.1.

3.3 Application to the Black-Scholes PDE

Recall the Black-Scholes pricing partial differential equation for a general option with price $U(S, \tau)$, written on an underlying asset following geometric Brownian motion with constant drift and volatility. Our space variable is now the stock price variable S. Recall that we reversed time using $\tau = T - t$, thus our pricing PDE is:

$$\frac{\partial U}{\partial \tau}(S, \tau) = \frac{1}{2}\sigma^2 S^2 \frac{\partial^2 U}{\partial S^2}(S, \tau) + rS\frac{\partial U}{\partial S}(S, \tau) - rU(S, \tau). \tag{3.16}$$

The initial and boundary conditions depend on the type of option contract. We will assume they are defined for the implementation of numerical methods.

We first need to replace our partial derivatives embedded in our pricing PDE with finite difference approximations. We assume that our time increment is given by $d\tau = dt$. Then using the fact that $S = mdS$ where dS is our stock price increment, our pricing PDE becomes:

$$\begin{aligned}\frac{U_m^{l+1} - U_m^l}{dt} = \frac{1}{2}\Bigg\{&\left[\frac{1}{2}\sigma^2(mdS)^2\left(\frac{U_{m+1}^l - 2U_m^l + U_{m-1}^l}{dS^2}\right) + rmdS\left(\frac{U_{m+1}^l - U_{m-1}^l}{2dS}\right) - rU_m^l\right] \\ &+ \left[\frac{1}{2}\sigma^2(mdS)^2\left(\frac{U_{m+1}^{l+1} - 2U_m^{l+1} + U_{m-1}^{l+1}}{dS^2}\right) + rmdS\left(\frac{U_{m+1}^{l+1} - U_{m-1}^{l+1}}{2dS}\right) - rU_m^{l+1}\right]\Bigg\},\end{aligned} \tag{3.17}$$

$$\begin{aligned} U_m^{l+1} - U_m^l = \frac{dt}{2}\Bigg[& \frac{1}{2}\sigma^2 m^2\Big(U_{m+1}^l - 2U_m^l + U_{m-1}^l\Big) + \frac{rm}{2}\Big(U_{m+1}^l - U_{m-1}^l\Big) - rU_m^l \\ & + \frac{1}{2}\sigma^2 m^2\Big(U_{m+1}^{l+1} - 2U_m^{l+1} + U_{m-1}^{l+1}\Big) + \frac{rm}{2}\Big(U_{m+1}^{l+1} - U_{m-1}^{l+1}\Big) - rU_m^{l+1}\Bigg]. \end{aligned} \tag{3.18}$$

Rearranging our finite difference approximations with all $l+1$ terms on the left hand side and all the l terms on the right hand side yields:

$$\begin{aligned} & -\frac{1}{4}mdt\Big(\sigma^2 m - r\Big)U_{m-1}^{l+1} + \left[1 + \frac{1}{2}dt\Big(\sigma^2 m^2 + r\Big)\right]U_m^{l+1} - \frac{1}{4}mdt\Big(\sigma^2 m + r\Big)U_{m+1}^{l+1} \\ & \quad = \frac{1}{4}mdt\Big(\sigma^2 m - r\Big)U_{m-1}^{l} + \left[1 - \frac{1}{2}dt\Big(\sigma^2 m^2 + r\Big)\right]U_m^{l} + \frac{1}{4}mdt\Big(\sigma^2 m + r\Big)U_{m+1}^{l}. \end{aligned} \tag{3.19}$$

Noticing our coefficients in our discretized PDE only vary with stock price, define:

$$a_m = \frac{1}{4}mdt\Big(\sigma^2 m - r\Big), \tag{3.20}$$

$$b_m = -\frac{1}{2}dt\Big(\sigma^2 m^2 + r\Big), \tag{3.21}$$

$$c_m = \frac{1}{4}mdt\Big(\sigma^2 m + r\Big). \tag{3.22}$$

Then,

$$-a_m U_{m-1}^{l+1} + \Big(1 - b_m\Big)U_m^{l+1} - c_m U_{m-1}^{l+1} = a_m U_{m-1}^l + \Big(1 + b_m\Big)U_m^l + c_m U_{m-1}^l. \tag{3.23}$$

This results in a linear system that needs to be solved for $\vec{U}^{l+1}$ at every time point $l+1$.

$$B\vec{U}^{l+1} = A\vec{U}^l, \tag{3.24}$$

where:

$$B = \begin{bmatrix} 1-b_2 & -c_3 & 0 & \dots & 0 \\ -a_2 & 1-b_3 & -c_4 & \ddots & \vdots \\ 0 & \ddots & \ddots & \ddots & 0 \\ \vdots & \ddots & \ddots & \ddots & -c_M \\ 0 & \dots & 0 & -a_{M-1} & 1-b_M \end{bmatrix},$$

and

$$A = \begin{bmatrix} 1+b_2 & c_3 & 0 & \dots & 0 \\ a_2 & 1+b_3 & c_4 & \ddots & \vdots \\ 0 & \ddots & \ddots & \ddots & 0 \\ \vdots & \ddots & \ddots & \ddots & c_M \\ 0 & \dots & 0 & a_{M-1} & 1+b_M \end{bmatrix}.$$

The matrices A and B are square and of size $M-1$. Notice that A and B do not vary with time, therefore we do not need to redefine their entries at every time iteration. Since we have boundary conditions that account for U_1^{l+1} and U_{M+1}^{l+1} for every time step $l+1$, we are once again only solving for the middle entries of the solution vector $\vec{U}^{l+1}$.

An illustrated example of implementing the Crank-Nicolson numerical scheme to solve for the call option value for a particular set of parameters given in Table 3.2 is shown in Figure 3.2.

Expected Return	r	0%
Volatility	σ	30%
Strike Price	K	\$100
Maturity Date	T	1 year
Number of Time Increments	$\tilde{L}$	252

Table 3.2: Parameters used in the implementation of the Crank-Nicolson numerical scheme for the Black-Scholes PDE.

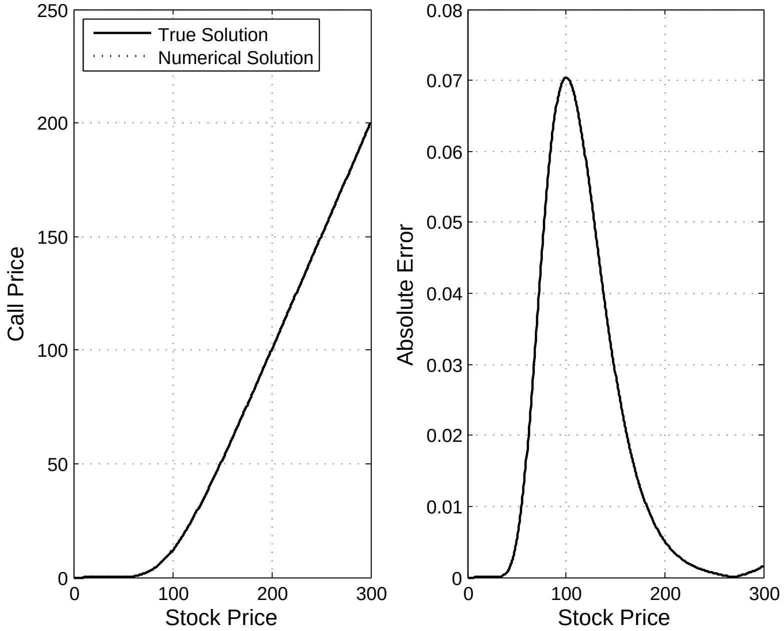

Figure 3.2: Comparison of the numerical and true solution for the Black-Scholes PDE at time $t = 0$. All parameters as given in Table 3.2.

The numerical solution shown in Figure 3.2 behaves as expected, displaying the same properties and curvature associated with the Black-Scholes call price. Once again the discrepancies are unobservable in the solution vector plot so the absolute error is considered. Since the call price solution has a magnitude of either 10^1 or 10^2 while the absolute error has a magnitude of

10^{-2}, the error is considered minimal. Thus solving the Black-Scholes PDE using numerical methods provides an accurate approximation to our true option price.

Since our regime-switching pricing problem is a coupled system of PDEs, it is advisable to first test the performance of the Crank-Nicolson numerical scheme on a system of simpler PDEs, such as coupled one-dimensional heat equations.

3.4 Application to Coupled One-Dimensional Heat Equations

In general, numerical schemes applied to coupled systems of equations are slightly more involved than those applied to uncoupled equations. This is due to the fact that there are now two solution grids which must be solved simultaneously. If we visualize this scenario, the result is two solution grids which must "talk" and provide information to one another at every time iteration in order for both equations to be solved numerically. Therefore it makes sense to consider a simple coupled system of equations before generalizing the results to our system of coupled pricing partial differential equations.

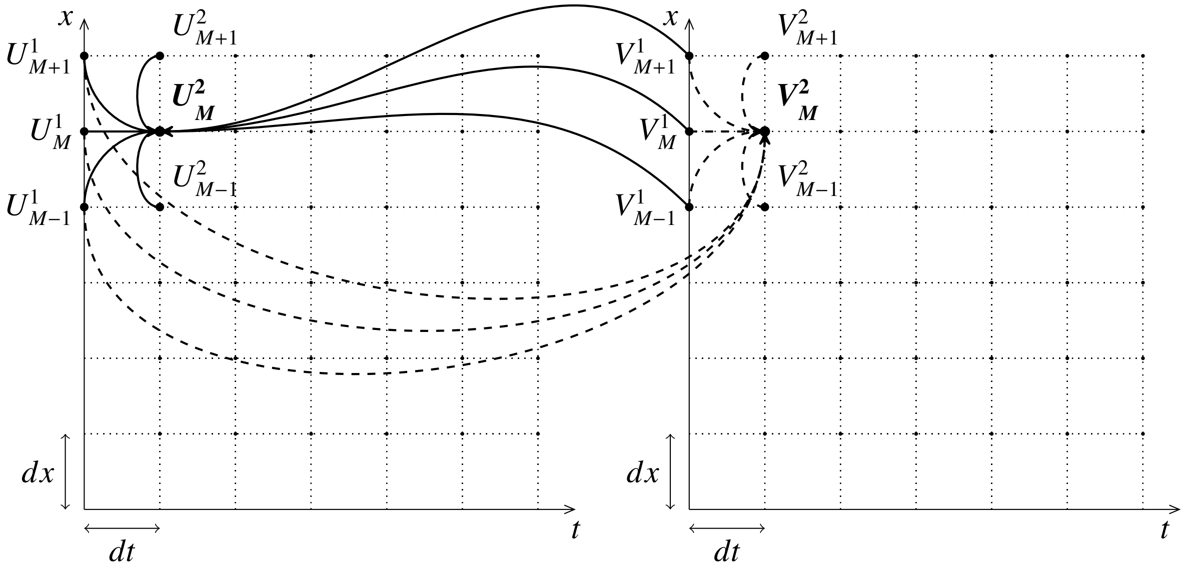

Figure 3.3: Visualization of coupled numerical grids interacting simultaneously to solve coupled PDEs for a single set of points (U^2_M, V^2_M).

Figure 3.3 allows us to visualize how the solution vectors for each grid depend directly on points from both numerical grids. This dependency adds a layer of complexity in the numerical methods used to solve the coupled systems. The dashed lines represent the points used to solve for the point V^2_M while the solid lines represent the points used to solve for the point U^2_M. When the Crank-Nicolson method is being fully implemented, the solution vectors for a specific time point $\vec{U}^{l+1}$ and $\vec{V}^{l+1}$ are solved simultaneously.

First we will consider a general coupled system of one-dimensional heat equations.

$$\frac{\partial U}{\partial t}(x,t) = P(x,t)\frac{\partial^2 U}{\partial x^2}(x,t) + Q(x,t)V(x,t), \tag{3.25}$$

$$\frac{\partial V}{\partial t}(x,t) = R(x,t)\frac{\partial^2 V}{\partial x^2}(x,t) + W(x,t)U(x,t). \tag{3.26}$$

The coefficients $P(x,t), Q(x,t), R(x,t)$ and $W(x,t)$ are assumed to be deterministic. The initial conditions and boundary conditions for both functions in this system are assumed to be defined.

For the first PDE, replacing the partial derivatives in the coupled system with finite difference approximations yields:

$$\begin{aligned}\frac{U_m^{l+1} - U_m^l}{dt} &= \frac{1}{2}\left\{\left[P_m^l\left(\frac{U_{m+1}^l - 2U_m^l + U_{m-1}^l}{dx^2}\right) + Q_m^l V_m^l\right]\right.\\ &\qquad \left. + \left[P_m^{l+1}\left(\frac{U_{m+1}^{l+1} - 2U_m^l + U_{m-1}^l}{dx^2}\right) + Q_m^{l+1} V_m^{l+1}\right]\right\},\end{aligned} \tag{3.27}$$

$$\begin{aligned}U_m^{l+1} - U_m^l &= \frac{1}{2}\frac{dt}{dx^2}P_m^l\left(U_{m+1}^l - 2U_m^l + U_{m-1}^l\right) + \frac{1}{2}dtQ_m^l V_m^l\\ &\qquad + \frac{1}{2}\frac{dt}{dx^2}P_m^{l+1}\left(U_{m+1}^{l+1} - 2U_m^{l+1} + U_{m-1}^{l+1}\right) + \frac{1}{2}dtQ_m^{l+1} V_m^{l+1}.\end{aligned} \tag{3.28}$$

Define:

$$a_m^l = \frac{1}{2}\frac{dt}{dx^2}P_m^l, \tag{3.29}$$

$$b_m^l = \frac{1}{2}dtQ_m^l. \tag{3.30}$$

Then,

$$\begin{aligned}&- a_m^{l+1}U_{m-1}^{l+1} + \left(1 + 2a_m^{l+1}\right)U_m^{l+1} - a_m^{l+1}U_{m+1}^{l+1} - b_m^{l+1}V_m^{l+1}\\ &\qquad = a_m^l U_{m-1}^l + \left(1 - 2a_m^l\right)U_m^l + a_m^l U_{m+1}^l + b_m^l V_m^l.\end{aligned} \tag{3.31}$$

Rewritten in matrix form:

$$B^{l+1}\vec{U}^{l+1} + C^{l+1}\vec{V}^{l+1} = A_m\vec{U}^l - C^l\vec{V}^l, \tag{3.32}$$

where:

$$B^{l+1} = \begin{bmatrix} 1 + 2a_2^{l+1} & -a_3^{l+1} & 0 & \dots & 0 \\ -a_2^{l+1} & 1 + 2a_3^{l+1} & -a_4^{l+1} & \ddots & \vdots \\ 0 & \ddots & \ddots & \ddots & 0 \\ \vdots & \ddots & \ddots & \ddots & -a_M^{l+1} \\ 0 & \dots & 0 & -a_{M-1}^{l+1} & 1 + 2a_M^{l+1} \end{bmatrix},$$

$$A^{l+1} = \begin{bmatrix} 1-2a_2^l & a_3^l & 0 & \dots & 0 \\ a_2^l & 1-2a_3^l & a_4^l & \ddots & \vdots \\ 0 & \ddots & \ddots & \ddots & 0 \\ \vdots & \ddots & \ddots & \ddots & a_M^l \\ 0 & \dots & 0 & a_{M-1}^l & 1-2a_M^l \end{bmatrix},$$

and

$$C^l = \begin{bmatrix} -b_2^l & 0 & \dots & 0 \\ 0 & -b_3^l & \ddots & \vdots \\ \vdots & \ddots & \ddots & 0 \\ 0 & \dots & 0 & -b_M^l \end{bmatrix}.$$

Similarly for the second PDE in our coupled system:

$$\begin{aligned} \frac{V_m^{l+1} - V_m^l}{dt} &= \frac{1}{2}\Bigg\{\left[R_m^l\left(\frac{V_{m+1}^l - 2V_m^l + V_{m-1}^l}{dx^2}\right) + W_m^l U_m^l\right] \\ &\quad + \left[R_m^{l+1}\left(\frac{V_{m+1}^{l+1} - 2V_m^{l+1} + V_{m-1}^{l+1}}{dx^2}\right) + W_m^{l+1} U_m^{l+1}\right]\Bigg\}, \end{aligned} \tag{3.33}$$

$$\begin{aligned} V_m^{l+1} - V_m^l &= \frac{1}{2}\frac{dt}{dx^2}R_m^l(V_{m+1}^l - 2V_m^l + V_{m-1}^l) + \frac{1}{2}dtW_m^l U_m^l \\ &\quad + \frac{1}{2}\frac{dt}{dx^2}R_m^{l+1}(V_{m+1}^{l+1} - 2V_m^{l+1} + V_{m-1}^{l+1}) + \frac{1}{2}dtW_m^{l+1}U_m^{l+1}. \end{aligned} \tag{3.34}$$

Define:

$$\tilde{a}_m^l = \frac{1}{2}\frac{dt}{dx^2}R_m^l, \tag{3.35}$$

$$\tilde{b}_m^l = \frac{1}{2}dtW_m^l. \tag{3.36}$$

Then,

$$\begin{aligned} &-\tilde{a}_m^{l+1}V_{m-1}^{l+1} + (1 + 2\tilde{a}_m^{l+1})V_m^{l+1} - \tilde{a}_m^{l+1}V_{m+1}^{l+1} - \tilde{b}_m^{l+1}U_m^{l+1} \\ &\quad = \tilde{a}_m^l V_{m-1}^l + (1 - 2\tilde{a}_m^l)V_m^l + \tilde{a}_m^l V_{m+1}^l + \tilde{b}_m^l U_m^l. \end{aligned} \tag{3.37}$$

Our linear system of equations is:

$$\tilde{B}^{l+1}\vec{V}^{l+1} + \tilde{C}^{l+1}\vec{U}^{l+1} = \tilde{A}^l\vec{V}^l - \tilde{C}^l\vec{U}^l, \tag{3.38}$$

where:

$$\tilde{B}^{l+1} = \begin{bmatrix} 1+2\tilde{a}_3^{l+1} & -\tilde{a}_3^{l+1} & 0 & \dots & 0 \\ -\tilde{a}_2^{l+1} & 1+2\tilde{a}_3^{l+1} & -\tilde{a}_4^{l+1} & \ddots & \vdots \\ 0 & \ddots & \ddots & \ddots & 0 \\ \vdots & \ddots & \ddots & \ddots & -\tilde{a}_M^{l+1} \\ 0 & \dots & 0 & -\tilde{a}_{M-1}^{l+1} & 1+2\tilde{a}_M^{l+1} \end{bmatrix},$$

$$\tilde{A}^l = \begin{bmatrix} 1-2\tilde{a}_2^l & \tilde{a}_3^l & 0 & \dots & 0 \\ \tilde{a}_2^l & 1-2\tilde{a}_3^l & \tilde{a}_4^l & \ddots & \vdots \\ 0 & \ddots & \ddots & \ddots & 0 \\ \vdots & \ddots & \ddots & \ddots & \tilde{a}_M^l \\ 0 & \dots & 0 & \tilde{a}_{M-1}^l & 1-2\tilde{a}_M^l \end{bmatrix},$$

and

$$\tilde{C}^l = \begin{bmatrix} -\tilde{b}_2^l & 0 & \dots & 0 \\ 0 & -\tilde{b}_3^l & \ddots & \vdots \\ \vdots & \ddots & \ddots & 0 \\ 0 & \dots & 0 & -\tilde{b}_M^l \end{bmatrix}.$$

Thus together, we have a system of two equations with two unknowns.

$$B^{l+1}\vec{U}^{l+1} + C^{l+1}\vec{V}^{l+1} = A^l\vec{U}^l - C^l\vec{V}^l, \tag{3.39}$$

$$\tilde{B}^{l+1}\vec{V}^{l+1} + \tilde{C}^{l+1}\vec{U}^{l+1} = \tilde{A}^l\vec{V}^l - \tilde{C}^l\vec{U}^l. \tag{3.40}$$

Taking linear combinations of the above equations, we can solve for $\vec{U}^{l+1}$ and $\vec{V}^{l+1}$ for all $l = 2\dots\tilde{L}+1$ since we are solving forward in time. First we will solve for the solution vector $\vec{U}^{l+1}$. Define:

$$D^l = A^l\vec{U}^l - C^l\vec{V}^l, \tag{3.41}$$

$$\tilde{D}^l = \tilde{A}^l\vec{V}^l - \tilde{C}^l\vec{U}_m. \tag{3.42}$$

Then our system becomes:

$$D^l = B^{l+1}\vec{U}^{l+1} + C^{l+1}\vec{V}^{l+1}, \tag{3.43}$$

$$\tilde{D}^l = \tilde{B}^{l+1}\vec{V}^{l+1} + \tilde{C}^{l+1}\vec{U}^{l+1}. \tag{3.44}$$

By multiplying equation (3.43) by $\tilde{B}^{l+1}$ and subtracting equation (3.44) which has been multiplied by C^{l+1}, we get:

$$\tilde{B}^{l+1}D^l - C^{l+1}\tilde{D}^l = \left(\tilde{B}^{l+1}B^{l+1} - C^{l+1}\tilde{C}^{l+1}\right)\vec{U}^{l+1}. \tag{3.45}$$

Defining,

$$F^{l+1} = \tilde{B}^{l+1}D^l - C^{l+1}\tilde{D}^l, \tag{3.46}$$

$$E^{l+1} = \tilde{B}^{l+1}B^{l+1} - C^{l+1}\tilde{C}^{l+1}, \tag{3.47}$$

we have the linear system of equations:

$$F^{l+1} = E^{l+1}\vec{U}^{l+1}. \tag{3.48}$$

The above system can be solved quickly in Matlab using the left division built-in function. We iterate through time, redefining the tridiagonal and diagonal matrices at each time step in order to solve for the full set of solution vectors. A very similar approach is taken to solve for the other solution vector, $\vec{V}^l$, for all $l = 2 \ldots \tilde{L} + 1$:

$$\tilde{F}^{l+1} = \tilde{E}^{l+1}\vec{V}^{l+1}, \tag{3.49}$$

where:

$$\tilde{F}^{l+1} = B^{l+1}\tilde{D}^{l} - \tilde{C}^{l+1}D^{l}, \tag{3.50}$$

$$\tilde{E}^{l+1} = B^{l+1}\tilde{B}^{l+1} - \tilde{C}^{l+1}C^{l+1}. \tag{3.51}$$

To test the accuracy of Crank-Nicolson on coupled PDEs, we will compare our numerical solutions for $U(x,t)$ and $V(x,t)$ to the true solutions for the following system of coupled heat equations.

$$\frac{\partial U}{\partial t}(x,t) = P\frac{\partial^2 U}{\partial x^2}(x,t) + V(x,t), \tag{3.52}$$

$$\frac{\partial V}{\partial t}(x,t) = R\frac{\partial^2 V}{\partial x^2}(x,t), \tag{3.53}$$

subject to:

$$U(0,t) = U(\tilde{M},t) = 0, \tag{3.54}$$

$$V(0,t) = V(\tilde{M},t) = 0, \tag{3.55}$$

$$U(x,0) = V(x,0)\sin\left(\frac{\pi x}{\tilde{M}}\right). \tag{3.56}$$

The above problem has the solution:

$$U(x,t) = \left[e^{-\frac{P\pi^2 t}{\tilde{M}^2}} + \frac{1}{P-R}\left(\frac{L}{\pi}\right)^2\left(e^{-\frac{R\pi^2 t}{\tilde{M}^2}} - e^{-\frac{P\pi^2 t}{\tilde{M}^2}}\right)\right]\sin\left(\frac{\pi x}{\tilde{M}}\right), \tag{3.57}$$

$$V(x,t) = e^{-\frac{R\pi^2 t}{\tilde{M}^2}}\sin\left(\frac{\pi x}{\tilde{M}}\right). \tag{3.58}$$

Diffusion Coefficient for $U(x,t)$	P	$\frac{1}{2}$
Diffusion Coefficient for $V(x,t)$	R	$\frac{1}{4}$
Length of Space Interval	$\tilde{M}$	10
Length of Time Interval	T	1
Number of Time Increments	$\tilde{L}$	100

Table 3.3: Parameters used in the implementation of the Crank-Nicolson numerical scheme for the coupled one-dimensional heat equations.

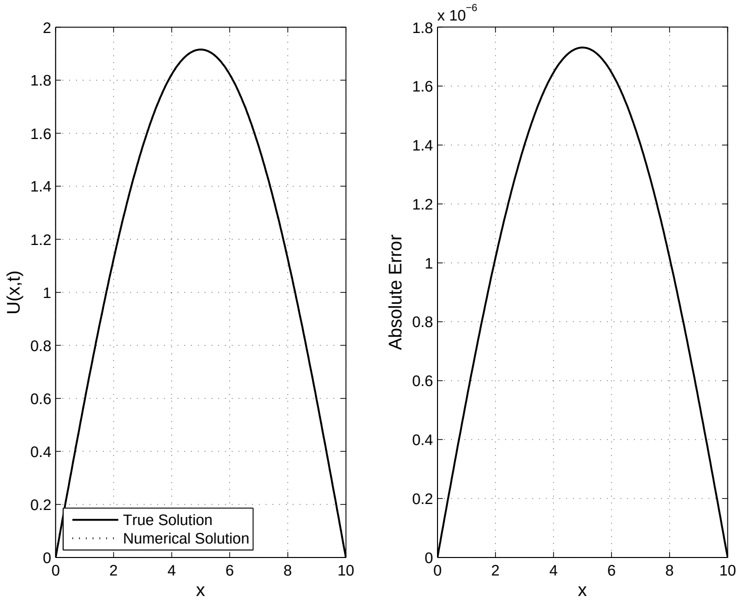

Figure 3.4: Comparison of the numerical and true solution for the coupled one-dimensional heat equation, $U(x, t)$, at time $t = 1$. All parameters as given in Table 3.3.

The results for our coupled system of one-dimensional heat equations mimics the results from our previous analysis of the uncoupled heat equation. In Figures 3.4 and 3.5, it can observed that the difference between the true and numerical solutions are unobservable for both solution vectors. When considering the absolute error associated with our numerical solution, we can see that for $U(x, t)$ this error is of size 10^{-6} while for $V(x, t)$ the error has a magnitude of 10^{-7}. Since the error is so small, it is essentially negligible. This indicates that even for a coupled system of PDEs, the Crank-Nicolson numerical scheme performs well and is able to accurately solve coupled equations.

As a result of this method's exceptional performance on the coupled heat equations, we will apply this method to solve our coupled system of pricing equations for an option written in a regime-switching market.

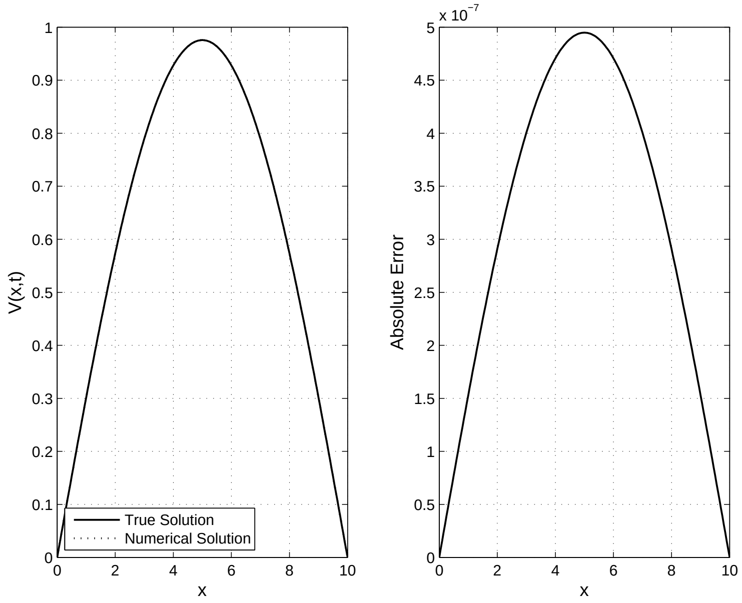

Figure 3.5: Comparison of the numerical and true solution for the coupled one-dimensional heat equation, $V(x,t)$, at time $t = 1$. All parameters as given in Table 3.3.

3.5 Application to Regime-Switching PDEs

Recall the generalized pricing PDE problem for a two-state regime-switching option $U^i(S,t)$, where i is the currently volatility state. With the time reversal $\tau = T - t$, our problem is now:

$$\frac{\partial U^i}{\partial \tau}(S,\tau) = \frac{1}{2}\sigma_i^2 S^2 \frac{\partial^2 U^i}{\partial S^2}(S,\tau) + rS\frac{\partial U^i}{\partial S}(S,\tau) - rU^i(S,\tau) - f_{ij}(S,\tau)\Big[U^j(S,\tau) - U^i(S,\tau)\Big], \quad (3.59)$$

where

$$f_{ij}(S,\tau) = -\Big(\lambda_{ij} - m_{ij}\Big), \quad (3.60)$$

for all $i \in \{H, L\}$ and $i \neq j$.

Like the constant volatility option, we are considering the generalized application of Crank-Nicolson where the initial and boundary conditions depend on the type of option contract.

Applying the Crank-Nicolson numerical scheme to the coupled pricing PDEs is slightly more involved as the value of an option in state i depends also on the value of that same option in state j. Using central differences for partial derivatives with respect to stock price, backward difference for the partial derivative with respect to time, and letting $S = mdS$ yields:

$$\frac{U_m^{i,l+1} - U_m^{i,l}}{dt} = \frac{1}{2}\Bigg\{\Bigg[\frac{1}{2}\sigma_i^2 (mdS)^2 \left(\frac{U_{m+1}^{i,l} - 2U_m^{i,l} + U_{m-1}^{i,l}}{dS^2}\right) + rmdS\left(\frac{U_{m+1}^{i,l} - U_{m-1}^{i,l}}{2dS}\right) - rU_m^{i,l}$$

$$
\begin{aligned}
&- f_{ij,m}^{l}\Big[U_{m}^{j,l} - U_{m}^{i,l}\Big]\Big] + \Big[\frac{1}{2}\sigma_i^2 (mdS)^2\Big(\frac{U_{m+1}^{i,l+1} - 2U_{m}^{i,l+1} + U_{m-1}^{i,l+1}}{dS^2}\Big) \\
&+ rmdS\Big(\frac{U_{m+1}^{i,l+1} - U_{m-1}^{i,l+1}}{2dS}\Big) - rU_{m}^{i,l+1} - f_{ij,m}^{l+1}\Big[U_{m}^{j,l+1} - U_{m}^{i,l+1}\Big]\Big]\Big\}, \qquad (3.61)
\end{aligned}
$$

$$
\begin{aligned}
U_{m}^{i,l+1} - U_{m}^{i,l} = \frac{1}{2}dt\Big[&\frac{1}{2}\sigma_i^2 m^2\Big(U_{m+1}^{i,l} - 2U_{m}^{i,l} + U_{m-1}^{i,l}\Big) + \frac{rm}{2}\Big(U_{m+1}^{i,l} - U_{m-1}^{i,l}\ Big) - (r - f_{ij,m}^{l})U_{m}^{i,l} \\
&- f_{ij,m}^{l}U_{m}^{j,l} + \frac{1}{2}\sigma_i^2 m^2\Big(U_{m+1}^{i,l+1} - 2U_{m}^{i,l+1} + U_{m-1}^{i,l+1}\Big) + \frac{rm}{2}\Big(U_{m+1}^{i,l+1} - U_{m-1}^{i,l+1}\Big) \\
&- (r - f_{ij,m}^{l+1})U_{m}^{i,l+1} - f_{ij,m}^{l+1}U_{m}^{j,l+1}\Big], \qquad (3.62)
\end{aligned}
$$

where $d\tau = dt$ represent the time increment and dS represents the stock price increment.

Separating based on the time index,

$$
\begin{aligned}
&- \frac{1}{4}mdt\Big(\sigma_i^2 m - r\Big)U_{m-1}^{i,l+1} + \Big[1 + \frac{1}{2}dt\Big(\sigma_i^2 m^2 + (r - f_{ij,m}^{l+1}\Big)\Big]U_{m}^{i,l+1} \\
&\quad - \frac{1}{4}mdt\Big(\sigma_i^2 m + r\Big)U_{m+1}^{i,l+1} + \frac{1}{2}f_{ij,m}^{l+1}U_{m}^{j,l+1} \\
&= \frac{1}{4}mdt\Big(\sigma_i^2 m - r\Big)U_{m-1}^{i,l} + \Big[1 - \frac{1}{2}dt\Big(\sigma_i^2 m^2 + (r - f_{ij,m}^{l}\Big)\Big]U_{m}^{i,l} \\
&\quad + \frac{1}{4}mdt\Big(\sigma_i^2 m + r\Big)U_{m+1}^{i,l} - \frac{1}{2}f_{ij,m}^{l+1}U_{m}^{j,l}. \qquad (3.63)
\end{aligned}
$$

Define:

$$
\begin{aligned}
a_{m}^{i,l} &= \frac{1}{4}mdt\Big(\sigma_i^2 m - r\Big), \qquad (3.64) \\
b_{m}^{i,l} &= -\frac{1}{2}dt\Big(\sigma_i^2 m^2 + r - f_{ij,m}^{l}\Big), \qquad (3.65) \\
c_{m}^{i,l} &= \frac{1}{4}mdt\Big(\sigma_i^2 m + r\Big). \qquad (3.66)
\end{aligned}
$$

Since the generalized regime-switching framework allows for the coefficients of the source terms coupling our state-dependent pricing equations to be deterministic, it follows that the coefficients defined above depend on both stock price and time. This affects how the Crank-Nicolson numerical scheme is carried out, which will be explained in greater detail later on. Thus,

$$
\begin{aligned}
&- a_{m}^{i,l+1}U_{m-1}^{i,l+1} + \Big(1 - b_{m}^{i,l+1}\Big)U_{m}^{i,l+1} - c_{m}^{i,l+1}U_{m+1}^{i,l+1} + \frac{1}{2}f_{ij,m}^{l+1}U_{m}^{j,l+1} \\
&= a_{m}^{i,l}U_{m-1}^{i,l} + \Big(1 + b_{m}^{i,l}\Big)U_{m}^{i,l} + c_{m}^{i,l}U_{m+1}^{i,l} - \frac{1}{2}f_{ij,m}^{l}U_{m}^{j,l}. \qquad (3.67)
\end{aligned}
$$

This results in:

$$B^{i,l+1}\vec{U}^{i,l+1} + C^{i,l+1}\vec{U}^{j,l+1} = A^{i,l}\vec{U}^{i,l} - C^{i,l}\vec{U}^{j,l}, \tag{3.68}$$

where:

$$B^{i,l+1} = \begin{bmatrix} 1-b_2^{l+1} & -c_3^{l+1} & 0 & \dots & 0 \\ -a_2^{l+1} & 1-b_3^{l+1} & -c_4^{l+1} & \ddots & \vdots \\ 0 & \ddots & \ddots & \ddots & 0 \\ \vdots & \ddots & \ddots & \ddots & -c_M^{l+1} \\ 0 & \dots & 0 & -a_{M-1}^{l+1} & 1-b_M^{l+1} \end{bmatrix},$$

$$A^{i,l} = \begin{bmatrix} 1+b_2^{l} & c_3^{l} & 0 & \dots & 0 \\ a_2^{l} & 1+b_3^{l} & c_4^{l} & \ddots & \vdots \\ 0 & \ddots & \ddots & \ddots & 0 \\ \vdots & \ddots & \ddots & \ddots & c_M^{l} \\ 0 & \dots & 0 & a_{M-1}^{l} & 1+b_M^{l} \end{bmatrix},$$

and

$$C^{i,l} = \begin{bmatrix} \frac{1}{2}f_{ij,2}^{l}dt & 0 & \dots & 0 \\ 0 & \frac{1}{2}f_{ij,3}^{l}dt & \ddots & \vdots \\ \vdots & \ddots & \ddots & 0 \\ 0 & \dots & 0 & \frac{1}{2}f_{ij,M}^{l}dt \end{bmatrix}.$$

The above matrices hold for all $i \in \{H, L\}$ where $i \neq j$. It turns out that when we consider equation (3.68) for both the high and low volatility states, we get a system of two equations with two unknowns: $\vec{U}^{H,l+1}$ and $\vec{U}^{L,l+1}$ which needs to be solved at every time iteration $l + 1$.

$$B^{H,l+1}\vec{U}^{H,l+1} + C^{H,l+1}\vec{U}^{L,l+1} = A^{H,l}\vec{U}^{H,l} - C^{H,l}\vec{U}^{L,l}, \tag{3.69}$$

$$B^{L,l+1}\vec{U}^{L,l+1} + C^{L,l+1}\vec{U}^{H,l+1} = A^{L,l}\vec{U}^{L,l} - C^{L,l}\vec{U}^{H,l}. \tag{3.70}$$

For simplicity, define:

$$D^{H,l} = A^{H,l}\vec{U}^{H,l} - C^{H,l}\vec{U}^{L,l}, \tag{3.71}$$

$$D^{L,l} = A^{L,l}\vec{U}^{L,l} - C^{L,l}\vec{U}^{H,l}. \tag{3.72}$$

Therefore, our coupled matrix system is now written as:

$$D^{H,l} = B^{H,l+1}\vec{U}^{H,l+1} + C^{H,l+1}\vec{U}^{L,l+1}, \tag{3.73}$$

$$D^{L,l} = B^{L,l+1}\vec{U}^{L,l+1} + C^{L,l+1}\vec{U}^{H,l+1}. \tag{3.74}$$

Multiplying equation (3.73) on the left by $B^{L,l+1}$ and equation (3.74) by $C^{H,l+1}$ and subtracting the second from the first:

$$B^{L,l+1}D^{H,l} - C^{H,l+1}D^{L,l} = \left(B^{L,l+1}B^{H,l+1} - C^{H,l+1}C^{L,l+1}\right)\vec{U}^{H,l+1}. \tag{3.75}$$

Define:

$$F^{H,l+1} = B^{L,l+1}D^{H,l} - C^{H,l+1}D^{L,l}, \tag{3.76}$$

$$E^{H,l+1} = B^{L,l+1}B^{H,l+1} - C^{H,l+1}C^{L,l+1}, \tag{3.77}$$

where $F^{H,l+1}$ is a vector of size $M-1$ and $E^{H,l+1}$ is a square matrix of size $M-1$.

Thus we require to solve the linear system of equations for $\vec{U}^{H,l}$.

$$F^{H,l+1} = E^{H,l+1}\vec{U}^{H,l+1}. \tag{3.78}$$

This can be easily solved using Matlab's built in left division function. A similar process is repeated to solve for $\vec{U}^{L,l+1}$, the option price for the low volatility state:

$$F^{L,l+1} = E^{L,l+1}\vec{U}^{L,l+1}, \tag{3.79}$$

where:

$$F^{L,l+1} = B^{H,l+1}D^{L,l} - C^{L,l+1}D^{H,l}, \tag{3.80}$$

$$E^{L,l+1} = B^{H,l+1}B^{L,l+1} - C^{L,l+1}C^{H,l+1}. \tag{3.81}$$

Assuming initial conditions given by the payoff function of a European call option and the associated boundary conditions, we can solve the regime-switching price PDEs for the high and low volatility call prices. The numerical solution for both the high and low state regime-switching call options is shown in Figure 3.6.

Expected Return	r	0%
High State Volatility	σ_H	40%
Low State Volatility	σ_L	10%
Strike Price	K	\$100
Daily High State Jump Intensity	λ_{LH}	15%
Daily Low State Jump Intensity	λ_{HL}	10%
High State MPVR	m_{HL}	0
Low State MPVR	m_{LH}	0
Maturity Date	T	1 year
Number of Time Increments	$\tilde{L}$	252

Table 3.4: Parameters used in the implementation of the Crank-Nicolson numerical scheme for the regime-switching coupled PDEs.

It can be observed that the numerical solution for the high state option, $C^H(S,t)$, and the solution for the low state option, $C^L(S,t)$, are both increasing with respect to the stock price. The call prices have the general shape and curvature that we expect for a European call price. Furthermore, the low state option price is less than the high state option price, most noticeably about the strike price of $K = \$100$, which is expected as financially we know that option prices increase as volatility levels increase.

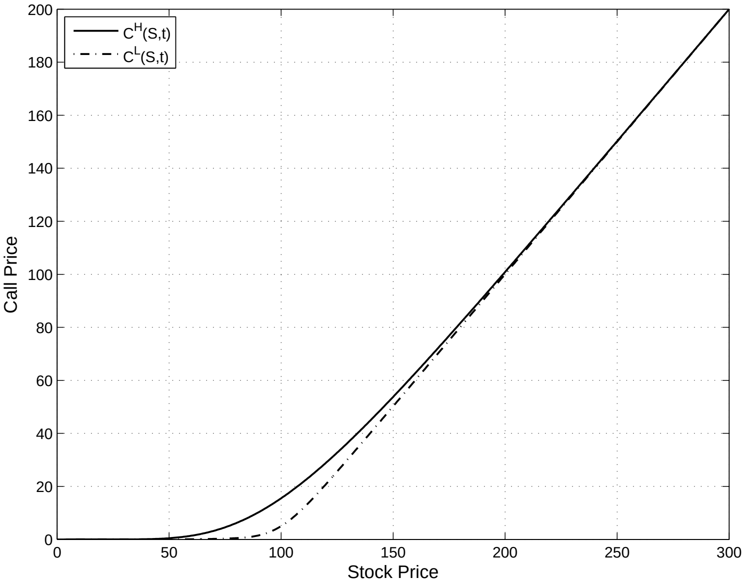

Figure 3.6: Crank-Nicolson numerical solution for the regime-switching coupled pricing PDEs at time $t = 0$. All parameters as given in Table 3.4.

By implementing the Crank-Nicolson numerical method on our regime-switching coupled pricing equations, we have obtained a benchmark solution technique to use in the following chapters. In particular we will use these numerical results to justify and support the financial validity of approximate solutions derived for our regimes-switching options. It is determining these approximate solutions that we turn our attention to in the next chapter.

Chapter 4

Approximate Solution

Our coupled regime-switching pricing partial differential equations derived in Chapter 2 do not have closed-form solutions for the state-dependent call prices. We are however, interested in studying the parameters embedded within our option pricing model, to analyse the effect that they have on the option prices. A parameter of particular interest is the state-dependent market price of volatility risk as it is a driving factor in the effect the coupled source term has on a particular regime's option price. In addition, numerical schemes do not allow as much insight to be built, driving us to consider an approximation to the solution that can easily be implemented. It is nice to understand the approximate behaviour of solutions, both for the insights these approximations bring and for the purpose of verifying more accurate, but more complicated numerical methods. Thus, obtaining an approximation to the solution of an option written in a financially realistic two-regime switching market would be useful.

Since our system of coupled PDEs cannot be solved directly, we use the classical Cauchy-Kowalevski Theorem, usually encountered in the very beginning of a PDE course, to derive approximate state-dependent option prices. In particular, we choose to reformulate our problem in terms of the well-known Black-Scholes option pricing equations in order to apply this applied mathematics theorem directly. This reformulation also provides an avenue to investigate further the financial intuition embedded within our problem. Specifically, the relationship between the backward error of our pricing problem and the possible trading gains/losses from our hedged position.

4.1 Review of Cauchy-Kowalevski Theorem

In general, the Cauchy-Kowalevski theorem is applied to an initial value problem, such as the one-dimensional heat equation. By taking a Taylor series expansion about the initial conditions, we can derive a series type solution. Existence of a solution is proven given the resulting series converges (Folland [20]; O'Neil [36]). A formal review of this theorem is given below.

Theorem 4.1.1 (Cauchy-Kowalevski)

Given the general Cauchy problem

$$\partial_t^k f = G(x, t, (\partial_x^\alpha \partial_t^j f)_{|\alpha|+j\le k, j<k}), \tag{4.1}$$

with initial condition

$$\partial_t^j f(x,0) = H_j(x). \tag{4.2}$$

Then if G and H_j are analytic near the origin $\forall j$, there exists a unique analytic solution in some neighbourhood about the origin. It follows that the Taylor series

$$\sum_\alpha \frac{\partial^\alpha f(x_0)}{\alpha!}(x - x_0)^\alpha, \tag{4.3}$$

converges absolutely to $f(x)$ if f is analytic near $x_0 \in \mathbb{R}^n$.

As we shall see, the Cauchy-Kowalevski Theorem will not directly apply to our problem since for a call option, the initial condition is not analytic for all possible stock prices. We will overcome this difficulty by using a "viscosity solution" type approach to find our approximation.

4.2 Reformulating our Regime-Switching Pricing Model

In order to analyse the effects of the state-dependent parameters, in particular the market prices of volatility risk, we require an approximation to our option price. The existence of a solution to a general initial value problem can typically be found by applying the Cauchy-Kowalevski Theorem and taking a Taylor series expansion about the initial point. First our regime-switching pricing problem is converted into an initial value problem by defining $\tau = T - t$.

$$\frac{\partial C^i}{\partial \tau}(S,\tau) = \frac{1}{2}\sigma_i^2 S^2 \frac{\partial^2 C^i}{\partial S^2}(S,\tau) + rS\frac{\partial C^i}{\partial S}(S,\tau) - rC^i(S,\tau) - f_{ij}(S,\tau)\Big[C^j(S,\tau) - C^i(S,\tau)\Big], \tag{4.4}$$

subject to

$$C^i(S,0) = C^j(S,0) = (S(0) - K)^+, \tag{4.5}$$

$$C^i(0,\tau) = C^j(0,\tau) = 0, \tag{4.6}$$

$$\lim_{S\to\infty} \frac{\partial C^i}{\partial S}(S,\tau) = \lim_{S\to\infty} \frac{\partial C^j}{\partial S}(S,\tau) = 1, \tag{4.7}$$

where

$$f_{ij}(S,\tau) = -\big(\lambda_{ij} - m_{ij}\big), \tag{4.8}$$

for all $i \in \{H, L\}$ and $i \neq j$. It should be noted that from now until otherwise noted, the Poisson intensities are assumed to be constant and denoted by λ_{ij}.

The initial condition for our problem is not differentiable about the strike price, K. Thus the European call option payoff is not consistent with the initial condition being analytic. We address this point by redefining our problem using financial intuition. We choose to redefine our regime-switching option prices to be functions of the corresponding Black-Scholes option prices. The well known Black-Scholes option pricing model [6] has been studied extensively and is well understood by practitioners and academics alike. For ease of reading, the following notation will be reduced: $f_{ij} \equiv f_{ij}(S,\tau)$.

$$C^H(S,\tau) = C^H_{BS}(S,\tau) - Y(S,\tau), \tag{4.9}$$
$$C^L(S,\tau) = C^L_{BS}(S,\tau) + X(S,\tau). \tag{4.10}$$

Our regime-switching option prices can be redefined this way due to our financial intuition regarding the effects of volatility switching. We know that all else being equal, option values are increasing in volatility. It is expected that the possibility of switching to a more stable regime makes the high state regime-switching option less valuable than an otherwise similar option in a single high volatility Black-Scholes world. On the other hand, the possibility of switching to a more volatile state is an attractive feature for an option and thus makes our regime-switching option price more valuable than an otherwise similar option in a single low volatility Black-Scholes world. Thus we need to use our new definitions of the option price to derive a new set of coupled PDEs. Thus $Y(S,\tau)$ and $X(S,\tau)$, which represent the difference between the Black-Scholes option price and the regime-switching price for the high and low state, respectively, are both non-negative. First, we substitute the newly redefined regime-switching option prices in the high state PDE.

$$\begin{aligned}\frac{\partial C^H_{BS}}{\partial \tau}(S,\tau) - \frac{\partial Y}{\partial \tau}(S,\tau) = {}& \frac{1}{2}\sigma_H^2 S^2 \frac{\partial^2 C^H_{BS}}{\partial S^2}(S,\tau) - \frac{1}{2}\sigma_H^2 S^2 \frac{\partial^2 Y}{\partial S^2}(S,\tau) \\ &+ rS\frac{\partial C^H_{BS}}{\partial S}(S,\tau) - rS\frac{\partial Y}{\partial S}(S,\tau) - rC^H_{BS}(S,\tau) + rY(S,\tau) \\ &- f_{HL}\Big[C^L_{BS}(S,\tau) + X(S,\tau) - C^H_{BS}(S,\tau) + Y(S,\tau)\Big]. \end{aligned} \tag{4.11}$$

For the constant volatility world where volatility is given by σ_i, we know that the Black-Scholes PDE holds.

$$\frac{\partial C^i_{BS}}{\partial \tau}(S,\tau) = \frac{1}{2}\sigma_i^2 S^2 \frac{\partial^2 C^i_{BS}}{\partial S^2}(S,\tau) + rS\frac{\partial C^i_{BS}}{\partial S}(S,\tau) - rC^i_{BS}(S,\tau). \tag{4.12}$$

It follows that:

$$\begin{aligned}\frac{\partial Y}{\partial \tau}(S,\tau) = {}& \frac{1}{2}\sigma_H^2 S^2 \frac{\partial^2 Y}{\partial S^2}(S,\tau) + rS\frac{\partial Y}{\partial S} - rY(S,\tau) \\ &- f_{HL}\Big[C^H_{BS}(S,\tau) - C^L_{BS}(S,\tau) - X(S,\tau) - Y(S,\tau)\Big]. \end{aligned} \tag{4.13}$$

Now, reformulating the low state PDE using equation (4.12).

$$\begin{aligned}\frac{\partial C^L_{BS}}{\partial \tau}(S,\tau) + \frac{\partial X}{\partial \tau}(S,\tau) = {}& \frac{1}{2}\sigma_L^2 S^2 \frac{\partial^2 C^L_{BS}}{\partial S^2}(S,\tau) + \frac{1}{2}\sigma_L^2 S^2 \frac{\partial^2 X}{\partial S^2}(S,\tau) \\ &+ rS\frac{\partial C^L_{BS}}{\partial S}(S,\tau) + rS\frac{\partial X}{\partial S}(S,\tau) - rC^L_{BS}(S,\tau) - rX(S,\tau) \\ &- f_{LH}\Big[C^H_{BS}(S,\tau) - Y(S,\tau) - C^L_{BS}(S,\tau) - X(S,\tau)\Big], \end{aligned} \tag{4.14}$$

$$\Rightarrow \frac{\partial X}{\partial \tau}(S,\tau) = \frac{1}{2}\sigma_L^2 S^2 \frac{\partial^2 X}{\partial S^2}(S,\tau) + rS\frac{\partial X}{\partial S}(S,\tau) - rX(S,\tau) - f_{LH}\Big[C_{BS}^H(S,\tau) - C_{BS}^L(S,\tau) - X(S,\tau) - Y(S,\tau)\Big]. \tag{4.15}$$

We arrive at a new system of coupled PDEs in terms of the new functions $Y(S,\tau)$ and $X(S,\tau)$. Our new pricing problem has analytic initial and boundary conditions although the non-smoothness of the original problem still enters, when $\tau = 0$, via the forcing term.

$$\frac{\partial Y}{\partial \tau}(S,\tau) = \frac{1}{2}\sigma_H^2 S^2 \frac{\partial^2 Y}{\partial S^2}(S,\tau) + rS\frac{\partial Y}{\partial S} - rY(S,\tau) - f_{HL}\Big[C_{BS}^H(S,\tau) - C_{BS}^L(S,\tau) - X(S,\tau) - Y(S,\tau)\Big], \tag{4.16}$$

$$\frac{\partial X}{\partial \tau}(S,\tau) = \frac{1}{2}\sigma_L^2 S^2 \frac{\partial^2 X}{\partial S^2}(S,\tau) + rS\frac{\partial X}{\partial S}(S,\tau) - rX(S,\tau) - f_{LH}\Big[C_{BS}^H(S,\tau) - C_{BS}^L(S,\tau) - X(S,\tau) - Y(S,\tau)\Big], \tag{4.17}$$

subject to:

$$Y(S,0) = X(S,0) = 0, \tag{4.18}$$

$$Y(0,\tau) = X(0,\tau) = 0, \tag{4.19}$$

$$\lim_{S\to\infty}\frac{\partial Y}{\partial S}(S,\tau) = \lim_{S\to\infty}\frac{\partial X}{\partial S}(S,\tau) = 0. \tag{4.20}$$

We can apply Cauchy-Kowalevski directly to our new coupled initial value problem as the initial condition is now analytic. Since are boundary conditions are homogeneous on an unbounded interval, we can ignore them during the application of the theorem and simply check that they are satisfied later.

Our coupled system depends on both the high and low volatility Black-Scholes option prices via the forcing term. If $\tau = 0$ in our coupled system for $Y(S,\tau)$ and $X(S,\tau)$ shown above, our forcing terms collapse. To consider the effect that the forcing terms have on our option price differences, we choose $\tau = \varepsilon$ instead. This motivates us to first apply the Cauchy-Kowalevski Theorem to the one-dimensional Black-Scholes problem where $\tau = \varepsilon$ for very small values of ε, which allow the initial and boundary conditions to be analytic.

4.2.1 Applying Cauchy-Kowalevski to the One-Dimensional Black-Scholes Problem

Consider the Black-Scholes call option price conditional on volatility state i, $C_{BS}^i(S,\tau)$. The pricing problem associated with this option is given below.

$$\frac{\partial C_{BS}^i}{\partial \tau}(S,\tau) = \frac{1}{2}\sigma^2 S^2 \frac{\partial^2 C_{BS}^i}{\partial S^2}(S,\tau) + rS\frac{\partial C_{BS}^i}{\partial S}(S,\tau) - rC_{BS}^i(S,\tau), \tag{4.21}$$

subject to:

$$C_{BS}^i(S,0) = (S(0) - K)^+, \tag{4.22}$$

$$C^{i}_{BS}(0,\tau) = 0, \tag{4.23}$$

$$\lim_{S\to\infty} \frac{\partial C^{i}_{BS}}{\partial S}(S,\tau) = 1. \tag{4.24}$$

The initial condition is not differentiable about the strike price K, thus the Cauchy-Kowalevski Theorem can not be applied directly. This motivates us to consider the Black-Scholes pricing problem under the assumption that there exists a solution for the problem such that the initial condition is evaluated at $\varepsilon > 0$ where ε is taken to be very small. Assume that there exists $C^{i,\varepsilon}_{BS}(S,\tau)$ that solves the parallel Black-Scholes pricing problem:

$$\frac{\partial C^{i,\varepsilon}_{BS}}{\partial \tau}(S,\tau) = \frac{1}{2}\sigma_i^2 S^2 \frac{\partial^2 C^{i,\varepsilon}_{BS}}{\partial S^2}(S,\tau) + rS\frac{\partial C^{i,\varepsilon}_{BS}}{\partial S}(S,\tau) - rC^{i,\varepsilon}_{BS}(S,\tau), \tag{4.25}$$

subject to:

$$C^{i,\varepsilon}_{BS}(S,0) = SN(d_1^\varepsilon) - Ke^{-r\varepsilon}N(d_2^\varepsilon), \tag{4.26}$$

$$C^{i,\varepsilon}_{BS}(0,\tau) = 0, \tag{4.27}$$

$$\lim_{S\to\infty} \frac{\partial C^{i,\varepsilon}_{BS}}{\partial S}(S,\tau) = 1, \tag{4.28}$$

where:

$$d_1^\varepsilon = \frac{\ln\frac{S}{K} + (r + \frac{1}{2}\sigma^2)\varepsilon}{\sigma\sqrt{\varepsilon}}, \tag{4.29}$$

$$d_2^\varepsilon = d_1^\varepsilon - \sigma\sqrt{\varepsilon}, \tag{4.30}$$

$$N(x) = \frac{1}{\sqrt{2\pi}}\int_{-\infty}^{x} e^{-\frac{z^2}{2}}\,dz. \tag{4.31}$$

If we consider $\varepsilon \to 0$, the following holds for all $n \geq 0$ since $C^{i,\varepsilon}_{BS}(S,0)$ is continuously differentiable with respect to S.

$$\lim_{\varepsilon\to 0}\frac{\partial^{(n)} C^{i,\varepsilon}_{BS}}{\partial S^{(n)}}(S,0) = \frac{\partial^{(n)} C^{i}_{BS}}{\partial S^{(n)}}(S,0), \tag{4.32}$$

$$\Rightarrow \lim_{\varepsilon\to 0}\frac{\partial^{(n)} C^{i,\varepsilon}_{BS}}{\partial \tau^{(n)}}(S,0) = \frac{\partial^{(n)} C^{i}_{BS}}{\partial \tau^{(n)}}(S,0). \tag{4.33}$$

Since this initial condition is analytic, we can now take a Taylor series expansion of $C^{i,\varepsilon}_{BS}(S,\tau)$ about the point $(S,0)$ and apply the Cauchy-Kowalevski Theorem.

$$C^{i,\varepsilon}_{BS}(S,\tau) = C^{i,\varepsilon}_{BS}(S,0) + \tau\frac{\partial C^{i,\varepsilon}_{BS}}{\partial \tau}(S,0) + \frac{1}{2}\tau^2\frac{\partial^2 C^{i,\varepsilon}_{BS}}{\partial \tau^2}(S,0) + \ldots, \tag{4.34}$$

$$\Rightarrow \lim_{\varepsilon\to 0} C^{i,\varepsilon}_{BS}(S,\tau) = \lim_{\varepsilon\to 0}\left[C^{i,\varepsilon}_{BS}(S,0) + \tau\frac{\partial C^{i,\varepsilon}_{BS}}{\partial \tau}(S,0) + \frac{1}{2}\tau^2\frac{\partial^2 C^{i,\varepsilon}_{BS}}{\partial \tau^2}(S,0) + \ldots\right], \tag{4.35}$$

$$= \lim_{\varepsilon\to 0} C^{i,\varepsilon}_{BS}(S,0) + \tau\lim_{\varepsilon\to 0}\frac{\partial C^{i,\varepsilon}_{BS}}{\partial \tau}(S,0) + \frac{1}{2}\tau^2\lim_{\varepsilon\to 0}\frac{\partial^2 C^{i,\varepsilon}_{BS}}{\partial \tau^2}(S,0) + \ldots, \tag{4.36}$$

$$= \sum_{n=0}^{\infty} \frac{\tau^n}{n!} \lim_{\varepsilon \to 0} \frac{\partial^{(n)} C_{BS}^{i,\varepsilon}}{\partial \tau^{(n)}}(S,0), \tag{4.37}$$

$$= \sum_{n=0}^{\infty} \frac{\tau^n}{n!} \frac{\partial^{(n)} C_{BS}}{\partial \tau^{(n)}}(S,0), \tag{4.38}$$

$$= C_{BS}^{i}(S,\tau), \tag{4.39}$$

$$\Rightarrow C_{BS}^{i}(S,\tau) = \sum_{n=0}^{\infty} \frac{\tau^n}{n!} \frac{\partial^{(n)} C_{BS}}{\partial \tau^{(n)}}(S,0). \tag{4.40}$$

Because we know that the one-dimensional Black-Scholes pricing problem has a unique solution, we can take equation (4.40) as being a shorthand denoting this solution. Before we can make use of this result, the error introduced into this system by our initial condition evaluated at ε must be investigated. Since we do not know the solution to our parallel Black-Scholes problem with the new initial condition, we will compare this problem to the classical Black-Scholes problem and another variation of the problem. Thus we have three initial value problems to consider.

The first case is our classical option pricing problem which considers an option $V_1(S,\tau)$ maturing at $\tau = 0$ with payoff $(S(0) - K)^+$. The second case considers an option $V_2(S,\tau)$ maturing at $\tau = \varepsilon$ with payoff $SN(d_1^\varepsilon) - Ke^{-r\varepsilon}N(d_2^\varepsilon)$. Our final case is that of our parallel Black-Scholes problem where an option $V_3(S,\tau)$ expires at $\tau = 0$ with payoff $SN(d_1^\varepsilon) - Ke^{-r\varepsilon}N(d_2^\varepsilon)$. Of interest is the error introduced by using our approximate option $V_3(S,\tau)$ as a substitution for $V_1(S,\tau)$ when applying the Cauchy-Kowalevski Theorem. An estimate of this error is obtained by examining the relationships between these three options.

It is known that for $\tau > \varepsilon$, $V_1(S,\tau) = V_2(S,\tau)$, since $V_2(S,\tau)$ has an initial condition that is the exact solution of $V_1(S,\tau)$ at $\tau = \varepsilon$. Thus it follows that $V_3(S,\tau) > V_2(S,\tau) = V_1(S,\tau-\varepsilon)$ for all τ. The error estimate that we examine is $\left|V_3(S,\tau) - V_1(S,\tau)\right| \approx \varepsilon \left|\frac{\partial V_1}{\partial \tau}(S,\tau-\varepsilon)\right|$ for $\tau > \varepsilon$. Various time points before maturity are considered as well as varying sizes for ε. A list of the parameters used in the example is given in Table 4.1.

Expected Return	r	0%
Volatility	σ	40%
Strike Price	K	\$100
Maximum Stock Price	S_{max}	\$300
Maturity Date	T	1 year
Number of Time Increments	$\tilde{L}$	200

Table 4.1: Parameters used in investigation of error estimate.

In Figure 4.1, the error introduced by using our parallel Black-Scholes option price diffuses as we move away from the initial condition. Although the error is the largest initially, it is more concentrated around the strike price. As we move forward in time, the absolute value of the error decreases, however it spreads out over more stock values. When considering the error associated with an option price, we are most interested in the error present when the option is priced. Options are priced at $t = 0$, so for our initial value problem this occurs at $\tau = T$.

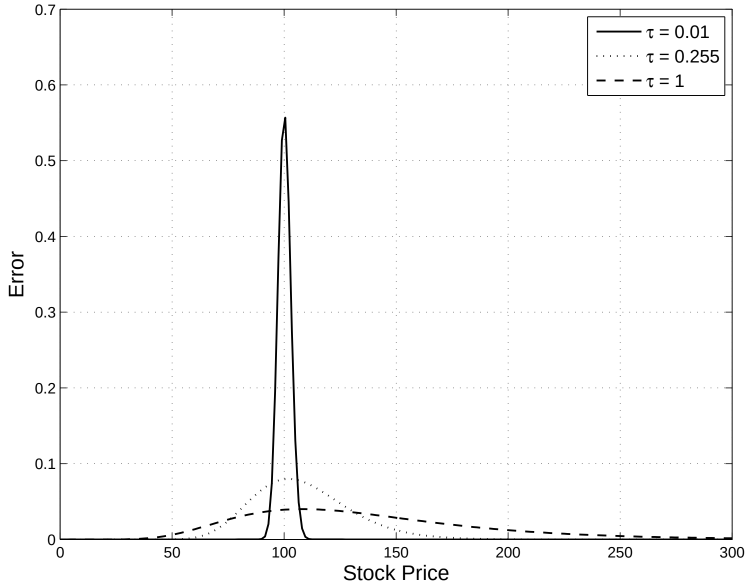

Figure 4.1: Comparison of the error estimate for various values of τ. $\varepsilon = 0.005$, all other parameters as given in Table 4.1.

Therefore the smallest error is present when we price our option however it is distributed over a wider range of stock prices.

Of greatest interest is the impact that the size of the time increment ε, by which we shift our parallel problem's evaluation of the initial condition, has on our error estimate. In Figure 4.2 the error introduced for various sizes of ε is investigated at the time the option is priced (i.e. $\tau = T$). It can be observed in Figure 4.2 that for large values of ε the error is quite large, however as $\varepsilon \to 0$ the error becomes minimal. Thus if we consider $\varepsilon \to 0$ in our parallel pricing problem, the approximation to the actual Black-Scholes option price is reasonable.

Now that an estimate of the error introduced into the system has been quantified, we apply the theorem to our coupled system for $Y(S,\tau)$ and $X(S,\tau)$.

4.2.2 Applying Cauchy-Kowalevski to the Regime-Switching Problem

We apply the Cauchy-Kowalevksi Theorem to our reformulated regime-switching problem, making use of the result given by equation (4.40) for the parallel Black-Scholes problem. In particular, we evaluate the Black-Scholes option prices in the forcing terms of our PDEs by using our parallel epsilon problem and taking the limit as $\varepsilon \to 0$.

First take a Taylor series expansion about the point $(S,0)$ for $Y(S,\tau)$. In order to apply the theorem, we have to make use of our previous result for the Black-Scholes prices and the fact that $\dfrac{\partial^{(n)} Y}{\partial S^{(n)}}(S,0) = 0$ for all $n \geq 0$.

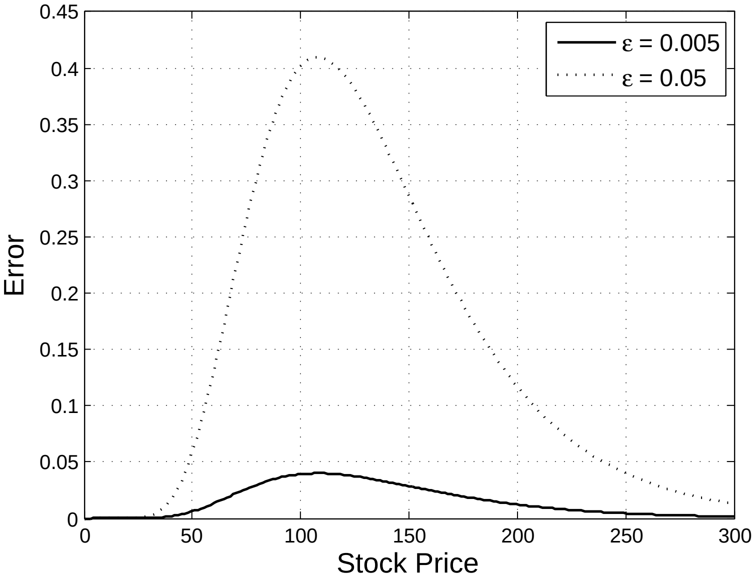

Figure 4.2: Comparison of the error estimate for various sizes of ε. $\tau = 1$, all other parameters as given in Table 4.1.

$$\begin{aligned}
Y(S,\tau) &= Y(S,0) + \tau\frac{\partial Y}{\partial \tau}(S,0) + \frac{1}{2!}\tau^2\frac{\partial^2 Y}{\partial \tau^2}(S,0) + \frac{1}{3!}\tau^3\frac{\partial^3 Y}{\partial \tau^3}(S,0) + \cdots, \qquad (4.41)\\
&= 0 + \tau\Big[-f_{HL}\Big(\lim_{\varepsilon\to 0} C_{BS}^{\varepsilon,H}(S,0) - \lim_{\varepsilon\to 0} C_{BS}^{\varepsilon,L}(S,0)\Big)\Big]\\
&\quad + \frac{1}{2!}\tau^2\Bigg[-f_{HL}\Bigg(\lim_{\varepsilon\to 0}\frac{\partial C_{BS}^{\varepsilon,H}}{\partial\tau}(S,0) - \lim_{\varepsilon\to 0}\frac{\partial C_{BS}^{\varepsilon,L}}{\partial\tau}(S,0)\Bigg)\\
&\qquad - f_{HL}(f_{HL}+f_{LH})\Big(\lim_{\varepsilon\to 0} C_{BS}^{\varepsilon,H}(S,0) - \lim_{\varepsilon\to 0} C_{BS}^{\varepsilon,L}(S,0)\Big)\Bigg]\\
&\quad + \frac{1}{3!}\tau^3\Bigg[-f_{HL}\Bigg(\lim_{\varepsilon\to 0}\frac{\partial^2 C_{BS}^{\varepsilon,H}}{\partial\tau^2}(S,0) - \lim_{\varepsilon\to 0}\frac{\partial^2 C_{BS}^{\varepsilon,L}}{\partial\tau^2}(S,0)\Bigg)\\
&\qquad - f_{HL}(f_{HL}+f_{LH})\Bigg(\lim_{\varepsilon\to 0}\frac{\partial C_{BS}^{\varepsilon,H}}{\partial\tau}(S,0) - \lim_{\varepsilon\to 0}\frac{\partial C_{BS}^{\varepsilon,L}}{\partial\tau}(S,0)\Bigg)\\
&\qquad - f_{HL}(f_{HL}+f_{LH})^2\Big(\lim_{\varepsilon\to 0} C_{BS}^{\varepsilon,H}(S,0) - \lim_{\varepsilon\to 0} C_{BS}^{\varepsilon,L}(S,0)\Big)\Bigg] + \cdots, \qquad (4.42)\\
&= -f_{HL}\tau\Bigg[\Bigg(\lim_{\varepsilon\to 0} C_{BS}^{\varepsilon,H}(S,0) + \tau\lim_{\varepsilon\to 0}\frac{\partial C_{BS}^{\varepsilon,H}}{\partial\tau}(S,0) + \frac{1}{2}\tau^2\lim_{\varepsilon\to 0}\frac{\partial^2 C_{BS}^{\varepsilon,H}}{\partial\tau^2}(S,0) + \cdots\Bigg)\\
&\qquad - \Bigg(\lim_{\varepsilon\to 0} C_{BS}^{\varepsilon,L}(S,0) + \tau\lim_{\varepsilon\to 0}\frac{\partial C_{BS}^{\varepsilon,L}}{\partial\tau}(S,0) + \frac{1}{2}\tau^2\lim_{\varepsilon\to 0}\frac{\partial^2 C_{BS}^{\varepsilon,L}}{\partial\tau^2}(S,0) + \cdots\Bigg)\Bigg]
\end{aligned}$$

$$
\begin{aligned}
&- f_{HL}(f_{HL} + f_{LH})\frac{\tau^2}{2!}\Bigg[\Bigg(\lim_{\varepsilon\to 0} C_{BS}^{\varepsilon,H}(S,0) + \tau \lim_{\varepsilon\to 0}\frac{\partial C_{BS}^{\varepsilon,H}}{\partial \tau}(S,0) + \cdots\Bigg) \\
&\qquad - \Bigg(\lim_{\varepsilon\to 0} C_{BS}^{\varepsilon,L}(S,0) + \tau \lim_{\varepsilon\to 0}\frac{\partial C_{BS}^{\varepsilon,L}}{\partial \tau}(S,0) + \cdots\Bigg)\Bigg] \\
&- f_{HL}(f_{HL} + f_{LH})^2\frac{\tau^3}{3!}\Big[\Big(\lim_{\varepsilon\to 0} C_{BS}^{\varepsilon,H}(S,0) + \cdots\Big) - \Big(\lim_{\varepsilon\to 0} C_{BS}^{\varepsilon,L}(S,0) + \cdots\Big)\Big] \\
&+ \cdots + \text{additional terms.}
\end{aligned} \tag{4.43}
$$

Much of the algebra is omitted for ease of reading. For further details please see Mielkie and Davison [33].

The additional terms that arise in our derivation have minimal impact on the regime-switching option price. This is due to the fact that as options approach their maturity date, the impact of volatility on their corresponding prices is negligible. In fact, the option prices written on two different volatility states converge at this point in time since we are considering the limit as we approach maturity. It follows that the difference between Greeks written on options with differing volatility is also negligible.

Additional terms arise in our Taylor series expansion that include the difference between the two state's Black-Scholes Greeks evaluated close to maturity (i.e. as $\varepsilon \to 0$). Since the effect of volatility is negligible on the option's Greeks right before expiration, these additional terms will have minimal impact on our approximate solution, a fact we will check in the subsequent error analysis discussion. Throwing away these terms in the Taylor series expansion allows us to write our result as an infinite sum with respect to the coefficients of the respective state's PDE source terms. Recall that these coefficients, f_{ij}, are functions of the intensities of the Poisson processes for all $i \in \{H, L\}$ where $i \neq j$.

$$
\begin{aligned}
Y(S,\tau) &\approx \left[\sum_{n=0}^{\infty}\frac{\tau^n}{n!}\lim_{\varepsilon\to 0}\frac{\partial^{(n)} C_{BS}^{\varepsilon,H}}{\partial \tau^{(n)}}(S,0) - \sum_{n=0}^{\infty}\frac{\tau^n}{n!}\lim_{\varepsilon\to 0}\frac{\partial^{(n)} C_{BS}^{\varepsilon,L}}{\partial \tau^{(n)}}(S,0)\right] \\
&\qquad \cdot (-f_{HL})\Bigg(\tau + (f_{HL} + f_{LH})\frac{\tau^2}{2!} + (f_{HL} + f_{LH})^2\frac{\tau^3}{3!} + \cdots\Bigg), \qquad (4.44) \\
&\approx -f_{HL}\Big[C_{BS}^{H}(S,\tau) - C_{BS}^{L}(S,\tau)\Big]\sum_{n=0}^{\infty}\frac{(f_{HL} + f_{LH})^n \tau^{n+1}}{(n+1)!}. \qquad (4.45)
\end{aligned}
$$

Our solution is now in terms of an infinite series. In order to prove existence of a solution, convergence must first be established. The series can be tested for convergence using d'Alembert's ratio test [41].

$$
\sum_{n=0}^{\infty}\frac{(f_{HL} + f_{LH})^n \tau^{n+1}}{(n+1)!}, \tag{4.46}
$$

$$
\Rightarrow \; a_n = \frac{(f_{HL} + f_{LH})^n \tau^{n+1}}{(n+1)!}, \tag{4.47}
$$

$$
\Rightarrow \; \lim_{n\to\infty}\left|\frac{a_{n+1}}{a_n}\right| = \lim_{n\to\infty}\left|\frac{(f_{HL} + f_{LH})\tau}{n+2}\right| = 0 < 1 \tag{4.48}
$$

Our series converges absolutely. Then using the known power series:

$$e^x - 1 = \sum_{n=0}^{\infty} \frac{x^{n+1}}{(n+1)!}, \tag{4.49}$$

$$\Rightarrow \frac{e^{(f_{HL}+f_{LH})\tau} - 1}{f_{HL}+f_{LH}} = \sum_{n=0}^{\infty} \frac{(f_{HL}+f_{LH})^n \tau^{n+1}}{(n+1)!}. \tag{4.50}$$

It follows that

$$Y(S,\tau) \approx -f_{HL}\Big[C^H_{BS}(S,\tau) - C^L_{BS}(S,\tau)\Big]\left(\frac{e^{(f_{HL}+f_{LH})\tau} - 1}{f_{HL}+f_{LH}}\right). \tag{4.51}$$

In our approximate solution for $Y(S,\tau)$, the Black-Scholes option prices $C^H_{BS}(S,\tau)$ and $C^L_{BS}(S,\tau)$ are treated as constant since we only have one value for each for a given S and τ.

Now, take a Taylor series expansion about $(S,0)$ for $X(S,\tau)$. Once again we make use of our previous result for the Black-Scholes prices and $\dfrac{\partial^{(n)}X}{\partial S^{(n)}}(S,0) = 0$ for all $n \geq 0$. The same logic and assumptions that were used for the derivation of $Y(S,\tau)$ are also used in this case.

$$\begin{aligned}
X(S,\tau) &= X(S,0) + \tau\frac{\partial X}{\partial \tau}(S,0) + \frac{1}{2!}\tau^2\frac{\partial^2 X}{\partial \tau^2}(S,0) + \frac{1}{3!}\tau^3\frac{\partial^3 X}{\partial \tau^3}(S,0) + \cdots, &(4.52)\\
&= 0 + \tau\Big[-f_{LH}\Big(\lim_{\varepsilon\to 0} C^{\varepsilon,H}_{BS}(S,0) - \lim_{\varepsilon\to 0} C^{\varepsilon,L}_{BS}(S,0)\Big)\Big]\\
&\quad + \frac{1}{2!}\tau^2\Bigg[-f_{LH}\left(\lim_{\varepsilon\to 0}\frac{\partial C^{\varepsilon,H}_{BS}}{\partial \tau}(S,0) - \lim_{\varepsilon\to 0}\frac{\partial C^{\varepsilon,L}_{BS}}{\partial \tau}(S,0)\right)\\
&\qquad\qquad - f_{LH}(f_{HL}+f_{LH})\Big(\lim_{\varepsilon\to 0} C^{\varepsilon,H}_{BS}(S,0) - \lim_{\varepsilon\to 0} C^{\varepsilon,L}_{BS}(S,0)\Big)\Bigg]\\
&\quad + \frac{1}{3!}\tau^3\Bigg[-f_{LH}\left(\lim_{\varepsilon\to 0}\frac{\partial^2 C^{\varepsilon,H}_{BS}}{\partial \tau^2}(S,0) - \lim_{\varepsilon\to 0}\frac{\partial^2 C^{\varepsilon,L}_{BS}}{\partial \tau^2}(S,0)\right)\\
&\qquad\qquad - f_{LH}(f_{HL}+f_{LH})\left(\lim_{\varepsilon\to 0}\frac{\partial C^{\varepsilon,H}_{BS}}{\partial \tau}(S,0) - \lim_{\varepsilon\to 0}\frac{\partial C^{\varepsilon,L}_{BS}}{\partial \tau}(S,0)\right)\\
&\qquad\qquad - f_{LH}(f_{HL}+f_{LH})^2\Big(\lim_{\varepsilon\to 0} C^{\varepsilon,H}_{BS}(S,0) - \lim_{\varepsilon\to 0} C^{\varepsilon,L}_{BS}(S,0)\Big)\Bigg] + \cdots, &(4.53)\\
&= f_{LH}\tau\Bigg[\left(\lim_{\varepsilon\to 0} C^{\varepsilon,L}_{BS}(S,0) + \tau\lim_{\varepsilon\to 0}\frac{\partial C^{\varepsilon,L}_{BS}}{\partial \tau}(S,0) + \frac{1}{2}\tau^2\lim_{\varepsilon\to 0}\frac{\partial^2 C^{\varepsilon,L}_{BS}}{\partial \tau^2}(S,0) + \cdots\right)\\
&\qquad\qquad - \left(\lim_{\varepsilon\to 0} C^{\varepsilon,H}_{BS}(S,0) + \tau\lim_{\varepsilon\to 0}\frac{\partial C^{\varepsilon,H}_{BS}}{\partial \tau}(S,0) + \frac{1}{2}\tau^2\lim_{\varepsilon\to 0}\frac{\partial^2 C^{\varepsilon,H}_{BS}}{\partial \tau^2}(S,0) + \cdots\right)\Bigg]\\
&\quad - f_{LH}(f_{HL}+f_{LH})\frac{\tau^2}{2!}\Bigg[\left(\lim_{\varepsilon\to 0} C^{\varepsilon,L}_{BS}(S,0) + \tau\lim_{\varepsilon\to 0}\frac{\partial C^{\varepsilon,L}_{BS}}{\partial \tau}(S,0) + \cdots\right)
\end{aligned}$$

$$
\begin{aligned}
&- \left(\lim_{\varepsilon\to 0} C_{BS}^{\varepsilon,H}(S,0) + \tau \lim_{\varepsilon\to 0} \frac{\partial C_{BS}^{\varepsilon,H}}{\partial\tau}(S,0) + \cdots \right) \Bigg] \\
&- f_{LH}(f_{HL} + f_{LH})^2 \frac{\tau^3}{3!} \Big[\Big(\lim_{\varepsilon\to 0} C_{BS}^{\varepsilon,L}(S,0) + \cdots \Big) - \Big(\lim_{\varepsilon\to 0} C_{BS}^{\varepsilon,H}(S,0) + \cdots \Big) \Big] \\
&+ \cdots + \text{additional terms}, \qquad (4.54)
\end{aligned}
$$

$$
\begin{aligned}
\approx & \Bigg[\sum_{n=0}^{\infty} \frac{\tau^n}{n!} \lim_{\varepsilon\to 0} \frac{\partial^{(n)} C_{BS}^{\varepsilon,H}}{\partial\tau^{(n)}}(S,0) - \sum_{n=0}^{\infty} \frac{\tau^n}{n!} \lim_{\varepsilon\to 0} \frac{\partial^{(n)} C_{BS}^{\varepsilon,L}}{\partial\tau^{(n)}}(S,0) \Bigg] \\
& \cdot (-f_{LH}) \left(\tau + (f_{HL} + f_{LH}) \frac{\tau^2}{2!} + (f_{HL} + f_{LH})^2 \frac{\tau^3}{3!} + \cdots \right), \qquad (4.55)
\end{aligned}
$$

$$
\approx -f_{LH} \Big[C_{BS}^{H}(S,\tau) - C_{BS}^{L}(S,\tau) \Big] \sum_{n=0}^{\infty} \frac{\tau^{n+1}}{(n+1)!} (f_{HL} + f_{LH})^n, \qquad (4.56)
$$

$$
\Rightarrow X(S,\tau) \approx -f_{LH} \Big[C_{BS}^{H}(S,\tau) - C_{BS}^{L}(S,\tau) \Big] \left(\frac{e^{(f_{HL}+f_{LH})\tau} - 1}{f_{HL} + f_{LH}} \right). \qquad (4.57)
$$

Algebraic details were omitted and can be found in Mielkie and Davison [33].

We now have approximate solutions for both of our volatility state's option price differences $X(S,\tau)$ and $Y(S,\tau)$.

$$
Y(S,\tau) \approx -f_{HL} \Big[C_{BS}^{H}(S,\tau) - C_{BS}^{L}(S,\tau) \Big] \left(\frac{e^{(f_{HL}+f_{LH})\tau} - 1}{f_{HL} + f_{LH}} \right) \qquad (4.58)
$$

$$
X(S,\tau) \approx -f_{LH} \Big[C_{BS}^{H}(S,\tau) - C_{BS}^{L}(S,\tau) \Big] \left(\frac{e^{(f_{HL}+f_{LH})\tau} - 1}{f_{HL} + f_{LH}} \right) \qquad (4.59)
$$

In our approximate solution for $Y(S,\tau)$, the Black-Scholes option prices $C_{BS}^{H}(S,\tau)$ and $C_{BS}^{L}(S,\tau)$ are treated as constant since we only have one value for a given S and τ. It is left to show that $Y(S,\tau)$ converges for all possible values of f_{HL}, f_{LH} and that $Y(S,\tau), X(S,\tau) \geq 0$ also holds. Since we are pricing under the risk-neutral measure (i.e. $m_{HL} = m_{LH} = 0$), it follows that $f_{HL}, f_{LH} \leq 0$ as:

$$
f_{HL} = -\lambda_{HL}, \qquad (4.60)
$$

$$
f_{LH} = -\lambda_{LH}, \qquad (4.61)
$$

where $\lambda_{HL}, \lambda_{LH} \geq 0$. In order to prove convergence of both $Y(S,\tau)$ and $X(S,\tau)$ and show that $Y(S,\tau), X(S,\tau) \geq 0$, the limits as $f_{ij} \to 0$ must be investigated for all i. First check the limit as $f_{ij} \to 0$ for $i \in \{H, L\}$ where $i \neq j$. Note if $f_{ij} = 0 \Rightarrow \lambda_{ij} = 0$, this essentially removes the switching effect for state i under the risk-neutral measure. We will also have to make use of the fact that the Black-Scholes call prices are bounded such that $0 \leq C_{BS}^{L}(S,\tau) \leq C_{BS}^{H}(S,\tau) < S$ holds. First, for $Y(S,\tau)$,

$$
\Rightarrow \lim_{f_{HL}\to 0} Y(S,\tau) = 0. \qquad (4.62)
$$

$$\lim_{f_{LH}\to 0} Y(S,\tau) = -\Big[C_{BS}^{H}(S,\tau) - C_{BS}^{L}(S,\tau)\Big]\Big(e^{f_{HL}\tau} - 1\Big), \tag{4.63}$$

$$\Rightarrow 0 \leq \lim_{f_{LH}\to 0} Y(S,\tau) < S. \tag{4.64}$$

$$\Rightarrow \lim_{f_{HL}=f_{LH}=F\to 0} Y(S,\tau) = -F\Big[C_{BS}^{H}(S,\tau) - C_{BS}^{L}(S,\tau)\Big]\frac{e^{2F\tau}-1}{2F} = 0. \tag{4.65}$$

Then for $X(S,\tau)$,

$$\Rightarrow \lim_{f_{LH}\to 0} X(S,\tau) = 0. \tag{4.66}$$

$$\lim_{f_{HL}\to 0} X(S,\tau) = -\Big[C_{BS}^{H}(S,\tau) - C_{BS}^{L}(S,\tau)\Big]\Big(e^{f_{LH}\tau} - 1\Big), \tag{4.67}$$

$$\Rightarrow 0 \leq \lim_{f_{HL}\to 0} X(S,\tau) < S. \tag{4.68}$$

$$\Rightarrow \lim_{f_{HL}=f_{LH}=F\to 0} X(S,\tau) = -F\Big[C_{BS}^{H}(S,\tau) - C_{BS}^{L}(S,\tau)\Big]\frac{e^{2F\tau}-1}{2F} = 0. \tag{4.69}$$

Now check all limits as $f_{ij} \to -\infty$ for $i \in \{H, L\}$ where $i \neq j$. First for $Y(S,\tau)$,

$$\lim_{f_{HL}\to -\infty} Y(S,\tau) = \Big[C_{BS}^{H}(S,\tau) - C_{BS}^{L}(S,\tau)\Big]\lim_{f_{HL}\to -\infty}\frac{f_{HL}}{f_{HL}+f_{LH}} \tag{4.70}$$

$$\overset{\text{L'H}}{=} \Big[C_{BS}^{H}(S,\tau) - C_{BS}^{L}(S,\tau)\Big], \tag{4.71}$$

$$\Rightarrow 0 \leq \lim_{f_{HL}\to -\infty} Y(S,\tau) < S. \tag{4.72}$$

$$\Rightarrow \lim_{f_{LH}\to -\infty} Y(S,\tau) = 0. \tag{4.73}$$

$$\begin{aligned}\lim_{f_{HL}=f_{LH}=F\to -\infty} Y(S,\tau) &= -F\Big[C_{BS}^{H}(S,\tau) - C_{BS}^{L}(S,\tau)\Big]\frac{e^{2F\tau}-1}{2F}\\ &= \frac{1}{2}\Big[C_{BS}^{H}(S,\tau) - C_{BS}^{L}(S,\tau)\Big],\end{aligned} \tag{4.74}$$

$$\Rightarrow 0 \leq \lim_{f_{HL}=f_{LH}=F\to -\infty} Y(S,\tau) < S. \tag{4.75}$$

Then for $X(S,\tau)$,

$$\lim_{f_{LH}\to -\infty} X(S,\tau) = \Big[C_{BS}^{H}(S,\tau) - C_{BS}^{L}(S,\tau)\Big]\lim_{f_{LH}\to -\infty}\frac{f_{LH}}{f_{HL}+f_{LH}} \overset{\text{L'H}}{=} \Big[C_{BS}^{H}(S,\tau) - C_{BS}^{L}(S,\tau)\Big], \tag{4.76}$$

$$\Rightarrow 0 \leq \lim_{f_{LH}\to -\infty} X(S,\tau) < S. \tag{4.77}$$

$$\Rightarrow \lim_{f_{HL}\to -\infty} X(S,\tau) = 0. \tag{4.78}$$

$$\begin{aligned}\lim_{f_{HL}=f_{LH}=F\to -\infty} X(S,\tau) &= -F\Big[C_{BS}^{H}(S,\tau) - C_{BS}^{L}(S,\tau)\Big]\frac{e^{2F\tau}-1}{2F}\\ &= \frac{1}{2}\Big[C_{BS}^{H}(S,\tau) - C_{BS}^{L}(S,\tau)\Big],\end{aligned} \tag{4.79}$$

$$\Rightarrow 0 \leq \lim_{f_{HL}=f_{LH}=F\to -\infty} X(S,\tau) < S. \tag{4.80}$$

Now that convergence and non-negativity has been proven, we can make use of our approximate solutions for $Y(S,\tau)$ and $X(S,\tau)$. Reversing time again by letting $t = T - \tau$, we derive approximate solutions for our state-dependent regime-switching option prices.

$$C^H(S,t) \approx C^H_{BS}(S,t) + f_{HL}\Big[C^H_{BS}(S,t) - C^L_{BS}(S,t)\Big]\left(\frac{e^{(f_{HL}+f_{LH})(T-t)} - 1}{f_{HL} + f_{LH}}\right), \tag{4.81}$$

$$C^L(S,t) \approx C^L_{BS}(S,t) - f_{LH}\Big[C^H_{BS}(S,t) - C^L_{BS}(S,t)\Big]\left(\frac{e^{(f_{HL}+f_{LH})(T-t)} - 1}{f_{HL} + f_{LH}}\right). \tag{4.82}$$

Since we know the Black-Scholes option prices are differentiable with respect to S (when $\tau > 0$), we also derive approximate solutions for the regime-switching Deltas. For our purposes, Delta is defined as the sensitivity of the option price to changes in the stock price.

$$\frac{\partial C^H}{\partial S}(S,t) \approx \frac{\partial C^H_{BS}}{\partial S}(S,t) + f_{HL}\left(\frac{\partial C^H_{BS}}{\partial S}(S,t) - \frac{\partial C^L_{BS}}{\partial S}(S,t)\right)\left(\frac{e^{(f_{HL}+f_{LH})(T-t)} - 1}{f_{HL} + f_{LH}}\right), \tag{4.83}$$

$$\frac{\partial C^L}{\partial S}(S,t) \approx \frac{\partial C^L_{BS}}{\partial S}(S,t) - f_{LH}\left(\frac{\partial C^H_{BS}}{\partial S}(S,t) - \frac{\partial C^L_{BS}}{\partial S}(S,t)\right)\left(\frac{e^{(f_{HL}+f_{LH})(T-t)} - 1}{f_{HL} + f_{LH}}\right) \tag{4.84}$$

Therefore by applying the Cauchy-Kowalevski Theorem, we can obtain expressions denoting state-dependent regime-switching option prices and their corresponding Deltas. Our approximate solution converged according to basic calculus techniques and results, thus unique state-dependent option price and corresponding Delta solutions do exist in a regime-switching market, given the appropriate initial condition. Below is the generalized version of our result for the two state case.

$$C^i(S,t) \approx C^i_{BS}(S,t) - f_{ij}\Big(C^j_{BS}(S,t) - C^i_{BS}(S,t)\Big)g(t,T), \tag{4.85}$$

$$\frac{\partial C^i}{\partial S}(S,t) \approx \frac{\partial C^i_{BS}}{\partial S}(S,t) - f_{ij}\left(\frac{\partial C^j_{BS}}{\partial S}(S,t) - \frac{\partial C^i_{BS}}{\partial S}(S,t)\right)g(t,T), \tag{4.86}$$

where for $i \in \{H, L\}$ and $i \neq j$,

$$f_{ij} = -\big(\lambda_{ij} - m_{ij}\big), \tag{4.87}$$

$$g(t,T) = \frac{e^{(f_{ij}+f_{ji})(T-t)} - 1}{f_{ij} + f_{ji}}, \tag{4.88}$$

$$C^k_{BS}(S,t) = S(t)N(d^k_1) - Ke^{-r(T-t)}N(d^k_2), \tag{4.89}$$

$$\frac{\partial C^k_{BS}}{\partial S}(S,t) = N(d^k_1), \tag{4.90}$$

$$d^k_1 = \frac{\ln\frac{S(t)}{K} + (r + \frac{1}{2}\sigma^2_k)(T-t)}{\sigma_k\sqrt{T-t}}, \tag{4.91}$$

$$d^k_2 = d^k_1 - \sigma_k\sqrt{T-t}, \tag{4.92}$$

$$N(x) = \frac{1}{\sqrt{2\pi}} \int_{-\infty}^{x} e^{-\frac{z^2}{2}} dz, \tag{4.93}$$

$$k = i, j. \tag{4.94}$$

4.3 Error Introduced by Approximate Solution

We seek to quantify the error introduced by our approximate continuous-time regime-switching option price given by equation (4.85). Since the true solution to our coupled pricing problem is unknown, we treat our problem as a root finding problem to determine the error. Our pricing equation is treated as an operator on the state-dependent option price. For this section, notation will be reduced for improved readability where $C^i \equiv C^i(S,t)$ and $C^i_{BS} \equiv C^i_{BS}(S,t)$.

$$\mathcal{L}_{R-S}(C^i) = \frac{\partial C^i}{\partial t} + \frac{1}{2}\sigma_i^2 S^2 \frac{\partial^2 C^i}{\partial S^2} + rS\frac{\partial C^i}{\partial S} - rC^i - f_{ij}\Big[C^j - C^i\Big]. \tag{4.95}$$

Recall that

$$C^i \approx C^i_{BS} - f_{ij}\Big[C^j_{BS} - C^i_{BS}\Big]g(t,T), \tag{4.96}$$

where for $i \in \{H, L\}$ and $i \neq j$:

$$g(t,T) = \frac{e^{(f_{ij}+f_{ji})(T-t)} - 1}{f_{ij} + f_{ji}}, \tag{4.97}$$

$$f_{ij} = -\big(\lambda_{ij} - m_{ij}\big), \tag{4.98}$$

and C^i_{BS} is the Black-Scholes call price dependent on volatility state i.

We consider the backward error associated with our approximate solution as a way to quantify the accuracy of our estimate compared to the actual solution (Bradie [10]; Sauer [38]) . Backward error is found by substituting the approximation back into the original problem, in our case into the coupled pricing equations. If a solution is exact, the associated backward error will be zero. To determine the error imposed by our approximate solution we consider the backward error $\Big|\mathcal{L}_{R-S}(C^i)\Big|$.

We will first simplify the notation for the regime-switching operator.

$$\mathcal{L}_{R-S}(C^i) = \theta^i + \frac{1}{2}\sigma_i^2 S^2 \Gamma^i + rS\Delta^i - rC^i - f_{ij}\Big[C^j - C^i\Big], \tag{4.99}$$

such that

$$\Delta^i \approx \Delta^i_{BS} - f_{ij}\Big[\Delta^j_{BS} - \Delta^i_{BS}\Big]g(t,T), \tag{4.100}$$

$$\Gamma^i \approx \Gamma^i_{BS} - f_{ij}\Big[\Gamma^j_{BS} - \Gamma^i_{BS}\Big]g(t,T), \tag{4.101}$$

$$\theta^i \approx \theta^i_{BS} - f_{ij}\Big[\theta^j_{BS} - \theta^i_{BS}\Big]g(t,T) + f_{ij}e^{(f_{ij}+f_{ji})(T-t)}\Big[\theta^j_{BS} - \theta^i_{BS}\Big], \tag{4.102}$$

where:

- $\Delta^i = \dfrac{\partial C^i}{\partial S}$ is the sensitivity of the option price with respect to the stock price
- $\Gamma^i = \dfrac{\partial^2 C^i}{\partial S^2} = \dfrac{\partial \Delta^i}{\partial S}$ is the sensitivity of Delta with respect to the stock price
- $\theta^i = \dfrac{\partial C^i}{\partial t}$ is the sensitivity of the option price with respect to time

The Greeks $\Delta^i_{BS}, \Gamma^i_{BS}, \theta^i_{BS}$, refer to those sensitivities with respect to the Black-Scholes option prices conditional on volatility state i. It was assumed that the Poisson intensities, λ_{ij}, and the state-dependent market prices of risk, $m_{ij}(S,t)$ are constant, thus the coefficients coupling the source terms, f_{ij}, are also constant for $i \in \{H, L\}$ where $i \neq j$. Substituting equations (4.100), (4.101), and (4.102) into equation (4.99), we get:

$$
\begin{aligned}
\mathcal{L}_{R\text{-}S}(C^i) = {} & \theta^i_{BS} - f_{ij}\Big[\theta^j_{BS} - \theta^i_{BS}\Big]g(t,T) + f_{ij}e^{(f_{ij}+f_{ji})(T-t)}\Big[\theta^j_{BS} - \theta^i_{BS}\Big] \\
& + \frac{1}{2}\sigma_i^2 S^2\Big(\Gamma^i_{BS} - f_{ij}\Big[\Gamma^j_{BS} - \Gamma^i_{BS}\Big]g(t,T)\Big) + rS\Big(\Delta^i_{BS} - f_{ij}\Big[\Delta^j_{BS} - \Delta^i_{BS}\Big]g(t,T)\Big) \\
& - r\Big(C^i_{BS} - f_{ij}\Big[C^j_{BS} - C^i_{BS}\Big]g(t,T)\Big) \\
& - f_{ij}\Big(C^j_{BS} - f_{ji}\Big[C^i_{BS} - C^j_{BS}\Big]g(t,T) - C^i_{BS} + f_{ij}\Big[C^j_{BS} - C^i_{BS}\Big]g(t,T)\Big), \qquad (4.103) \\
\Rightarrow \mathcal{L}_{R\text{-}S}(C^i) = {} & \theta^i_{BS} + \frac{1}{2}\sigma_i^2 S^2\Gamma^i_{BS} + rS\,\Delta^i_{BS} - rC^i_{BS} \\
& + f_{ij}g(t,T)\Big(\theta^i_{BS} + \frac{1}{2}\sigma_i^2 S^2\Gamma^i_{BS} + rS\,\Delta^i_{BS} - rC^i_{BS}\Big) \\
& - f_{ij}g(t,T)\Big(\theta^j_{BS} + \frac{1}{2}\sigma_i^2 S^2\Gamma^j_{BS} + rS\,\Delta^j_{BS} - rC^j_{BS}\Big) \\
& + f_{ij}e^{(f_{ij}+f_{ji})(T-t)}\Big[C^j_{BS} - C^i_{BS}\Big] - f_{ij}\Big(1 + (f_{ij} + f_{ji})g(t,T)\Big)\Big[C^j_{BS} - C^i_{BS}\Big]. \qquad (4.104)
\end{aligned}
$$

We know from the Black-Scholes option pricing model [6] that the following holds:

$$
\theta^i_{BS} + \frac{1}{2}\sigma_i^2 S^2\Gamma^i_{BS} + rS\,\Delta^i_{BS} - rC^i_{BS} = 0. \qquad (4.105)
$$

Then,

$$
\begin{aligned}
\mathcal{L}_{R\text{-}S}(C^i) &= -f_{ij}g(t,T)\Big(\theta^j_{BS} + \frac{1}{2}\sigma_i^2 S^2\Gamma^j_{BS} + rS\,\Delta^j_{BS} - rC^j_{BS}\Big) \\
&\quad + f_{ij}e^{(f_{ij}+f_{ji})(T-t)}\Big[C^j_{BS} - C^i_{BS}\Big] - f_{ij}\Big(1 + (f_{ij} + f_{ji})g(t,T)\Big)\Big[C^j_{BS} - C^i_{BS}\Big] \\
&\quad + \frac{1}{2}\sigma_j^2 S^2\Gamma^j_{BS} f_{ij}g(t,T) - \frac{1}{2}\sigma_j^2 S^2\Gamma^j_{BS} f_{ij}g(t,T), \qquad (4.106) \\
&= -f_{ij}g(t,T)\Big(\theta^j_{BS} + \frac{1}{2}\sigma_j^2 S^2\Gamma^j_{BS} + rS\,\Delta^j_{BS} - rC^j_{BS}\Big)
\end{aligned}
$$

$$
\begin{aligned}
&-\frac{1}{2}(\sigma_i^2-\sigma_j^2)S^2\Gamma_{BS}^j f_{ij}g(t,T)\\
&+f_{ij}\Big[C_{BS}^j-C_{BS}^i\Big]\Big(e^{(f_{ij}+f_{ji})(T-t)}-\Big(1+(f_{ij}+f_{ji})g(t,T)\Big)\Big), \qquad (4.107)\\
=&-\frac{1}{2}(\sigma_i^2-\sigma_j^2)S^2\Gamma_{BS}^j f_{ij}g(t,T)\\
&+f_{ij}\Big[C_{BS}^j-C_{BS}^i\Big]\Big(e^{(f_{ij}+f_{ji})(T-t)}-\Big(1+(f_{ij}+f_{ji})g(t,T)\Big)\Big). \qquad (4.108)
\end{aligned}
$$

Substituting in equation (4.97),

$$
\begin{aligned}
\mathcal{L}_{R-S}(C^i)=&-\frac{1}{2}(\sigma_i^2-\sigma_j^2)S^2\Gamma_{BS}^j f_{ij}\left(\frac{e^{(f_{ij}+f_{ji})(T-t)}-1}{f_{ij}+f_{ji}}\right)\\
&+f_{ij}\Big[C_{BS}^j-C_{BS}^i\Big]\left[e^{(f_{ij}+f_{ji})(T-t)}-\left(1+(f_{ij}+f_{ji})\left(\frac{e^{(f_{ij}+f_{ji})(T-t)}-1}{f_{ij}+f_{ji}}\right)\right)\right], \qquad (4.109)\\
\Rightarrow \mathcal{L}_{R-S}(C^i)=&\ \frac{1}{2}\frac{f_{ij}}{f_{ij}+f_{ji}}(\sigma_i^2-\sigma_j^2)\Big(1-e^{(f_{ij}+f_{ji})(T-t)}\Big)S^2\Gamma_{BS}^j. \qquad (4.110)
\end{aligned}
$$

Therefore it follows that the backward error associated with our approximate regime-switching solution is:

$$
\Big|\mathcal{L}_{R-S}(C^i)\Big|=\frac{1}{2}\frac{f_{ij}}{f_{ij}+f_{ji}}\Big|\sigma_i^2-\sigma_j^2\Big|\Big(1-e^{(f_{ij}+f_{ji})(T-t)}\Big)S^2\Gamma_{BS}^j, \qquad (4.111)
$$

where for $i\in\{H,L\}$, $i\neq j$,

$$
\begin{aligned}
\Gamma_{BS}^j&=\frac{N'(d_1^j)}{S\sigma_j\sqrt{T-t}}, \qquad (4.112)\\
d_1^j&=\frac{\ln\frac{S}{K}+\Big(r+\frac{1}{2}\sigma_j^2\Big)(T-t)}{\sigma_j\sqrt{T-t}}, \qquad (4.113)\\
N'(d_1^j)&=\frac{1}{\sqrt{2\pi}}e^{-\frac{1}{2}(d_1^j)^2}. \qquad (4.114)
\end{aligned}
$$

Recall that our regime-switching PDE is derived using standard hedging and arbitrage arguments. Financially, this means that the price of the option obtained by solving this pricing equation must be the fair price for all investors taking a position in the option. In other words, since it is assumed that we are continuously rebalancing our hedge position against both volatility and stock price movements, the investor should not obtain a risk-less profit (i.e. on average trading gains/losses must net out to zero). If, in this sense, the option is priced fairly, the left hand side of the PDE should equate to zero when the option value and their corresponding Greeks are substituted back in. If the price of the option does not allow for the PDE and hence our backward error to be zero, this means that the price of our option is allowing for an investor to experience trading gains/losses from their hedged position. Specifically, the backward error associated with our problem represents the rate of money generation/loss for an investor holding a hedged position in the regime-switching option. If a non-zero backward error persists for a large range of stock price values about the option's strike price, trading gains/losses are imminent and unavoidable.

Using financially intuitive checks, we examined the backwards error associated with our approximate regime-switching option price solution. The first of these checks is to consider when we can no longer switch out of current volatility regime i. This implies that $\lambda_{ij} \to 0 \Rightarrow f_{ij} \to 0$. It should be pointed that if the market were in the opposing regime j, it still could switch to regime i but once we entered this regime, we will no longer be able to leave it.

$$\lim_{f_{ij}\to 0}\left|\mathcal{L}_{R\text{-}S}(C^i)\right| = \lim_{f_{ij}\to 0}\frac{1}{2}\frac{f_{ij}}{f_{ij}+f_{ji}}\left|\sigma_i^2-\sigma_j^2\right|\left(1-e^{(f_{ij}+f_{ji})(T-t)}\right)S^2\Gamma_{BS}^j = 0. \tag{4.115}$$

The above result is consistent with intuition as we expect that the error vanishes when regimes persist forever and thus the pricing equations decouple. When the pricing equations decouple, our approximate solution for regime i becomes the Black-Scholes option pricing equation conditional on the current volatility state occupation. We know that the Black-Scholes PDE can be directly solved by the Black-Scholes call price, so the resulting backwards error is zero.

We can also consider what happens when we can no longer switch between the two volatility states in our framework. It should be noted that in order for $f_{ij}+f_{ji} = 0$ to hold, since $f_{ij} \leq 0$ it follows that all $f_{ij} = 0$ for $i \in \{H, L\}$ where $i \neq j$. Thus let $f_{ij} = F$ and take the limit as F approaches zero.

$$\lim_{F\to 0}\left|\mathcal{L}_{R\text{-}S}(C^i)\right| = \lim_{F\to 0}\frac{1}{2}\frac{F}{2F}\left|\sigma_i^2-\sigma_j^2\right|\left(1-e^{2F(T-t)}\right)S^2\Gamma_{BS}^j \tag{4.116}$$

$$= \frac{1}{4}\left|\sigma_i^2-\sigma_j^2\right|\lim_{F\to 0}\left(1-e^{2F(T-t)}\right)S^2\Gamma_{BS}^j \tag{4.117}$$

$$\Rightarrow \lim_{F\to 0}\left|\mathcal{L}_{R\text{-}S}(C^i)\right| = 0 \tag{4.118}$$

Once again, we expected the error to vanish as our model reduced to a decoupled system of state-dependent Black-Scholes pricing equations for which we know the exact solution.

Finally, we can check what happens to our error as we approach maturity.

$$\lim_{t\to T}\left|\mathcal{L}_{R\text{-}S}(C^i)\right| = \lim_{f_{ij}\to 0}\frac{1}{2}\frac{f_{ij}}{f_{ij}+f_{ji}}\left|\sigma_i^2-\sigma_j^2\right|\left(1-e^{(f_{ij}+f_{ji})(T-t)}\right)S^2\Gamma_{BS}^j = 0. \tag{4.119}$$

The error vanishes since the regime-switching option's payoffs are independent of volatility state occupation. In other words, since the options priced under our regime-switching framework satisfy the same final conditions as do those under the Black-Scholes framework, it is expected that the error associated with our approximate solution vanishes.

Overall, the equation derived for our backwards error estimate for the approximate regime-switching option pricing solution shows that the error introduced into our state-dependent pricing PDEs is a weighted (by Poisson intensities) time-valued measure of the opposing regime's sensitivity to changes in the underlying asset's price. The approximate solution and its backward error are discussed in greater detail in the following section.

4.4 Discussion

Consider the generalized approximate solutions for our two volatility regimes: high and low,

$$C^H(S,t) \approx C^H_{BS}(S,t) + f_{HL}\Big[C^H_{BS}(S,t) - C^L_{BS}(S,t)\Big]g(t,T), \tag{4.120}$$

$$C^L(S,t) \approx C^L_{BS}(S,t) - f_{LH}\Big[C^H_{BS}(S,t) - C^L_{BS}(S,t)\Big]g(t,T), \tag{4.121}$$

$$\frac{\partial C^H}{\partial S}(S,t) \approx \frac{\partial C^H_{BS}}{\partial S}(S,t) + f_{HL}\left[\frac{\partial C^H_{BS}}{\partial S}(S,t) - \frac{\partial C^L_{BS}}{\partial S}(S,t)\right]g(t,T), \tag{4.122}$$

$$\frac{\partial C^L}{\partial S}(S,t) \approx \frac{\partial C^L_{BS}}{\partial S}(S,t) - f_{LH}\left[\frac{\partial C^H_{BS}}{\partial S}(S,t) - \frac{\partial C^L_{BS}}{\partial S}(S,t)\right]g(t,T), \tag{4.123}$$

where:

$$g(t,T) = \frac{e^{(f_{HL}+f_{LH})(T-t)} - 1}{f_{HL} + f_{LH}}, \tag{4.124}$$

$$f_{HL} = -\big(\lambda_{HL} - m_{HL}\big), \tag{4.125}$$

$$f_{LH} = -\big(\lambda_{LH} - m_{LH}\big). \tag{4.126}$$

It would seem logical to state an ansatz where the regime-switching solution is a weighted combination of the high and low volatility Black-Scholes options prices and solve the corresponding partial differential equations for the state-dependent weights. Unfortunately, assuming that $f_{HL} \neq f_{LH}$, the coupled partial differential equations for the weights are in fact more complicated than those of the original problem and there is no improvement which warrants using this approach over our proposed method.

Financially, f_{ij} acts as an adjustment term for a particular state's option price. Given the intensity of our Poisson process and our current state's level of volatility, f_{ij} allows for the price to reflect the immediate market conditions. Intuitively, these state-dependent relations make financial sense because, if we assumed $f_{HL} = f_{LH} = 0$, the pricing partial differential equations decouple and reduce to the state-dependent Black-Scholes pricing equations [6], as expected. In addition, if the high and low regime volatilities were the same, the source terms driven by f_{HL}, f_{LH} would vanish, once again leaving Black-Scholes type option pricing equations.

Since the $\lambda_{HL}, \lambda_{LH} \geq 0$, it follows that $f_{HL}, f_{LH} \leq 0$ under the risk-neutral measure. It is interesting to consider our approximate option price solution and its associated backward error under the risk neutral measure, found by substituting equations (4.124), (4.125), and (4.126) into equations (4.120), (4.121), and (4.111). This gives us the following relations:

$$C^H(S,t) \approx C^H_{BS}(S,t)[1 - \alpha_H(t)] + C^L_{BS}(S,t)\alpha_H(t), \tag{4.127}$$

$$C^L(S,t) \approx C^L_{BS}(S,t)[1 - \alpha_L(t)] + C^H_{BS}(S,t)\alpha_L(t), \tag{4.128}$$

$$\Big|\mathcal{L}_{R-S}(C^H)\Big| = \frac{1}{2}\alpha_H(t)(\sigma_H^2 - \sigma_L^2)S^2\Gamma^L_{BS}, \tag{4.129}$$

$$\Big|\mathcal{L}_{R-S}(C^L)\Big| = \frac{1}{2}\alpha_L(t)(\sigma_H^2 - \sigma_L^2)S^2\Gamma^H_{BS}, \tag{4.130}$$

where:

$$\alpha_H(t) = \frac{\lambda_{HL}}{\lambda_{HL} + \lambda_{LH}}\Big(1 - e^{-(\lambda_{HL}+\lambda_{LH})(T-t)}\Big), \tag{4.131}$$

$$\alpha_L(t) = \frac{\lambda_{LH}}{\lambda_{HL} + \lambda_{LH}}\Big(1 - e^{-(\lambda_{HL}+\lambda_{LH})(T-t)}\Big), \tag{4.132}$$

such that $\lambda_{HL} + \lambda_{HL} \neq 0$, which holds due to our previous assumption that the arrival rates of the Poisson processes must be strictly positive.

The weights $\alpha_H(t), \alpha_L(t)$ are time dependent, decaying as we approach the maturity date of the option, T. Our state-dependent regime switching option prices depend on the percentage of time volatility switches to the opposing regime, conditional on switching regimes at all. The impact of the probability of switching regimes on our state-dependent option price is greatest at the initiation of the contract (i.e. at $t = 0$). For example, it is clear that as $t \to T$, the impact of switching to the low regime on our high option price becomes less influential and that for sufficiently small time left until maturity, our regime-switching price can be approximated by the corresponding Black-Scholes price. Thus as we approach maturity, our option price solution approaches the corresponding Black-Scholes option price and thus to the given final conditions. In addition, since both state's errors decay as $t \to T$, our approximate solution introduces the most error into the regime-switching pricing PDE about the strike price, K, at contract initiation, $t = 0$.

We can consider what occurs to our state-dependent regime-switching option prices as one of the Poisson intensities becomes infinitely large. First consider when the intensity λ_{HL} of the process driving jumps to the low volatility regime becomes infinitely large:

$$\lim_{\lambda_{HL}\to\infty} C^{H,L}(S,t) = C^L_{BS}(S,t), \tag{4.133}$$

$$\lim_{\lambda_{HL}\to\infty} \left|\mathcal{L}_{R-S}(C^H)\right| = \frac{1}{2}(\sigma_H^2 - \sigma_L^2)S^2\Gamma^L_{BS}, \tag{4.134}$$

$$\lim_{\lambda_{HL}\to\infty} \left|\mathcal{L}_{R-S}(C^L)\right| = 0. \tag{4.135}$$

Now consider as the intensity, λ_{LH}, of the process driving jumps to the high regime becomes large:

$$\lim_{\lambda_{LH}\to\infty} C^{H,L}(S,t) = C^H_{BS}(S,t), \tag{4.136}$$

$$\lim_{\lambda_{LH}\to\infty} \left|\mathcal{L}_{R-S}(C^H)\right| = 0, \tag{4.137}$$

$$\lim_{\lambda_{LH}\to\infty} \left|\mathcal{L}_{R-S}(C^L)\right| = \frac{1}{2}(\sigma_H^2 - \sigma_L^2)S^2\Gamma^H_{BS}. \tag{4.138}$$

It can be noted that when the intensity of the process governing jumps to one regime is infinitely large, both state-dependent regime-switching option prices are approximated by the corresponding Black-Scholes option price. This is due to the fact that the market will always switch back to this regime no matter what, therefore it makes sense to price the option as if we are in a constant volatility world.

Furthermore, it is interesting to consider what values our option prices take on as the intensities of both Poisson processes become extremely large (i.e. approach infinity). We get:

$$\lim_{\lambda_{HL},\lambda_{LH}\to\infty} C^{H,L}(S,t) \approx \frac{1}{2}\Big[C^{H}_{BS}(S,t) + C^{L}_{BS}(S,t)\Big], \tag{4.139}$$

$$\lim_{\lambda_{HL},\lambda_{LH}\to\infty} \Big|\mathcal{L}_{R-S}(C^{H})\Big| = \frac{1}{4}(\sigma^2_H - \sigma^2_L)S^2\Gamma^{L}_{BS}, \tag{4.140}$$

$$\lim_{\lambda_{HL},\lambda_{LH}\to\infty} \Big|\mathcal{L}_{R-S}(C^{L})\Big| = \frac{1}{4}(\sigma^2_H - \sigma^2_L)S^2\Gamma^{H}_{BS}. \tag{4.141}$$

When there are infinitely many regime switches possible, neither the initial regime or currently occupied regime have an impact on the option price. Thus our regime-switching option price is written as an equally weighted combination of the possible state's Black-Scholes option prices. The error introduced by our regime-switching option price approximations depend directly on the sensitivity of the option with respect to the underlying if it occupied the other regime. Furthermore, if the intensities of our respective Poisson processes are equal (i.e. $\lambda_{HL} = \lambda_{LH} = \tilde{\lambda}$ where $\tilde{\lambda}$ is a constant), then our regime-switching option price is an equally weighted combination of Black-Scholes option prices conditional on high or low volatility state.

$$C^{H,L}(S,t) \approx \frac{1}{2}\Big[C^{H}_{BS}(S,t) + C^{L}_{BS}(S,t)\Big], \tag{4.142}$$

$$\Big|\mathcal{L}_{R-S}(C^{H})\Big| = \frac{1}{4}(\sigma^2_H - \sigma^2_L)S^2\Gamma^{L}_{BS}, \tag{4.143}$$

$$\Big|\mathcal{L}_{R-S}(C^{L})\Big| = \frac{1}{4}(\sigma^2_H - \sigma^2_L)S^2\Gamma^{H}_{BS}. \tag{4.144}$$

It is important to note that when infinitely many regime switches are allowed, where the probability of leaving the currently occupied regimes are constant for all possible regimes, the actual probability has no effect on option price as it is computed using equal weights. The errors become almost identical but are still weighted with respect to the opposing regime's sensitivity to the underlying's price. For example, a higher volatility option is more sensitive to underlying movements in stock price, especially when the option is at the money. This is attributed to the fact that the error of the high volatility option is a function of the low volatility option's gamma, which takes on a value of higher magnitude about the strike. Therefore, the magnitude of the error introduced into the high regime PDE by the high state option increases as well.

Expected Return	r	0%
High State Volatility	σ_H	40%
Low State Volatility	σ_L	10%
Strike Price	K	\$100
Maximum Stock Price	S_{max}	\$300
Maturity Date	T	1 year
Daily High Jump Intensity	λ_{HL}	5%
Daily Low Jump Intensity	λ_{LH}	5%
High State MPVR	m_{HL}	0
Low State MPVR	m_{LH}	0
Number of Time Increments	$\tilde{L}$	252

Table 4.2: Parameters used in the implementation of the Crank-Nicolson numerical scheme.

To determine the reliability of our approximate solution, we compared it to the numerical solution of our coupled equations. A comparison of our approximate solutions to the numerical solutions in Figures 4.3 and 4.4 show that our approximate state-dependent solutions are fairly accurate over most stock prices. However, there is a larger discrepancy near the strike price. This is because we evaluated our Black-Scholes terms within the forcing terms using our initial condition evaluated at ε. The error in our approximate solution is largest in magnitude about the strike price, which is illustrated in the figure. However our goal was to find an approximate solution that had the same behaviour as the numerical solution, which was in fact realized as shown in Figures 4.3 and 4.4. Our result provides a quick and easy method to evaluate regime-switching options, and can be applied to other types of options only exercisable at maturity.

To further support our state-dependent error term, we compare the backward error associated with implementing the Crank-Nicolson numerical scheme on both the state-dependent decoupled Black-Scholes equations and the coupled regime-switching pricing partial differential equations. The backward error quantifies how the unknown error introduced by the approximate solution is magnified when introduced back into the original pricing PDE. The parameters are consistent with those previously used. The results of this calculation are summarized in Figures 4.5, 4.6 and 4.7.

It can be observed that the backward error plots of Figures 4.5, 4.6 and 4.7 all have a similar shape, suggesting that our approximate solution is a reasonable solution for our coupled pricing equation. Even in the implementation of Crank-Nicolson on the classical Black-Scholes PDE, the error introduced back into the PDE by the numerical solution has the largest magnitude about the strike price. As well, for our regime-switching error term, the greatest error is experienced when the option is at-the-money, $S = K$, although this error does dissipate as the exercise date of the option is approached. The magnitude of our error term is significantly greater, most notably near the money, which is expected as the error introduced from the approximate solution gets magnified when substituted back into the pricing equation.

In general, when considering the backward error associated with the Crank-Nicolson numerical solution of both the Black-Scholes and regime-switching PDEs, it can be observed that both states take on the largest error about the strike price, however the high state's error is greater or equal to the low state error for all stock prices. In comparison, when we consider our error term it can be noted that for the high state, the error is concentrated and of largest magni-

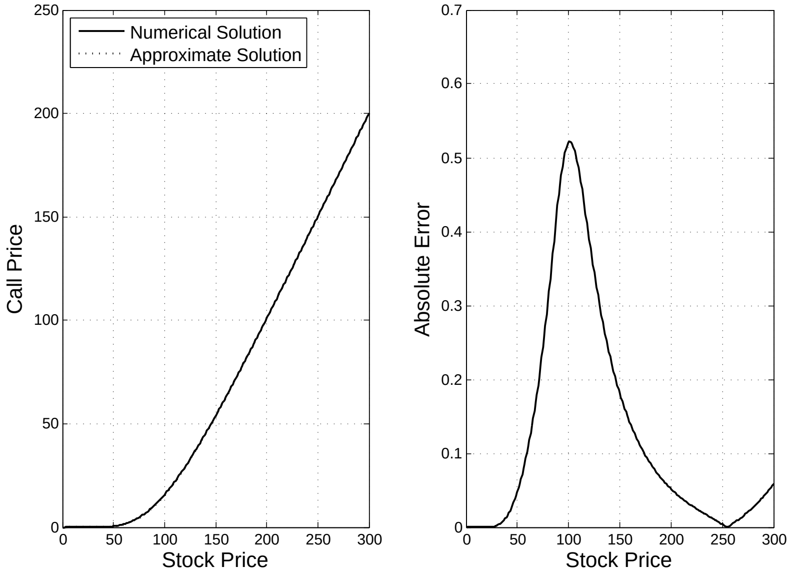

Figure 4.3: Comparison of the numerical and approximate solution of the high state regime-switching risk-neutral call option at $t = 0$. Parameters as given in Table 4.2.

tude near the stock price. The low state error is consistently smaller in magnitude but persists for most stock values. The persistence of the error among the stock prices is the main difference between our analytical backward error function and the numerical backward error found using Crank-Nicolson. Using the numerical scheme, the error introduced back into the PDE persists for almost all possible stock values, however our error is more concentrated around the strike, especially for the high regime option. This suggests that although our error is of greater magnitude, there is a smaller range of stock price values for which our method produces inaccurate approximations compared with the Crank-Nicholson numerical method. It is important to recall that substituting the approximate option price back into the PDE magnifies the error. The error between our approximate solution and the true solution are smaller in magnitude, as illustrated in Figures 4.3 and 4.4. For an option trader, smaller more persistent discrepancies in the option price could accumulate to more portfolio losses as compared to less likely larger errors in the price. Although the results produced by our approximate solution are not always as accurate as those found numerically, our result provides an easily understood, financially intuitive approximation.

Finally, the L^2-norm was computed to analyse the error between our approximate solution and the numerical solution found through the implementation of the Crank-Nicholson method. The first case considers the effect of time on the error introduced by our approximation. As shown in Figure 4.8, for both the high and low state options, the error decreases significantly as time approaches maturity. All parameters remained the same as in the previous example. This is consistent with our intuition that our approximate option prices would be the most inaccurate at the option's inception date. However, as our option prices diffuse to their boundary

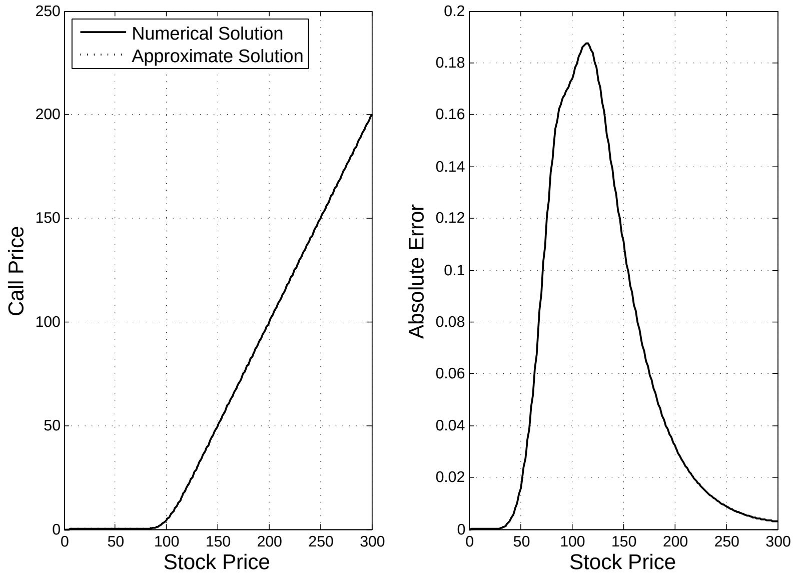

Figure 4.4: Comparison of the numerical and approximate solution of the low state regime-switching risk-neutral call option at $t = 0$. Parameters as given in Table 4.2.

conditions, the error diminishes.

Given that the greatest error observed between our solution and the numerical solution occurs at option inception, the last case will consider the error introduced at the initial time step $t = 0$, while varying the solution grid size. As the grid size increases, the step size, dt, decreases. The increments shown in Figure 4.9 are those associated with the time steps. As we decrease the size of the increments, the error increases. It is well known that the finer the numerical grid (i.e. smaller increments), the more accurate the numerical result. Since the L^2-norm is shown to grow with increased grid size, it can be concluded that it is the approximate solution, not the numerical solution, that is contributing to this increased error. It should be pointed out that in all three cases, the high state option price has a greater discrepancy error (larger L^2-norm) than the low state option price, indicating that our approximate solution is better suited for pricing in the low volatility regime than the high volatility regime.

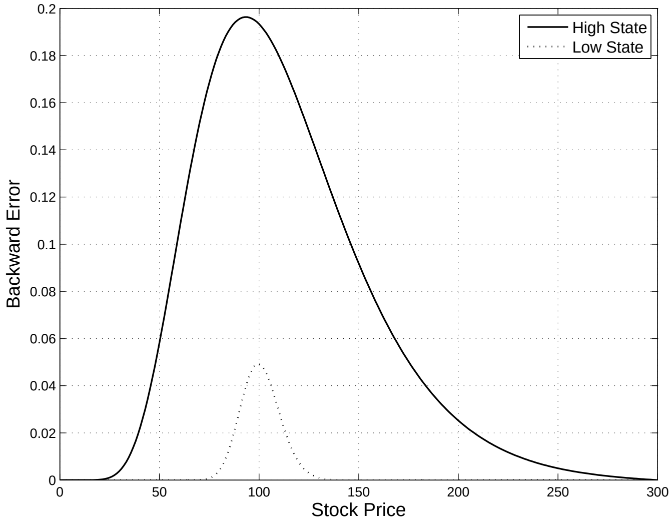

Figure 4.5: Comparison of the backward error associated with solving the state-dependent Black-Scholes PDEs at $t = 0$ using the Crank-Nicolson numerical scheme. Parameters as given in Table 4.2.

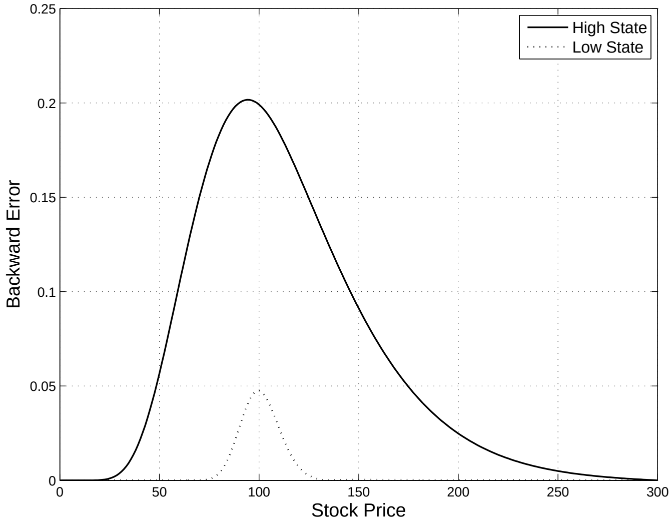

Figure 4.6: Comparison of the backward error associated with solving the coupled regime-switching risk-neutral PDEs at $t = 0$ using the Crank-Nicolson numerical scheme. Parameters as given in Table 4.2.

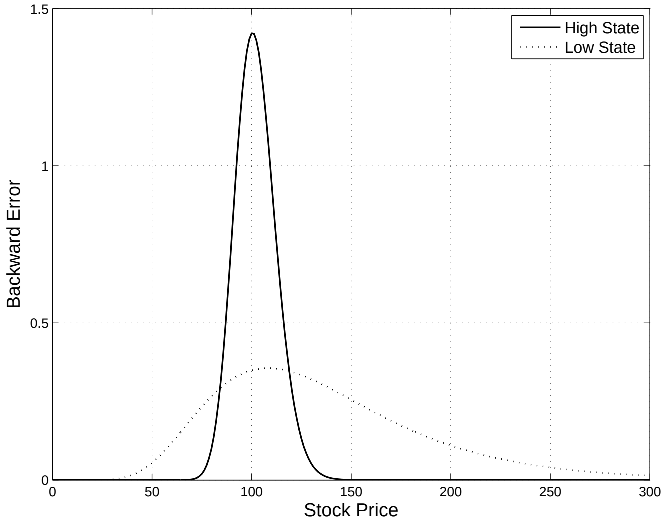

Figure 4.7: Comparison of the backward error associated with our approximate regime-switching risk-neutral solution at $t = 0$. Parameters as given in Table 4.2.

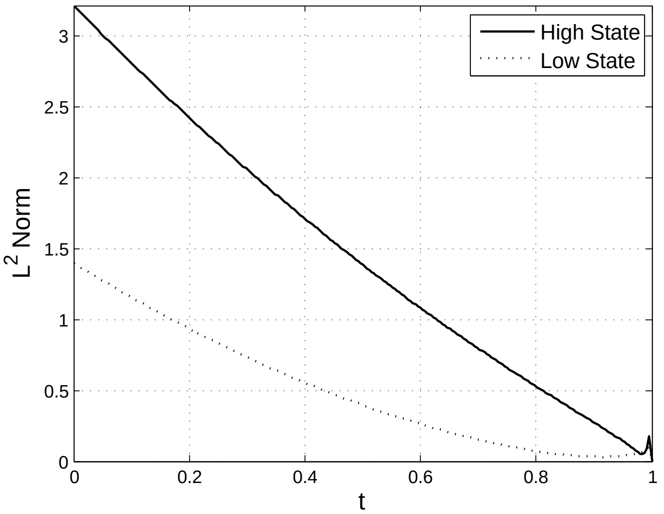

Figure 4.8: Effect of time on the L^2 norm associated with the difference between the approximate and numerical solutions for the regime-switching risk-neutral coupled PDEs. Parameters as given in Table 4.2.

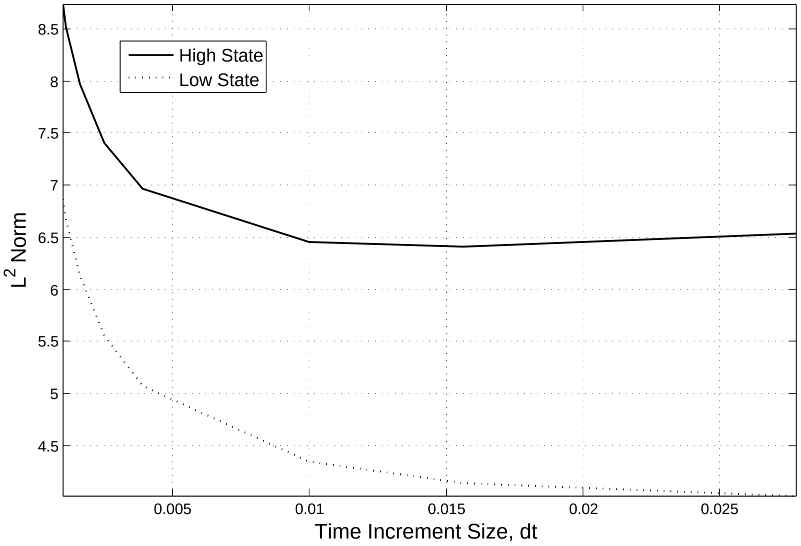

Figure 4.9: Effect of varying the time increments, dt, on the L^2 norm associated with the difference between the approximate and numerical solutions at $t = 0$ for the regime-switching risk-neutral coupled PDEs. Parameters as given in Table 4.2

4.5 Summary

In the presence of regime-switching volatility we derived coupled pricing partial differential equations dependent on the market price of volatility risk. Using the Cauchy-Kowalevski Theorem, the existence of unique state-dependent option prices was proven, and approximate solutions were derived from a series-type solution. Considering financial intuition, our problem was redefined to be a function of the corresponding volatility state's Black-Scholes option prices. As a result, continuous-time state-dependent solutions for both regime-switching option prices and Deltas were derived as functions of both the Black-Scholes option prices and the coefficients coupling the partial differential equation source terms. Overall, an examination of our results show that the impact of regime-switching is time-sensitive and decays as an option approaches its maturity date. Our new analytic approximation provides an easy and effective approximation technique that can easily be applied to other options written on underlyings with regime-switching volatility.

One of the main parameters embedded within the coefficients of the PDE source terms is the market price of volatility risk. Given our approximate solutions for the regime-switching option prices and Deltas, it is interesting to investigate the impact that varying the magnitude and sign of the risk premia has on these financial terms. This question will be addressed in the next chapter.

Chapter 5

Impact of Market Price of Volatility Risk

For decades, it has been of great importance to explain the differences between option prices obtained from option pricing models and the actual prices of options traded on stock exchanges around the world. Since the introduction of the seminal Black and Scholes [6] option pricing model, academics and practitioners have tried to quantify the discrepancies between theoretically predicted and observed option prices: to understand the difference between implied and realized volatility. Jackwerth and Rubinstein [29] found that an option's implied volatility is biased high compared to historical volatility. This difference has been attributed to the existence of volatility risk premia. Much work in financial econometrics supports the hypothesis that volatility risk premia are non-positive. Carr and Wu [12] used US equity data to support the existence of volatility risk premia. Boswijk [8] showed, using Dutch market data, evidence to prove the existence of the market price of volatility risk in equity markets.

The market price of volatility risk is important as it provides a way to measure a market's appetite for risk. Bakshi and Kapadia [5] showed in the presence of stochastic volatility that the underperformance of a delta-hedged portfolio was related to the existence of a negative market price of volatility risk. Work has also been done to show the existence of a negative market price of volatility risk in commodities markets. Doran and Ronn [16] used New York Mercantile Exchange options and futures data to show that the difference between the implied and realized volatility was directly related to the existence of a negative market price of volatility risk in energy markets (i.e. natural gas, crude oil, and heating oil).

The focus of this chapter is to examine the theoretical impact of the market price of volatility risk on pricing options in a regime-switching market. We saw in Chapter 2 that the market price of volatility risk arises in a coupled system of partial differential equations (PDEs) representing the price of a option written on an underlying with regime-switching volatility. In this model, the market price of volatility risk is a driving force in the effect the coupled source term has on a particular regime's option price. Since closed-form solutions are not available for the system of equations, approximate solutions for the option prices and hedge ratios were obtained through an application of a classical PDE theorem. The form of the approximate solutions, particularly with respect to the impact of the market price of volatility risk term, gives rise to financially intuitive results.

In general, an option seller takes on more risk in the high volatility state since greater uncertainty exists in the future price of the underlying asset relative to the low state. It is therefore natural to investigate the consequence of state-dependent market prices of volatility risk.

Duarte and Jones [17] showed that the volatility risk premium varies positively with the overall level of market volatility. As well as being positively correlated to volatility movement, Coval and Shumway [13] previously found evidence that the market price of volatility risk is time varying through their analysis of Chicago Board Options Exchange call and put price data. We will show theoretically that the existence of such option prices and their corresponding hedge ratios depend directly on restrictions placed on the market price of volatility risk, otherwise financially unrealistic solutions may arise. In particular, we will prove that state-dependent market prices of volatility risk must be negative, otherwise pricing model results defy basic financial intuition.

For the analysis presented in this chapter, we assume that λ_{ij} and m_{ij} are constant for each regime i where $i \in \{H, L\}$ such that $i \neq j$. In order for the problem to make sense we assume that $\lambda_{HL} > 0$ and $\lambda_{LH} > 0$ to avoid certain pathological cases.

5.1 Restrictions Derived Directly from Coupled Pricing Equations

Our financial intuition allows us to expect the regime-switching option prices to be bounded by the corresponding Black-Scholes option prices. Due to the possibility of switching to a different regime, the high regime option becomes less valuable and the low state option becomes more valuable in the presence of volatility switching. This motivates us to consider the difference between regime-switching and constant-volatility options. Recall that in Chapter 4 we redefined our regime-switching options in terms of these inherent differences, $Y(S,t)$ and $X(S,t)$, and derived a new set of coupled pricing equations.

$$C^H(S,t) = C^H_{BS}(S,t) - Y(S,t), \tag{5.1}$$

$$C^L(S,t) = C^L_{BS}(S,t) + X(S,t), \tag{5.2}$$

where $X(S,t), Y(S,t) \geq 0$.

The dynamics of the option prices can be analysed using the coupled PDEs directly. The time reversal transformation $\tau = T - t$ as well as the transformations in equations (5.1) and (5.2) yielded a new coupled system of PDEs given by equations (4.16) and (4.17) .

Although our new system of coupled equations for $X(S,\tau)$ and $Y(S,\tau)$ has analytic initial conditions, non-smoothness arises in the problem via the Black-Scholes relations found in the forcing terms. Given that the initial condition for the Black-Scholes pricing problem is not analytic, we previously considered a similar pricing problem conditional on volatility state i with solution $C^{i,\varepsilon}_{BS}(S,\tau)$ having an analytic initial condition:

$$C^{i,\varepsilon}_{BS}(S,0) = SN(d^{i,\varepsilon}_1) - Ke^{-r\varepsilon}N(d^{i,\varepsilon}_2), \tag{5.3}$$

where

$$d^{i,\varepsilon}_1 = \frac{\ln\frac{S}{K} + (r + \frac{1}{2}\sigma_i^2)\varepsilon}{\sigma_i\sqrt{\varepsilon}}, \tag{5.4}$$

$$d^{i,\varepsilon}_2 = d^{i,\varepsilon}_1 - \sigma_i\sqrt{\varepsilon}, \tag{5.5}$$

$$N(x) = \frac{1}{\sqrt{2\pi}} \int_{-\infty}^{x} e^{-\frac{z^2}{2}} dz. \tag{5.6}$$

For very small values of ε such that ε approaches zero, we assume the following:

$$C^{i}_{BS}(S,0) = \lim_{\varepsilon\to 0} C^{i,\varepsilon}_{BS}(S,0). \tag{5.7}$$

Analyzing our system of PDES at $\tau = 0$ and making use of the analytic initial condition of the closely related Black-Scholes problem:

$$\frac{\partial Y}{\partial \tau}(S,0) = -f_{HL}\left[\lim_{\varepsilon\to 0} C^{H,\varepsilon}_{BS}(S,0) - \lim_{\varepsilon\to 0} C^{L,\varepsilon}_{BS}(S,0)\right], \tag{5.8}$$

$$\frac{\partial X}{\partial \tau}(S,0) = -f_{LH}\left[\lim_{\varepsilon\to 0} C^{H,\varepsilon}_{BS}(S,0) - \lim_{\varepsilon\to 0} C^{L,\varepsilon}_{BS}(S,0)\right]. \tag{5.9}$$

Now, consider a Taylor series expansion of our option price differences about the point $\tau = 0$.

$$Y(S,\tau) = Y(S,0) + \tau\frac{\partial Y}{\partial \tau}(S,0) + \frac{1}{2}\tau^2\frac{\partial^2 Y}{\partial \tau^2}(S,0) + \ldots, \tag{5.10}$$

$$X(S,\tau) = X(S,0) + \tau\frac{\partial X}{\partial \tau}(S,0) + \frac{1}{2}\tau^2\frac{\partial^2 X}{\partial \tau^2}(S,0) + \ldots. \tag{5.11}$$

Then for very small τ such that $\tau >> \tau^2$, it follows that all terms of order $O(\tau^2)$ and higher may be neglected in our Taylor series expansions.

$$Y(S,\tau) = -f_{HL}\tau\left[\lim_{\varepsilon\to 0} C^{H,\varepsilon}_{BS}(S,0) - \lim_{\varepsilon\to 0} C^{L,\varepsilon}_{BS}(S,0)\right], \tag{5.12}$$

$$X(S,\tau) = -f_{LH}\tau\left[\lim_{\varepsilon\to 0} C^{H,\varepsilon}_{BS}(S,0) - \lim_{\varepsilon\to 0} C^{L,\varepsilon}_{BS}(S,0)\right]. \tag{5.13}$$

We know that $X(S,\tau), Y(S,\tau) \geq 0$ for all values of $\tau \geq 0$. Since it is well known that $\lim_{\varepsilon\to 0} C^{H,\varepsilon}_{BS}(S,0) - \lim_{\varepsilon\to 0} C^{L,\varepsilon}_{BS}(S,0) \geq 0$, it follows that:

$$Y(S,\tau) \geq 0, \tag{5.14}$$

$$-f_{HL}\tau\left[\lim_{\varepsilon\to 0} C^{H,\varepsilon}_{BS}(S,0) - \lim_{\varepsilon\to 0} C^{L,\varepsilon}_{BS}(S,0)\right] \geq 0, \tag{5.15}$$

$$\Rightarrow f_{HL} < 0. \tag{5.16}$$

Similarly,

$$X(S,\tau) \geq 0, \tag{5.17}$$

$$- f_{LH}\tau\left[\lim_{\varepsilon\to 0} C_{BS}^{H,\varepsilon}(S,0) - \lim_{\varepsilon\to 0} C_{BS}^{L,\varepsilon}(S,0)\right] \geq 0, \tag{5.18}$$

$$\Rightarrow f_{LH} < 0. \tag{5.19}$$

From equations (5.12) and (5.13), we can have the following relationship:

$$Y(S,\tau) = \frac{f_{HL}}{f_{LH}} X(S,\tau). \tag{5.20}$$

The relation given by (5.20) only holds for very small values of τ. Therefore when we are approaching maturity, the difference between the high state Black-Scholes option price and the corresponding regime-switching option price is a scaled difference between the low volatility Black-Scholes and regime-switching option prices. The scaling of this difference relies explicitly on the Poisson intensities and the state-dependent market prices of volatility risk. Since it was assumed that $X(S,\tau), Y(S,\tau) \geq 0$ and since Black-Scholes option prices are everywhere positive, it follows that both $f_{HL}, f_{LH} < 0$ also holds here. For all possible volatility states, if the coefficient of the source term coupling the pricing equations f_{ij} is negative, the state-dependent market prices of volatility risk are also negative for any possible Poisson intensity, λ_{ij}, as shown below.

$$f_{ij} < 0, \tag{5.21}$$

$$-\left(\lambda_{ij} - m_{ij}\right) < 0, \tag{5.22}$$

$$\Rightarrow m_{ij} < \lambda_{ij}. \tag{5.23}$$

Our regime-switching framework defined $\lambda_{ij} > 0$ to ensure switching occurs between volatility states. This implies that $m_{ij} \leq 0$ for any choice of hedge rebalancing period and for all possibly Poisson intensities. Thus in order to get economically reasonable regime-switching option prices, the state-dependent market prices of volatility risk must be negative. It remains to show that the same restrictions must hold for our approximate solutions.

5.2 Restrictions Derived from Approximate Solutions

In order to determine if the same restrictions for the state-dependent market prices of volatility risk exist for our approximate option prices, we write equations (4.85) and (4.86) explicitly for the high and low volatility regimes.

$$C^H(S,t) \approx C_{BS}^H(S,t) + f_{HL}[C_{BS}^H(S,t) - C_{BS}^L(S,t)]g(t,T), \tag{5.24}$$

$$C^L(S,t) \approx C_{BS}^L(S,t) - f_{LH}[C_{BS}^H(S,t) - C_{BS}^L(S,t)]g(t,T), \tag{5.25}$$

$$\frac{\partial C^H}{\partial S}(S,t) \approx \frac{\partial C_{BS}^H}{\partial S}(S,t) + f_{HL}\left[\frac{\partial C_{BS}^H}{\partial S}(S,t) - \frac{\partial C_{BS}^L}{\partial S}(S,t)\right]g(t,T), \tag{5.26}$$

$$\frac{\partial C^L}{\partial S}(S,t) \approx \frac{\partial C_{BS}^L}{\partial S}(S,t) - f_{LH}\left[\frac{\partial C_{BS}^H}{\partial S}(S,t) - \frac{\partial C_{BS}^L}{\partial S}(S,t)\right]g(t,T), \tag{5.27}$$

where:

$$f_{HL} = -\big(\lambda_{HL} - m_{HL}\big), \tag{5.28}$$

$$f_{LH} = -\big(\lambda_{LH} - m_{LH}\big), \tag{5.29}$$

$$g(t,T) = \frac{e^{(f_{HL}+f_{LH})(T-t)} - 1}{f_{HL} + f_{LH}}. \tag{5.30}$$

It is easy to show that $g(t,T) \geq 0$ for all $t \leq T$ and $f_{HL}, f_{LH} < 0$.

$$\begin{aligned} f_{HL} + f_{LH} < 0 \text{ and } -1 \leq e^{(f_{HL}+f_{LH})(T-t)} - 1 \leq 0, \\ \Rightarrow g(t,T) = \frac{e^{(f_{HL}+f_{LH})(T-t)} - 1}{f_{HL} + f_{LH}} \geq 0. \end{aligned} \tag{5.31}$$

Since f_{ij} is a function of the market price of volatility risk m_{ij} for $i \in \{H, L\}$ where $i \neq j$, we consider restrictions on f_{ij} which in turn define individual restrictions on m_{ij}. Financially, f_{ij} acts as an adjustment term for a particular state's option price, specifically as implied Poisson intensities for their respective Poisson processes, which will be discussed in more detail in the subsequent section. Intuitively, these state-dependent relations make financial sense because the assumption that $f_{HL} = f_{LH} = 0$ would decouple pricing partial differential equations, reducing them to the state-dependent Black-Scholes pricing equations. In addition, if the high and low regime volatilities were the same, the source terms driven by f_{HL}, f_{LH} would vanish, once again leaving Black-Scholes type option pricing equations.

When options go too far in or out of the money, their state-dependent option prices converge to the same value, especially towards maturity. At this point the option dynamics no longer include much of the risk of switching between volatility regimes, as volatility has minimal effect on the option price. This is consistent with Bakshi and Kapadia's [5] statement that options deep in/out of the money cannot provide insight about the market price of volatility risk. Therefore we are only concerned with the case where $C^H(S,t) \approx C^L(S,t)$ does not hold such that there exists a non-negligible source term coupling the equations. This implies that at least one of the following must also be true:

$$\lambda_{HL} \neq m_{HL}, \tag{5.32}$$

$$\lambda_{LH} \neq m_{LH}. \tag{5.33}$$

Since our purpose is to determine if any restrictions must be imposed on the market prices of volatility risk, and thus on the coefficients of the source terms in the pricing equations, we will consider financially intuitive constraints which the approximate solutions of the option price and hedge ratios must satisfy.

First, elementary arbitrage considerations imply that a call option price must be positive and bounded above by the stock price. Second, the Delta of a call option must lie between zero and one, as its seller need never hold more than one nor less than zero shares to fully hedge their risk. This is because a call option gives its owner the right to exercise at maturity in order to buy one share of the stock from their counterparty (i.e. investor who sold the option). Since the seller does not want to be stuck with buying the one full share of the stock for a premium (i.e. market value) if the option is exercised, they accumulate their position in the stock over time. Third, in a regime-switching market, there exists the possibility of switching to a more volatile or stable regime, depending on our initial regime, which in turn affects the option value. For a low state option, we know that the price is bounded below by the low volatility state Black-Scholes option price, since the possibility of switching to a more volatile state makes the position more valuable. On the other hand, a high state regime-switching option is bounded above by the high volatility state Black-Scholes option price. Since it is possible to shift to a more stable regime, the option is not worth as much. In other words,

$$0 \le C_{BS}^L(S,t) \le C^L(S,t) \le C^H(S,t) \le C_{BS}^H(S,t) < S. \tag{5.34}$$

As previously discussed, it is also true that

$$g(t,T) \ge 0 \text{ for all } f_{HL}, f_{LH}. \tag{5.35}$$

Our intuition indicates that the coefficients driving the source terms must be negative, however this can also be proved mathematically.

It can easily be observed that the state-dependent option prices and Deltas depend on a common term $g(t,T)$, for all $0 \le t \le T$. Checking the behaviour of this function at the initial time point and at maturity, it can be noted that the boundedness of the approximate solutions depend solely on the behaviour of this function.

5.2.1 Behaviour of $g(t,T)$

As we approach maturity, $\lim_{t \to T} g(t,T) \to 0$ for all f_{ij}, which decouples the state-dependent solutions, making them solely dependent on the Black-Scholes functions conditional on volatility state occupation. This is expected as the option boundary conditions are independent of the volatility model.

On the other hand, as the time to maturity becomes quite large, the convergence of the function $g(t,T)$ is not as clear-cut. Since this function depends on the relation $f_{HL} + f_{LH}$, we will examine convergence for three cases: $f_{HL} + f_{LH} = 0$, $f_{HL} + f_{LH} > 0$, and $f_{HL} + f_{LH} < 0$.

For $f_{HL} + f_{LH} = 0$ where both f_{HL}, f_{LH} can't be zero since we assumed that $\lambda_{HL}, \lambda_{LH} > 0$ to ensure regime-switching. First expand $e^{(f_{HL}+f_{LH})(T-t)}$ in a Taylor series about $(f_{HL}+f_{LH})(T-t) = 0$.

$$e^{(f_{HL}+f_{LH})(T-t)} = \Big(1 + (f_{HL} + f_{LH})(T-t) + \frac{1}{2}(f_{HL} + f_{LH})^2(T-t)^2 + \dots\Big) - 1. \tag{5.36}$$

Consider $g(t,T)$ now and evaluate at $f_{HL} + f_{LH} = 0$.

$$g(t,T)\Big|_{f_{HL}+f_{LH}=0} = \frac{1 + (f_{HL} + f_{LH})(T-t) + \frac{1}{2}(f_{HL} + f_{LH})^2(T-t)^2 + \dots}{f_{HL} + f_{LH}}\Big|_{f_{HL}+f_{LH}=0}, \tag{5.37}$$

$$\Rightarrow g(t,T)\Big|_{f_{HL}+f_{LH}=0} = T - t. \tag{5.38}$$

For $f_{HL} + f_{LH} > 0$,

$$e^{(f_{HL}+f_{LH})(T-t)} \geq 1, \tag{5.39}$$

$$\lim_{T-t\to\infty} g(t,T) = \lim_{T-t\to\infty} \frac{e^{(f_{HL}+f_{LH})(T-t)} - 1}{f_{HL} + f_{LH}} \to \infty. \tag{5.40}$$

Finally, check $f_{HL} + f_{LH} < 0$,

$$0 \leq e^{(f_{HL}+f_{LH})(T-t)} \leq 1, \tag{5.41}$$

$$\lim_{T-t\to\infty} g(t,T) = \lim_{T-t\to\infty} \frac{e^{(f_{HL}+f_{LH})(T-t)} - 1}{f_{HL} + f_{LH}} = -\frac{1}{f_{HL} + f_{LH}} \geq 0. \tag{5.42}$$

As the time to maturity becomes quite large, the function $g(t,T)$ diverges when $f_{HL} + f_{LH} \geq 0$. Therefore the option prices and hedge ratios are unbounded with respect to time when $f_{HL} + f_{LH} \geq 0$. Since this violates basic financial principles, in order to ensure bounded option prices and Deltas in a regime-switching market, the coefficients of the source terms must form a strictly negative sum, $f_{HL} + f_{LH} < 0$.

This result is intuitive if we consider the difference between the two state's option prices.

$$C^H(S,t) - C^L(S,t) \approx C^H_{BS}(S,t) - C^L_{BS}(S,t) + (f_{HL} + f_{LH})(C^H_{BS}(S,t) - C^L_{BS}(S,t))g(t,T) \tag{5.43}$$

Since we expect the difference between the option prices to decrease in the presence of regime-switching, as low regime options become increasingly more valuable and high regime options less valuable, this is only possible if $f_{HL} + f_{LH} < 0$.

It remains to show that given $f_{HL} + f_{LH} < 0$, some individual restrictions on both f_{HL}, f_{LH} must hold such that following financial constraints are satisfied.

$$0 \leq C^L_{BS}(S,t) \leq C^L(S,t) < S, \tag{5.44}$$

$$0 \leq C^H(S,t) \leq C^H_{BS}(S,t) < S, \tag{5.45}$$

$$0 \leq \frac{\partial C^L}{\partial S}(S,t) \leq 1, \tag{5.46}$$

$$0 \leq \frac{\partial C^H}{\partial S}(S,t) \leq 1. \tag{5.47}$$

In the following sections, we summarize the results from the mathematical proofs. For further detail, please see Mielkie and Davison [34]. For the proofs, notation will be reduced as follows for simplicity: $C^i \equiv C^i(S,t)$, $\frac{\partial C^i}{\partial S} \equiv \frac{\partial C^i}{\partial S}(S,t)$, $C^i_{BS} \equiv C^i_{BS}(S,t)$, and $\frac{\partial C^i_{BS}}{\partial S} \equiv \frac{\partial C^i_{BS}}{\partial S}(S,t)$

5.2.2 Case 1: $f_{HL} \in \mathbb{R}$, $f_{HL} + f_{LH} < 0$

For this case, we will only consider the effects of the source term coefficient on the high regime option price and Delta.

Since $f_{HL} + f_{LH} < 0$, we will assume that $f_{HL} > 0 \Rightarrow f_{LH} < 0$, $|f_{HL}| \geq |f_{HL} + f_{LH}|$. Let $f_{HL} + f_{LH} = -A$ and $f_{HL} = B$ where $A, B > 0$ and $\frac{A}{B} \geq 1$. Hence it follows that $g(t,T)$ as defined by equation (5.30) can be rewritten as $g(t,T) = \dfrac{1 - e^{-A(T-t)}}{A} \leq \dfrac{1}{A}$.

Satisfy $0 \leq C^H \leq C^H_{BS} < S$

$$0 \leq C^H_{BS} - C^L_{BS} \leq C^H_{BS}, \tag{5.48}$$

$$\Rightarrow 0 \leq C^H_{BS} \leq C^H_{BS} + Bg(t,T)[C^H_{BS} - C^L_{BS}] \leq \Big(1 + \frac{B}{A}\Big)C^H_{BS} < \Big(1 + \frac{B}{A}\Big)S, \tag{5.49}$$

$$\Rightarrow 0 \leq C^H_{BS} \leq C^H < \Big(1 + \frac{B}{A}\Big)S. \tag{5.50}$$

However, since we require $0 \leq C^H \leq C^H_{BS} < S$, and since $f_{HL} > 0 \Rightarrow C^H \geq C^H_{BS}$ and $C^H > S$, we have a contradiction. Therefore in order to have bounded and positive high state option prices, we require that $f_{HL}, f_{LH} < 0$.

Satisfy $0 \leq \dfrac{\partial C^H}{\partial S} \leq 1$

$$0 \leq \frac{\partial C^H_{BS}}{\partial S} - \frac{\partial C^L_{BS}}{\partial S} \leq \frac{\partial C^H_{BS}}{\partial S}, \tag{5.51}$$

$$0 \leq \frac{\partial C^H_{BS}}{\partial S} \leq \frac{\partial C^H_{BS}}{\partial S} + Bg(t,T)\Big[\frac{\partial C^H_{BS}}{\partial S} - \frac{\partial C^L_{BS}}{\partial S}\Big] \leq \Big(1 + \frac{B}{A}\Big)\frac{\partial C^H_{BS}}{\partial S}, \tag{5.52}$$

$$\Rightarrow 0 \leq \frac{\partial C^H}{\partial S} \leq \Big(1 + \frac{B}{A}\Big)\frac{\partial C^H_{BS}}{\partial S}. \tag{5.53}$$

To satisfy financial intuition, we require $0 \leq \frac{\partial C^H}{\partial S} \leq 1$, and since $f_{HL} > 0 \Rightarrow \frac{\partial C^H}{\partial S} \geq 1$, we have a contradiction. Therefore in order to have bounded and positive high state Deltas, we require that $f_{HL}, f_{LH} < 0$.

5.2.3 Case 2: $f_{LH} \in \mathbb{R}$, $f_{HL} + f_{LH} < 0$

For this case, we will only consider the effects of the source term coefficient on the low regime option price and Delta.

Since $f_{HL} + f_{LH} < 0$, we will assume that $f_{LH} > 0 \Rightarrow f_{HL} < 0$, $|f_{LH}| \geq |f_{HL} + f_{LH}|$. Let $f_{HL} + f_{LH} = -A$ and $f_{LH} = B$ where $A, B > 0$ and $\frac{A}{B} \geq 1$.

Satisfy $0 \leq C^L_{BS} \leq C^L < S$

$$0 \leq C^H_{BS} - C^L_{BS} \leq C^H_{BS}, \tag{5.54}$$

$$C^L_{BS} - \frac{B}{A}C^H_{BS} \leq C^L_{BS} - Bg(t,T)[C^H_{BS} - C^L_{BS}] \leq C^L_{BS} < S, \tag{5.55}$$

$$\Rightarrow C^L_{BS}[1 - \frac{B}{A}] \leq C^L \leq C^L_{BS} < S. \tag{5.56}$$

However, since we require $0 \leq C^L_{BS} \leq C^L < S$, and since $f_{LH} > 0 \Rightarrow C^L \leq 0$ and $C^L \leq C^L_{BS}$, we have a contradiction. Therefore in order to have bounded and positive low state option prices, we require that $f_{HL}, f_{LH} < 0$.

Satisfy $0 \leq \dfrac{\partial C^L}{\partial S} \leq 1$

$$0 \leq \frac{\partial C^H_{BS}}{\partial S} - \frac{\partial C^L_{BS}}{\partial S} \leq \frac{\partial C^H_{BS}}{\partial S}, \tag{5.57}$$

$$\frac{\partial C^L_{BS}}{\partial S} - \frac{B}{A}\frac{\partial C^H_{BS}}{\partial S} \leq \frac{\partial C^L_{BS}}{\partial S} - Bg(t,T)\Big[\frac{\partial C^H_{BS}}{\partial S} - \frac{\partial C^L_{BS}}{\partial S}\Big] \leq \frac{\partial C^L_{BS}}{\partial S} \leq 1, \tag{5.58}$$

$$\Rightarrow \frac{\partial C^L_{BS}}{\partial S}\Big[1 - \frac{B}{A}\Big] \leq \frac{\partial C^L}{\partial S} \leq 1. \tag{5.59}$$

Financially, we require $0 \leq C^L_{BS} \leq C^L < S$, and since $f_{LH} > 0 \Rightarrow \frac{\partial C^L}{\partial S} \leq 0$, we have a contradiction. Therefore in order to have bounded and positive low state option Deltas, we require that $f_{HL}, f_{LH} < 0$.

To summarize we found that for the high state option price and Delta, we found that the financial constraints were violated when $f_{HL} > 0$. The high state option was not bounded above by either the Black-Scholes option price or the stock price and the Delta could take on values greater than one. On the other hand, when we considered $f_{LH} > 0$ for the low regime, it was found that both the option and its Delta violated the non-negativity constraints. As previously discussed, a negative coefficient coupling the source terms implies that negative state-dependent market prices of volatility risk are required for financially reasonable regime-switching option prices.

Further analysis shows that given negative market prices of volatility risk, changing the magnitude of the low (respectively high) prices of risk has a more pronounced effect on the low (respectively high) state's option price and Delta value.

$$\frac{f_{ij}}{f_{ij} + f_{ji}} \geq \frac{f_{ji}}{f_{ij} + f_{ji}}, \text{ for all } i \in \{H, L\}, i \neq j. \tag{5.60}$$

Since

$$C^i(S,t) \approx C^i_{BS}(S,t) - f_{ij}(C^j_{BS}(S,t) - C^i_{BS}(S,t))\left(\frac{e^{(f_{ij}+f_{ji})(T-t)} - 1}{f_{ij} + f_{ji}}\right), \tag{5.61}$$

$$\frac{\partial C^i}{\partial S}(S,t) \approx \frac{\partial C^i_{BS}}{\partial S}(S,t) - f_{ij}\left(\frac{\partial C^j_{BS}}{\partial S}(S,t) - \frac{\partial C^i_{BS}}{\partial S}(S,t)\right)\left(\frac{e^{(f_{ij}+f_{ji})(T-t)} - 1}{f_{ij} + f_{ji}}\right), \tag{5.62}$$

are our approximate solutions, the relative change in a state-dependent option price and corresponding Delta are directly proportional to the change in magnitude of its state-dependent market price of volatility risk.

It follows that for all regime-switching options in a two state market, no matter what volatility state is occupied, the corresponding market price of volatility risk must be negative in order for the option values and hedge ratios to satisfy financially intuitive conditions.

To illustrate the necessity of the restriction of state-dependent market prices of volatility risk to negative values, a Crank-Nicolson numerical scheme was used to solve the coupled PDEs for the two-state case.

Expected Return	r	0%
High State Volatility	σ_H	40%
Low State Volatility	σ_L	10%
Strike Price	K	\$100
Maturity Date	T	1 year
Daily High State Jump Intensity	λ_{HL}	5%
Daily Low State Jump Intensity	λ_{LH}	5%
Number of Time Increments	$\tilde{L}$	252

Table 5.1: Parameters used in the implementation of the Crank-Nicolson numerical scheme.

As can be noted in Figure 5.1, when the low state market price of volatility risk is given a positive value (i.e. $m_{LH} = 4$), financially impossible negative option prices can be observed about the strike price. Therefore the numerical solution exhibits the same behaviour as our approximate solution, and our claim in support of negative state-dependent market prices of volatility risk is illustrated.

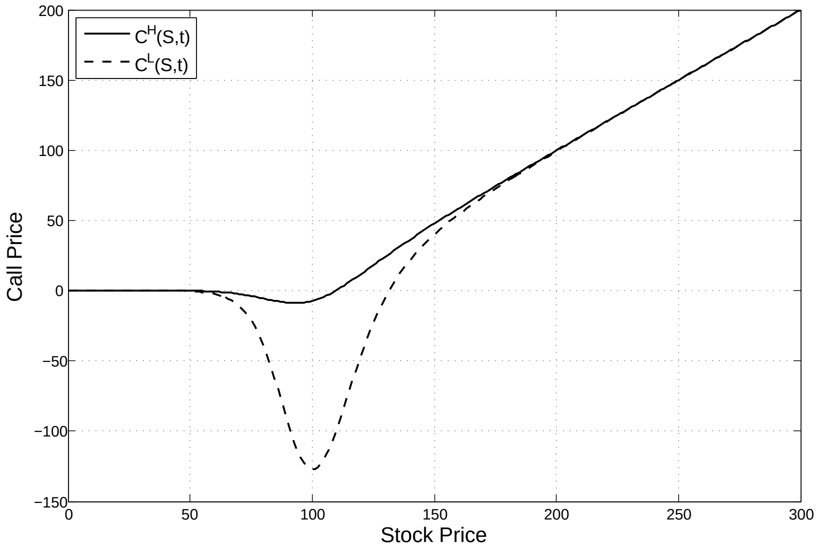

Figure 5.1: Crank-Nicolson numerical solutions for the coupled pricing PDEs. $m_{HL} = -1, m_{LH} = 4$, all other parameters as given in Table 5.1.

Furthermore, a comparison of our approximate solutions to the numerical solutions in Figure 5.2 and Figure 5.3 show that our approximate state-dependent solutions are fairly accurate, although with some discrepancy about the strike price. This error was quantified and discussed in detail in Chapter 4. However given different combinations of state-dependent market prices of volatility risk, it is observed that the numerical solution has the same behaviour as the approximate solution. As desired, Figure 5.2 and Figure 5.3 illustrate that given negative state dependent market prices of volatility risk, regime-switching option prices are in fact positive and bounded above by the underlying asset's price.

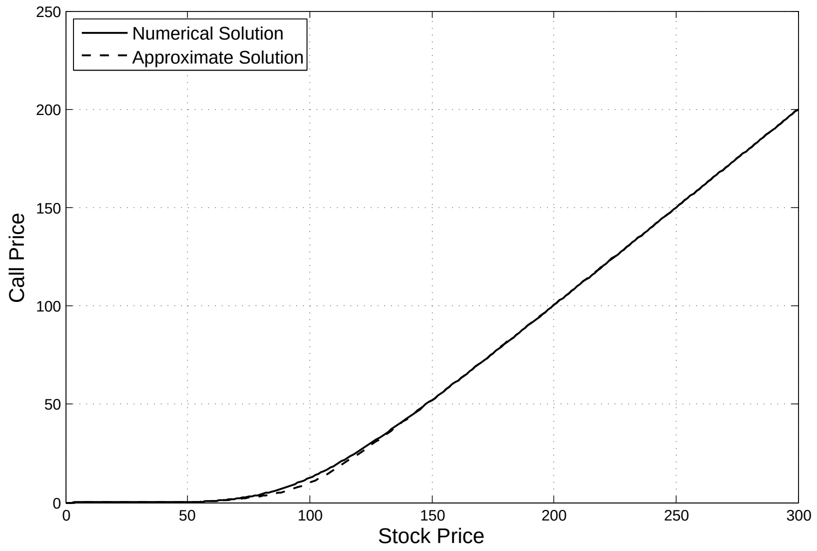

Figure 5.2: Comparison of the numerical and approximate solution of the high state pricing PDE. $m_{HL} = m_{LH} = -2$, all other parameters as given in Table 5.1.

We have shown that, in order for option prices to make sense financially, the state-dependent market price of volatility risk must take on negative values. However, what does this negative market price of volatility risk imply financially for regime-switching options? Doran and Ronn [16] stated that, in energy markets, options buyers pay a premium for downside protection against declines in the market, which in turn leads to a increase in implied volatility levels. Delta hedged option sellers favour low volatility as larger price movements could lead to them losing money from their hedged position in the stock. On the other hand, investors with a hedged position in a long option desire high volatility since to hedge their exposure to the option they buy low and sell high in the underlying asset thus earning a small profit every time they rebalance their portfolio. We can extend this logic to our regime-switching framework from an unhedged point of view. When we occupy the low volatility state, option buyers are motivated to pay a premium as there exists the risk of transitioning to a more volatile state where the future value of the underlying asset is more unknown. In a more volatile state, the probability of the underlying asset price moving until the option is in- or out-of-the-money increases. Although in the high volatility state since the market can switch to a stabler regime, investors need to hedge against the current volatility state occupation and will pay a premium

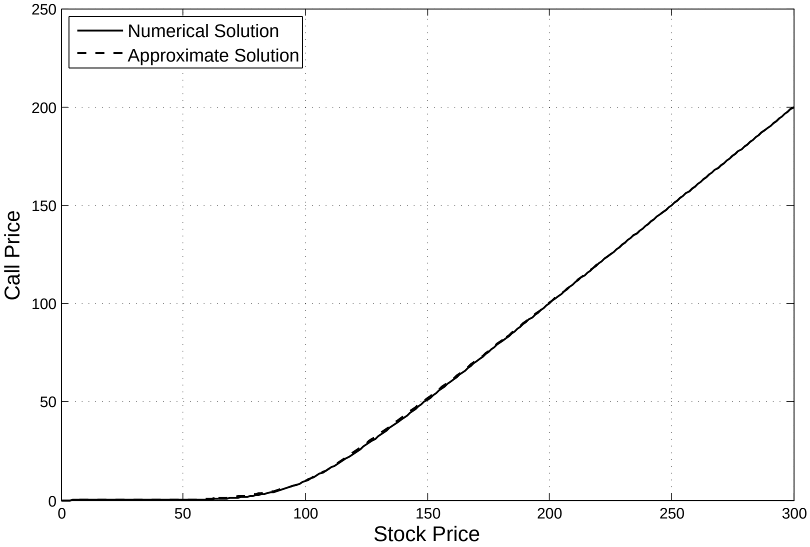

Figure 5.3: Comparison of the numerical and approximation solution of the low state pricing PDE. $m_{HL} = m_{LH} = -2$, all other parameters as given in Table 5.1.

to do so. Thus under the regime-switching framework, investors justify incorporating a premium within the option prices, through the existence of negative volatility risk premia, for options that allow to hedge the exposure to either the current volatility state occupation or the possibility of future volatility state occupation.

5.3 Implied Volatility Smiles

The difference between implied volatility and historical volatility can be used to measure the discrepancy between market and model prices of options. Traders make daily use of implied volatility as it allows them to determine the risk associated with an option struck at a particular strike price. Since there are usually a handful of options corresponding to a particular maturity date available on financial markets, determining the associated implied volatility with these options will help them decide which option fits their trading strategy and also fits the risk preferences of their clients.

Volatility smiles describe the relationship between the strike price of an option and an option's implied volatility, and are similar for both calls and puts. The observed smile shows that in- and out-of-the-money options' corresponding implied volatility is higher than those options trading at-the-money. A common explanation for this result is of more demand for these options by traders for use in their trading activities, and for use as leverage when the price of the underlying asset changes (Hull [28]).

Volatility smiles have been observed by practitioners in modern equity markets; their existence was first noticed after the financial crisis in October 1987. Furthermore, volatility smiles have been found in various option pricing models derived within the last few decades. In fact, many models are derived for the sole purpose of fitting the volatility smile phenomenon. Bollen [7] showed that volatility smiles could be backed out from regime-switching European options for various strike prices and maturity dates, priced using a pentanomial lattice. More recently, Yao *et al.* [56] illustrated the volatility smiles and volatility term structures that can be computed from options priced under a risk-neutral regime-switching model. They showed that the existence of this phenomenon remained consistent when the jump size between the two regimes and the frequency of jumps were varied. These results are not surprising as the dependence of an option's price on its underlying volatility becomes inconsequential when an option is too far in- or out-of-the-money.

We have already demonstrated that the state-dependent market prices of volatility risk must be negative in order to produce option prices satisfying basic financial intuition. Building upon our earlier claim that volatility risk premia must be negative, we investigate the effect of different values for the price of risk on the implied volatility smiles. Our benchmark for analysis is shown in Figure 5.4, when the corresponding high and low state implied volatility smiles are shown for a risk-neutral regime-switching European call option. The European call options with a one year maturity, were priced using a Crank-Nicolson numerical scheme. Using Matlab's built-in implied volatility solver 'blsimpv' found in the Financial Toolbox, implied volatility was backed out from our numerical option prices for a range of strike prices.

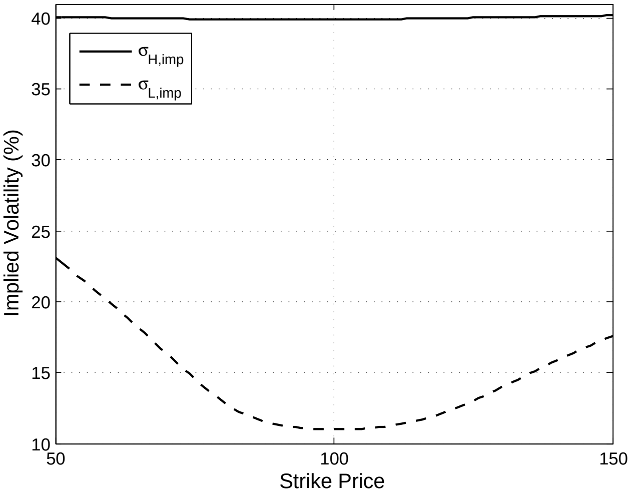

Figure 5.4: Implied volatility smile corresponding to high and low state risk-neutral regime-switching options prices. $m_{HL} = m_{LH} = 0$ and $S = \$100$, all other parameters as given in Table 5.1.

With the parameters given in Table 5.1, Figure 5.4 shows the volatility smile for the low regime option is more pronounced than that for the high regime option. The state transitions in the market have a greater impact on those options priced in a low volatility state than those in a high volatility state, as they are more sensitive to movements in the underlying asset.

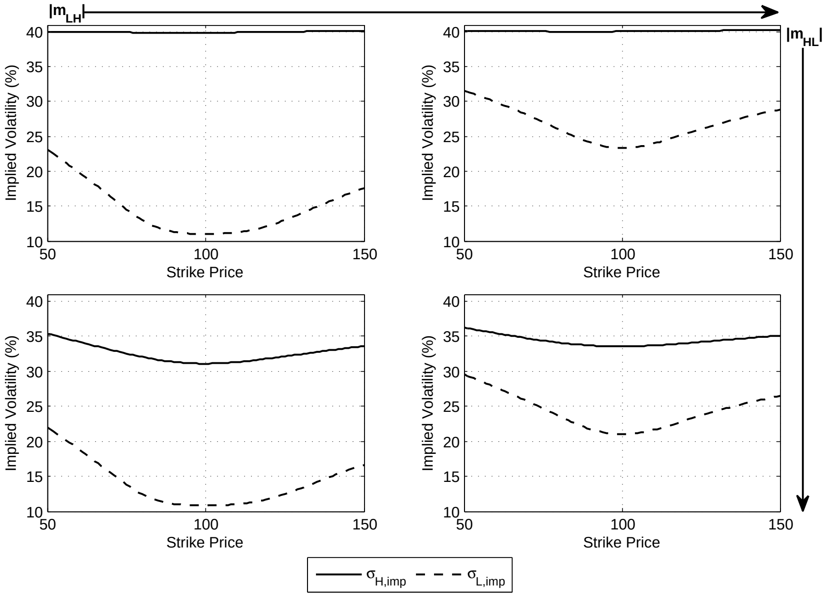

Figure 5.5: State-dependent implied volatility smiles resulting from varying the market prices of volatility risk. $m_{HL} = \{0, -1\}$, $m_{LH} = \{0, -1\}$, $S = \$100$, all other parameters as given in Table 5.1.

Both the magnitude of the high and low state-dependent market prices of volatility risk were varied in order to observe the effect on the option's implied volatility smiles. It was found, as shown in Figure 5.5, that increasing just the magnitude of the high state price of risk caused both state's implied volatility smiles to shift lower and become more pronounced. On the other hand, increasing the magnitude of the low state price of risk while leaving the high state price constant caused both states' smiles to shift upwards and become less pronounced. Both these effects were more significant with respect to the price of risk's corresponding state's option price. Since the market price of volatility risk can be thought of as a premium compensating investors for the possibility of the market switching to a differing volatility regime, these observations make intuitive sense. Recall that increasing the magnitude of the high state market price of volatility risk decreases the high state option value due to the possibility of switching to a stabler regime. In turn this would also decrease the implied volatility with respect to the risk neutral case. Low state options were found to increase in value when their state's price of risk was increased in magnitude. Since there is a possible switch to a more volatile regime, the option is now worth more. As a result, the implied volatility increases as well. When both states' prices of risk are altered by the same amount, the observed effects are the same, however the change from our benchmark case is not as much.

Many investors are concerned with the overall level of risk they acquire when taking a position in the market. When trading in a market with underlying regime-switching volatility, there always exists some risk that the volatility will switch to a less desirable regime. To account for this, many investors require compensation through the premia embedded in the option price. Of interest, in relation to volatility smiles, is how big do these premia need to be in order for a risk-averse investor to take a position in a particular option.

Recall that the coupling coefficients of the pricing PDEs given by equation (2.48) and f_{HL}, f_{LH} as given by equation (2.52), are functions of the Poisson arrival rates governing the switching between the two regimes. Since they are also functions of the state-dependent market prices of volatility risk, which compensate for the risk of switching regimes, we may consider these coefficients to be risk-adjusted Poisson arrival rates, interpreted as implied transitional probabilities which compensate for the current market conditions as well as the market's aversion to these conditions. Doing so lends to further analysis of the market price of volatility risk and the resulting implied volatility.

First, consider an investor who has a long position in an option. This individual fears low volatility since an option price at a lower volatility level is worth less than an otherwise identical option priced at a higher volatility level. Such an investor would require a fairly large high state market price of risk to compensate for the possibility of switching to a lower volatility regime. Given that $m_{HL}(S,t) \to -\infty$ it follows that $f_{HL} \to -\infty$ as well. We will first analyse the effect that the high state coupling coefficient has on the approximate regime-switching option prices. To do so, we will assume that the low state coefficient takes on a constant and finite negative value $f_{LH} = -F$ where $F \geq 0$.

First, check the high state price.

$$\lim_{\substack{f_{HL}\to-\infty \\ f_{LH}=-F}} C^H(S,t) \approx \lim_{\substack{f_{HL}\to-\infty \\ f_{LH}=-F}} \left[C^H_{BS}(S,t) + f_{HL}\Big(C^H_{BS}(S,t) - C^L_{BS}(S,t)\Big)\left(\frac{e^{(f_{HL}+f_{LH})(T-t)} - 1}{f_{HL}+f_{LH}}\right)\right], \tag{5.63}$$

$$\approx C^H_{BS}(S,t) + \Big(C^H_{BS}(S,t) - C^L_{BS}(S,t)\Big) \cdot \left[\lim_{f_{HL}\to-\infty} \frac{f_{HL}}{f_{HL}-F}\right] \cdot \left[\lim_{f_{HL}\to-\infty} \Big(e^{(f_{HL}-F)(T-t)} - 1\Big)\right], \tag{5.64}$$

$$\overset{\text{L'H}}{\approx} C^H_{BS}(S,t) - \Big(C^H_{BS}(S,t) - C^L_{BS}(S,t)\Big), \tag{5.65}$$

$$\Rightarrow \lim_{\substack{f_{HL}\to-\infty \\ f_{LH}=-F}} C^H(S,t) \approx C^L_{BS}(S,t). \tag{5.66}$$

Now for the low state call price,

$$\lim_{\substack{f_{HL}\to-\infty \\ f_{LH}=-F}} C^L(S,t) \approx \lim_{\substack{f_{HL}\to-\infty \\ f_{LH}=-F}} \left[C^L_{BS}(S,t) - f_{LH}\Big(C^H_{BS}(S,t) - C^L_{BS}(S,t)\Big)\left(\frac{e^{(f_{HL}+f_{LH})(T-t)} - 1}{f_{HL}+f_{LH}}\right)\right], \tag{5.67}$$

$$\approx C^L_{BS}(S,t) + F\Big(C^H_{BS}(S,t) - C^L_{BS}(S,t)\Big) \cdot \left[\lim_{f_{HL}\to-\infty} \frac{\Big(e^{(f_{HL}-F)(T-t)} - 1\Big)}{f_{HL}-F}\right], \tag{5.68}$$

$$\Rightarrow \lim_{\substack{f_{HL}\to-\infty \\ f_{LH}=-F}} C^L(S,t) \approx C^L_{BS}(S,t). \tag{5.69}$$

Therefore if a market compensates for the possible switch to the low regime, our option will be priced as though we are in a constant low volatility world. A flat implied volatility smile is shown to exist under these circumstances.

$$\sigma_{H,imp} = \sigma_{L,imp} = \sigma_L. \tag{5.70}$$

This makes economic sense as investors would like to price their options to minimize the risk of switching to an undesirable regime. This is equivalent to picking m_{HL} large enough that the option is priced assuming that switches to the low regime happen with absolute certainty (i.e. $\lambda_{HL}dt = 1$).

Investors worried about switching into a low regime want to be compensated for the risk associated with possibly staying in this regime given they at some point switch into it. Since volatility can switch continuously, this can be intuitively associated with a higher risk premium demanded. If this compensation is given, the option they sell will be priced as if it were trading in a low regime constant volatility world. It turns out that a risk-averse option buyer would rather buy an option at a lower price than face the risks associated with switching regimes.

Now we can investigate the risks faced by option sellers and what price of risk a risk-averse short position in an option would require. Option sellers fear the volatility rising over the life of the option. Using the same logic as before, we know that these types of investors would require a fairly large price of risk to compensate for the risk of switching to the more volatile state. In order to analyse the effect of the low state coefficient, the high state coefficient will take on a constant, negative value $f_{HL} = -F$ where $F \geq 0$.

For the high state switching option,

$$\lim_{\substack{f_{HL}=-F \\ f_{LH}\to-\infty}} C^H(S,t) \approx \lim_{\substack{f_{HL}=-F \\ f_{LH}\to-\infty}} \left[C^H_{BS}(S,t) + f_{HL}\Big(C^H_{BS}(S,t) - C^L_{BS}(S,t)\Big)\left(\frac{e^{(f_{HL}+f_{LH})(T-t)} - 1}{f_{HL}+f_{LH}}\right)\right], \tag{5.71}$$

$$\approx C^H_{BS}(S,t) - F\Big(C^H_{BS}(S,t) - C^L_{BS}(S,t)\Big)\cdot\left[\lim_{\substack{f_{HL}=-F \\ f_{LH}\to-\infty}} \frac{e^{(-F+f_{LH})(T-t)} - 1}{-F+f_{LH}}\right], \tag{5.72}$$

$$\Rightarrow \lim_{\substack{f_{HL}=-F \\ f_{LH}\to-\infty}} C^H(S,t) \approx C^H_{BS}(S,t). \tag{5.73}$$

Now for the low state option,

$$\lim_{\substack{f_{HL}=-F \\ f_{LH}\to-\infty}} C^L(S,t) \approx \lim_{\substack{f_{HL}=-F \\ f_{LH}\to-\infty}} \left[C^L_{BS}(S,t) - f_{LH}\Big(C^H_{BS}(S,t) - C^L_{BS}(S,t)\Big)\left(\frac{e^{(f_{HL}+f_{LH})(T-t)} - 1}{f_{HL}+f_{LH}}\right)\right], \tag{5.74}$$

$$\approx C^L_{BS}(S,t)$$

$$-\left(C_{BS}^{H}(S,t)-C_{BS}^{L}(S,t)\right)\cdot\left[\lim_{f_{LH}\to-\infty}\frac{f_{LH}}{-F+f_{LH}}\right]\cdot\left[\lim_{f_{LH}\to-\infty}\left(e^{(-F+f_{LH})(T-t)}-1\right)\right], \tag{5.75}$$

$$\overset{\text{L'H}}{\approx} C_{BS}^{L}(S,t)+\left(C_{BS}^{H}(S,t)-C_{BS}^{L}(S,t)\right), \tag{5.76}$$

$$\Rightarrow \lim_{\substack{f_{HL}=-F\\ f_{LH}\to-\infty}} C^{L}(S,t)\approx C_{BS}^{H}(S,t). \tag{5.77}$$

The risk associated with a short position in our regime-switching options results in the state-dependent options being priced as if they were in a constant high volatility world. As a result, a flat implied volatility smile taking on the high volatility value across all strike prices arises from the model.

$$\sigma_{H,imp}=\sigma_{L,imp}=\sigma_{H}. \tag{5.78}$$

Like before, pricing our option in such a way is equivalent to picking our risk premium large enough so that it mimics a framework where the volatility switches to the high regime with absolute certainty (i.e. $\lambda_{LH}dt = 1$).

Our option buyers want to be compensated for the risk of the volatility staying high that they have taken on by entering into a position in this option. Once again, investors require a higher risk premium. This is equivalent to our risk-averse option seller requesting more for an option from their counterparty in order to minimize their potential future risks than face the uncertainty of the underlying volatility in the market.

Finally, both risk-averse option buyers and sellers may consider the most extreme cases when negotiating the premia added to their option prices. An interesting case is to consider that volatility in a two-regime world will on average spend half of its time in the high regime, and the other half in the low regime. It turns out that if both investors require large prices of risk to compensate for their opposing risks, we would price the options in such a way. Now consider what occurs to the state-dependent option prices as the magnitude of both coefficients of the coupling source terms become infinitely large.

For simplicity, let $f_{HL} = af_{LH}$ where $f_{LH} = F$ and $a \geq 0$. Take the limit as $F \to -\infty$. For the high state option,

$$\lim_{\substack{f_{HL}=aF, f_{LH}=F\\ F\to-\infty}} C^{H}(S,t)\approx \lim_{\substack{f_{HL}=aF, f_{LH}=F\\ F\to-\infty}}\left[C_{BS}^{H}(S,t)+f_{HL}\left(C_{BS}^{H}(S,t)-C_{BS}^{L}(S,t)\right)\left(\frac{e^{(f_{HL}+f_{LH})(T-t)}-1}{f_{HL}+f_{LH}}\right)\right], \tag{5.79}$$

$$\begin{aligned}\approx\ & C_{BS}^{H}(S,t)\\ &+\left(C_{BS}^{H}(S,t)-C_{BS}^{L}(S,t)\right)\cdot\left[\lim_{F\to-\infty}\frac{aF}{(a+1)F}\right]\cdot\left[\lim_{F\to-\infty}\left(e^{(a+1)F(T-t)}-1\right)\right],\end{aligned} \tag{5.80}$$

$$\approx C_{BS}^{H}(S,t)-\frac{a}{a+1}\left(C_{BS}^{H}(S,t)-C_{BS}^{L}(S,t)\right), \tag{5.81}$$

$$\Rightarrow \lim_{\substack{f_{HL}=aF, f_{LH}=F\\ F\to-\infty}} C^{H}(S,t)\approx \frac{1}{a+1}C_{BS}^{H}(S,t)+\frac{a}{a+1}C_{BS}^{L}(S,t). \tag{5.82}$$

Finally, for the low state call option,

$$\lim_{\substack{f_{HL}=aF, f_{LH}=F \\ F\to-\infty}} C^L(S,t) \approx \lim_{\substack{f_{HL}=aF, f_{LH}=F \\ F\to-\infty}} \left[C^L_{BS}(S,t) - f_{LH}\Big(C^H_{BS}(S,t) - C^L_{BS}(S,t)\Big)\left(\frac{e^{(f_{HL}+f_{LH})(T-t)}-1}{f_{HL}+f_{LH}}\right)\right], \tag{5.83}$$

$$\approx C^L_{BS}(S,t)$$

$$- \Big(C^H_{BS}(S,t) - C^L_{BS}(S,t)\Big)\cdot\left[\lim_{F\to-\infty}\frac{F}{(a+1)F}\right]\cdot\left[\lim_{F\to-\infty}\Big(e^{(a+1)F(T-t)}-1\Big)\right], \tag{5.84}$$

$$\approx C^L_{BS}(S,t) + \frac{1}{a+1}\Big(C^H_{BS}(S,t) - C^L_{BS}(S,t)\Big), \tag{5.85}$$

$$\Rightarrow \lim_{\substack{f_{HL}=aF, f_{LH}=F \\ F\to-\infty}} C^L(S,t) \approx \frac{1}{a+1}C^H_{BS}(S,t) + \frac{a}{a+1}C^L_{BS}(S,t). \tag{5.86}$$

If investors are concerned about a market which ends up permanently in the opposing regime, then paying a weighted average of the two regime's option prices will eliminate some risk associated with both of their positions. This is equivalent to the fair price that both investors (i.e. long and short position) would accept to set up their positions in the presence of uncertain volatility. It should be noted that the implied volatility arising under these assumptions is not a weighted average of the volatility values of the two regimes.

$$\sigma_{H,imp} = \sigma_{L,imp} \neq \frac{1}{a+1}\sigma_H + \frac{a}{a+1}\sigma_L. \tag{5.87}$$

A special case of our generalized result is when $a = 1$. This implies that our Poisson intensities controlling our switches into the opposing regimes have the same magnitude. If this were the case, investors would simply take the average of the two state option prices to set up their hedge positions.

5.4 Summary

By using the approximate solutions for state-dependent option prices and corresponding Deltas, we were able to analyse the impact of the market price of volatility risk on these relations, both intuitively and mathematically. Utilizing basic financial principles, we were able to show that negative state-dependent market prices of volatility risk were necessary to have reasonable theoretical option prices in a regime-switching market. The proof of existence of such negative state-dependent market prices of volatility risk allowed us to quantify the market's attitudes about uncertainty in a regime-switching volatility framework. Specifically, the negative market price of volatility risk acts as an option premium. The option will be worth more due to its ability to hedge against movements between volatility regimes. It was found that the both the occupation and potential occupation of a volatile regime causes investors to pay this premium for options that allow them to hedge against this risk. We investigated the state-dependent premia required by risk-averse option buyers and sellers to eliminate the risk they face in the market. Finally, the consequence of varying the magnitude of the state-dependent market prices of volatility risk on the implied volatility smiles was shown to alter both the slope and the magnitude of the smile when compared to the risk-neutral case.

Now that our regime-switching coupled pricing equations have been solved using both a numerical method and an approximation technique, we can now consider what hedging strategies we can use to effectively hedge against both the movements in the underlying asset and in the unknown jumps between volatility regimes. A basic introduction to hedging and arbitrage arguments follows along with an empirical analysis of both volatility-dependent and naive hedging strategies.

Chapter 6

Hedging Strategies

Throughout this chapter, we consider an investor who takes a short position in a European call option. Recall that a European call option gives its owner the right but not the obligation to buy the underlying asset for the strike price K at the maturity date of the option T. This right will only be exercised if it is cheaper to buy the stock at the strike price than it would be to go directly to the market and do so. An investor having shorted (i.e. sold) the option is exposed to the risk of the contract's counterparty coming at maturity to buy the share, one unit of the underlying asset. Due to this, a short position in a call option has an asymmetric loss/gain profile where we are exposed to unlimited downside risk if the option expires in-the-money. As a result, we must hedge against this risk by cleverly investing in a portfolio of financial instruments.

In this chapter, we will be comparing various different hedging strategies that can be employed to hedge both against random movements in the volatility and in the underlying asset. As we will see, these strategies will give us distinct hedge ratios for our different hedging instruments employed in our portfolios. The number of hedging instruments and their respective hedge positions will be defined by each strategy. However there are a few similarities between the strategies studied, in particular we will always take a position in the underlying asset to directly hedge against asset risk. This position will be unique for each strategy and defined by Δ_1^i. The discrepancies lie in how we approach hedging out our regime-switching volatility risk. Recall that we assume that volatility cannot be hedged directly and thus we choose to take positions in hedging options to do so. Given N volatility regimes, we will assume that we have $N-1$ hedging options available to us. The positions in these hedging instruments will be given by Δ_n^i for $n = 2, \ldots, N$ and will be hedging strategy and volatility state dependent.

In particular we will focus on strategies that allow us to completely hedge out all the risks embedded within our model. Mathematically we show that we can fully hedge against these risks, however financial implications arise motivating more advanced hedging techniques. Finally, we will compare our regime-switching hedging strategies with more naive Black-Scholes style hedge portfolios conditional on different estimates of constant volatility. An overview of the Black-Scholes hedging model is presented as a benchmark model for hedging, setting the stage for the set-up and derivation of our regime-switching hedge portfolios. All strategies are first presented mathematically and then compared within a numerical simulation study.

6.1 Simulation Framework

In order to compare the mean profit/loss of different hedging strategies employed under our regime-switching volatility framework, we must first discuss how the stock price and volatility paths are simulated. All simulations in this chapter are implemented in Matlab.

6.1.1 Simulating Regime-Switching Volatility

This thesis is based on the assumption that volatility can switch between a finite number of regimes, in particular a high and low volatility state. The equation below shows how our stochastic volatility path is simulated at every time increment dt.

$$\sigma_{t+dt} = \sigma_t + (\sigma_H - \sigma_t)dq_{LH,t} + (\sigma_L - \sigma_t)dq_{HL,t}, \tag{6.1}$$

where $dq_{LH,t}, dq_{HL,t}$ are draws from independent binomial distributions with respective probabilities $\lambda_{LH}dt, \lambda_{HL}dt$. Draws for random variables occur at every time increment. Recall that λ_{ij} is the intensity of the Poisson process associated with the jump from the ith volatility regime to the jth volatility regime while dt represents the time increment used for simulating GBM.

For simulation purposes, we assume that the initial volatility state occupation, σ_0, depends on the unconditional probability of being in either of the two regimes.

$$\begin{bmatrix} P_H \\ P_L \end{bmatrix}_{unconditional} = \begin{bmatrix} \dfrac{\lambda_{LH}}{\lambda_{LH} + \lambda_{HL}} \\ \dfrac{\lambda_{HL}}{\lambda_{LH} + \lambda_{HL}} \end{bmatrix}.$$

A fraction $P_{H,unconditional}$ of paths begin in the high volatility state while a fraction $P_{L,unconditional}$ begin in the low volatility state.

6.1.2 Simulating Geometric Brownian Motion

As discussed in Chapter 2, it is assumed that our underlying asset (i.e. stock) follows geometric Brownian motion (GBM). In order to simulate the price paths, we must choose a time increment dt at which every increment the stock can change price. The equation below illustrates how we simulate the stochastic differential equation for GBM.

$$S_{t+dt} = S_t e^{\left(\mu - \frac{1}{2}\sigma_t^2\right)dt + \sigma_t \sqrt{dt} Z_t}, \tag{6.2}$$

where Z is a draw from a standard normal distribution. Recall that a standard normal random variable has mean 0 and variance 1. Due to the dependency of the volatility state on the price path, the volatility state at time t, σ_t, is simulated first. The initial stock price S_0 is always assumed to be given.

6.2 Simulating Hedging Strategies

After simulating sample volatility paths and their corresponding stock price paths, we are ready to implement all of our hedging strategies on these paths. First we need to compute the regime-switching option prices. In Chapter 3 we saw that numerical methods were necessary to solve our coupled system of regime-switching pricing equations. Solving these equations using the Crank-Nicolson numerical scheme gives us both the high and low volatility option prices. Since we computed our option prices on a numerical grid, if the value of the stock price falls between two grid points, we use linear interpolation to find the exact option price for a particular choice of S and t. For simplicity, linear interpolation was implemented via a built-in Matlab function 'interp2'. If a stock price in our sample path exceeds the maximum stock price in our numerical grid, we use the following approximation for the call option price.

$$C^i(S,t) = S - Ke^{-r(T-t)}, \tag{6.3}$$

for all $i \in \{H, L\}$.

The above approximation was employed when $S > S_{max}$. It is important to note that when we numerically solved our PDEs, the stock vector used could be generalized by $S = [0 \dots S_{max}]^T$. Since we know that stock prices must be non-negative, no approximation was necessary on the lower bound since the stock prices cannot fall below the lower bound of the vector used in our numerical scheme, however they can go above S_{max}. Finally, we require that our option price corresponds to the correct volatility state, thus we must identify which state we occupy at every time point to determine if we use the high or low price and the high or low hedge ratios. The strategy specific hedge ratios will be described in detail later on in the chapter.

$$C(S,t) = \begin{cases} C^H(S,t) \text{ if } \sigma(t) = \sigma_H \\ C^L(S,t) \text{ if } \sigma(t) = \sigma_L \end{cases}, \tag{6.4}$$

$$\Delta_n = \begin{cases} \Delta_n^H \text{ if } \sigma(t) = \sigma_H \\ \Delta_n^L \text{ if } \sigma(t) = \sigma_L \end{cases}, \tag{6.5}$$

for all $n = 1 \cdots N$.

The best indication of how our hedging strategies perform is to compute the mean profit/loss over Q sample stock price and volatility paths. The mean and 95% confidence interval will give us a good indication of whether or not an investor utilizing a hedge portfolio would break-even or lose/earn money on average. The equations below give us an idea of how profit/loss is computed for our hedge portfolios initially, at every time increment, and when we close out our portfolio. For a finite number N of hedging instruments,

$$\text{Profit}_0 = C_{1,0} - \Delta_{1,0}S_0(1 + sgn(\Delta_{1,0})TC_{stock}) - \sum_{n=2}^{N} \Delta_{n,0}C_{n,0}(1 + sgn(\Delta_{n,0})TC_{option}), \tag{6.6}$$

$$\begin{aligned} \text{Profit}_{t+dt} &= (1 + rdt)\text{Profit}_t - (\Delta_{1,t+dt} - \Delta_{1,t})S_{t+dt}\Big(1 + sgn(\Delta_{1,t+dt} - \Delta_{1,t})TC_{stock}\Big) \\ &\quad - \sum_{n=2}^{N}(\Delta_{n,t+dt} - \Delta_{n,t})C_{n,t+dt}\Big(1 + sgn(\Delta_{n,t+dt} - \Delta_{n,t})TC_{option}\Big), \end{aligned} \tag{6.7}$$

$$\text{Profit}_T = (1 + rdt)\text{Profit}_{T-dt} - (\Delta_{1,T} - \Delta_{1,T-dt})S_T\Big(1 + sgn(\Delta_{1,T} - \Delta_{1,T-dt})TC_{stock}\Big)$$

$$- \sum_{n=2}^{N} (\Delta_{n,T} - \Delta_{n,T-dt}) C_{n,t+dt} \Big(1 + sgn(\Delta_{n,T} - \Delta_{n,T-dt}) TC_{option} \Big)$$

$$+ \Delta_{1,T} S_T - (S_T - K_1)^+ + \sum_{n=2}^{N} \Delta_{n,T} (S_T - K_n)^+, \tag{6.8}$$

where:

$$sgn(x) = \begin{cases} -1 & \text{if } x < 0 \\ 0 & \text{if } x = 0 \\ 1 & \text{if } x > 0 \end{cases}.$$

Since we are setting up all hedging strategies from the point of view of an investor with a short position in a European call option, we will initially sell this option to a counterparty for $C_{1,0} \equiv C_1(S(0), 0)$ dollars. We then either earn additional profit or spend money when setting up our positions (long/short) in our financial hedging instruments. We assume that the profit from time t earns the risk-free rate of interest over every time increment dt. If profit is non-negative, this means that we earn the risk-free rate of interest; if profit is negative, this means we are being charged the risk-free rate of interest for borrowing money from a counterparty (i.e. a bank).

At maturity, we must close out our hedge portfolios by fulfilling our side of the multiple contracts we have entered into. A detailed discussion about how hedge portfolios are closed out will be given in the proceeding sections detailing the different hedging strategies.

For all our hedging models, we assume that the transaction costs incurred are proportional. This means that the total amount charged per transaction depends directly on the amount of a particular financial product traded. The transaction cost, measured in basis points, is constant. Typically, proportional option transaction costs are much greater than proportional stock transaction costs. For simplicity we assume that all hedging options are changed the same transaction costs, TC_{option}, while the changes in position in our underlying asset are charged the rate defined by TC_{stock} where $TC_{option} >> TC_{stock}$.

6.3 Black-Scholes Hedging

We will first discuss a benchmark model for hedging to illustrate how and why hedge portfolios are set up. In the constant volatility world, otherwise known as the Black-Scholes framework [6], we must consider what risks we are exposed to as an investor. From a hedging perspective, risks can be defined as things that can affect the profit/loss of our portfolio and are unknown and uncontrollable. If we consider taking a position in any financial option contract written on a stock, we are exposed to the movements in this stock. Stock prices cannot be predicted nor controlled, thus there exists huge stock risk associated with buying or selling an option.

Under the constant volatility framework, we can assume that the stock price follows geometric Brownian motion and as a result, we can mathematically determine how to hedge against this risk. To hedge against the risk of movements in an underlying asset, intuitively it makes sense for us to hold some fraction, Δ_1^i, of the asset in our portfolio. Our notation for the Black-Scholes call price will remain the same as in previous chapters, to maintain consistency.

Thus $C^i_{BS}(S,t)$ represents the Black-Scholes call option price conditional on volatility state i. Our portfolio $\Pi^i(S,t)$ is represented mathematically as follows:

$$\Pi^i(S,t) = -C^i_{BS}(S,t) + \Delta^i_1 S. \tag{6.9}$$

We are interested in investigating the effect that the stock price has on changes in the value of the hedge portfolio, thus:

$$d\Pi^i(S,t) = -dC^i_{BS}(S,t) + \Delta^i_1 dS. \tag{6.10}$$

The dynamics of our constant volatility option show that the option is only exposed to random movements, dS, in the underlying asset.

$$dC^i(S,t) = \left(\frac{\partial C^i}{\partial t}(S,t) + \frac{1}{2}\sigma_i^2 S^2 \frac{\partial^2 C^i}{\partial S^2}(S,t)\right)dt + \frac{\partial C^i}{\partial S}(S,t)dS. \tag{6.11}$$

It follows that:

$$\begin{aligned} d\Pi^i(S,t) &= -\left[\left(\frac{\partial C^i}{\partial t}(S,t) + \frac{1}{2}\sigma_i^2 S^2 \frac{\partial^2 C^i}{\partial S^2}(S,t)\right)dt + \frac{\partial C^i}{\partial S}(S,t)dS\right] + \Delta^i_1 dS, && (6.12)\\ &= -\left(\frac{\partial C^i}{\partial t}(S,t) + \frac{1}{2}\sigma_i^2 S^2 \frac{\partial^2 C^i}{\partial S^2}(S,t)\right)dt + \left(\Delta^i_1 - \frac{\partial C^i}{\partial S}(S,t)\right)dS. && (6.13)\end{aligned}$$

To eliminate the risk from our portfolio, we must choose our hedge ratio $\Delta^i_1 = \frac{\partial C^i_{BS}}{\partial S}(S,t)$ so that the coefficient in front of dS vanishes, to eliminate all risk in our hedge portfolio. We end up with the Black-Scholes pricing PDE:

$$\frac{\partial C^i}{\partial t}(S,t) + \frac{1}{2}\sigma_i^2 S^2 \frac{\partial^2 C^i}{\partial S^2}(S,t) + rS\frac{\partial C^i}{\partial S}(S,t) - rC^i(S,t) = 0, \tag{6.14}$$

subject to the standard payoff function and boundary conditions associated with a European call option as denoted in equations (2.49) - (2.51).

This well-known pricing equation has a closed-form solution for the value of a European call option and for the hedge ratio (Delta). The hedge ratio is used to determine the number of shares of the underlying asset an investor needs to own in order to hedge against the risk of movement in the underlying asset.

$$\begin{aligned} C^i_{BS}(S,t) &= SN(d^i_1) - Ke^{-r(T-t)}N(d^i_2), && (6.15)\\ \Delta^i_1 &= N(d^i_1), && (6.16)\end{aligned}$$

where:

$$\begin{aligned} d^i_1 &= \frac{\ln\frac{S}{K} + \left(r + \frac{1}{2}\sigma_i^2\right)(T-t)}{\sigma_i\sqrt{T-t}}, && (6.17)\\ d^i_2 &= d^i_1 - \sigma_i\sqrt{T-t}, && (6.18)\end{aligned}$$

and $N(x)$ represents the standard normal cumulative distribution function (CDF). From the properties of the normal distribution we know that $0 \leq N(d^i_1) \leq 1$. The hedge ratio for our position in the underlying asset is defined by $\Delta_1^i = N(d_1^i)$, which is a bounded, increasing function in the stock price. This result makes sense financially as we only ever need one full share of the stock to completely hedge out the risk of our counterparty exercising the option at maturity. Thus as the stock price rises, we buy a higher quantity of the stock to hedge against the risk of the option being exercised. When the stock price falls, we will sell off small quantities of our stock as the likelihood of the option being exercised decreases. This results in option sellers like us buying high and selling low in order to hedge against the inherent stock price movement risk. Over time, the money used to hedge out our risk will eat away at the profit we initially obtained by selling the call option. However, since under the constant volatility framework there exists no arbitrage opportunity, our profits and losses will net out as there is no way to make a risk-less profit from our hedge portfolio. This is of course given that transaction costs are neglected.

6.4 Overview of Hedging Strategies

We will once again assume that our volatility process can only switch between the high and low volatility regimes. For all hedging strategies we consider that we have available three options $C_1^i(S,t), C_2^i(S,t), C_3^i(S,t)$ with strike prices K_1, K_2, K_3 respectively such that $K_3 < K_1 < K_2$. We also have access to the underlying asset, S. The first option $C_1^i(S,t)$ is the option in which we take a short position, also known as our pricing option. Options $C_2^i(S,t)$ and $C_3^i(S,t)$ will be our hedging options for which strategies will be devised to use them to hedge against volatility risk. It is important to note that whatever hedging options we use, the maturity date of these options must be dated at or after the maturity date of the original option sold (i.e. $T_1 \leq T_n$ for $n = 2,3$). Since we are hedging against the switching risk, we must always have a hedging option available while the original option is still exposed to volatility risk.

A detailed discussion of all the hedging strategies used follows. A numerical study of these hedging portfolios and a detailed analysis follows in Section 6.5.

6.4.1 Portfolio I: Hedging with One Option

We assume an investor takes a short position in a European call option $C_1^i(S,t)$ struck at price K_1 and maturing at time T_1. To hedge the exposure taken on by selling an option, we will also continuously adjust positions in the underlying asset S, and another call option $C_n^i(S,t)$ struck at K_n, maturing at T_n for $n = 2,3$. We generalize our hedge ratio and pricing equation derivations for either one of the two possible hedging options $C_2^i(S,t)$ or $C_3^i(S,t)$ where $K_3 < K_1 < K_2$ is assumed to hold. We will investigate later the effects of choosing one over the other in our portfolio. For simplicity, Δ_n^i will refer only to the hedge ratio used for the particular hedging option $C_n^i(S,t)$.

Since we only have the risk of switching out of our currently occupied volatility regime, we only require one hedging option in our portfolio. Our state-dependent portfolio is as follows:

$$\Pi^i(S,t) = -C_1^i(S,t) + \Delta_1^i S + \Delta_n^i C_n^i(S,t). \tag{6.19}$$

Both $C_1^i(S,t)$ and $C_n^i(S,t)$ have the same dynamics but at least one of $K_1 \neq K_n$ and/or $T_1 \neq T_n$ must hold. Recall the dynamics of a regime-switching option which hold for all options in our portfolio.

$$dC^i(S,t) = \left(\frac{\partial C^i}{\partial t}(S,t) + \frac{1}{2}\sigma_i^2 S^2 \frac{\partial^2 C^i}{\partial S^2}(S,t)\right)dt + \frac{\partial C^i}{\partial S}(S,t)dS + \Big[C^j(S,t) - C^i(S,t)\Big]dq_{ij}(t). \tag{6.20}$$

Then the change in portfolio value is:

$$\begin{aligned}
d\Pi^i(S,t) &= -dC_1^i(S,t) + \Delta_1^i dS + \Delta_n^i dC_n^i(S,t), && (6.21)\\
&= -\Bigg[\left(\frac{\partial C_1^i}{\partial t}(S,t) + \frac{1}{2}\sigma_i^2 S^2 \frac{\partial^2 C_1^i}{\partial S^2}(S,t)\right)dt + \frac{\partial C_1^i}{\partial S}(S,t)dS \\
&\quad + \Big[C_1^j(S,t) - C_1^i(S,t)\Big]dq_{ij}(t)\Bigg] \\
&\quad + \Delta_1^i dS + \Delta_n^i \Bigg[\left(\frac{\partial C_n^i}{\partial t}(S,t) + \frac{1}{2}\sigma_i^2 S^2 \frac{\partial^2 C_n^i}{\partial S^2}(S,t)\right)dt + \frac{\partial C_n^i}{\partial S}(S,t)dS \\
&\quad + \Big[C_n^j(S,t) - C_n^i(S,t)\Big]dq_{ij}(t)\Bigg], && (6.22)\\
&= \left[\Delta_n^i\left(\frac{\partial C_n^i}{\partial t}(S,t) + \frac{1}{2}\sigma_i^2 S^2 \frac{\partial C_n^i}{\partial S^2}(S,t)\right) - \frac{\partial C_1^i}{\partial t}(S,t) - \frac{1}{2}\sigma_i^2 S^2 \frac{\partial^2 C_1^i}{\partial S^2}(S,t)\right]dt \\
&\quad + \left[\Delta_1^i - \frac{\partial C_1^i}{\partial S}(S,t) + \Delta_n^i \frac{\partial C_n^i}{\partial S}(S,t)\right]dS \\
&\quad + \Big[\Delta_n^i\Big(C_n^j(S,t) - C_n^i(S,t)\Big) - \Big(C_n^j(S,t) - C_n^i(S,t)\Big)\Big]dq_{ij}(t). && (6.23)
\end{aligned}$$

To hedge against movements in the stock price,

$$\Delta_1^i = \frac{\partial C_1^i}{\partial S}(S,t) - \Delta_n^i \frac{\partial C_n^i}{\partial S}(S,t). \tag{6.24}$$

To hedge against upwards and downwards jumps in volatility,

$$\Delta_n^i = \frac{C_1^j(S,t) - C_1^i(S,t)}{C_n^j(S,t) - C_n^i(S,t)}. \tag{6.25}$$

It is interesting to note a mathematical characteristic of our above hedge ratio for the hedging option our portfolio. It is known that option prices are monotonically increasing with respect to volatility levels. Thus if $\sigma_i \leq \sigma_j$, it follows that $C_n^i(S,t) \leq C_n^j(S,t)$ and $\Delta_n^i \geq 0$ for all S, t, n. Even if we assumed $\sigma_i \geq \sigma_j$ it still follows that $\Delta_n^i \geq 0$ due to the structure of the equation. Thus it is clear that to hedge against our shorted option, we will be taking a dynamic long position in our hedging option.

In general, given the current volatility regime i, our hedging strategy is

$$\Delta_1^i = \frac{\partial C_1^i}{\partial S}(S,t) - \left[\frac{C_1^j(S,t) - C_1^i(S,t)}{C_n^j(S,t) - C_n^i(S,t)}\right]\frac{\partial C_n^i}{\partial S}(S,t), \tag{6.26}$$

$$\Delta_n^i = \frac{C_1^j(S,t) - C_1^i(S,t)}{C_n^j(S,t) - C_n^i(S,t)}. \tag{6.27}$$

Such a hedging strategy makes financial sense, since if both call options $C_1^i(S,t)$ and $C_n^i(S,t)$ were struck at the same strike price and expired on the same date, their values would be equivalent and the hedging strategy would reduce to $\Delta_1^i = 0$ and $\Delta_n^i = 1$. This is just a static hedge in which we take an opposite position, in our case a long position, in the call option we originally sold.

Taking into account our hedging strategy, our state-dependent portfolio is

$$\begin{aligned} d\Pi^i(S,t) = \Bigg[&\frac{C_1^j(S,t) - C_1^i(S,t)}{C_n^j(S,t) - C_n^i(S,t)}\left(\frac{\partial C_n^i}{\partial t}(S,t) + \frac{1}{2}\sigma_i^2 S^2 \frac{\partial^2 C_n^i}{\partial S^2}(S,t)\right) \\ &- \frac{\partial C_1^i}{\partial t}(S,t) - \frac{1}{2}\sigma_i^2 S^2 \frac{\partial^2 C_1^i}{\partial S^2}(S,t)\Bigg]dt. \end{aligned} \tag{6.28}$$

With our choice of Δ_1^i, Δ_n^i, the change in the value of the portfolio only depends on the deterministic change in time. Therefore the no arbitrage conditions allow this to be equated to the risk-free return on the portfolio.

$$d\Pi^i(S,t) = r\Pi^i(S,t)dt, \tag{6.29}$$

$$= r(-C_1^i(S,t) + \Delta_1^i S + \Delta_n^i C_n^i(S,t))dt \tag{6.30}$$

$$\begin{aligned} &\Bigg(-rC_1^i(S,t) + rS\left[\frac{\partial C_1^i}{\partial S}(S,t) - \frac{\partial C_n^i}{\partial S}(S,t)\left(\frac{C_1^j(S,t) - C_1^i(S,t)}{C_n^j(S,t) - C_n^i(S,t)}\right)\right] \\ &\quad + rC_n^i(S,t)\left(\frac{C_1^j(S,t) - C_1^i(S,t)}{C_n^j(S,t) - C_n^i(S,t)}\right)\Bigg)dt \end{aligned}$$

$$\begin{aligned} = \Bigg[&\frac{C_1^j(S,t) - C_1^i(S,t)}{C_n^j(S,t) - C_n^i(S,t)}\left(\frac{\partial C_n^i}{\partial t}(S,t) + \frac{1}{2}\sigma_i^2 S^2 \frac{\partial^2 C_n^i}{\partial S^2}(S,t)\right) \\ &- \frac{\partial C_1^i}{\partial t}(S,t) - \frac{1}{2}\sigma_i^2 S^2 \frac{\partial^2 C_1^i}{\partial S^2}(S,t)\Bigg]dt, \end{aligned} \tag{6.31}$$

$$\begin{aligned} \Rightarrow &\frac{1}{C_1^j(S,t) - C_1^i(S,t)}\left[\frac{\partial C_1^i}{\partial t}(S,t) + \frac{1}{2}\sigma_i^2 S^2 \frac{\partial^2 C_1^i}{\partial S^2}(S,t) + rS\frac{\partial C_1^i}{\partial S}(S,t) - rC_1^i(S,t)\right] \\ &= \frac{1}{C_n^j(S,t) - C_n^i(S,t)}\left[\frac{\partial C_n^i}{\partial t}(S,t) + \frac{1}{2}\sigma_i^2 S^2 \frac{\partial^2 C_n^i}{\partial S^2}(S,t) + rS\frac{\partial C_n^i}{\partial S}(S,t) - rC_n^i(S,t)\right]. \end{aligned} \tag{6.32}$$

Since we selected the two options $C_1^i(S,t)$ and $C_n^i(S,t)$ such that at least one of $T_1 \neq T_n$, $K_1 \neq K_n$ applies, the only way the above relation can hold is if both sides are independent of their type of option contract. Thus both sides can only be a function of their dependent variables, S, σ, t. Therefore the state-dependent function $f_{ij}(S,t)$ is introduced.

$$\frac{1}{C^j(S,t) - C^i(S,t)}\left[\frac{\partial C^i}{\partial t}(S,t) + \frac{1}{2}\sigma_i^2 S^2 \frac{\partial^2 C^i}{\partial S^2}(S,t) + rS\frac{\partial C^i}{\partial S}(S,t) - rC^i(S,t)\right] = f_{ij}(S,t). \tag{6.33}$$

Motivated by Heston [27], let $f_{ij}(S,t)$ be a function of the volatility's drift and the market price of volatility risk where $f_{ij}(S,t) = -\left(\lambda_{ij} - m_{ij}\right)$ and m_{ij} represents the state-dependent market price of volatility risk. Then we get our general coupled pricing final value problem for $i \in \{H, L\}$ where $i \neq j$.

$$\frac{\partial C^i}{\partial t}(S,t) + \frac{1}{2}\sigma_i^2 S^2 \frac{\partial^2 C^i}{\partial S^2}(S,t) + rS\frac{\partial C^i}{\partial S}(S,t) - rC^i(S,t) - f_{ij}\Big[C^j(S,t) - C^i(S,t)\Big], \tag{6.34}$$

subject to the standard European call payoff function and boundary conditions given in equations (2.49) - (2.51).

The above pricing PDE can be solved numerically, as shown in Chapter 3, or by using an approximation technique detailed in Chapter 4. Although mathematically, the inherent risks are completely hedged against using our choice of portfolio, it turns out that issues can nonetheless arise. These financially rooted issues will be discussed later on in this section. First, we will discuss the two different ways to utilize this portfolio given our arsenal of hedging options available.

Hedging with $C_2^i(S,t)$

Since we assumed that $K_1 < K_2$, ideally we would choose to hedge with $C_2^i(S,t)$ given that we expected the stock price to rise. Intuitively, if the stock price rises, we know that eventually the option we shorted will be exercised by the counterparty. Upon exercise, it is our obligation to sell one share of the underlying asset to our counterparty for K_1 dollars. It turns out that if the stock price rises high enough such that $S_T > K_2$, if we have a long position in our hedging option $C_2^i(S,t)$, we can choose to exercise this option at maturity to obtain ownership of one share of a stock by only paying K_2. We then turn around and close out our short position with our counterparty. In this scenario, our costs to close out our portfolio are lower since exercising our hedging option allowed us to take ownership of the stock for less than the trading price on the market. On the other hand, if the stock price at option expiration was such that $K_1 < S_T < K_2$, the strike price of our hedging option, we would simply choose to buy the remaining quantity of our stock directly from the market in order to have one share on hand to sell to our counterparty. For completeness, the portfolio and hedge ratios for this strategy are outlined below.

$$\Pi^i(S,t) = -C_1^i(S,t) + \Delta_1^i S + \Delta_2^i C_2^i(S,t), \tag{6.35}$$

$$\Delta_1^i = \frac{\partial C_1^i}{\partial S}(S,t) - \left(\frac{C_1^j(S,t) - C_1^i(S,t)}{C_2^j(S,t) - C_2^i(S,t)}\right)\frac{\partial C_2^i}{\partial S}(S,t), \tag{6.36}$$

$$\Delta_2^i = \frac{C_1^j(S,t) - C_1^i(S,t)}{C_2^j(S,t) - C_2^i(S,t)}. \tag{6.37}$$

Hedging with $C_3^i(S,t)$

On the other hand, if as an investor we expected the stock price to fall, we would choose to hedge against volatility risk with $C_3^i(S,t)$ since $K_3 < K_1$. Our main concern is the possibility that the counterparty from our original short option position may choose to exercise the option at maturity. If this occurs, we need to have one share of the stock on hand to sell to them for K_1. If the stock price falls enough such that $S_T < K_1$, the counterparty will choose to not exercise their option as it is now out-of-the-money and has no intrinsic value to them. The concern is if the stock price falls slightly but remains in-the-money. This occurs when $S_T > K_1$ at which point the option will be exercised by the counterparty. Since we are hedging with $C_3^i(S,t)$ which is also in-the-money at expiration, we will choose to exercise our option and buy one share of the underlying asset for K_3. we then turn around and sell the share of the stock to our counterparty for K_1, thus pocketing the difference $K_1 - K_3$. The portfolio and hedge ratios for this strategy are given below.

$$\Pi^i(S,t) = -C_1^i(S,t) + \Delta_1^i S + \Delta_3^i C_3^i(S,t), \tag{6.38}$$

$$\Delta_1^i = \frac{\partial C_1^i}{\partial S}(S,t) - \left(\frac{C_1^j(S,t) - C_1^i(S,t)}{C_3^j(S,t) - C_3^i(S,t)}\right)\frac{\partial C_3^i}{\partial S}(S,t), \tag{6.39}$$

$$\Delta_3^i = \frac{C_1^j(S,t) - C_1^i(S,t)}{C_3^j(S,t) - C_3^i(S,t)}. \tag{6.40}$$

In reality, we cannot predict long or short term variations in the stock price. As a result, an investor does not know which hedging option is ideal to use in their portfolio. The risk of going deep in-the-money or deep out-of-the-money can change the dynamics of some or all of the options in the portfolio. When setting up our arbitrage arguments to derive our pricing equation, it was assumed that all options dynamics were exposed to the same market risks. If this is not the case, financially rooted issues arise with our portfolio which will be discussed in detail in the next section.

Issues with Portfolio I

When hedging against various uncontrollable random factors such as stock price movement and stochastic volatility, issues are bound to arise. In particular, it is a well known fact in mathematical finance that there exists cases of moneyness in which the option price is no longer impacted by the volatility levels. When this occurs the options prices in all volatility states are approximately equivalent $C_n^j(S,t) \approx C_n^i(S,t)$.

In general, moneyness refers to the relationship between the trading price of an underlying asset and the strike price of our option. Of concern to us is the effect that an option being too deep in-the-money and too deep out-of-the-money has on the hedging positions in our portfolio. A call option is considered in-the-money when the stock price is trading above the strike price and is considered out-of-the-money when the stock price is trading below the strike price [28]. If a European call option is too deep in the money, this implies that $S >> K$ such that $C(S,t) = S - Ke^{-r(T-t)}$. On the other hand if a European call option is too deep out-of-the-money, this implies that $S << K$ such that $C(S,t) = 0$. In both of these cases we can clearly see that the option values are independent of volatility levels. If $T_n >> T_1$ the issue with respect to being too deep in-the-money could be minimized, however it does not take care of the out-of-the-money case.

We concern ourselves with two call options in our portfolio: the option we initially sold, $C_1^i(S,t)$, and the hedging option, $C_n^i(S,t)$, we use to hedge our volatility exposure. When the option's values are no longer dependent on volatility levels, it turns out that their dynamics change as well:

$$dC_n^i(S,t) = \left(\frac{\partial C_n^i}{\partial t}(S,t) + \frac{1}{2}\sigma_i^2 S^2 \frac{\partial^2 C_n^i}{\partial S^2}(S,t)\right)dt + \frac{\partial C_n^i}{\partial S}(S,t)dS, \tag{6.41}$$

for all $n = 1, \ldots, 3$.

It can be noted that an option being too deep in- or out-of-the-money has dynamics now only exposed to movements in the underlying asset.

If the option originally shorted, $C_1^i(S,t)$, no longer possesses regime-switching volatility dynamics, it is intuitive to realize that we no longer need an additional hedging instrument in our portfolio as we are now only exposed to movements in the underlying asset. This is due to the fact that our short call option is no longer sensitive to volatility movement and we would proceed by hedging Black-Scholes [6] style. This would involve us continuously adjusting our position in the underlying asset. It makes sense as this point to liquidate our position in our hedging option by letting $\Delta_n^i = 0$. It follows that our hedge ratio for the hedging option given by equation (6.27), is defined in such a way that allows for the position to be liquidated automatically.

The more involved situation is when the hedging option $C_n^i(S,t)$, where $n = 2, 3$, no longer possesses the regime-switching volatility dynamics. Recall that we want to hedge against our volatility switching with an option written on the same underlying with the same switching dynamics. If this option is no longer exposed (or sufficiently exposed) to volatility switching, it is now considered an inappropriate hedging instrument. It should be noted that although the hedging option price becomes insensitive to volatility movements, as a result, the associated hedge ratio becomes hugely sensitive. As can be noted in equation (6.27), insensitivity to volatility in the hedging option causes the magnitude of the hedge ratio to become quite large. The main issue lies with the case where our hedging option is no longer sensitive to volatility but the original option we shorted is. This motivates us to consider a new portfolio incorporating an additional hedging option with different contract specifications. Although there is a immense basket of options available, we choose our hedging option in such a way that the structure the two hedging options strike prices straddle the shorted option's strike price. We must choose our options to have strike prices to exist in some range around K_1 such that they do not begin deep in- or out-of-the-money. This is realistic as options on financial markets have strike prices that allow them to be sold at- or about-the-money. This ensures that one of two hedging options used will still be sensitive to volatility switching when the other hedging option is not. Setting up our portfolio in this way can be though of as a type of insurance option straddling to insure that we always have appropriate hedging options available to hedge against the embedded switching risk. Such a portfolio will be presented in the next section.

6.4.2 Portfolio II: Hedging with Two Options

Given the issues that can possibly arise while hedging using Portfolio I, we introduce an additional arbitrary hedging option to our portfolio $C_3^i(S,t)$ struck at K_3 and maturing at T_3, to also be used to hedge against movements in the volatility. It is assumed that $K_3 < K_1 < K_2$. Choosing hedging options with strike prices straddling the original strike price is deliberate as this ensures that if and when one hedging option can no longer be used to hedge volatility risk, there is another option available in the portfolio to do so with. This set up also ensures that the original option will lose its exposure to volatility before both of the hedging options do.

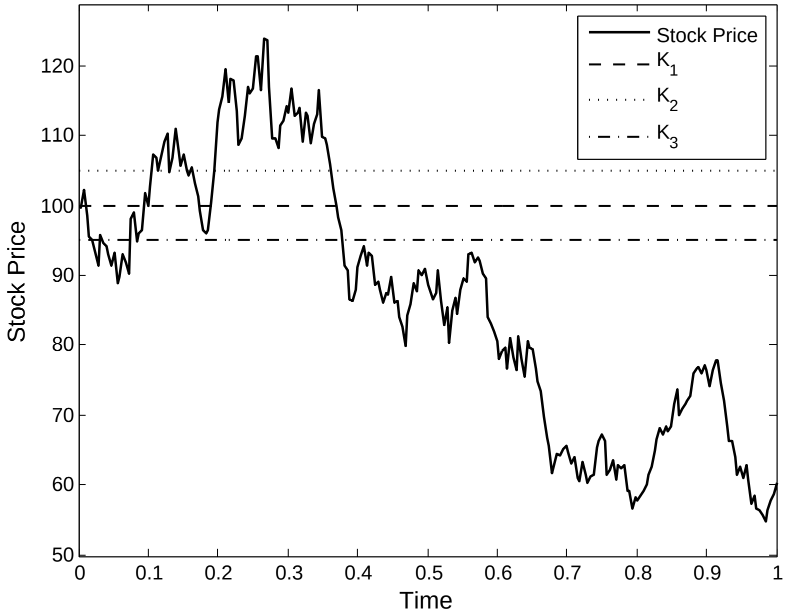

Figure 6.1: Example of Portfolio II set-up when $S_T < K_3$.

This is more clear by considering Figures 6.1 and 6.2 which depict the two cases that our portfolio set-up protects against. In Figure 6.1, it is observed that the stock price falls below all the strike prices at the maturity date. As the stock price begins to fall, the first option to go deep out-of-the-money is $C_2^i(S,t)$ with strike price K_2. Therefore this option is no longer a useful hedging option for us. However, while the shorted option is still exposed to the switching volatility dynamics, we have our other hedging option $C_3^i(S,t)$ with strike price K_3 that we can still use. As the stock price continues to fall, the option we shorted will go deep out-of-the-money before our last hedging option, at which point we only need to proceed with taking a position in our underlying asset. Thus it was illustrated that as the stock price falls, we are assured that there will always be a hedging option available to us containing the regime-switching dynamics, as long as our original option so requires.

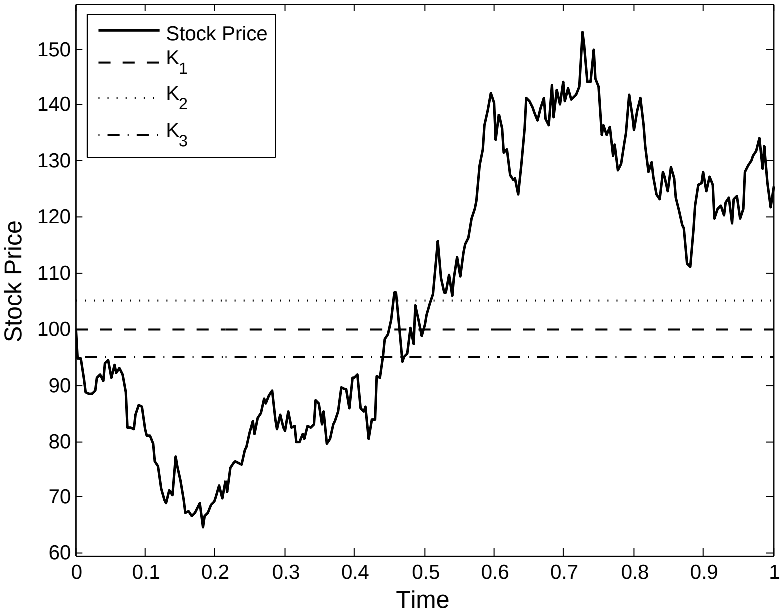

Figure 6.2: Example of Portfolio II set-up when $S_T > K_2$.

Figure 6.2 depicts the opposite scenario where the stock price rises above all the strike prices at the maturity date. As the stock price begins to rise, the first option to go deep in-the-money and to be no longer dependent on volatility levels is our hedging option $C_3^i(S,t)$ with strike price K_3. However, given the clever set-up of our portfolio, there still is another hedging option $C_2^i(S,t)$ available to use against volatility switching. As the stock price continues to rise, the option we shorted will first become deep in-the-money before our remaining hedging option. At this point, we would only need to hedge as if we were in the Black-Scholes world. Once again, for the life of the shorted option in which it was exposed to volatility switching dynamics, our portfolio always contained a hedging option that could be utilized.

Now that the motivation behind the set-up of Portfolio II is clear, we can investigate what hedge ratios and pricing equations follow under this framework. Our new hedge portfolio, Portfolio II, is given below.

$$\Pi^i(S,t) = -C_1^i(S,t) + \Delta_1^i S + \Delta_2^i C_2^i(S,t) + \Delta_3^i C_3^i(S,t). \tag{6.42}$$

The change in value of our portfolio is:

$$d\Pi^i(S,t) = -dC_1^i(S,t) + \Delta_1^i dS + \Delta_2^i dC_2^i(S,t) + \Delta_3^i dC_3^i(S,t). \tag{6.43}$$

Since all options in the portfolio are written on the same underlying asset with regime-switching volatility, they all have the same option dynamics.

$$d\Pi^i(S,t) = -\left[\left(\frac{\partial C_1^i}{\partial t}(S,t) + \frac{1}{2}\sigma_i^2 S^2 \frac{\partial^2 C_1^i}{\partial S^2}(S,t)\right)dt + \frac{\partial C_1^i}{\partial S}(S,t)dS + \left[C_1^j(S,t) - C_1^i(S,t)\right]dq_{ij}(t)\right] + \Delta_1^i dS$$

$$\begin{aligned}
&+\Delta_2^i\Big[\Big(\frac{\partial C_2^i}{\partial t}(S,t)+\frac{1}{2}\sigma_i^2S^2\frac{\partial^2C_2^i}{\partial S^2}(S,t)\Big)dt+\frac{\partial C_2^i}{\partial S}(S,t)dS+\Big[C_2^j(S,t)-C_2^i(S,t)\Big]dq_{ij}(t)\Big]\\
&+\Delta_3^i\Big[\Big(\frac{\partial C_3^i}{\partial t}(S,t)+\frac{1}{2}\sigma_i^2S^2\frac{\partial^2C_3^i}{\partial S^2}(S,t)\Big)dt+\frac{\partial C_3^i}{\partial S}(S,t)dS+\Big[C_3^j(S,t)-C_3^i(S,t)\Big]dq_{ij}(t)\Big],
\end{aligned} \tag{6.44}$$

$$\begin{aligned}
={}&\Big[\Delta_2^i\Big(\frac{\partial C_2^i}{\partial t}(S,t)+\frac{1}{2}\sigma_i^2S^2\frac{\partial^2C_2^i}{\partial S^2}(S,t)\Big)+\Delta_3^i\Big(\frac{\partial C_3^i}{\partial t}(S,t)+\frac{1}{2}\sigma_i^2S^2\frac{\partial^2C_3^i}{\partial S^2}(S,t)\Big)\\
&-\Big(\frac{\partial C_1^i}{\partial t}(S,t)+\frac{1}{2}\sigma_i^2S^2\frac{\partial^2C_1^i}{\partial S^2}(S,t)\Big)\Big]dt\\
&+\Big(\Delta_1^i-\frac{\partial C_1^i}{\partial S}(S,t)+\Delta_2^i\frac{\partial C_2^i}{\partial S}(S,t)+\Delta_3^i\frac{\partial C_3^i}{\partial S}(S,t)\Big)dS\\
&+\Big(\Delta_2^i\Big[C_2^j(S,t)-C_2^i(S,t)\Big]+\Delta_3^i\Big[C_3^j(S,t)-C_3^i(S,t)\Big]-\Big[C_1^j(S,t)-C_1^i(S,t)\Big]\Big).
\end{aligned} \tag{6.45}$$

To hedge against movements in the underlying asset,

$$\Delta_1^i=\frac{\partial C_1^i}{\partial S}(S,t)-\Delta_2^i\frac{\partial C_2^i}{\partial S}(S,t)-\Delta_3^i\frac{\partial C_3^i}{\partial S}(S,t). \tag{6.46}$$

To hedge against movements between the volatility regimes,

$$\Delta_2^i\Big[C_2^j(S,t)-C_2^i(S,t)\Big]+\Delta_3^i\Big[C_3^j(S,t)-C_3^i(S,t)\Big]=C_1^j(S,t)-C_1^i(S,t). \tag{6.47}$$

Since we have more unknown variables (i.e. our hedge ratios) than equations, either Δ_2^i or Δ_3^i can be arbitrarily chosen. For us, this would depend on our initial choice of hedging option. For Portfolio I, we had two hedge ratios to determine with two equations. That procedure was straightforward and involved solving a linear system of equations. For Portfolio II, both mathematical methods and methods motivated by financial intuition will be investigated.

Minimum Variance Hedging Approach

We will first approach this problem by investigating what hedge ratio is necessary for our second hedging option in order to minimize the variance of the portfolio. Since we previously saw that our choice of hedge ratios hedged against all risks, our change in portfolio value depends solely on the deterministic change in time. Thus it follows that:

$$\begin{aligned}
d\Pi^i(S,t)&=r\Pi^i(S,t)dt, &(6.48)\\
&=r\Big[-C_1^i(S,t)+\Delta_1^iS+\Delta_2^iC_2^i(S,t)+\Delta_3^iC_3^i(S,t)\Big]dt. &(6.49)
\end{aligned}$$

Since we chose Δ_3^i to be arbitrary, we will rewrite equation (6.47) to represent the hedge ratio Δ_2^i.

$$\Delta_2^i=\frac{C_1^j(S,t)-C_1^i(S,t)}{C_2^j(S,t)-C_2^i(S,t)}-\Delta_3^i\Big(\frac{C_3^j(S,t)-C_3^i(S,t)}{C_2^j(S,t)-C_2^i(S,t)}\Big). \tag{6.50}$$

As we will be minimizing the variance of our portfolio, we need to first derive an expression for the portfolio variance.

$$\begin{aligned}
\mathrm{Var}[d\Pi^i(S,t)] &= \mathbb{E}[(d\Pi^i(S,t) - \mathbb{E}[d\Pi^i(S,t)])^2], && (6.51)\\
&= \mathbb{E}[(d\Pi^i(S,t))^2] - (\mathbb{E}[d\Pi^i(S,t)])^2, && (6.52)\\
&= -(\mathbb{E}[d\Pi^i(S,t)])^2, && (6.53)
\end{aligned}$$

since $\mathbb{E}[dt^2] = 0$.

$$\begin{aligned}
\mathbb{E}[d\Pi^i(S,t)] &= r\Big[-C_1^i(S,t) + \Delta_1^i S + \Delta_2^i C_2^i(S,t) + \Delta_3^i C_3^i(S,t)\Big], && (6.54)\\
\mathrm{Var}[d\Pi^i(S,t)] &= -r^2\Big(-C_1^i(S,t) + \Delta_1^i S + \Delta_2^i C_2^i(S,t) + \Delta_3^i C_3^i(S,t)\Big)^2. && (6.55)
\end{aligned}$$

We want to solve $\dfrac{d\mathrm{Var}[d\Pi^i(S,t)]}{d\Delta_3^i} = 0$ for Δ_3^i.

$$\frac{d}{d\Delta_3^i}\left[-r^2\Big(-C_1^i(S,t) + \Delta_1^i S + \Delta_2^i C_2^i(S,t) + \Delta_3^i C_3^i(S,t)\Big)^2\right] = 0, \tag{6.56}$$

$$-2r^2\Big(-C_1^i(S,t) + \Delta_1^i S + \Delta_2^i C_2^i(S,t) + \Delta_3^i C_3^i(S,t)\Big)\left(\frac{d\Delta_1^i}{d\Delta_3^i}S + \frac{d\Delta_2^i}{d\Delta_3^i}C_2^i(S,t) + C_3^i(S,t)\right) = 0, \tag{6.57}$$

where:

$$\begin{aligned}
\frac{d\Delta_1^i}{d\Delta_3^i}(S,t) &= -\frac{d\Delta_2^i}{d\Delta_3^i}\frac{\partial C_2^i}{\partial S}(S,t) - \frac{\partial C_3^i}{\partial S}(S,t), && (6.58)\\
\frac{d\Delta_2^i}{d\Delta_3^i}(S,t) &= -\frac{C_3^j(S,t) - C_3^i(S,t)}{C_2^j(S,t) - C_2^i(S,t)}. && (6.59)
\end{aligned}$$

The above derivatives are constant for a given value of S and t (i.e. they no longer depend on the hedge ratio Δ_3^i). Then,

$$-C_1^i(S,t) + \Delta_1^i S + \Delta_2^i C_2^i(S,t) + \Delta_3^i C_3^i(S,t) = 0, \tag{6.60}$$

$$\left(\frac{\partial C_1^i}{\partial S}(S,t) - \Delta_2^i\frac{\partial C_2^i}{\partial S}(S,t) - \Delta_3^i\frac{\partial C_3^i}{\partial S}(S,t)\right)S + \Delta_2^i C_2^i(S,t) + \Delta_3^i C_3^i(S,t) = C_1^i(S,t), \tag{6.61}$$

$$\Delta_2^i\left(C_2^i(S,t) - S\frac{\partial C_2^i}{\partial S}(S,t)\right) + \Delta_3^i\left(C_3^i(S,t) - S\frac{\partial C_3^i}{\partial S}(S,t)\right) = C_1^i(S,t) - S\frac{\partial C_1^i}{\partial S}(S,t), \tag{6.62}$$

$$\begin{aligned}
&\left[\frac{C_1^j(S,t) - C_1^i(S,t)}{C_2^j(S,t) - C_2^i(S,t)} - \Delta_3^i\frac{C_3^j(S,t) - C_3^i(S,t)}{C_2^j(S,t) - C_2^i(S,t)}\right]\left(C_2^i(S,t) - S\frac{\partial C_2^i}{\partial S}(S,t)\right)\\
&\quad + \Delta_3^i\left(C_3^i(S,t) - S\frac{\partial C_3^i}{\partial S}(S,t)\right) = C_1^i(S,t) - S\frac{\partial C_1^i}{\partial S}(S,t).
\end{aligned} \tag{6.63}$$

Rearranging for Δ_3^i yields our minimum variance hedge ratio for our arbitrary hedging option $C_3^i(S,t)$.

$$\Delta_3^i = \frac{\left[C_2^j(S,t) - C_2^i(S,t)\right]\left(C_1^i(S,t) - S\frac{\partial C_1^i}{\partial S}(S,t)\right) - \left[C_1^j(S,t) - C_1^i(S,t)\right]\left(C_2^i(S,t) - S\frac{\partial C_2^i}{\partial S}(S,t)\right)}{\left[C_2^j(S,t) - C_2^i(S,t)\right]\left(C_3^i(S,t) - S\frac{\partial C_3^i}{\partial S}(S,t)\right) - \left[C_3^j(S,t) - C_3^i(S,t)\right]\left(C_2^i(S,t) - S\frac{\partial C_2^i}{\partial S}(S,t)\right)}. \tag{6.64}$$

It follows that:

$$\Delta_2^i = \frac{\left[C_1^j(S,t) - C_1^i(S,t)\right]\left(C_3^i(S,t) - S\frac{\partial C_3^i}{\partial S}(S,t)\right) - \left[C_3^j(S,t) - C_3^i(S,t)\right]\left(C_1^i(S,t) - S\frac{\partial C_1^i}{\partial S}(S,t)\right)}{\left[C_2^j(S,t) - C_2^i(S,t)\right]\left(C_3^i(S,t) - S\frac{\partial C_3^i}{\partial S}(S,t)\right) - \left[C_3^j(S,t) - C_3^i(S,t)\right]\left(C_2^i(S,t) - S\frac{\partial C_2^i}{\partial S}(S,t)\right)}. \tag{6.65}$$

Although these hedge ratios are chosen such that our portfolio variance is minimized, it turns out that they do not make sense intuitively. In financial mathematics, intuition is a huge guide to the appropriateness of mathematical assumptions and methodologies chosen. The results obtained by these models must also be supported by expert financial intuition in order for them to be justified. This cyclical pattern of intuition and mathematics is common in applied mathematics. In our case, the minimized variance hedge ratios give us results that show that in times when we do not need to be hedged against volatility switching, we are taking unnecessary positions in options. This in turn can eat away at our initial profit obtained from selling the option especially if transaction costs are considered. Thus it makes more financially intuitive sense to employ a strategy to minimize the use of hedging options such that our profit is not whittled away by unnecessary trades in our hedging option. We can consider initially hedging with one hedging option and if and when this option becomes unusable to us (i.e. its dynamics no longer contain regime-switching properties), we can begin employing our other hedging option to counteract this issue. This will resolve all financial issues that arose in our initial hedging portfolio, Portfolio I, while not taking and/or maintaining unnecessary positions in options.

Given that $K_3 < K_1 < K_2$, there are several cases that naturally arise for which we can investigate whether or not our minimized hedge ratios allow us to properly hedge against our underlying market risks. Two main subsets of cases are: $C_1^i(S,t) \neq C_1^j(S,t)$ and $C_1^i(S,t) \approx C_1^j(S,t)$.

Case 1: $C_1^i(S,t) \neq C_1^j(S,t)$

Given that $K_1 < K_2$, $C_2^i(S,t) \approx C_2^j(S,t)$ occurs when the stock price falls significantly such that $S << K_2$. Our positions for our hedging options are as follows:

$$\Delta_2^i = \frac{\left[C_3^j(S,t) - C_3^i(S,t)\right]\left(S\frac{\partial C_1^i}{\partial S}(S,t) - C_1^i(S,t)\right) - \left[C_1^j(S,t) - C_1^i(S,t))\right]\left(S\frac{\partial C_3^i}{\partial S}(S,t) - C_3^i(S,t)\right)}{\left[C_3^j(S,t) - C_3^i(S,t)\right]\left(S\frac{\partial C_2^i}{\partial S}(S,t) - C_2^i(S,t)\right)}, \tag{6.66}$$

$$\Delta_3^i = \frac{C_1^j(S,t) - C_1^i(S,t)}{C_3^j(S,t) - C_3^i(S,t)}. \tag{6.67}$$

Since the dynamics of the hedging option $C_2^i(S,t)$ no longer include the risk of volatility switching, we intuitively expected that $\Delta_2^i = 0$. This is due to the fact that if the hedging option's dynamics are not exposed to the same risks are our original shorted option then it can no longer be used to hedge against the volatility switching. Since we have another option in our portfolio to use, it makes the most sense to liquidate our position in the asset completely. Even maintaining a static position in this unusable option would be more efficient as we would not incur any additional transaction costs.

The other scenario is when the stock price rises where $S >> K_3$. At this point, one of our hedging options $C_3^i(S,t)$ is deep in-the-money where option value is independent of volatility level. Our positions for our hedging options are as follows:

$$\Delta_2^i = \frac{C_1^j(S,t) - C_1^i(S,t)}{C_2^j(S,t) - C_2^i(S,t)}, \tag{6.68}$$

$$\Delta_3^i = \frac{\left[C_2^j(S,t) - C_2^i(S,t)\right]\left(S\frac{\partial C_1^i}{\partial S}(S,t) - C_1^i(S,t)\right) - \left[C_1^j(S,t) - C_1^i(S,t)\right]\left(S\frac{\partial C_2^i}{\partial S}(S,t) - C_2^i(S,t)\right)}{\left[C_2^j(S,t) - C_2^i(S,t)\right]\left(S\frac{\partial C_3^i}{\partial S}(S,t) - C_3^i(S,t)\right)}. \tag{6.69}$$

Since the hedging option $C_3^i(S,t)$ becomes independent of volatility level, we would expect to liquidate our position in this option, $\Delta_3^i = 0$, and fully hedge with our other hedging option $C_2^i(S,t)$. However, the minimized variance approach dictates that we should still keep a dynamic position in this hedging instrument, thus continuously incurring unnecessary hedging costs through changing our position and transaction costs over time. Technically, we only need one hedging option to hedge against the possible jump to another volatility regime, thus holding a dynamic position in two options seems excessive and costly.

Overall, we can see that when we still require to hedge against all risks (i.e. stock price movement and volatility switching) associated with our shorted call option, the minimized variance method does not seem to fully satisfy financial intuition and may cause additional costs over time. It remains to analyse what happens when the shorted option no longer posses regime-switching dynamics.

Case 2: $C_1^i(S,t) \approx C_1^j(S,t)$

We know that we need to hedge against the option we sold: $C_1^i(S,t)$. Given the dynamics of all regime-switching call options, we know that if $C_l^j(S,t) \approx C_l^i(S,t)$ then the option no longer possesses an exposure to volatility switching. If this occurs for the option we sold, intuitively we know that we should only need to hedge Black-Scholes style (i.e. against movement in the underlying asset). Given the structure of our hedging options (i.e. $K_3 < K_1 < K_2$), $C_1^j(S,t) \approx C_1^i(S,t)$ can only occur if one of $C_2^j(S,t) \approx C_2^i(S,t)$ or $C_3^j(S,t) \approx C_3^i(S,t)$ also holds.

First, we examine what happens when the stock price falls where $S << K_1 < K_2$ such that both $C_1^i(S,t)$ and $C_2^i(S,t)$ become insensitive to volatility. Our hedge ratios are:

$$\Delta_2^i = \frac{S\frac{\partial C_1^i}{\partial S}(S,t) - C_1^i(S,t)}{S\frac{\partial C_2^i}{\partial S}(S,t) - C_2^i(S,t)} \neq 0, \tag{6.70}$$

$$\Delta_3^i = 0. \tag{6.71}$$

Given that our original option no longer is exposed to volatility switching, we should only have to take a position in the underlying asset in order to hedge against our remaining risk from movements in the stock price. However, the minimized variance method denotes that we should liquidate our position in one of our hedging options, while still maintaining a position in our other hedging option. Intuitively, this is not what we would expect financially and we would be incurring additional hedging costs by keeping a dynamic position in an additional, unnecessary hedging instrument.

On the other hand, when the stock price rises such that $S >> K_1 > K_3$ and $C_3^i(S,t) \approx C_3^j(S,t)$, our positions for our hedging options are as follows:

$$\Delta_2^i = 0 \tag{6.72}$$

$$\Delta_3^i = \frac{S\frac{\partial C_1^i}{\partial S}(S,t) - C_1^i(S,t)}{S\frac{\partial C_3^i}{\partial S}(S,t) - C_3^i(S,t)} \neq 0 \tag{6.73}$$

Once again, we expect to liquidate positions in both of our hedging options, although the minimum variance method dictates that we do so for one only option. By keeping a hedge position in an additional hedging instrument, over time more and more hedging losses can be easily incurred especially when proportional transaction costs are taken into consideration.

The inconsistencies that arise when choosing our hedge ratios for Portfolio II via minimized variance motivate us to consider putting restrictions in place on our hedge portfolio. This would ensure that we are not losing unnecessary money from dynamically changing positions in hedging instruments not deemed appropriate to use for hedging.

Hedging with a Limit

Thinking back to Portfolio I, we recall that our hedge ratio for our hedging options as follows:

$$\Delta_n^i = \frac{C_1^j(S,t) - C_1^i(S,t)}{C_n^j(S,t) - C_n^i(S,t)}. \tag{6.74}$$

We can easily see that as $C_n^i(S,t) \to C_n^j(S,t)$, the above hedge ratio ”blows up”. This is equivalent with taking a non-finite position in the hedging option. It is not realistic to take a infinite position in an option nor is it realistic to take a large finite position in this option. This motivates us to put a limit on the number of hedging options we can buy in order to hedge against the inherent volatility switching risk of our shorted option. In addition, the further we go in- or out-of-the-money, the less volatility impacts option value (i.e. $C_n^i(S,t) \approx C_n^j(S,t)$. In such cases, it would make sense to completely liquidate our position in this hedging option and begin to hedge using only the additional hedging option whose value is still dependent on volatility level. We will assume that we start hedging with one hedging option $C^i_n(S,t)$ where $n \in \{2,3\}$ in addition to hedging with the underlying asset S. Our additional hedging option $C^i_{n^\star}(S,t)$ will be available for use, but only utilized if the original hedging option's hedging ratio breaches a limit or when it goes too deep in- or out-of-the-money. If the hedging limit is not breached, we will hedge using the initial hedging instruments in our portfolio. Our initial portfolio is as follows:

$$\Pi^i(S,t) = -C^i_1(S,t) + \Delta^i_1 S + \Delta^i_n C^i_n(S,t) + \Delta^i_{n^\star} C^i_{n^\star}(S,t), \tag{6.75}$$

where:

$$\Delta^i_1 = \frac{\partial C^i_1}{\partial S}(S,t) - \Delta^i_n \frac{\partial C^i_n}{\partial S}(S,t) - \Delta^i_{n^\star} \frac{\partial C^i_{n^\star}}{\partial S}(S,t). \tag{6.76}$$

Initially, $\Delta^i_{n^\star} = 0$, since we do not utilize this hedging option unless absolutely necessary. The values for Δ^i_n and $\Delta^i_{n^\star}$ are case dependent and as such there are three scenarios that can arise that are described in detail below. We are generalizing our results for all possible cases. The following cases hold for both $K_{n^\star} < K_1 < K_n$ and $K_n < K_1 < K_{n^\star}$. Note that $n^\star, n = 2,3$ where $n^\star \neq n$.

Case 1: $0 \leq \Delta^i_n < N_{lim}$

The first case to consider is when the hedging ratio of our initial hedging option does not breach the imposed limit. If the limit is not breached, this means two things. First, that the hedging option still possesses the dynamics containing volatility switching, thus making it an appropriate financial instrument to hedge volatility. Second, that our equation for our hedge ratio dictates that we take a position of reasonable finite magnitude in our hedging option, following with our intuition. The hedge ratios for all possible options we can use are expressed below.

$$\Delta^i_n = \frac{C^j_1(S,t) - C^i_1(S,t)}{C^j_n(S,t) - C^i_n(S,t)}, \tag{6.77}$$

$$\Delta^i_{n^\star} = 0. \tag{6.78}$$

While the limit is not breached, our hedging strategy is identical to that of Portfolio I, discussed earlier on in this chapter.

Case 2: $\Delta^i_n \geq N_{lim}$

Our hedging limit N_{lim} is breached as the hedging option becomes less and less sensitive to volatility levels. This occurs as $C^i_n(S,t) \to C^j_n(S,t)$ which in turn "blows up" our ratio. In this case, it is more advisable to maintain a static hedge in our initial hedging option, and bring in our secondary hedging option $C^i_{n^\star}(S,t)$ to dynamically hedge against the possible volatility switching. The corresponding hedge ratios are defined below.

$$\Delta^i_n = N_{lim}, \tag{6.79}$$

$$\Delta^i_{n^\star} = \frac{C^j_1(S,t) - C^i_1(S,t)}{C^j_{n^\star}(S,t) - C^i_{n^\star}(S,t)}\left[1 - N_{lim}\left(\frac{C^j_n(S,t) - C^i_n(S,t)}{C^j_1(S,t) - C^i_1(S,t)}\right)\right]. \tag{6.80}$$

The static hedge in our initial hedging option allows us to avoid unnecessary transactions costs by closing out this position. At this point in time, this option still possesses the regime-switching dynamics and is still a usable hedging option if the stock price moves in a direction such that the limit is no longer breached. If this occurs, it would be far less costly to readjust our position from the static hedge than it would be to completely re-set-up our position from a liquidated hedge.

It was shown earlier that $\dfrac{C^j_1(S,t) - C^i_1(S,t)}{C^j_n(S,t) - C^i_n(S,t)} \geq 0$ and we chose $N_{lim} > 0$ since we take a long position in our hedging option. Thus it follows that:

$$N_{lim} < \frac{C^j_1(S,t) - C^i_1(S,t)}{C^j_n(S,t) - C^i_n(S,t)}, \tag{6.81}$$

$$0 \leq N_{lim}\left(\frac{C^j_n(S,t) - C^i_n(S,t)}{C^j_1(S,t) - C^i_1(S,t)}\right) < 1, \tag{6.82}$$

$$0 < 1 - N_{lim}\left(\frac{C^j_n(S,t) - C^i_n(S,t)}{C^j_1(S,t) - C^i_1(S,t)}\right) \leq 1. \tag{6.83}$$

Given equation (6.80), and since we know that the limit gets breached as $C^i_n(S,t) \to C^j_n(S,t)$. This allows us to assume that while the limit is breached, the follow is true:

$$\Delta^i_{n^\star} \approx \frac{C^j_1(S,t) - C^i_1(S,t)}{C^j_{n^\star}(S,t) - C^i_{n^\star}(S,t)}. \tag{6.84}$$

This is the same hedge ratio used if we had assumed we were only going to hedge with our additional hedging option $C^i_{n^\star}(S,t)$.

Case 3: $C^i_n(S,t) \approx C^j_n(S,t)$

Finally, Case 3 represents the scenario that Portfolio I could not insure against. When the initial hedging option goes too deep in-the-money or deep out-of-the-money, its value becomes insensitive to volatility level. At this point, the option's dynamics are no longer exposed to the shifts between the two volatility regimes. We know from basic hedging arguments, that the hedging instrument must be exposed to the same risks as the initial option we sold. Thus it makes financial sense to liquidate this position and employ our additional hedging option on hand. It is assumed that this extra hedging option has the same dynamics as our original option. The new hedge ratios are given below.

$$\Delta^i_n = 0, \tag{6.85}$$

$$\Delta^i_{n^\star} = \frac{C^j_1(S,t) - C^i_1(S,t)}{C^j_{n^\star}(S,t) - C^i_{n^\star}(S,t)}. \tag{6.86}$$

It can be observed that these hedge positions are the same as those employed in Portfolio I, however we are now hedging with $C^i_{n^\star}(S,t)$ instead of $C^i_n(S,t)$.

For the above defined cases for Portfolio II, we will price all of the options contained in our portfolio using the pricing PDE defined by equation (6.34). This is due to the fact that for this pricing equation holds directly for Cases 1 and 3. In Case 2, where we hold a static hedge in one of our hedging options, since it is assumed that this option is on its way to be completely independent of volatility levels, it makes intuitive sense to use the pricing PDE derived from the portfolio with one hedging option.

Although we have discussed in detail ways to hedge against the additional risk embedded within our options via volatility switching, it may not always be beneficial for an investor to take positions in multiple hedging instruments especially when transaction costs are taken into account. We will now consider several different hedging approaches which assume constant volatility.

6.4.3 Hedging with Constant Volatility

For an investor it may not always be the most profitable to dynamically change hedge ratios in multiple financial instruments. This is also more pertinent given the fact that volatility generally does not shift between regimes too often. Individual state occupation can last a matter of months or years. Over time, especially in the presence of transaction costs, readjusting a portfolio too often can accumulate unwanted and unnecessary transaction costs. As a result, investors might be better off to hedge assuming constant volatility and assuming that switching will not occur over the life of the option they hold in their portfolio. No matter what, we cannot assume that a stock price will not change, thus we still need to hedge against the underlying as defined by the Black-Scholes option pricing model [6]. This hedging method was described in detail in Section 6.3.

The basic set-up of the constant volatility hedge portfolios and their ratios are consistent across strategies. What differs per strategy is how we estimate our volatility level, which is assumed to be constant. This method is equivalent to the Black-Scholes hedge, now conditional on our volatility estimate $\sigma_{i^\star}$ where $i^\star$ represents our constant volatility state occupation.

$$\Pi^{i^\star}(S,t) = -C^{i^\star}_{BS}(S,t) + \Delta^{i^\star}_{BS} S, \tag{6.87}$$

$$C^{i^\star}_{BS}(S,t) = S N(d^{i^\star}_1) - K e^{-r(T-t)} N(d^{i^\star}_2), \tag{6.88}$$

$$\Delta^{i^\star}_{BS} = N(d^{i^\star}_1), \tag{6.89}$$

where:

$$d^{i^\star}_1 = \frac{\ln\frac{S}{K} + \left(r + \frac{1}{2}(\sigma^\star_i)^2\right)(T-t)}{\sigma^\star_i \sqrt{T-t}}, \tag{6.90}$$

$$d_2^{i^\star} = d_1^{i^\star} - \sigma_{i^\star}\sqrt{T-t}, \tag{6.91}$$

$$N(x) = \frac{1}{\sqrt{2\pi}}\int_{\infty}^{x} e^{-\frac{z^2}{2}}dz. \tag{6.92}$$

We will hedge against movements in the underlying asset using our Black-Scholes Delta given by equation (6.89). The price at which we sell our call option will be determined by equation (6.88).

The main issue facing us now is what volatility level would we choose to hedge with. This choice should not be arbitrary and the estimate of volatility should be rooted in financial intuition. The current market state and the investor's risk preferences should both be considered when determining an estimate of the volatility level. We can consider both a probabilistic approach to defining the volatility or a financially intuitive method based on the type of investor setting up the portfolio. Various approaches to estimating the volatility will be discussed in detail in this section.

Unconditional Volatility

If we consider the long term behaviour of volatility, it may be useful to consider the unconditional probabilities of occupying either the high or low volatility state. We can use these unconditional probabilities to compute a weighted average of the high and low volatility levels in order to give us an estimate for our constant volatility state level.

$$\sigma_{i^\star} = \sigma_H P_{H,unconditional} + \sigma_L P_{L,unconditional}, \tag{6.93}$$

where:

$$\begin{bmatrix} P_H \\ P_L \end{bmatrix}_{unconditional} = \begin{bmatrix} \dfrac{\lambda_{LH}}{\lambda_{LH}+\lambda_{HL}} \\ \dfrac{\lambda_{HL}}{\lambda_{LH}+\lambda_{HL}} \end{bmatrix}.$$

This gives us an estimate of the volatility which reflects the market conditions over time. The estimate will be pulled towards the volatility level for the state that we occupy the majority of the time.

Hedging Given Investor's Risk Preferences

In Chapter 5, it was observed that investors are concerned with the overall risk they take on when setting up a position in a market with a financial instrument. In particular, under our regime-switching framework investors are highly concerned with the potential to switch to a less desirable volatility regime which could hinder their hedging strategy. We saw that investors who are scared of such a switching risk will demand compensation for taking on this risk via the volatility risk premium. This premium is embedded within the coupling coefficient of our pricing equations, given by equation (2.52), which acts as a risk-adjusted Poisson intensity. Given that this compensation was considered to be large enough to alleviate their risks, in all cases, we could approximate our regime-switching call option values by assuming constant volatility. A discussion of these preferences and how they relate to our constant volatility hedging strategies is given.

Preferences of a Short Position

We previously saw that an investor with a short position in a regime-switching option fears high volatility, all else being equal. Option prices are monotonically increasing with respect to volatility thus, a decrease in volatility leads to a decrease in option value. From the short position's perspective, their probability of their counterparty exercising the option increases with volatility and thus they require a large volatility risk premium to compensate them for their risk. As we saw, this results in the regime-switching option being priced as if we are in a constant high volatility world. Thus we will hedge against only movements in the underlying asset assuming we are occupying the high volatility regime where $\sigma_{i^\star} = \sigma_H$.

From the analysis in previous chapters we know that $C^i(S,t) \leq C^H_{BS}(S,t)$ for all $i \in \{H, L\}$. Thus the investor sells the option for more than it would have if it had been priced fairly using the regime-switching pricing PDEs. This premium the short gets paid via the increased option price compensates them for having a higher possibility of having to fulfill their end of the call option contract. Since they are charging more than the fair price of the option, it is expected that they will incur a risk-less profit from their portfolio. Since the investor is not hedging against volatility movement, over time this will allow them to incur lower hedging costs as they won't be readjusting their position in an additional hedging instrument. They will only be readjusting their position in the underlying asset.

Although this hedging strategy is set up from the perspective of a short position, it is important to recall that there exists a counterparty with whom they initially sold the call option to. This counterparty took a long position in the option, having paid a higher premium than the fair price to do so. It is expected that over time, the long position would lose on average more money while hedging their risks, in comparison to the case where it is assumed they paid the fair price for the option. The profits they earn by hedging their risk in the underlying asset through selling high and buying low, may not be enough to cover the cost of buying the option.

Preferences of a Long Position

Recall that an investor taking a long position in a call option fears low volatility. If the option is trading out-of-the-money and the volatility is low, the probability of the option going in-the-money over its lifetime is small. Since the probability of exercising the option decreases, they require a large volatility risk premium to compensate them for their risk. This results in the regime-switching option being priced as if the market permanently occupied the low volatility regime.

As such our estimate of the volatility level, $\sigma_{i^\star} = \sigma_L$, leads to the option being sold for a lower price than it would have been otherwise (i.e. $C^L_{BS}(S,t) \leq C^i(S,t)$ for all $i \in \{H, L\}$. Effectively, the investor taking a long position in this option gets a discounted price which is their way of being compensated for taking on the volatility switching risk and getting a less desirable option. Since the investor paid less than the fair price and will be hedging their option position by shorting shares of the underlying asset, over time they should incur a risk-less trading profit by selling high and buying low in the underlying.

Again, we need to consider the effect of the risk-adjusted option price on the counterparty of the option contract. In this case, the counterparty will be an investor with a short position. Since they sold the option for less than the fair price, it can be expected that over time they will lose money on average as they hedge against movements in the underlying asset by taking a long position in the underlying asset. The lower premium they charge for the option will be eaten away at quicker through the process of buying high and selling low in the stock.

Preferences of Both Long and Short Positions

We saw in Chapter 5 that when both the long and short positions in an option contract have their respective risks they want to hedge against, the option is priced via a weighted average of the corresponding Black-Scholes call option prices. This result can be thought of as the risk-adjusted fair price of the regime-switching call option, as it takes into account the risks of both counterparties.

$$C(S,t) = \frac{1}{a+1} C^H_{BS}(S,t) + \frac{a}{a+1} C^L_{BS}(S,t), \tag{6.94}$$

where $f_{HL} = a f_{LH}$.

For simplicity in the numerical analysis presented in the next section, we will assume that $f_{HL} = f_{LH}$ such that $a = 1$ in the above equation. This allows us to hedge with implied volatility such that the option price is an average of the high and low state option prices. We compute the implied volatility using a built-in Black-Scholes implied volatility solver ('blsimpv') which is part of the Financial Toolbox in Matlab. It is assumed that the regime-switching option is the average of the individual Black-Scholes option prices conditional on high and low volatility regime.

$$C(S,0) = \frac{1}{2}\Big(C^H_{BS}(S,0) + C^L_{BS}(S,0)\Big). \tag{6.95}$$

Using the implied volatility solver, we back out an implied volatility value at contract initiation using the option price given by equation (6.95). We then use this implied volatility value as our estimate for the constant volatility level. This allows us to hedge by taking a dynamic position in the underlying asset over the lifetime of our shorted call option.

6.5 Hedging Strategies Analysis

Our main goal of this chapter was to compare the performance of the different hedging strategies under our regime-switching volatility framework. The best indicator of hedge portfolio performance is considered the profit/loss. We perform a Monte Carlo simulation where we simulate $Q = 10,000$ sample volatility paths and their corresponding stock price paths. All of our hedging strategies are applied to each set of paths, and a mean terminal profit/loss is computed using all Q paths. We also consider the 95% confidence intervals of our terminal profit/loss in order to determine the reliability of our estimate of the mean profit resulting from our strategies. Unless otherwise denoted, the parameters used in our numerical analysis and comparison of hedging strategies are given in Table 6.1.

Expected Return	r	0%
High State Volatility	σ_H	40%
Low State Volatility	σ_L	10%
$C_1^i(S,t)$ Strike Price	K_1	\$100
$C_2^i(S,t)$ Strike Price	K_2	\$105
$C_3^i(S,t)$ Strike Price	K_3	\$95
High State Daily Jump Intensity	λ_{LH}	1%
Low State Daily Jump Intensity	λ_{HL}	1%
High State Market Price of Volatility Risk	m_{HL}	0
Low State Market Price of Volatility Risk	m_{LH}	0
Maturity Date	T	1 year
Number of Time Increments	N	252
Initial Stock Price	S_0	\$100.00
Stock Transaction Cost	TC_{stock}	0 bps
Option Transaction Cost	TC_{option}	0 bps
Number of Price Paths	Q	10,000

Table 6.1: Parameters used in the analysis of hedging strategies for varying stock price path drifts.

For simplicity, we assume that the market prices of volatility risk are negligible ($m_{HL} = m_{LH} = 0$), as our main focus is on how well the hedging strategies perform under different market conditions. It is assumed that there are 252 trading days in one year and that volatility and stock price change daily. In addition, our positions in all financial instruments in our hedge portfolios are rebalanced every trading day. It is assumed that portfolio rebalancing is independent of transaction costs. In other words, the presence and level of transaction costs has no effect on whether or not we rebalance our portfolio. The switching mechanisms between volatility regimes are driven by the jump intensities which were assumed to be identical and equal to 1% daily. Thus no matter what state we occupy, we have a 1% chance every trading day to switch into the opposing regime. We have picked a small switching intensity to correspond with the fact that volatility does not switch states very often, corresponding to a small probability of switching.

Table 6.2 summarizes state occupation and transition data for our simulation study. For clarity, the same $Q = 10,000$ sample paths were utilized for all of our numerical analysis presented in this chapter.

It can be observed that on average, volatility spends half of its time in the low volatility regime and the other half in the high volatility regime. The percentages of state transitions clarifies that switches between regimes were scarce, occurring on average 0.50% of the time. On the other hand, staying in a currently occupied regime occurred 50% of the time. We can conclude that once the market switched into a particular volatility regime, it occupied that regime for a large percentage of our time. This indicates that flip-flopping between regimes was infrequent.

Of particular interest in our study is the performance of our hedging strategies given different stock price drifts, μ. In addition we consider the effect of the Delta limit on portfolios performance as well as the effect of varying transaction costs, TC_{stock} and TC_{option}. We are

Data Type	Mean (%)	95% C.I. (%)
Total High State Occupation	50.16	[49.61, 50.70]
Total Low State Occupation	49.84	[49.30, 50.39]
Total H|H Transitions	49.66	[49.11, 50.21]
Total L|H Transitions	0.50	[0.49, 0.51]
Total L|L Transitions	49.34	[48.80, 49.89]
Total H|L Transitions	0.50	[0.49, 0.51]

Table 6.2: Summary of total state occupations and total state transitions for price paths used in hedging analysis.

specifically interested in the effect that the Delta limit has on Portfolio II's mean profit/loss, as well as percentage of trading days the Delta limit is actually breached. We will start with analysing results for the stock drift.

6.5.1 Effect of Stock Price Drift

Given the way in which we set up our hedging option's strike prices to straddle the shorted option's strike prices in Portfolio II, we need to analyse various magnitudes and directions of stock price drifts, in order to determine the efficacy of our method under differing market conditions. It is also useful to see how this financially rooted portfolio performs against more naive strategies and our basic regime-switching strategy of Portfolio I.

Two interesting cases to investigate are when the shorted option finishes either in- or out-of-the-money. To investigate when the original option we hedge against finishes out-of-the-money we assume $\mu = -5\%$. On average, the terminal stock price finished at \$95.35 ($S_0 e^{\mu T} =$ \$95.12), below the strike price of K_1. In these instances, the option would not be exercised by the counterparty. When the shorted option finishes in-the-money, it is expected that the counterparty is expected to exercise their right to buy one share of the underlying from us. Thus we must cover our position by taking some position in the underlying asset and/or hedging option. Depending on where the stock price finishes such that $S_T > K_1$, different hedging instruments in Portfolio II can be utilized to close out our shorted position. This motivates us to analyse the mean profit/loss when $\mu = 0\%, 5\%, 10\%$.

When $\mu = 0\%$, the stock price on average finishes at \$100.24 ($S_0 e^{\mu T} =$ \$100.00). It can be expected that some of the paths in our sample data finished above the strike price and some above. For $\mu = 5\%$, the mean terminal stock price was \$105.38 ($S_0 e^{\mu T} =$ \$105.13). For stock price paths that finish such that $K_1 < S_T < K_2$, it is assumed that the hedging option $C_3^i(S,t)$ would be utilized to close out our short position. It is cheaper to exercise that option and buy the share of the stock for K_3 and then sell it for K_1, pocketing the difference. This method also allows us to take possession of one share of the stock at a cheaper rate than market price.

Finally, when $\mu = 10\%$ the mean terminal stock price was \$110.79 ($S_0 e^{\mu T} =$ \$110.52). Under this scenario, our hedging option $C_2^i(S,t)$ is in-the-money and by exercising this option we could obtain the stock for $K_2 < S_T$ allowing us limit our losses from not having to purchase the share directly off the market for a higher price.

The results from our hedging simulation for varying stock price drifts are given in Table 6.3.

Hedging Strategy	$\mu = -5\%$		$\mu = 0\%$	
	Mean	95% C.I.	Mean	95% C.I.
Terminal Stock Price	\$95.35	[\$94.78, \$95.93]	\$100.24	[\$99.64, \$100.84]
Portfolio I: $C_2^i(S,t)$	0.34¢	[-0.55¢, 1.22¢]	0.97¢	[0.10¢, 1.83¢]
Portfolio I: $C_3^i(S,t)$	0.82¢	[-0.08¢, 1.71¢]	1.36¢	[0.49¢, 2.23¢]
Portfolio II: $C_2^i(S,t)$, $N_{lim} = 1$	0.54¢	[-0.23¢, 1.31¢]	0.06¢	[-0.72¢, 0.83¢]
Portfolio II: $C_2^i(S,t)$, $N_{lim} = 2$	0.41¢	[-0.39¢, 1.21¢]	0.00¢	[-0.79¢, 0.79¢]
Portfolio II: $C_3^i(S,t)$, $N_{lim} = 1$	0.88¢	[0.07¢, 1.69¢]	0.65¢	[-0.08¢, 1.39¢]
Portfolio II: $C_3^i(S,t)$, $N_{lim} = 2$	1.01¢	[0.18¢, 1.83¢]	0.77¢	[0.00¢, 1.54¢]
Implied Volatility	-123.10¢	[-130.20¢, -116.00¢]	-123.13¢	[-130.33¢, -115.93¢]
High Volatility	457.07¢	[450.00¢, 464.15¢]	467.89¢	[460.68¢, 475.09¢]
Low Volatility	-702.22¢	[-713.49¢, -690.95¢]	-712.98¢	[-724.20¢, -701.76¢]
Unconditional Volatility	-120.39¢	[-127.48¢, -113.29¢]	-120.36¢	[-127.56¢, -113.17¢]

Hedging Strategy	$\mu = 5\%$		$\mu = 10\%$	
	Mean	95% C.I.	Mean	95% C.I.
Terminal Stock Price	\$105.38	[\$104.75, \$106.01]	\$110.79	[\$110.12, \$111.45]
Portfolio I: $C_2^i(S,t)$	0.76¢	[-0.09¢, 1.62¢]	-0.01¢	[-0.86¢, 0.83¢]
Portfolio I: $C_3^i(S,t)$	1.55¢	[0.64¢, 2.45¢]	0.48¢	[-0.43¢, 1.39¢]
Portfolio II: $C_2^i(S,t)$, $N_{lim} = 1$	-0.12¢	[-0.79¢, 0.55¢]	-0.11¢	[-0.96¢, 0.74¢]
Portfolio II: $C_2^i(S,t)$, $N_{lim} = 2$	-0.28¢	[-0.97¢, 0.42¢]	-0.31¢	[-1.17¢, 0.55¢]
Portfolio II: $C_3^i(S,t)$, $N_{lim} = 1$	0.42¢	[-0.25¢, 1.09¢]	0.28¢	[-0.53¢, 1.08¢]
Portfolio II: $C_3^i(S,t)$, $N_{lim} = 2$	0.58¢	[-0.13¢, 1.29¢]	0.52¢	[-0.29¢, 1.33¢]
Implied Volatility	-123.69¢	[-130.91¢, -116.47¢]	-126.12¢	[-133.24¢, -118.99¢]
High Volatility	471.42¢	[464.22¢, 478.62¢]	466.21¢	[459.18¢, 473.24¢]
Low Volatility	-714.58¢	[-725.81¢, -703.35¢]	-706.08¢	[-717.30¢, -694.87¢]
Unconditional Volatility	-120.91¢	[-128.12¢, -113.70¢]	-123.36¢	[-130.48¢, -116.25¢]

Table 6.3: Hedging analysis for varying stock price path drifts using numerical option prices. Parameters as given in Table 6.1.

Overall, the performance of each hedging strategy is fairly consistent across market conditions. First, let's compare our two hedging strategies tailored to hedge against all of our market risks. Both Portfolio I and Portfolio II are observed to break-even on average. It should be noted that the difference in mean profit/loss between these two strategies is on the order of tenths of a cent. The portfolios hedging with $C_3^i(S,t)$ do tend to perform slightly better which could be attributed to the fact that this option is more likely in-the-money at maturity, given the average terminal stock prices, thus the investor can utilize it to close out their initial short position, if necessary. Overall, Portfolio II does provide a tighter confidence interval than Portfolio I indicating that the results have less variation. The tightness in these confidence intervals differ by tenths of a cent, making it almost negligible to the average investor since commonly available market data is not quoted beyond cents.

Financially, it can be observed that the differences across market conditions are negligible as they differ by tenths of a cent for both Portfolio I and Portfolio II. This allows us to state that our portfolios are set up and hedge in such a way that we are indifferent to the overall direction of the market. This makes financial sense when we recall our pricing PDE which only depended on the risk-free rate of interest and the volatility level. By hedging the risk of the stock price movements, we made our portfolio indifferent to the drift of the stock price, assuming no transaction costs.

For the cases involving Portfolio II, we chose to investigate the portfolio's terminal profit/loss for two values of the option hedge ratio limit: $N_{lim} = 1, 2$. The first value, $N_{lim} = 1$, was chosen as intuitively we know that at maturity an investor would only require one share of a hedging option to close out their original short position, if the shorted option is exercised by their counterparty. We also chose to investigate mean profit/loss of Portfolio II when the hedge ratio limit is allowed to be slightly higher. The motivation behind this stems from the fact that the higher the hedge ratio, the lower the percentage of trading days we will breach this limit. A more detailed analysis of this relationship follows in Section 6.5.2. Overall, for portfolios with a higher hedge ratio limit, their confidence intervals were not as tight, indicating that there is a higher variability in the associated terminal profit/loss. Furthermore, if we began hedging with $C_2^i(S,t)$, we experience lower terminal profit (or higher loss), than when we imposed a stricter $N_{lim} = 1$ on our hedge ratios. This could be due to the fact that it in most cases, hedging with $C_3^i(S,t)$ allows for us to have an in-the-money option at maturity to close out our short position with. When we breach our limit, we can make use of this in-the-money option. The opposite was true for portfolios when we hedged with $C_3^i(S,t)$ in which we experienced a slightly higher terminal profit. In this case, we begin hedging with the higher valued option, thus by increasing the hedge ratio limit, we can continue to use this option for longer as opposed to setting up a new position in an option that may or may not end up in-the-money. However, the differences between the two hedging limit cases are on the order of tenths and hundreds of cents, making them almost negligible in the long run.

Overall, our naive hedging strategies do not perform as well as our strategies developed specifically to eliminate volatility risk. This can be expected as we are leaving our portfolio completely exposed to volatility risk, which affects the stock price path. The unconditional volatility method and the implied volatility method produce approximately the same losses. Recall that the implied volatility method took into account compensating both the short and long positions for taking on their respective risks.

Since we set up our portfolio from the perspective of a short position, it makes sense that the constant high volatility strategy yields a significant profit. All else being equal, if the short position is compensated for their risk of potentially switching to a lower regime, they will initially demand more money for the option they sold. Along the same lines, if the short position decides to follow a constant volatility trading strategy, they will sell their option for less than it is worth and thus incur significant trading losses as we can see in Table 6.3. Of course, in the grand scheme of things these losses are considered significant when compared to the profit/losses of the other strategies.

The hedging strategies that took into account volatility switching were re-run using our approximate call option prices derived in Chapter 4. These results are given in Table 6.4. Recall that our approximate option prices are given by equation (4.85). If we consider this approximation in our generalized hedge ratio, we get:

$$\Delta_n^i \approx \frac{C^j_{1,BS}(S,t) - C^i_{1,BS}(S,t)}{C^j_{n,BS}(S,t) - C^i_{n,BS}(S,t)}, \tag{6.96}$$

where $C^i_{n,BS}(S,t)$ and $n = 1,2,3$ denotes the Black-Scholes call price conditional on volatility state i for all $i \in \{H, L\}$ where $i \neq j$.

Analysing the approximate hedge ratio utilized in the comparison of hedge portfolios, gives rise to some nice intuition. From equation (6.96), it can be observed that the hedge ratio utilizing the approximate option prices results in a ratio of the difference between the Black-Scholes constant volatility option prices conditional on volatility states i and j for the shorted option over the hedging option. Since our volatility process is memoryless, intuitively it is reasonable to assume that our hedge ratio would only take into account the change in option value if we switched into the opposing regime, regardless of the frequency of this jump occurring. We know that this switch is possible at any time point, therefore we need to consistently hedge against this risk.

Hedging Strategy	$\mu = -5\%$		$\mu = 0\%$	
	Mean	95% C.I.	Mean	95% C.I.
Terminal Stock Price	\$95.35	[\$94.78, \$95.93]	\$100.24	[\$99.64, \$100.84]
Portfolio I: $C_2^i(S,t)$	-94.38¢	[-99.28¢, -89.48¢]	-93.30¢	[-98.21¢, -88.40¢]
Portfolio I: $C_3^i(S,t)$	-93.06¢	[-98.06¢, -88.05¢]	-96.40¢	[-101.39¢, -91.40¢]
Portfolio II: $C_2^i(S,t)$, $N_{lim} = 1$	-8.43¢	[-9.93¢, -6.92¢]	-2.61¢	[-4.17¢, -1.06¢]
Portfolio II: $C_2^i(S,t)$, $N_{lilm} = 2$	-31.62¢	[-33.40¢, -29.84¢]	-24.36¢	[-26.18¢, -22.53¢]
Portfolio II: $C_3^i(S,t)$, $N_{lim} = 1$	7.10¢	[5.56¢, 8.65¢]	0.56¢	[-0.95¢, 2.08¢]
Portfolio II: $C_3^i(S,t)$, $N_{lim} = 2$	-16.94¢	[-18.87¢, -15.00¢]	-26.38¢	[-28.30¢, -24.46¢]

Hedging Strategy	$\mu = 5\%$		$\mu = 10\%$	
	Mean	95% C.I.	Mean	95% C.I.
Terminal Stock Price	\$105.38	[\$104.75, \$106.01]	\$110.79	[\$110.12, \$111.45]
Portfolio I: $C_2^i(S,t)$	-89.90¢	[-94.84¢, -84.97¢]	-85.13¢	[-90.11¢, -80.15¢]
Portfolio I: $C_3^i(S,t)$	-98.32¢	[-103.36¢, -93.28¢]	-98.82¢	[-103.92¢, -93.72¢]
Portfolio II: $C_2^i(S,t)$, $N_{lim} = 1$	3.71¢	[2.19¢, 5.22¢]	10.87¢	[9.27¢, 12.46¢]
Portfolio II: $C_2^i(S,t)$, $N_{lim} = 2$	-16.34¢	[-18.15¢, -14.53¢]	-7.35¢	[-9.23¢-5.47¢]
Portfolio II: $C_3^i(S,t)$, $N_{lim} = 1$	-5.98¢	[-7.44¢, -4.52¢]	-11.00¢	[-12.48¢, -9.52¢]
Portfolio II: $C_3^i(S,t)$, $N_{lim} = 2$	-35.33¢	[-37.21¢, -33.46¢]	-42.48¢	[-44.34¢-40.63¢]

Table 6.4: Hedging analysis for varying stock price path drifts using approximate option prices. Parameters as given in Table 6.1.

It can be observed that on average, when hedging with the approximate solutions, we lose money. Furthermore, a comparison of Portfolio II for the different hedge ratio limits shows that having a higher limit results in consistently losing more money and having higher variability in our hedging results (i.e. wider confidence interval). These consistent losses across all portfolios could be attributed to the fact that the approximate option prices may produce prices which on average are lower than those computed numerically via Crank-Nicolson. This assumption arises from the fact that when we analysed our results for constant volatility, hedging a shorted position with low volatility yielded losses while hedging with high volatility resulted in a substantial profit in proportion to other results. This is consistent with our previous discussions on investor risk preferences and the market price of volatility risk. Thus it is logical to assume that the approximate solutions compute lower option prices than their equivalent numerical solutions thus allowing a short position to incur losses on average. This is due to the fact that a lower price means the investor will initially receive less money for selling the option to a counterparty and as a result, can incur losses in their hedge position as this price does not exactly represent the risk inherent in the market. This absolute error between the approximate price and the numerical price can be assumed to be the source of the losses observed in our numerical study. The variation in these results is also wider than previous simulations with it being of magnitude of cents instead of tenths of cents. Overall, we can see that it is best to use a numerically accurate option price when implementing hedging strategies especially when rebalancing occurs more often.

6.5.2 Effect of Delta Limit

Recall that the Delta limit, N_{lim} was imposed on the initial hedging option employed in Portfolio II. This was put in place to insure that the hedge ratio would not "blow up" thus requiring that the investor take an infinite position in an option. We are interested to determine what effect, if any, the magnitude of this Delta limit has on the mean profit/loss of our trading strategies and on the percentage of time this limit is actually breached over the course of trading.

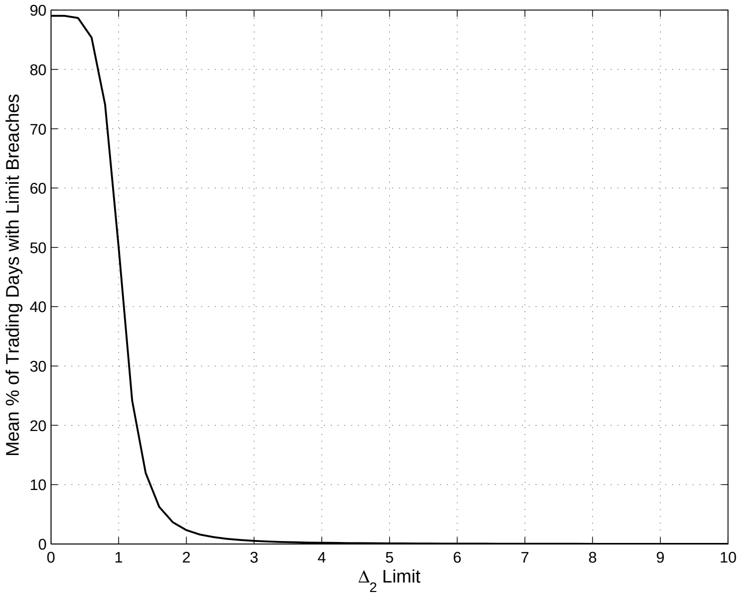

Figure 6.3: Effect of Δ_2 limit on mean % of trading days with limit breaches. $\mu = 0\%$, all other parameters as given in Table 6.1.

It was found that the overall percentage of limit breaches was independent of both stock price drift and on which option we initially hedged with. We only show results for one choice

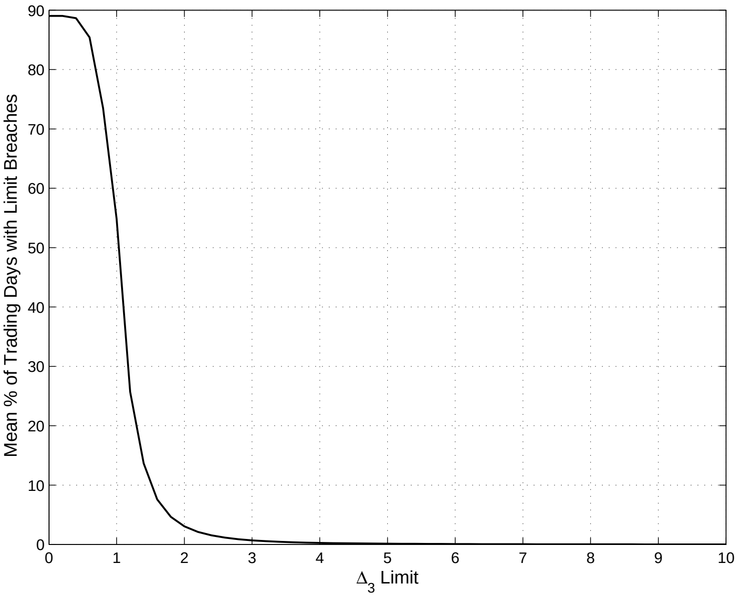

Figure 6.4: Effect of Δ_3 limit on mean % of trading days with limit breaches. $\mu = 0\%$, all other parameters as given in Table 6.1.

of stock drift, $\mu = 0\%$, however similar results follow for other market conditions. Figures 6.3 and 6.4 show that when the limit is a fraction of an option, the limit is breached between 50% and 90% of the time. There is an exponential decay that can be observed in the percentage of limit breaches as the Delta limit increases. No observable change is observed for values above $N_{lim} = 4$ as limit breaches become non-existent. It should be noted that almost identical results are observed for when we start hedging Portfolio II with either $C_2^i(S,t)$ or $C_3^i(S,t)$.

Finally, we investigated the effect that the Delta limit has on the mean profit/loss of Portfolio II. The same effects for increases in Delta limit were observed for all market conditions. Figure 6.5 illustrates the effect that the Delta limit has on the mean profit/loss of Portfolio I when we choose to hedge with $C_2^i(S,t)$ such that $K_1 < K_2$. The mean profit/loss and corresponding 95% confidence intervals decrease with respect to the Δ_2 limit. As the hedge ratio limit increases, the mean profit/loss decreases by a magnitude of a few tenths of cents. This decrease appears to flatten out for larger values of the limit. When Δ_2 limit take on the value of zero, financially this means that we will only be hedging with our additional hedging option $C_3^i(S,t)$. Figure 6.5 indicates that hedging with our additional hedging option produces maximum portfolio performance.

Similarly, Figure 6.6 shows the effect that the Delta limit has on the mean profit/loss of Portfolio II when we choose to hedge with $C_3^i(S,t)$ such that $K_3 < K_1$. Increases in the Delta limit are shown to cause increases in our mean profit/loss. This difference in profit/loss is only a few cents in comparison and this begins to flatten out over time. There is a peak in the mean profit/loss which occurs between $N_{lim} = 1$ and $N_{lim} = 2$. This suggests that for this portfolio, there is an optimal limit to impose to maximize our portfolio performance. When the limit takes on the value of zero, this is a scenario in which we would only be hedging with

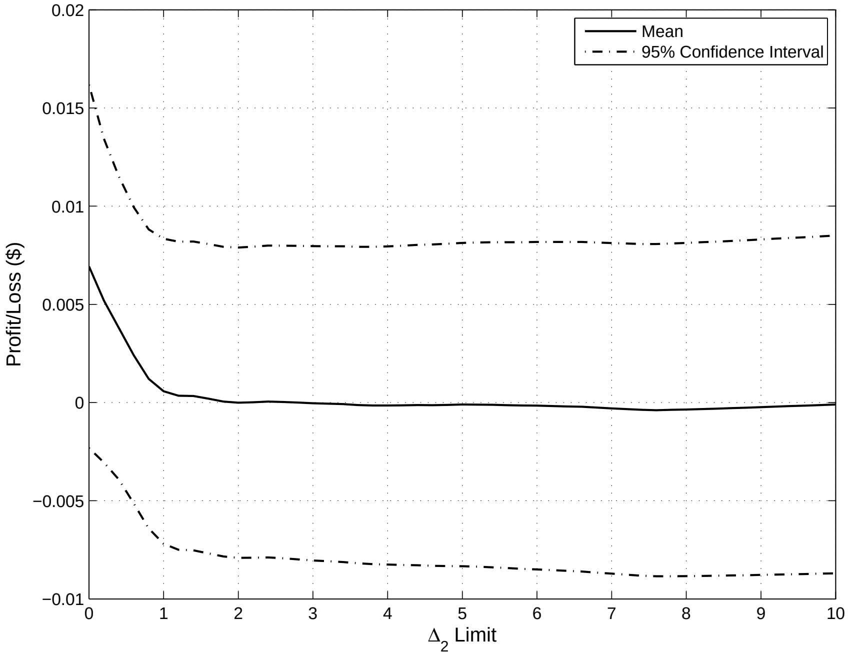

Figure 6.5: Effect of Δ_2 limit on profit/loss of Portfolio II. $\mu = 0\%$, all other parameters as given in Table 6.1.

our additional option, $C_2^i(S,t)$. Figure 6.6 indicates that this scenario would lead to our worst portfolio performance for all values of the hedge ratio limit.

In general, larger values for our Delta limit will allow us to take larger positions in our first hedging option. If this limit is breached, we must introduce a new hedging option which will incur additional costs. For the portfolio starting with $C_2^i(S,t)$, when the limit is breached, we must also start hedging with $C_3^i(S,t)$. Recall that it was assumed that $K_3 < K_1 < K_2$. All else being equal, it turns out that $C_3^i(S,t) > C_2^i(S,t)$. However, given that all hedging options are in-the-money, it will always be cheaper at maturity to exercise $C_3^i(S,t)$ to buy one share of the stock for the low price of K_3. Therefore keeping some dynamic position in this option over the life of the portfolio is cheaper in the long run, rather than trying to set up a large position in it closer to maturity. Thus increasing the hedging ratio limit such that we will use our original hedging option $C_2^i(S,t)$ will result in a lower terminal portfolio profit. On the other hand, for the portfolio in which we begin hedging with $C_3^i(S,t)$, our initial hedging option is the more expensive option of the two available to us. However since this option is more likely to finish in-the-money, making it the most beneficial hedging instrument in our portfolio, it is advisable to maintain a dynamic position in it for longer through a larger hedging limit. If our hedging limit is too low, our dynamic position would be in the other option $C_2^i(S,t)$, which due to the set-up of the portfolio with respect to the strike prices, is less likely to finish in-the-money. This makes it a less desirable hedging option in the long run since we want an option in our portfolio which enables us, if necessary, to buy one share of the stock at maturity for the cheapest price

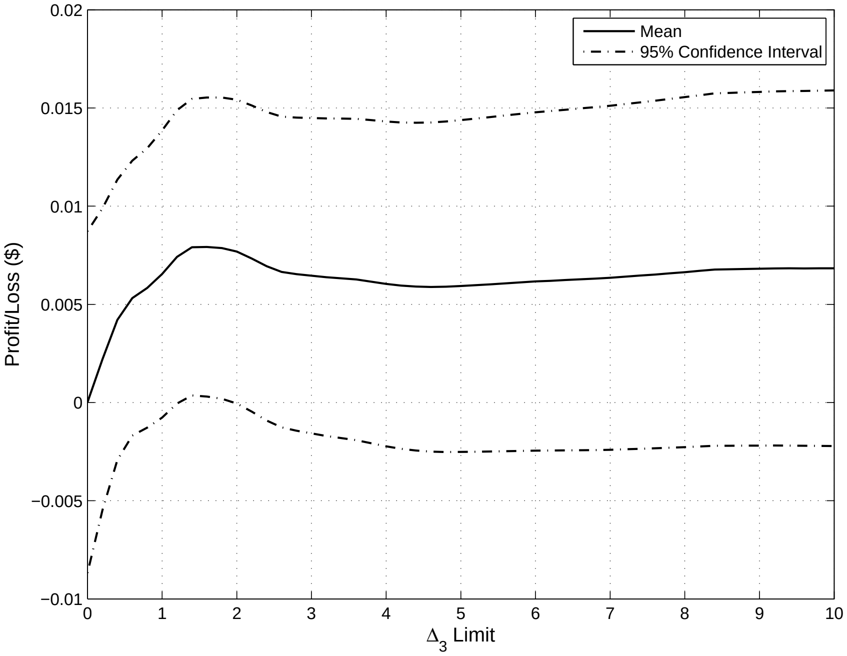

Figure 6.6: Effect of Δ_3 limit on profit/loss of Portfolio II. $\mu = 0\%$, all other parameters as given in Table 6.1.

in order to close out our short position.

Using the results illustrated in Figures 6.3 and 6.5 together, we can observe that it is most profitable to have a hedge limit as low as possible for $C_2^i(S,t)$, in order to ensure that we will hedge with our option that has a higher probability of finishing the money. On the other hand, the results of Figures 6.4 and 6.6, indicate that there is an optimal Delta limit which would maximize our profit. This limit would ensure that we always have a position in our original option $C_3^i(S,t)$, whether dynamic or static, which has a higher probability of being in-the-money at maturity. The additional option would provide some added value in hedging against the inherent risks, while minimizing trading costs associated with our higher valued, original hedging option.

6.5.3 Effect of Transaction Costs

In the implementation of our hedging strategies, it was assumed that the transaction costs were proportional to the amount traded. In other words, how much we are charged to complete a transaction is dependent on how much we buy/sell of a particular financial instrument in readjusting our hedge. All transaction costs are denoted in basis points. A basis point is one percent of one percent. In particular we investigated three sets of stock transaction costs TC_{stock} and option transaction costs, TC_{option} and analysed the mean profit/loss of four portfolios for varying stock drifts. In general, we allowed our option transaction costs to be higher than those for the stock due to the fact that they are proportional costs. One basis point of \$100 is significantly less than one basis point of \$10. Since options usually cost fractions of what the stock it is written on is trading for, it makes sense to allow the transaction costs to take on higher values.

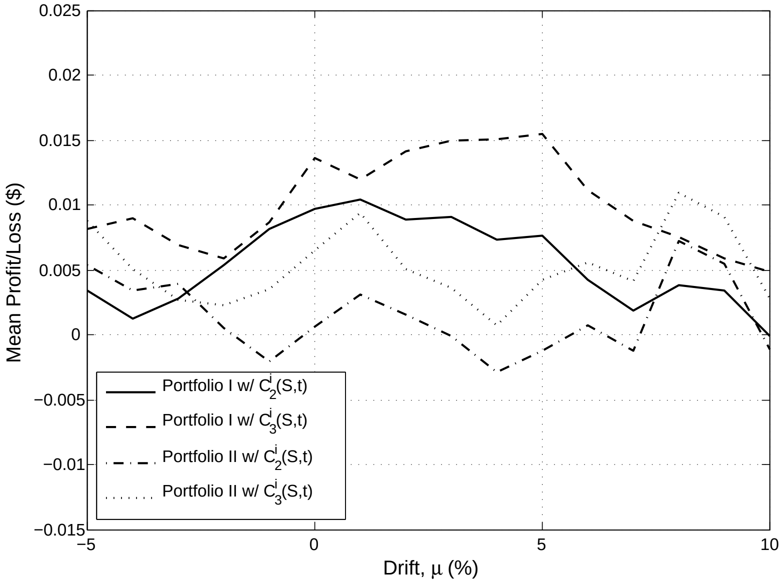

Figure 6.7: Effect of stock price drift, μ, on the mean profit/loss of differing portfolios. $N_{lim} = 1$, $TC_{stock} = 0$ bps and $TC_{option} = 0$ bps, all other parameters as given in Table 6.1.

Figure 6.7 provides a benchmark for future analysis since to compute profit/loss, transaction costs are not included. In the absence of transaction costs, there is no observable pattern between mean profit/loss and increasing the stock drift. It should be noted that the magnitude of the mean profit/loss depicted in this figure are on the magnitude of tenths of cents. Therefore these differences observed are negligible since all profits/losses would round out to approximately zero dollars on average.

With the introduction of option transaction costs, we begin to observe differences between the four portfolios plotted in Figure 6.8. Both variations of Portfolio II began to perform better than their respective variations of Portfolio I. Since Portfolio II doesn't allow the investor to take extreme option positions, fewer transaction costs are incurred over the life of the portfolio. Thus capping the number of options we can hedge with has a positive impact on our overall profit/loss as we are not losing money through changing our position by large magnitudes and as a result, not accumulating unnecessary transaction costs.

Following the assumption that option transaction costs are much greater than stock transaction costs, we can see that Portfolio II clearly outperforms Portfolio I in terms of profit/loss, as shown in Figure 6.9. This performance is indicated by the overall mean loss incurred by

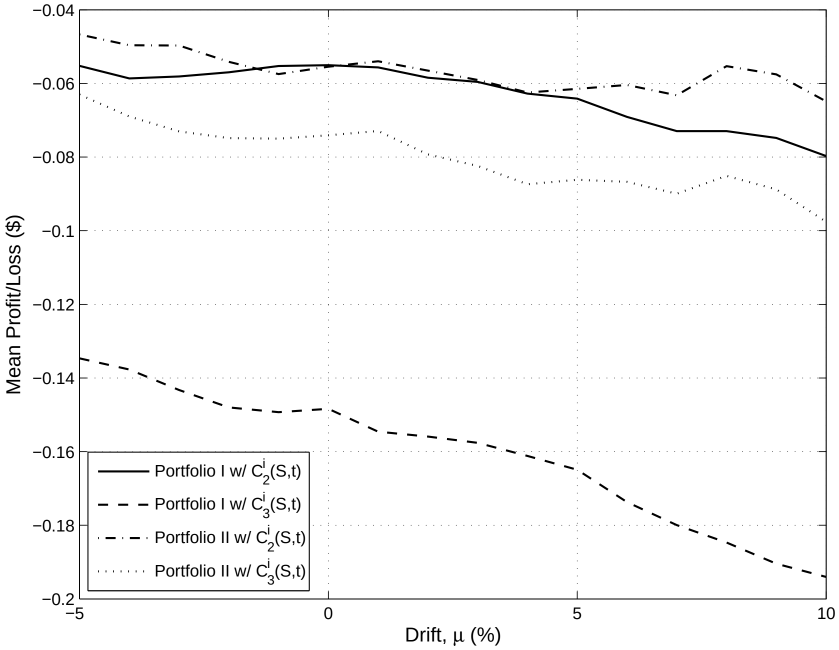

Figure 6.8: Effect of stock price drift, μ, on the mean profit/loss of differing portfolios. $N_{lim} = 1$, $TC_{stock} = 0$ bps and $TC_{option} = 10$ bps, all other parameters as given in Table 6.1.

the portfolio over time. Now that higher transaction costs are being taken into account, there exists an observable impact of the stock drift with respect to portfolio profit/loss. As stock drift increase in the positive direction, all portfolios lose more money. This indicates that as the stock price drifts upwards and away from the strike prices of all three possible options in our portfolio, our hedge positions are increasing in magnitude thus incurring more transaction costs every time we readjust our position (i.e. daily). As a result, these accumulated transaction costs have a negative effect on the value of our portfolio.

Overall, when transaction costs were introduced into our hedging portfolios, they caused the portfolios on average to lose money. However these losses varied between \$0.05 and \$2.10, depending on the portfolio. It is important to note that the introduction and/or magnitude of transaction costs did not influence how we readjusted our positions in our financial instruments. This is directly attributed to the decrease in profit/loss observed in the figures as transaction costs were increased. Realistically, transaction costs would have a direct impact on how much and how frequently an investor chooses to adjust their hedged positions.

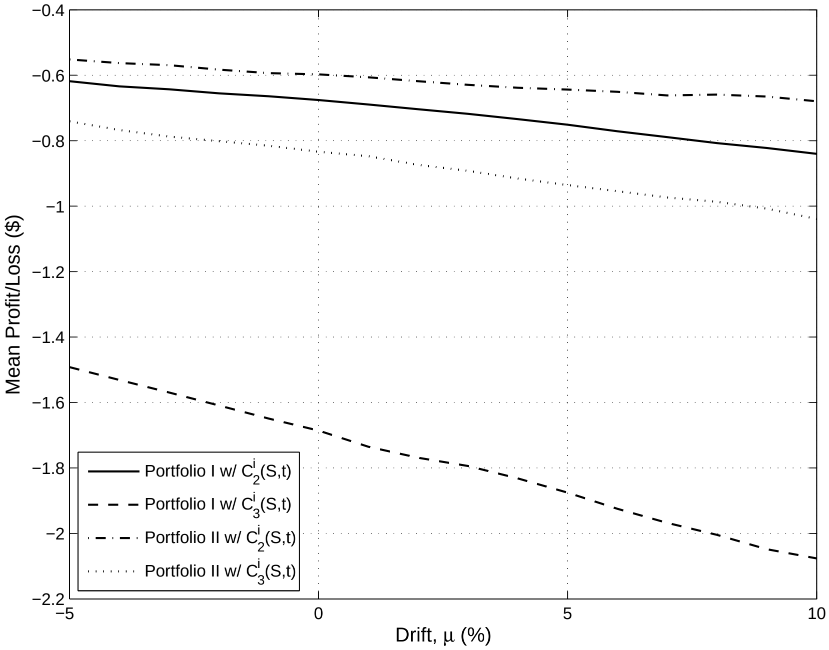

Figure 6.9: Effect of stock price drift, μ, on the mean profit/loss of differing portfolios. $N_{lim} = 1$, $TC_{stock} = 1$ bps and $TC_{option} = 100$ bps, all other parameters as given in Table 6.1.

6.6 Summary

The investigation of various hedging strategies under our regime-switching volatility framework were analysed both mathematically and through a numerical study. We considered portfolios designed to directly hedge out the risk of volatility switching as well as the risk of stock price movements, in addition to more naive constant volatility hedging approaches. Although we found that the set up of Portfolio I was mathematically sound, financial issues arose which limited the practicality of this hedging method. As a result, more sophisticated portfolios were considered where a basket of two hedging options was available to the investor. Given the assumption that the strike prices of the hedging options must straddle the strike price of the shorted option, this portfolio allowed for there always to be a usable hedging option in the portfolio. A hedging limit was also introduced to ensure that an investor did not take extreme positions in their hedging options. This hedging limit proved especially useful in limiting losses when transaction costs were taken into account. Overall, we found that portfolios that were set up to directly hedge against the volatility switching mechanism in our market performed substantially better than those taking a more naive approach to hedging.

Furthermore, the relationship between the hedge ratio limit and mean profit/loss of the portfolios was studied, and it was found that this limit has a direct impact on the profitability of these strategies conditional on initial hedging option choice. Finally, it was found that in the presence of transaction costs, Portfolio II performs significantly better than an otherwise similar Portfolio I. For all volatility switching portfolios, the inclusion of transaction costs illustrated the existence of a decreasing relationship between stock price drift and portfolio profitability.

All analysis contained within this thesis up until this point assumed that the Poisson intensities driving the frequency of volatility switching were constant. Now that solid mathematical and financial intuition has been built around this model, it follows to investigate the consequence of deterministic Poisson intensities on the pricing of options under our regime-switching framework. A natural extension of our framework is to consider the effect of upcoming financial events on our regime-switching volatility.

Chapter 7

Deterministic Poisson Intensities

In Chapter 2 we introduced a generalized framework for pricing a call written on an underlying asset in a market with regime-switching volatility. From Chapter 2 until now, the intensities of the Poisson processes driving the switching mechanisms between states were assumed to be constant. However, as one might realistically expect, these intensities are non-constant and fluctuate with changes in the market. These changes can be unsystematic and company specific or they could be systematic and as a result affect an entire financial market. In particular, there has been much research into the impact of company specific public information on equity and fixed income prices, and in particular their volatility levels.

Patell and Wolfson [37] found that earnings releases and dividend announcements affect the intraday behaviour of stock prices trading on New York Stock Exchange, with these stocks quickly incorporating the new information into their prices within hours. An interesting result of their study found that these price adjustments began before the actual announcement was made. By analysing the relationship between firms' earnings volatility and earnings forecasts, Waymire [48] showed that firms who report earnings more frequently experience lower volatility than firms who do not. The firms compared had earnings forecasts of similar accuracy. Jennings and Starks [30] were able to show that companies with quarterly earnings reports containing additional information have stocks whose prices start adjusting before the release of information. However, the average speed of adjustment is shown to be several trading days longer than companies with reports containing less information. Furthermore, French and Roll [21] investigated the impact of information flow during trading days and exchange holidays, using weekly US equity return data. They concluded that increased volatility is directly related to the differences in information flow of public and private information during trading hours as opposed to non-trading hours. Interestingly, Skinner [40] found that companies with exchange traded options listed on their stock experience smaller stock price reaction associated with the reporting of earnings releases. This was attributed to the fact that companies with listed options have more analysts forecasting the earnings for these firms and as a result there exists a lower level of surprise for investors when earnings are filed.

More recently, Ederington and Lee [18] analysed the impact of the employment report, consumer price index (CPI) and the producer price index (PPI) on the T-bond, Eurodollar and Deutsche mark futures markets. They considered intraday volatility patterns during trading hours over which news releases occurred. They show that news releases do cause an increase in volatility levels compared to days where no news release were made, with prices adjusting quickly, within one minute in very active markets. It was found however that increased volatility persists longer. Harvey and Huang [26] examined the impact of public information disclosures on market volatility in the Eurodollar and Treasury bill futures markets and found that bad macroeconomic news, released just before trading begins, is in fact associated with higher volatility levels. As well, they found there exists a relationship between the size of the surprise of such news and the magnitude of the increase in volatility levels.

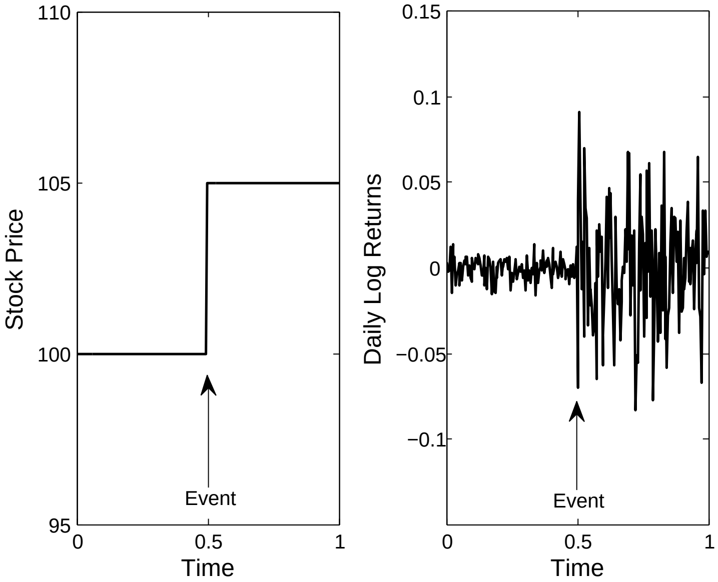

Figure 7.1: Two types of event studies: discontinuous stock price movement and volatility regime change.

Although many event studies focus on discrete shifts in stock price, as shown in the left plot of Figure 7.1, we focus on the shift in the volatility levels associated with stock price paths. These volatility shifts are observable when considering the daily log returns of a price path, as illustrated in the right plot contained in Figure 7.1. Recall that increases in the magnitude of the log returns are associated with an increase in the volatility level.

All in all, there is much empirical evidence and past studies supporting an observed impact of financial news on volatility, in particular that news tends to cause an increase in volatility levels. Often similar regime-switching frameworks are considered for modelling business phase cycles and volatility switching. Filardo [19] showed that a Markov model with time-varying transitional probabilities was better to model business cycles than fixed constant transitional probabilities. The enhanced model was able to take into account turning points that can occur where the market shifts states (i.e. between expansions and contractions). Since the release of information can result in a shift in the volatility states much like Filardo's shifts between business cycle phases, we will model our switching intensities to take into account the release dates of company specific financial news. Since options are written on company stock which experience price and volatility changes coinciding with news releases, it is intuitive to want to price this future risk into our options pricing framework in order to provide the fairest price possible for investors.

7.1 Motivation

As we have discussed, economic literature has investigated the influence of different financial and economic events on fixed income and equity volatility. In particular, financial events such as earnings releases, company mergers and acquisitions, and dividend payments are shown to trigger changes in the volatility levels of individual publicly traded companies. Uncertainty in the company may occur, as the known event date approaches, which results in an increase in short-term volatility levels. As a result, there may be a positive or negative impact on the stock price, depending on the outcome of the event. Following an empirical study done by Patell and Wolfson [37] which found that earnings announcements had a more pronounced impact on stock prices than dividend announcements, we choose to model our Poisson intensities as functions of upcoming quarterly earnings releases.

All publicly traded companies must report their earnings after every quarter. Earnings are filed as a report and allow shareholders and the public to know how the company performed during the last quarter. Usually, companies experience a delay of approximately one month between the end of the quarter and the date that the quarterly earnings are released. There is usually uncertainty about a particular company's financial results. Financial analysts report their expectations for a company's quarterly performance which can lead to earnings surprises when the reports are made publicly available. Earnings surprises, either positive or negative, occur when the reported earnings are above or below the analyst's expectations.

Since every publicly traded company has a different risk and return profile affected by their core business, we will examine empirical data from two companies in different industries. First, we will consider one of the big six banks in Canada, Toronto-Dominion Bank, a bank involved in retail, commercial and investment banking headquartered in Toronto, Ontario. We also consider Apple Inc., the second largest technology company in the world, which has experienced significant growth over the past decade and is headquartered in Cupertino, California. Due to their differing industries, we expect that the volatility levels of each company's publicly traded stock to differ, however for them both to be influenced by the arrival of information pertaining to earnings.

Quarter	Dates	
	End of Quarter	Earnings Release
Q1	January 31, 2013	February 28, 2013
Q2	April 30, 2013	May 23, 2013
Q3	July 31, 2013	August 29, 2013
Q4	October 31, 2013	December 5, 2013

Table 7.1: Quarter end and earnings release dates for Toronto Dominion bank for fiscal year 2013. Ticker symbol TD.TO on TSX. Data obtained from [42], [43], [44], and [45].

Quarter	Dates	
	End of Quarter	Earnings Release
Q1	December 29, 2012	January 23, 2013
Q2	March 30, 2013	April 23, 2013
Q3	June 29, 2013	July 23, 2013
Q4	September 28, 2013	October 28, 2013

Table 7.2: Quarter end and earnings release dates for Apple for fiscal year 2013. Ticker symbol APPL on Nasdaq. Data obtained from [1], [2], [3], and [4].

Tables 7.1 and 7.2 contain the quarter end dates and the subsequent earnings release dates for Toronto-Dominion (TD) Bank and Apple Inc., respectively. As mentioned above, there is usually a lag of approximately one month between the end of quarter and the date the earnings are released. Each quarter's earnings release date is known well before the quarter end and this information is made public before the actual release date.

7.1.1 5-Day Moving Average Volatility

It is not expected that the impact of earnings releases on stock prices and on the volatility level of the company to be long-term. Any observed effects are assumed to be short-term as the price of the company stock, through trading, is expected to incorporate this information into its price. This price adjustment occurs through the normal continuous trading in the stock by investors. Therefore, we consider the weekly (5-day) moving average of historical volatility for each of these companies, in order to capture any short-term changes in volatility levels around the end of quarter dates and the earnings release dates.

In both Figures 7.2 and 7.3, we can observe increases in volatility levels occurring just before or on the earnings release date. One explanation is to assume that there exists uncertainty in the quarterly results that the company will officially file thus causing the price to fluctuate at a higher level as investors short/long the stock due to increasing fears. Over the fiscal year 2013, it can be observed that Apple Inc. has higher volatility levels than TD Bank. As was mentioned before, the technology industry is more volatile than a bank in the stable Canadian banking system. As a result, Apple Inc. experiences a higher number of transactions in its company stock. This can be supported by considering the weekly (5-day) moving average trading volume for both publicly traded companies.

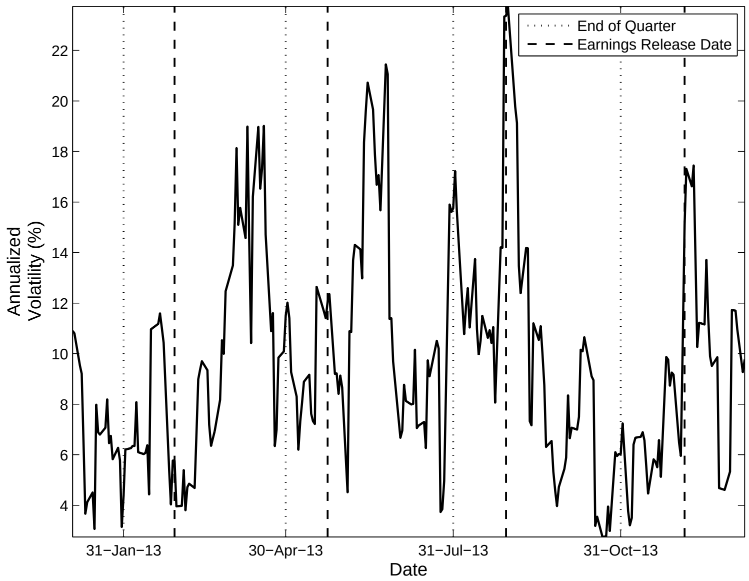

Figure 7.2: 5-day moving average volatility for TD Bank for fiscal year 2013. Data obtained from Yahoo Canada Finance [52].

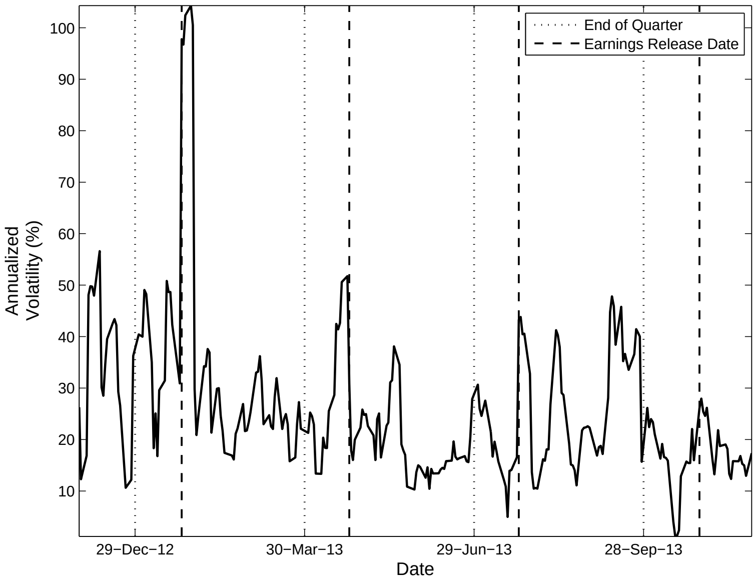

Figure 7.3: 5-day moving average volatility for Apple for fiscal year 2013. Data obtained from Yahoo Canada Finance [50].

7.1.2 5-Day Moving Average Trading Volume

Stock prices are affected by many factors, one of them being their daily trading volume. Bid-ask spreads are readjusted to account for trading volume. The higher the demand, the higher the ask price can be for a stock, which shifts the spread upwards. Trading volume on general can be thought to increase as an uncertain financial event looms, as the outcome of the event could trigger more permanent shifts in the stock price. Since future movements in the stock are both unknown and uncontrollable, investors may seek to change their positions dramatically as the event approaches.

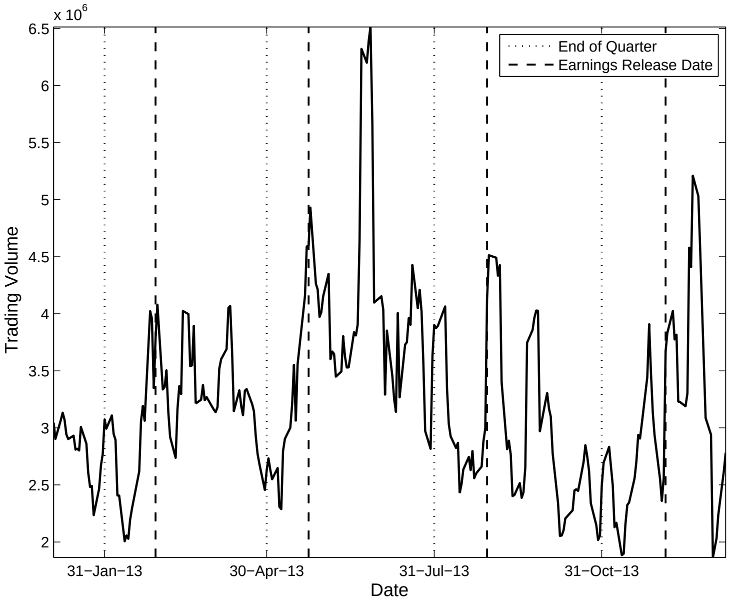

Figure 7.4: 5-day moving average of daily trading volume for TD Bank for fiscal year 2013. Data obtained from Yahoo Canada Finance [52].

These sentiments are reflected in Figures 7.4 and 7.5, which plot the 5-day moving average of daily trading volume against the end of quarter and earnings release dates.

It can be observed that as the quarterly earnings release dates approach, both TD Bank and Apple Inc. experience large variations in their trading volume. The most observable variation in the trading volume is for Apple Inc. at the end of their first quarter. On average, we can also observe that the volume of Apple Inc. shares is much higher than TD Bank shares. It should be noted that Apple Inc. trades on the Nasdaq in New York City while TD Bank trades on the Toronto Stock Exchange, which may have some effect on these differences. This data indicates that investors do care about financial events when readjusting their portfolios. Risk-averse investors may liquidate their shares if they fear an upcoming downward drift in the stock price while risk-taking investors may set up options strategies coupled with short stock strategies in order to profit off of similar financial outcomes. Overall, the empirical evidence along with previous studies done by economists and practitioners provide a solid foundation for exploring

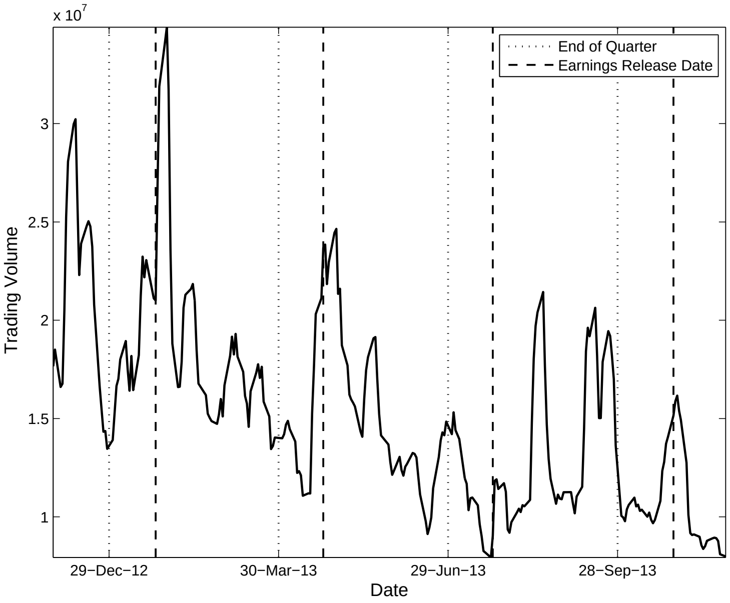

Figure 7.5: 5-day moving average of daily trading volume for Apple for fiscal year 2013. Data obtained from Yahoo Canada Finance [50].

event-driven regime-switching intensities.

7.2 Earnings Release Framework

Our earnings release volatility switching framework will build upon the regime-switching framework introduced in Chapter 2. For consistency, we will continue to consider that the volatility can switch between two regimes, with the switches being driven by independent Poisson processes. This framework is given by equations (2.45), (2.46) and (2.47). Since our regime-switching pricing equations were derived under a generalized model where the Poisson intensities were taken to be deterministic functions, our pricing PDE remains the same as in previous chapters and is given by equation (2.48) with payoff and boundary conditions consistent for a European call option.

For the remainder of this chapter, the difference will be that instead of letting the Poisson intensities take on constant values, as assumed for Chapters 4 through 6, we will allow our Poisson intensities to be functions of both time and stock price. Recall that the general form of our risk-adjusted Poisson intensities for state i is given by:

$$f_{ij}(S,t) = -(\lambda_{ij}(S,t) - m_{ij}), \tag{7.1}$$

where $i \in \{H, L\}$ such that $i \neq j$.

The focus of this chapter is on the different forms that the Poisson intensity $\lambda_{ij}(S,t)$ can take, reflecting the market and company conditions surrounding a particular underlying asset. As a result, we also consider the associated pricing and hedging results.

Under our event-driven regime-switching framework, we will assume that the date of quarterly earnings release is known and occurs at $t = \tau^\star$. It will also be assumed that the probability of switching regimes is an increasing function with respect to the time to event, $\tau^\star - t$. The closer we are to the event occurring, the higher the magnitude of our Poisson intensity triggering the switching process. If the event occurs before option maturity, the intensity will decrease as we move forward in time away from the event date. A time intensity parameter, κ is introduced to control the time growth and/or decay of our jump intensities. We will also further extend our framework to incorporate the effect of stock price levels. Throughout this chapter, we will analyze both mathematically and numerically the differences in pricing and hedging options where the event occurs at option maturity and when the event occurs before option maturity. Since several cases of deterministic intensities, depending on both time and stock, builds upon our model considering solely time as a dependent variable, we will first consider the time varying Poisson intensity model.

7.2.1 Time Varying Poisson Intensities

First we consider the simpler case in which the intensities of the Poisson processes depend only on time. Since we expect on average for a shift to an opposing regime to occur as the event approaches, we model the intensities to increase as the event date approaches. For all cases, $\lambda^\star_{ij}$ is assumed to be the maximum Poisson intensity that the process can ever reach. Thus we have defined an upper bound on the intensity of our process. As previously stated κ is the time intensity parameter and $m_{ij}(S,t)$ is the state-dependent market price of volatility risk. For the discussion presented, assume that the state-dependent market prices of volatility risk take on constant values (i.e. $m_{ij} \equiv m_{ij}(S,t)$).

We restrict our time intensity parameter to only take on strictly positive values such that $\kappa > 0$. If $\kappa = 0$, this would insinuate that time has no impact on the switching intensity and thus our framework reduces to that where the Poisson intensities take on constant fixed values. When the event occurs at maturity, we model the intensities to increase as the event date approaches. On the other hand, when the event date does not occur at option maturity, the intensities increase as we approach the event date and decrease after the event has occurred. In general our deterministic time-varying model is as follows:

$$\lambda_{ij}(t) = \lambda^{\star}_{ij} e^{-\kappa(\tau^{\star}-t)sgn(\tau^{\star}-t)}, \tag{7.2}$$

where

$$sgn(\tau^{\star} - t) = \begin{cases} -1 & \text{if } t > \tau^{\star} \\ 0 & \text{if } t = \tau^{\star} \\ 1 & \text{if } t < \tau^{\star} \end{cases}.$$

When the event occurs at maturity such that $\tau^{\star} = T$, it follows that $sgn(T - t) = 1$ since $t \leq T$ for all t. The above result reduces to:

$$\lambda_{ij}(t) = \lambda^{\star}_{ij} e^{-\kappa(T-t)}. \tag{7.3}$$

The function $e^{-\kappa(\tau^{\star}-t)sgn(\tau^{\star}-t)}$ acts as a control on the Poisson intensity and due to its mathematical properties, allows it to vary between zero and $\lambda^{\star}_{ij}$. Thus our deterministic intensity is a bounded function: $0 \leq \lambda_{ij}(t) \leq \lambda^{\star}_{ij}$. If $\kappa(\tau^{\star} - t) \to \infty$ this would imply that $\lambda_{ij}(t) \to 0$. Thus if either the time to event or the chosen value for κ is very large, the switching effect would be turned off completely. This would result in the volatility never being able to switch out of its currently occupied regime. A more detailed investigation of the time-intensity parameter, κ, with respect to option maturity dates and event dates is presented in Section 7.3. For now, it is safe to assume that $\kappa(\tau^{\star} - t)$ is finite such that the switching mechanism is enabled within our regime-switching framework. In other words, we only consider a finite time horizon.

For the remainder of this chapter, we will analyse numerical results pertaining to the time varying Poisson intensities in two separate cases. Case 1 describes a case in which the financial event occurs at option maturity, while Case 2 will refer to events that occur before maturity, $\tau^{\star} < T$. We will first analyse how our time varying intensities are modelled for both of these cases separately. Since our intensities are independent of stock price, Figures 7.6 and 7.7 plot the intensities against time alone.

In Figure 7.6, we can observe that the Poisson intensity increases as the maturity date of the option approaches, which coincides with the date of the financial event. Thus as we approach the financial event, it becomes more and more likely that our Poisson process will trigger a switch to the opposing regime. The speed at which the intensity changes with respect to time is controlled by the magnitude of κ and will be discussed later on.

Figure 7.7 illustrates the observable difference when the financial event occurs before option maturity. As we approach the financial event at $\tau^{\star}$, the Poisson intensity increases. It reaches it maximum intensity at the event date $t = \tau^{\star}$ and decreases as we move further away from the date and towards maturity $\tau^{\star} < t \leq T$. The intensity is modelled in this way as it is assumed that if the switch does not occur before or on the event that, it becomes highly unlikely that it will switch regimes afterwards. This is due to the fact that after the event has occurred

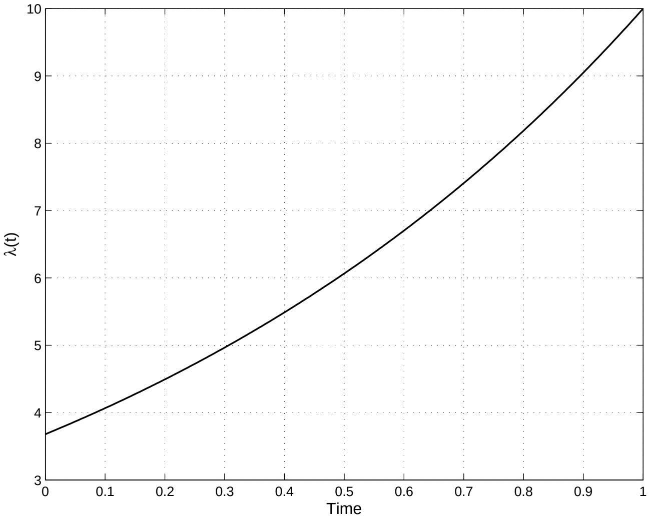

Figure 7.6: Time varying Poisson intensity assuming the financial event occurs at maturity. $\kappa = 1$, $\lambda^\star = 10\%$ (daily), and $T = 1$ year.

and the information disclosed is now public, investors no longer have this unknown risk in their portfolio. Thus it is likely that if the volatility does not switch before or on the event date, that it will not switch at all. Once again, κ controls the speed at which the time varying intensity grows and decays.

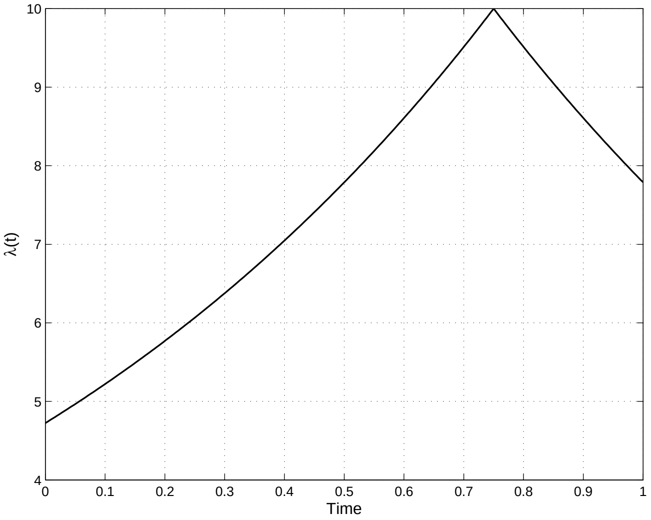

Figure 7.7: Time varying Poisson intensity assuming the financial event occurs before maturity. $\kappa = 1$, $\lambda^\star = 10\%$ (daily), $\tau^\star = 9$ months, and $T = 1$ year.

7.2.2 Time and Stock Varying Poisson Intensities

Building upon the time varying Poisson intensity model given by equation (7.2), we will now adjust this expression to be a function of another dependent variable, the stock price. One way to do so is to use the level that the stock price is trading at with respect to a benchmark level ξ, as a trigger on the magnitude of the Poisson intensity.

As we previously saw, regime-switching options become insensitive to volatility switching when the option is too far in- or out-of-the-money. However, when the option is trading around or at-the-money, volatility levels have a significant effect on pricing and hedging strategies. Any little movement in the underlying asset about the strike price can effect whether or not the option has intrinsic value. Incorporating the underlying asset's value as a dependent variable within the switching mechanism is a way for the option price to take into acccount the impact of future volatility levels given a particular price level. One way to consider this trigger within the Poisson intensity is to have it increase with stock price level. In Wilmott [49], the impact of Delta hedging a stock is found to have an impact on an underlying asset's value. Changes in an asset's value are directly related to changes in the associated volatility levels. Financially, it makes sense to incorporate this hedge ratio into our intensity model, allowing our switching intensities to incorporate the amount the stock was hedged.

Since volatility levels do have a significant impact on the stock price's level, they also have an impact on the amount an investor may earn (or have to pay out) at option maturity. In this scenario, we would want our intensity to reflect the maximum Poisson intensity defined within our market. Of course, time value would still have to be taken into account, however our stock price trigger could take on values between zero and one. This results in having our new time and stock varying Poisson intensities being bounded both above and below.

$$0 \leq \lambda_{ij}(S,t) \leq \lambda^{\star}_{ij} e^{-\kappa(\tau^{\star}-t)sgn(\tau^{\star}-t)}. \tag{7.4}$$

As previously discussed in detail in Chapter 6, when our regime-switching option is trading deep in- or out-of-the-money, volatility has little to no impact on the price of the option. It is important to remember that volatility still has an impact on the actual stock price level. Under these two scenarios, our regime-switching option is equivalent to a constant volatility option. The properties of the constant volatility Black-Scholes Delta can fulfill our intuitive constraints placed on stock price trigger, making it an ideal multiplier within our intensity model. This constant volatility hedge ratio conditional on volatility level, σ_i, is given by:

$$\Delta^i_1 = N(d^i_1), \tag{7.5}$$

where:

$$d^i_1 = \frac{\log\left(\frac{S}{\xi}\right) + \left(r + \frac{1}{2}\sigma^2_i\right)(T-t)}{\sigma_i \sqrt{T-t}}, \tag{7.6}$$

$$N(x) = \frac{1}{\sqrt{2\pi}} \int_{-\infty}^{x} e^{-\frac{z^2}{2}} dz. \tag{7.7}$$

The hedge ratio, Δ^i_1, under the Black-Scholes model is defined by the normal cumulative distribution function (CDF). As per the properties of the normal CDF, we know that $0 \leq N(d^i_1) \leq 1$. Thus we can use the hedge ratio as our stock price trigger to control the size of the Poisson intensity, dependent on where the stock price is trading with respect to our benchmark price ξ. As we can see, if the stock prices are trading at high values compared to ξ (i.e. deep in-the-money), the trigger's value will be one. If the stock prices are trading at levels well below ξ, its value will be zero. When the stock is trading around the stock price, the trigger will be a factor between zero and one. Thus, the generalized time varying Poisson intensity model which incorporates a stock trigger is given below.

$$\lambda_{ij}(S,t) = \lambda^{\star}_{ij} N(d^{i,\star}_1) e^{-\kappa(\tau^{\star}-t)sgn(\tau^{\star}-t)}, \tag{7.8}$$

where:

$$sgn(\tau^{\star}-t) = \begin{cases} -1 & \text{if } t > \tau^{\star} \\ 0 & \text{if } t = \tau^{\star} \\ 1 & \text{if } t < \tau^{\star} \end{cases},$$

and

$$d^{i,\star}_1 = \frac{\log\left(\frac{S}{\xi}\right) + \left(r + \frac{1}{2}\sigma^2_i\right)(\tau^{\star}-t)sgn(\tau^{\star}-t)}{\sigma_i \sqrt{(\tau^{\star}-t)sgn(\tau^{\star}-t)}}, \tag{7.9}$$

$$N(x) = \frac{1}{\sqrt{2\pi}} \int_{-\infty}^{x} e^{-\frac{z^2}{2}} dz. \tag{7.10}$$

It is important to note that this model is similar in structure to our time varying Poisson intensity model, with the addition of the new stock price trigger component.

For completeness, when the event occurs at maturity such that $\tau^\star = T$, the above result reduces to:

$$\lambda_{ij}(S,t) = \lambda^\star_{ij} N(d^i_1) e^{-\kappa(T-t)}, \tag{7.11}$$

where

$$d^i_1 = \frac{\log\left(\frac{S}{\xi}\right) + \left(r + \frac{1}{2}\sigma_i^2\right)(T-t)}{\sigma_i \sqrt{T-t}}, \tag{7.12}$$

$$N(x) = \frac{1}{\sqrt{2\pi}} \int_{-\infty}^{x} e^{-\frac{z^2}{2}} dz. \tag{7.13}$$

Once again, we will analyse our time and stock varying Poisson intensities for two different cases, pertaining to the relationship between event and option maturity dates.

Expected Return	r	0%
Volatility	σ	30%
Benchmark Price Level	ξ	\$100
Daily Maximum Poisson Intensity	$\lambda^\star$	10%
Event Date	$\tau^\star$	9 months
Maturity Date	T	1 year

Table 7.3: Parameters used in the analysis of time and stock varying Poisson intensities.

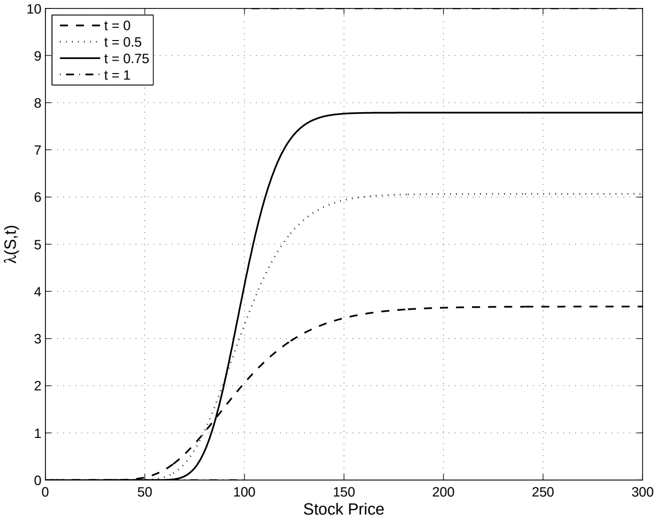

Figure 7.8: Time and stock varying Poisson intensity assuming the financial event occurs at maturity. Parameters as given in Table 7.3.

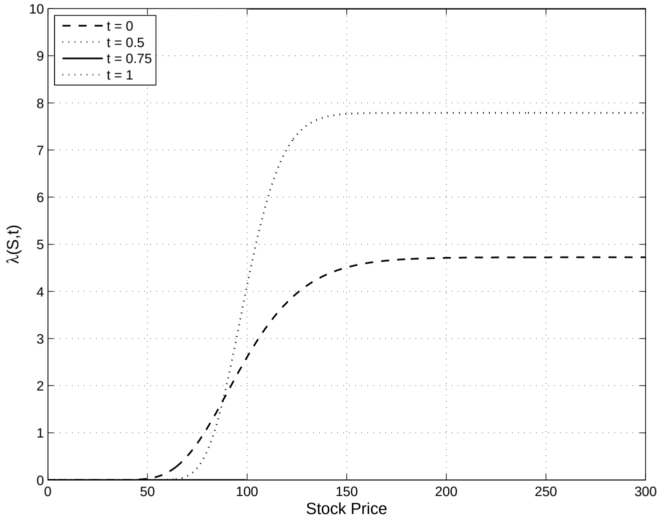

Figure 7.9: Time and stock varying Poisson intensity assuming the financial event occurs before maturity. Parameters as given in Table 7.3.

Case 3 will describe when the financial event occurs at option maturity, while Case 4 will refer to events that occur before maturity, $\tau^\star < T$. Figures 7.8 and 7.9 plot the intensities solely against stock price for different time points.

In Figure 7.8, we can observe that for all time points plotted, when the stock price is trading well below the strike price, the value of the Poisson intensity is zero. On the other hand, when the stock price is trading above the strike price, the value of the Poisson intensity approaches the value defined by the maximum Poisson intensity and by the time factor. This is the upper bound of our function. At maturity, when $t = \tau^\star = T$, we can see that the Poisson intensity takes on a value of zero when $S \leq K$ and a value of $\lambda^\star$ when $S > K$. Thus at option and event maturity, we can either switch with our maximum defined intensity or not at all. Our plain vanilla option will inherently be priced based on these factors since its value depends directly on the Poisson intensities embedded within the model.

Figure 7.9 considers the evolution of the Poisson intensity when the event date occurs before the maturity date of the option. We notice similar changes in the value of the intensity as we approach the event date. Once again at event maturity, the Poisson intensity can take on either the value of zero or the maximum Poisson intensity, dependent on where the stock price is trading with respect to the strike price. The key difference here is since the option maturity is after the event date, we see a downwards shift in the intensity function as we move away from the event date. In particular since both $t = 0.5$ and $t = 1$ are equidistant from the event date and due to the form of our equations, they both have the same resultant Poisson intensities.

7.3 Effect of the Time Intensity Parameter, κ

Each of the four cases outlined in the previous section depend on the time intensity parameter κ. Recall that κ is assumed to take on strictly finite positive values in order to incorporate event timing into our model. Financially, we can interpret κ as a measure of the stock's sensitivity to approaching earnings releases. Their sensitivity is based in the market, on which their equity trades reaction to their quarter end results. Either good or bad performance could trigger an increase in trading volume and have an impact on short-term price drift and volatility.

Financially, we can consider a small κ value to be associated with a publicly traded company that is unstable and for whom an earnings announcement would have little impact on stock volatility levels. The low level of impact would be due to the high volatility of the stock and thus an increase in volatility would not be uncharacteristic. An exception may be a buyout or takeover of the company. An example of such a company stock could be a small start-up technology company. If the company's stock is not expected to be affected by an upcoming financial event, κ is taken to be small such that we can consider that particular company's switching intensity to be non-time dependent. In other words, if $\kappa \to 0$ this implies that $\lambda^{\star}_{ij} e^{-\kappa(\tau^{\star}-t)sgn(\tau^{\star}-t)} \to \lambda^{\star}_{ij}$. Companies with a larger κ are those relatively stable companies for which the uncertainty of a quarterly earnings release would cause an impact of some magnitude on their stock price levels. An example of such a company could be any of the big six Canadian banks.

Since all cases are built upon our original time-varying intensity model, we will explore varying magnitudes of the time intensity parameter for Cases 1 and 2.

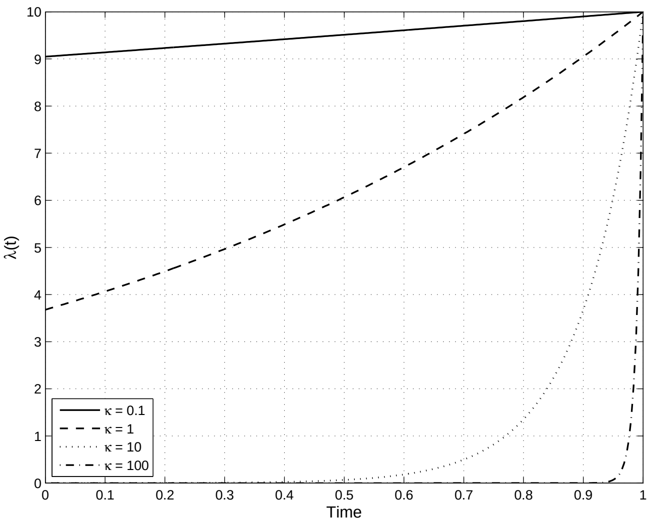

Figure 7.10: Impact of κ on the time-dependent Poisson intensity assuming the event occurs at option maturity. $\lambda^{\star} = 10\%$ (daily) and $T = 1$ year.

In Figure 7.10, it can be observed that for small values of κ, the change in the Poisson intensity appears to be linear in time. The larger κ, the more the Poisson intensity ramps up closer to the event. For very large values of κ, the effect of time is almost negligible until just before the financial event at which point, the intensity increases at a rapid speed to its maximum value, $\lambda^{\star}_{ij}$.

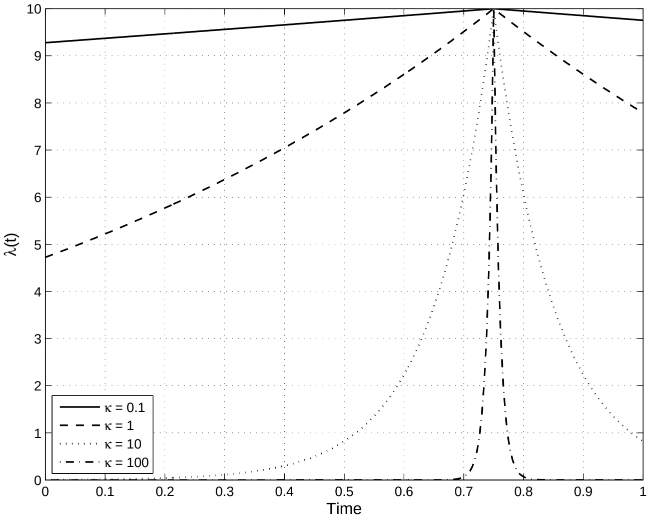

Figure 7.11: Impact of κ on the time-dependent Poisson intensity assuming the event occurs before option maturity. $\lambda^{\star} = 10\%$ (daily), $\tau^{\star} = 9$ months, and $T = 1$ year.

Figure 7.11 shows similar results to those analysed in Figure 7.10. The main difference is that the financial event occurs before option maturity, and thus the Poisson intensity must decrease as we move away from the event date. The speed at which the Poisson intensity decreases depends on the magnitude of κ. For a quick decay in intensity, larger values of κ are required while a lower value of κ allows for the intensity to decrease linearly.

Since the dates of big financial events are made public within their respective quarter, it makes financial sense to hedge against these information releases using shorter dated options. In particular, with earnings release, as we saw the company releases quarterly results approximately one month after the end of quarter. These dates are made publicly available about three months before they occur, thus allowing investors to set up appropriate hedge portfolios to profit on these events or at least mitigate potential losses.

7.4 Discussion

Now that the time intensity parameter and different functional forms of the deterministic Poisson intensities have been investigated, we now must analyse the effects that these time and stock varying Poisson intensities have on our regime-switching European option values. We will separately analyse all cases outlined in this chapter and compare them to a benchmark case. For ease of analysis, our benchmark case will be the constant Poisson intensity model which was discussed in detail in Chapters 4 through 6. The benchmark model assumes we our Poisson processes takes on the maximum Poisson intensity $\lambda^{\star}_{ij}$ at every time increment.

Expected Return	r	0%
High State Volatility	σ_H	40%
Low State Volatility	σ_L	10%
Maximum Daily High State Jump Intensity	$\lambda^{\star}_{LH}$	99%
Maximum Daily Low State Jump Intensity	$\lambda^{\star}_{HL}$	99%
High State Market Price of Volatility Risk	m_{HL}	0
Low State Market Price of Volatility Risk	m_{LH}	0
Maturity Date	T	1 year
Number of Time Increments	$\tilde{L}$	252
Time Intensity Parameter	κ	10
Event Date[†]	$\tau^{\star}$	9 months

Table 7.4: Parameters used in the analysis of option pricing for deterministic Poisson intensities. Note: [†] This event date is only used for Case 2 and Case 4 where it is assumed that the event occurs before the maturity date of our regime-switching call option.

All options will be priced numerically using the Crank-Nicolson method outlined in Chapter 3. The parameters used are given in Table 7.4 and will be consistent throughout this section, unless otherwise noted. The maximum daily high and low state jump intensities were taken to be 99% in order for us to effectively observe and analyse the differences in option prices. Empirical evidence from both Apple Inc. and TD Bank show that as a financial event approaches, volatility tends to spike upwards, as illustrated in Figures 7.2 and 7.3. This is why our parameters allow for such a high probability of switching to a more volatile regime as the event approaches. After said financial event occurs, it is most likely that the stock process will revert to a lower volatility level since the risk of the event has passed. This accounts for the high probability of switching from the high to low regime. Another parameter of particular interest is the magnitude chosen for the time intensity parameter κ. In our analysis of this parameter in the preceding section, we saw that higher values of κ allowed for the speed of the change in intensity to increase at a higher rate closer to the event date. Since we want the switch to have the highest probability of occurring closest to the event, we did not choose a small κ in order to avoid having a linear-like change in our Poisson intensity parameters. As a result, we chose a moderate value for the time intensity parameter, $\kappa = 10$, to ensure switching is more likely to occur closer to the event date.

We will show illustrated examples of our numerical option prices in the following subsections. Option prices are plotted for the entire stock interval over which they are computed. Figures which zoom in around the strike price can be found in Appendix A.

7.4.1 Case 1: Time Varying, Maturity Event Poisson Intensities

Recall that Case 1 considers switches between volatility regimes driven by deterministic time varying Poisson intensities. We have priced call options written on underlying assets with these dynamics.

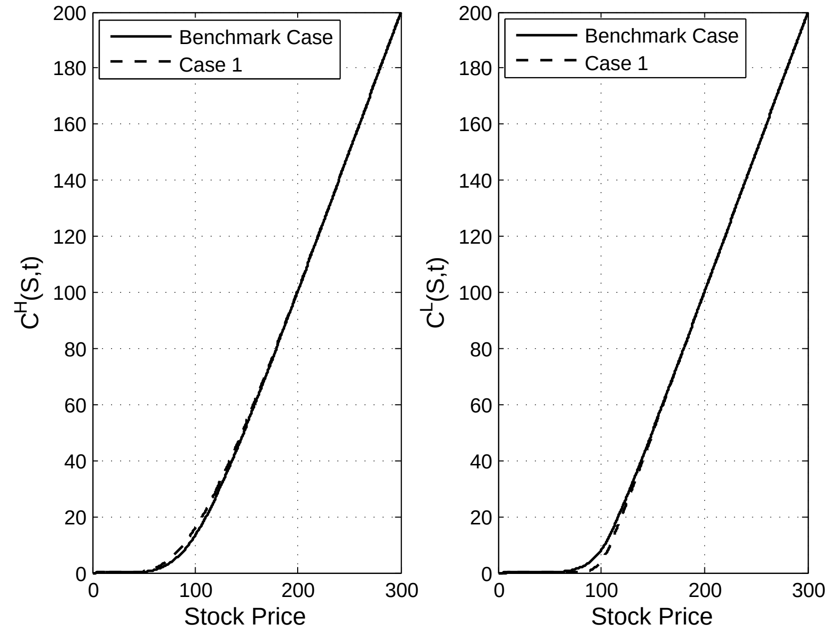

Figure 7.12: Comparison of numerical regime-switching option prices between the benchmark case and Case 1 at $t = 0$. Parameters as given in Table 7.4.

In Figure 7.12, it can be observed that the introduction of time-varying Poisson intensities into our regime-switching framework makes the high state option more valuable with respect to the constant intensity options. On the other hand, the introduction of these deterministic intensities price our low state option lower than the otherwise similar constant intensity option.

As noted in Figure 7.13, these differences with respect to the benchmark case hit a maximum at the strike price. When the option is deep in- or out-of-the-money, the impact of time-varying intensities is minimal. These differences can also be observed when considering the implied volatility smiles associated with these numerical option prices.

In Figure 7.14, we can observe that Case 1's high state implied volatility smile is pulled upwards in comparison with the benchmark case. However, the low state implied volatility smile is pulled downwards. This supports the previous observations with respect to the option prices. It is interesting to note that the difference between both state's implied volatility smiles and the benchmark is greater as the strike price increases, with the greatest difference occurring when the option is at-the-money. This indicates that the impact of event timing has caused out-of-the-money low state regime-switching call options to be priced at an even lower level comparatively to the in-the-money options. The reverse is shown for the high state, where out-of-the-money calls are priced at a relatively higher volatility value than before, in comparison with the in-the-money options

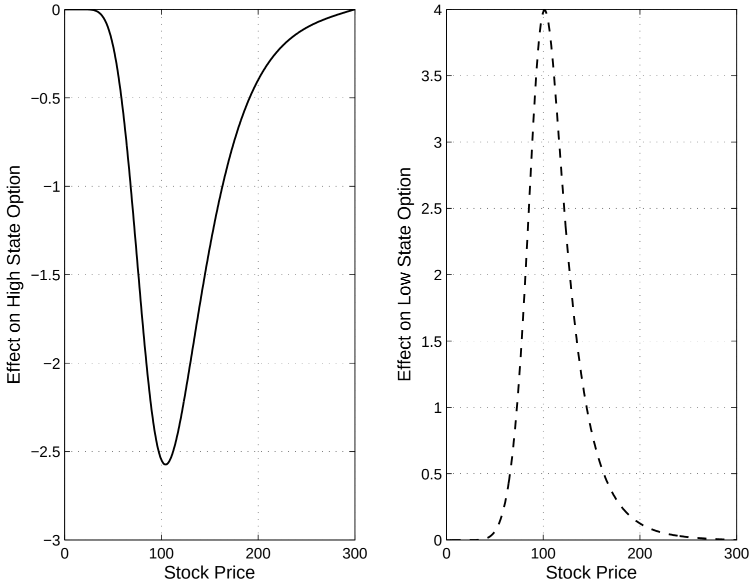

Figure 7.13: Difference between the benchmark case and Case 1 numerical option prices at $t = 0$. Parameters as given in Table 7.4.

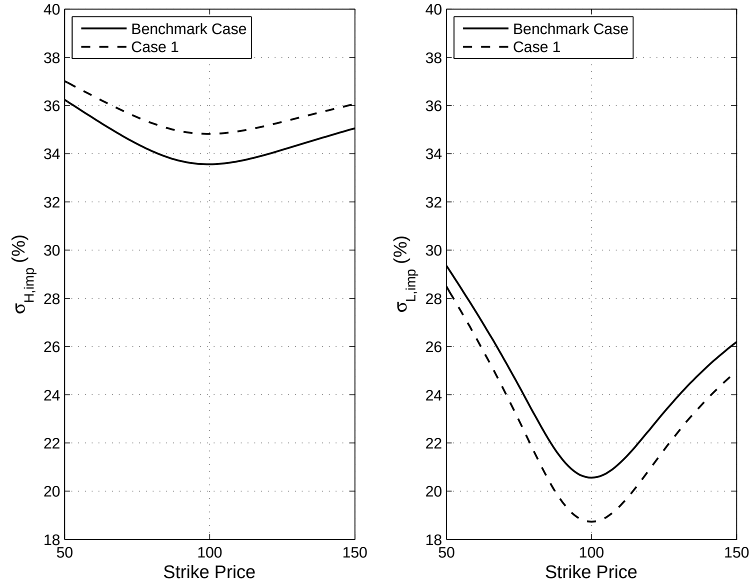

Figure 7.14: Implied volatility smiles corresponding to option prices for the benchmark case and Case 1. S = \$100, all other parameters as given in Table 7.4.

7.4.2 Case 2: Time Varying, Non-Maturity Event Poisson Intensities

Case 2 considers a call option priced on an underlying asset whose earnings release date occurs before option expiry. This company stock's dynamics include regime-switching volatility which is driven by a deterministic time-dependent Poisson intensities.

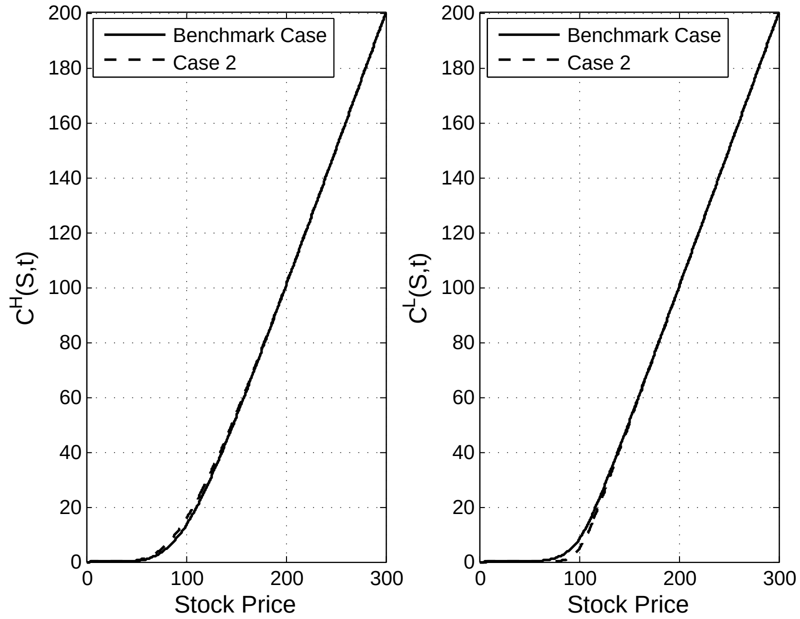

Figure 7.15: Comparison of regime-switching option prices between the benchmark case and Case 2 at $t = 0$. Parameters as given in Table 7.4.

For Case 2, we find similar results to those of Case 1. High state option prices are pulled upwards while low state option prices are pulled downwards with the inclusion of the time varying intensities, as shown in Figures 7.15 and 7.16. Recall that the only difference between these two models is the timing of the company's financial event.

It can be observed that Case 1 experienced a difference of higher magnitude between option prices than in Case 2. This could be attributed to the fact that the increase in the magnitude of the Poisson intensities in Case 1 occurs over the whole life of the option. Thus when pricing the option at option initiation, the cumulative effect of intensities with higher magnitudes has more of an effect on the option price. In Case 2, the Poisson intensities increase up until the event date which occurs before the option expiration. During the time between the event date and option expiration, the Poisson intensities decrease as it becomes more unlikely to have a volatility state shift at this point. This would result in a lower cumulative effect of the intensities on the option prices.

Considering the implied volatility allows us to observe that once again the high state implied volatility is pulled upwards and the low state implied volatility is pulled downwards with respect to the benchmark case, as shown in Figure 7.17. Similarly to Case 1, the difference between the implied volatility smiles increases as the option becomes out-of-the-money. The

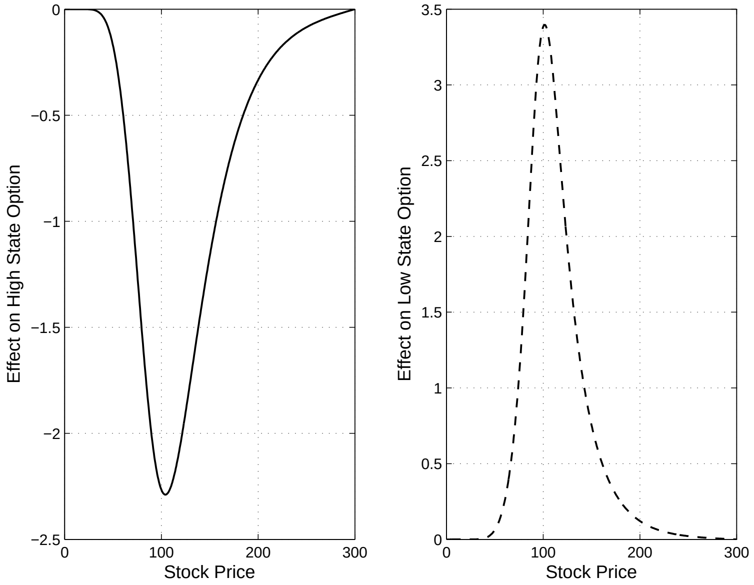

Figure 7.16: Difference between the benchmark case and Case 2 numerical option prices at $t = 0$. Parameters as given in Table 7.4.

greatest difference is observed when the option is at-the-money. However, the difference with respect to the benchmark case is less than we observed for Case 1. A similar interpretation of volatility smile results follow from Case 1.

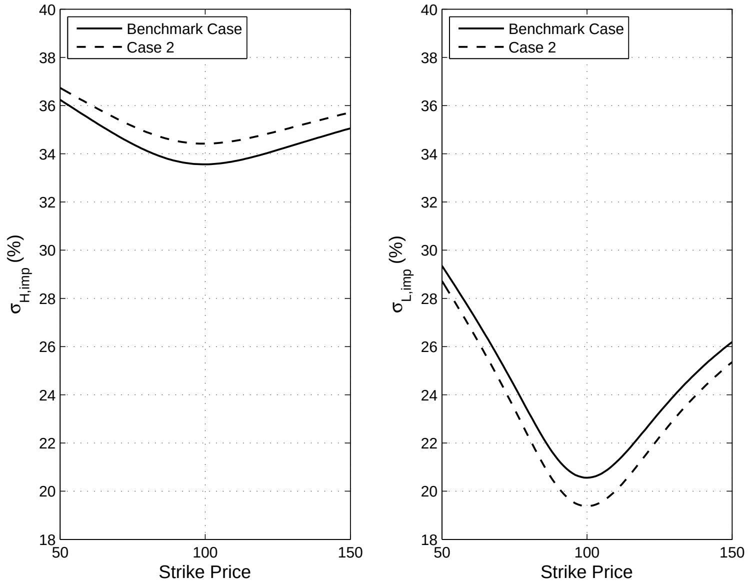

Figure 7.17: Implied volatility smiles corresponding to option prices for the benchmark case and Case 2. $S = \$100$, all other parameters as given in Table 7.4.

7.4.3 Case 3: Time and Stock Varying, Maturity Event Poisson Intensities

In Case 3, we allow for the level of the stock price to have a trigger effect on the magnitude of the Poisson intensities. It is assumed that the financial event will occur at option maturity.

Although the intensities now vary for different stock price levels, we can observe that the impact on the initial price of the option is similar to the previous cases where the intensity was only dependent on time. In Figure 7.18 we can see that the effect of our stock and time dependent intensities results in the high state option price being pulled upwards while the low state option price is pulled downwards and priced lower than before. As is confirmed in Figure 7.19, the most observable effects on the option price are about the strike price. Although the hedge ratio, which we use as a form of stock price trigger for the Poisson intensities, turns off completely when we are deep out-of-the-money or allows the Poisson intensity to take on the maximum intensity when the option is deep in-the-money, this is also where volatility has little to no effect on option prices. If we compare the magnitude of the differences about the strike price for Figure 7.19 to Figure 7.13, observe that a greater magnitude of difference occurs when our intensities are both time and stock dependent. This results in our options for Case 3 being priced at a slightly higher value for the high state option and a slightly lower value for the low state option in comparison to Case 1. These differences can be attributed to the inclusion of the stock price trigger. When the stock is trading about the strike price, its future evolution is important in regards to whether or not the European call option will be exercisable at maturity. Since the trigger acts as a factor multiplier for the Poisson intensities, the results indicate

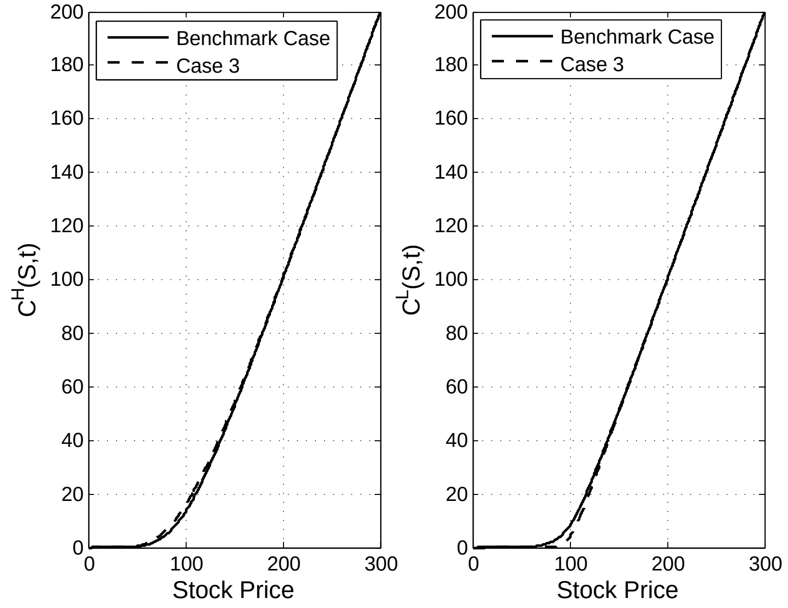

Figure 7.18: Comparison of regime-switching option prices between the benchmark case and Case 3 at $t = 0$. Parameters as given in Table 7.4.

that since the stock is trading about the strike price, the switching intensity has a decreased magnitude, lowering the probability of switching to a stabler less valuable regime. As a result, the option's value increases. Similarly, an intensity with decreased magnitude controlling the switch from the low to high state, results in the process assuming we will stay in a more stable volatility regime, thus resulting in the call option's value being lower.

Through an observation of the implied volatility smiles, it is apparent that the shapes of the smiles changed for Case 3 in comparison to the benchmark case. Figure 7.20 shows that both state's volatility smiles now look like volatility skews due to their asymmetric shape. For the high state, the volatility skew takes on larger values than the benchmark case, with the difference increasing as the strike price rises and the options become out-of-the-money. The difference between the low state volatility smiles increase once again with increases in stock price. This indicates that the combination of the time and stock variables on the Poisson intensities has more of an impact on implied volatility and thus on option prices as the options go further out-of-the-money. The impact of the stock trigger via the constant volatility hedge ratio results in the volatility smile for the high state being a forward skew. The more a high state option is out-of-the-money, the more less valuables it is, as it is unlikely that we will switch states to the low regime. On the other hand, the low volatility smile is now a reverse skew. This corresponds to an out-of-the-money call that is highly unlikely to switch regimes due to the stock price trigger being turned off. Thus the option is priced at a lower value, reflecting its permanency in the low volatility regime.

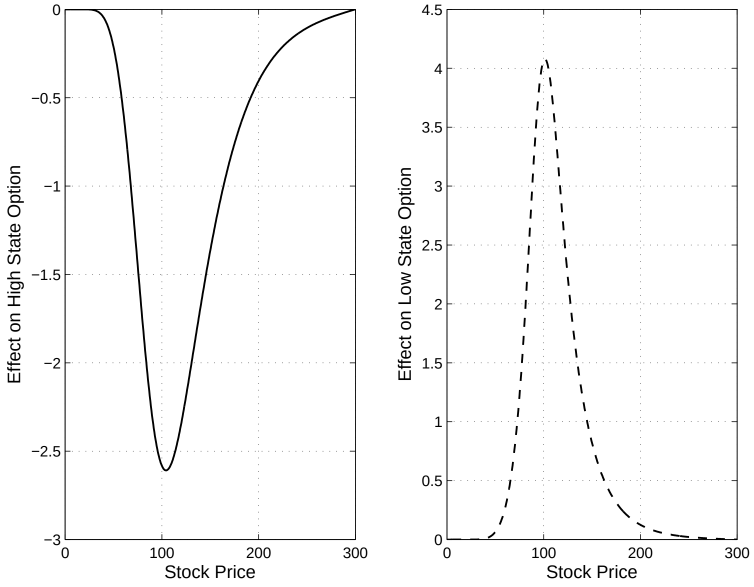

Figure 7.19: Difference between the benchmark case and Case 3 numerical option prices at $t = 0$. Parameters as given in Table 7.4.

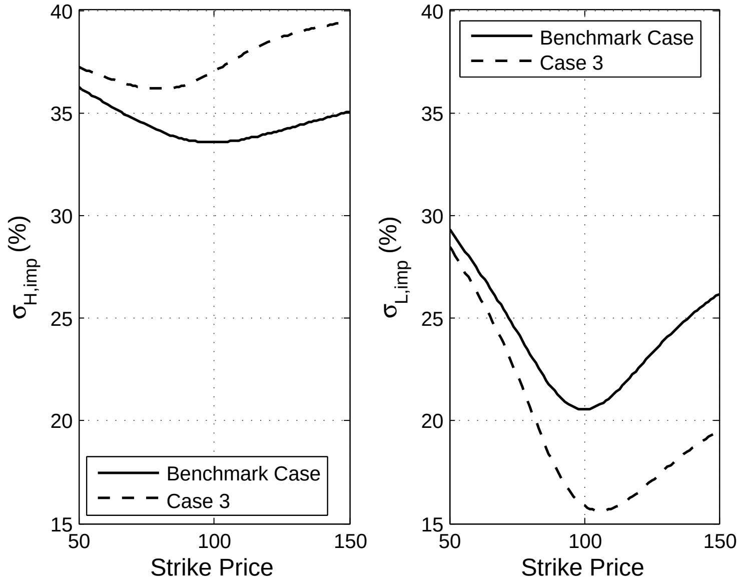

Figure 7.20: Implied volatility smiles corresponding to option prices for the benchmark case and Case 3. $S = \$100$, all other parameters as given in Table 7.4.

7.4.4 Case 4: Time and Stock Varying, Non-Maturity Event Poisson Intensities

Our final case, Case 4, differs from Case 3 only with respect to the timing of the financial event. It is now assumed that the financial event will occur before the expiration of our call option.

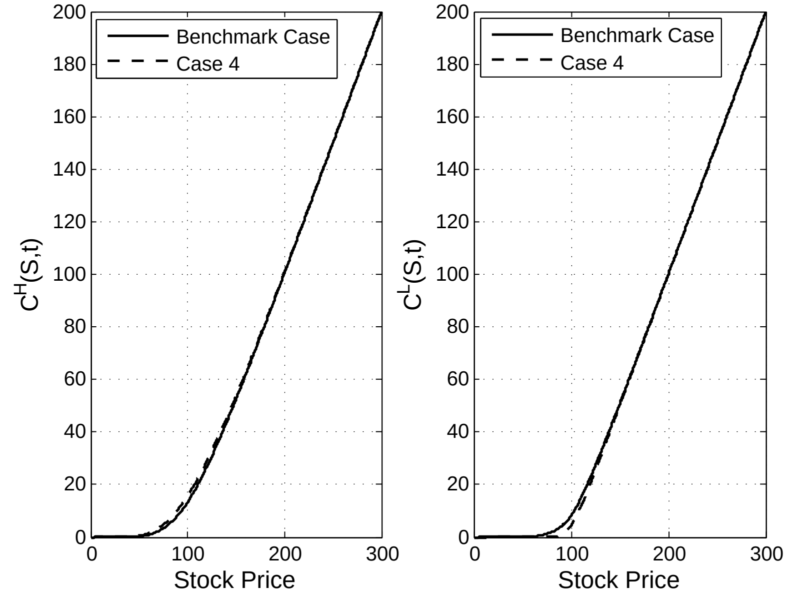

Figure 7.21: Comparison of regime-switching option prices between the benchmark case and Case 4 at $t = 0$. Parameters as given in Table 7.4.

The results of Case 4 with respect to the benchmark constant intensity case are very similar to those of Case 3. Once again the high state option prices are pulled upwards while low state option prices are pulled downwards as shown in Figures 7.21 and 7.22. The only difference between these Case 3 and Case 4 is the company's financial event occurring before the option expiration.

There is a slight decrease observed in magnitude of the differences between the benchmark and Case 4 option prices than we previously saw for Case 3. As we previously stated, when pricing the option at option initiation, the cumulative effect of intensities has more of an effect on option prices. Since the intensities are increasing for all stock values up until the event and option maturation date in Case 3, there is this increase in cumulative intensity effect. As we previously saw during the intensity exploration section, as we move away from the event date, the intensities reverse and begin to decrease over time. This results in a lower cumulative effect of daily intensities in the computation of the option price.

The results for the implied volatility are similar to those found in Case 3. In Figure 7.23, a forward skew is observed for the high volatility smile, while a reverse skew (or volatility smirk) is observed for the resulting low volatility smile. The main difference when comparing the two time and stock intensity cases is that the shift upward (downward) in the high (low) volatility

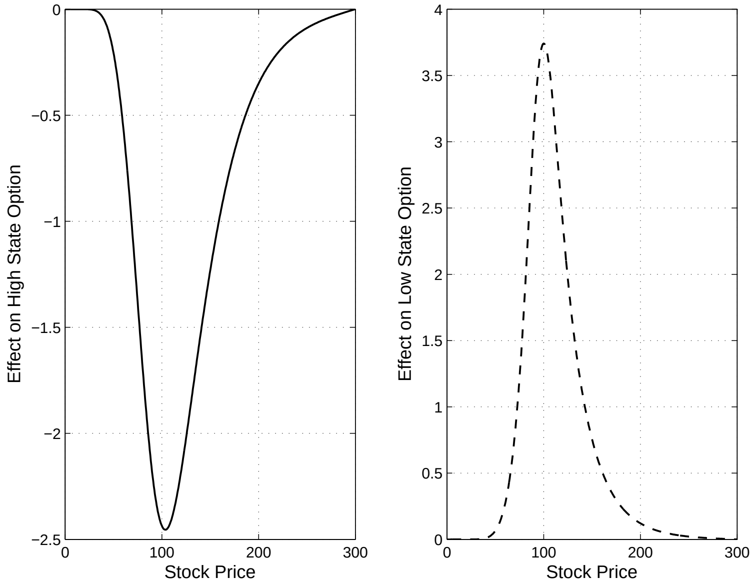

Figure 7.22: Difference between the benchmark case and Case 4 numerical option prices at $t = 0$. Parameters as given in Table 7.4.

smile is not as pronounced for Case 4 as it was in Case 3. Similar intuition arises under our non-maturity, time and stock varying intensity model as was discussed for Case 3.

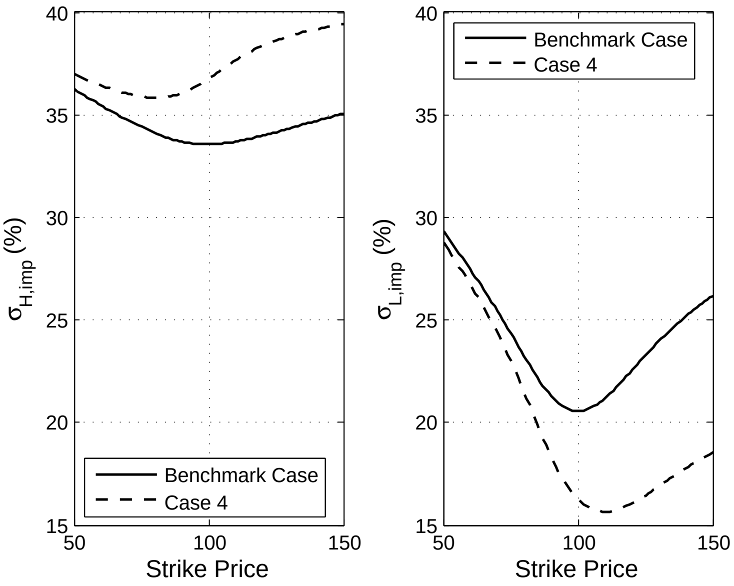

Figure 7.23: Implied volatility smiles corresponding to option prices for the benchmark case and Case 4. $S = \$100$, all other parameters as given in Table 7.4.

7.5 Hedging Strategies

As we have seen previously, the risks faced by investors are dependent on the position they take in an option and/or stock. Recall our investor from Chapters 5 and 6, who had a short position in our regime-switching option. Such an investor was scared of the potential of switching to a high volatility regime. Since we have shown that volatility levels can increase as a financial event such as a quarterly earnings release date approaches, this investor would be scared of the risk associated with the positive or negative outcome of this event. As we saw in our discussion in Chapter 5, one thing this investor could demand to hedge their risk is a higher risk premium to compensate them for this event-driven volatility risk. A higher risk premium would result in them being compensated for their risk by paying a lower price for the option at contract initiation. Many options are regulated and exchange-traded and as such, there is no negotiation between the buyer and seller. This type of compensation would have to be inherently priced within the options value before it hits the market.

A basic and common strategy that one could set up involves shorting one share of the stock and longing one call option. Usually, investors short a stock with the expectation that the price will fall over time. With earnings releases, there is no way to predict, without illegal insider information, whether or not the outcome will be positive or negative. Therefore we do not know if we should hedge against a decrease or increase in the stock price. If we long an option and short a share of the stock, we can protect against the drift in the stock. If there is bad news, it can be expected that company's stock will become volatile and a price decrease is imminent as soon as investors start selling off their shares. When the price falls, we buy back the stock at market price and return it to our investor. If our option is in-the-money, we will exercise our right to buy one share of the underlying, otherwise we will buy back the share from the market directly. Since we originally shorted the stock we must now return it to the owner. If the earnings release contained good news about the company's quarterly business, then it is most likely that the price will increase. At this point, we will have to exercise our option in order to return the share of the stock to its owner. The only way to ensure profits with this strategy is to originally short the share for more money than the discounted strike price and option premium combined.

Investors do have control over which options they can buy based on the expiration dates set by the exchange. There are several options written on a single stock, with varying maturity dates as well as with varying strikes. We can take advantage of such options by buying and exercising these options at an optimal time with respect to earnings release dates. An investor interested in taking a position in a call option written on a company's stock with an upcoming financial event who is however scared of high volatility has choices of hedging strategies related to the timing of option maturity. An investor can choose to invest in an option that expires before the earnings release date. This way their payoff is not affected by the risk associated with the upcoming quarterly earnings filings. Since quarterly earnings releases happen at approximately three month intervals, it is best for an investor to choose shorter dated call options as opposed to longer dated options. Since there is more risk associated with owning the stock around the event date than owning an option on the stock, the investor can roll their options with maturity dates straddling the earnings release dates. In other words, an investor could choose to buy a three month call option expiring before the event date. At option expiration, if the call is in the money, they will exercise and obtain a share of the stock. The investor can then turn around, sell this share on the market for the current value and then roll their profits into another option. Since they will sell the stock for more than what they paid (i.e. the strike price), they will make some profit even after setting up their subsequent long call position.

Finally, it is expected that investors hedging against upcoming financial events, will hedge more aggressively as the event approaches. This would be reflected in the hedge ratios for both the positions in the hedging options and in the underlying asset. Both of these hedge ratios depend directly on the state-dependent option prices which are now more sensitive to the upcoming financial event. Depending on where the stock is trading, there may be a significant shift in the number of shares an investor holds in their hedge portfolio. With the underlying Poisson intensity reaching its maximum switching level as the event approaches, investors who are especially risk-averse would be willing to take positions in the underlying and possibly some hedging options in order to ensure they can profit or at the very least break-even.

7.6 Summary

Incorporating deterministic Poisson intensities into our model allowed for the stock price's evolution and volatility levels to take into account major upcoming financial events. By allowing our regime-switching volatility framework to have intensities dependent on time and stock price, we were able to effectively model our volatility as event-driven. We discussed the time intensity parameter and how its magnitude can be thought of as being company and/or industry specific and is significant in determining the switching behaviour of the volatility process.

By incorporating the effect of a company's quarterly earnings release dates into our volatility model, the resultant options have been priced more fairly as their information is now embedded within the pricing framework. A summary of the results for each new Poisson intensity model is given in the table below.

Dependent Variables	Model	Comparison to Benchmark Case	
		Option Prices	Implied Volatility
Time	$\lambda_{ij}^{\star} e^{-\kappa(\tau^{\star}-t) sgn(\tau^{\star}-t)}$	$C^H(S,t) \uparrow$ $C^L(S,t) \downarrow$ $C^H_{\tau^{\star}=T}(S,t) \geq C^H_{\tau^{\star}<T}(S,t)$ $C^L_{\tau^{\star}=T}(S,t) \leq C^L_{\tau^{\star}<T}(S,t)$	$\sigma_{H,imp} \uparrow$ $\sigma_{L,imp} \downarrow$ $\sigma_{H,imp,\tau^{\star}=T} \geq \sigma_{H,imp,\tau^{\star}<T}$ $\sigma_{L,imp,\tau^{\star}=T} \leq \sigma_{L,imp,\tau^{\star}<T}$
Time & Stock	$\lambda_{ij}^{\star} N(d_1^{i,\star}) e^{-\kappa(\tau^{\star}-t) sgn(\tau^{\star}-t)}$	$C^H(S,t) \uparrow$ $C^L(S,t) \downarrow$ $C^H_{\tau^{\star}=T}(S,t) \geq C^H_{\tau^{\star}<T}(S,t)$ $C^L_{\tau^{\star}=T}(S,t) \leq C^L_{\tau^{\star}<T}(S,t)$	$\sigma_{H,imp} \uparrow$ $\sigma_{L,imp} \downarrow$ $\sigma_{H,imp,\tau^{\star}=T} \geq \sigma_{H,imp,\tau^{\star}<T}$ $\sigma_{L,imp,\tau^{\star}=T} \leq \sigma_{L,imp,\tau^{\star}<T}$

Table 7.5: Summary of results for the time varying and time and stock varying Poisson intensity cases.

Overall, no matter what hedging strategy is used, since the time line corresponding to most company's financial events is short term (i.e. under a year), short-dated options are the best choice for investors over long-dated options. We discussed how this allows them to protect themselves against the risk associated with financial events by straddling their option maturity dates around the event date. More risk-loving investors could take advantage of upcoming earnings release dates by setting up strategies that may allow them to profit.

Chapter 8

Concluding Remarks

This thesis focused on pricing and hedging options under a realistic two-regime volatility framework. We conclude with a summary of results presented within this thesis and a brief overview of possible future research extensions that could arise from this work.

8.1 Summary

In the presence of regime-switching volatility, we derived coupled pricing partial differential equations dependent on the market price of volatility risk. Numerical solution techniques, in particular the Crank-Nicolson numerical scheme, were first implemented on a classical initial value problem, the one-dimensional heat equation, both in singular and system form in order to justify its accuracy in solving partial differential equations. We used this method to solve our problem of interest, the coupled regime-switching option pricing PDEs. Doing so provided a benchmark pricing technique for which we compared our subsequent analysis with.

Redefining our problem in terms of the corresponding volatility state's Black-Scholes option prices allowed us to derive continuous-time state-dependent approximate solutions for both regime-switching option prices and Deltas. These approximate solutions were obtained through the application of the Cauchy-Kowalevski Theorem which gave a series-type solution. We quantified the error of our approximate solution by treating our problem as a related root-finding problem and using backwards error analysis. The performance of our option price approximations were compared to numerical results. It was found that our approximation performed well, although there exists slight variability around the strike price of the option. In addition, we showed that regime-switching options are less sensitive to volatility levels near option expiry. Our new analytic approximation provided an easy and effective approximation technique that can easily be applied to other options written on underlying assets with regime-switching volatility.

By using these approximate solutions for the state-dependent option prices and their corresponding Deltas, we were able to analyse the impact of the market price of volatility risk on these relations, both intuitively and mathematically. Utilizing basic financial principles, we were able to show that negative state-dependent market prices of volatility risk were necessary to have financially meaningful option prices in a regime-switching market. The proof of existence of such negative state-dependent market prices of volatility risk allowed us to quantify the investors' risk attitudes surrounding uncertainty in a market with regime-switching volatility. Specifically, the negative market price of volatility risk acts as an option premium compensating investors for taking on volatility risk. It was found that both the occupation and potential occupation of a volatile regime causes investors to pay this premium for options that allow them to hedge against this risk. We investigated the state-dependent premia required by risk-averse option buyers and sellers to eliminate the risk they face in the market. Finally, the consequence of varying the magnitude of the state-dependent market prices of volatility risk on the implied volatility smiles was shown to alter both the slope and the magnitude of the smile when compared to the risk-neutral case.

Building upon basic hedging and arbitrage arguments introduced under the assumption of constant volatility, we set up portfolios that were mathematically designed to hedge against both the risk of movement in the underlying asset and the risk of jumping to the opposing volatility regime. One assumption was that one hedging option was needed to hedge against our risk of switching to one other volatility regime. We found that financial issues can limit the practical applicability of this assumption. An option's moneyness has to be considered when using it as a hedging option. When an option is too far in- or out-of-the-money, volatility has little impact on regime-switching option prices thus making them inappropriate hedging options. We showed that creating a basket of two options, cleverly chosen such that their respective strike prices straddled the shorted option's strike price, allowed for our portfolio to always contain a usable hedging option. The inclusion of a hedging limit in this portfolio prohibited an investor from taking too extreme a position in a particular hedging option thus reducing portfolio losses. The financial insight obtained about the volatility risk premium led to a set of naive hedging strategies against which we compared our more sophisticated regime-switching portfolios. On average, it was found that the portfolios set up to directly hedge against volatility switching performed the best in that they broke even on average and had the least variability in their mean terminal profit/loss, in the absence of transaction costs. It was also shown that in the presence of increased transaction costs, in particular for the hedging options, the portfolios containing the basket of options lost less money on average due to the control of the magnitude of the option positions.

Finally, we extended our regime-switching volatility framework to include deterministic Poisson intensities. This extension, motivated by the impact of earnings releases on publicly traded companies' volatility levels, studied the impact of both time and stock price level on the frequency of the switching mechanism. We first modelled time-dependency into our framework by allowing the intensities to grow exponentially, constrained by a time-intensity parameter, up until the quarterly earnings release date. If the option did not expire on this same date, the intensity was modelled to decay as we moved forward in time, away from the earnings date. A similar set up was used for our second set of cases in which the intensity's magnitude was now dependent on both the time and stock price levels. It was found that the high state regime-switching option became more valuable with the inclusion of the deterministic intensities, while the low state option became less valuable. These differences were most observable around the strike price, where the option is most sensitive to movements in the underlying asset and volatility. As a result, the associated implied volatility smiles were pulled upwards for high state and downwards for the low case. When the earnings releases occurred on option expiry, there was a more pronounced impact on option prices than when the events occurred before option expiry. This was attributed to the compounding impact of the varying intensities over time due to the fact that options are priced at contract initiation.

8.2 Future Work

The work presented in this thesis can lead to many possible extensions. Throughout this thesis, it was assumed that the state-dependent market prices of volatility risk were constant within a respective volatility state occupation. An obvious extension would be to consider non-constant risk premiums allowing them to be a deterministic function of the dependent variables, stock price and time. Financial intuition suggests that movement in the underlying asset affects the risk attitudes of investors dependent on their position (i.e. long/short) in an option. As such the premium they demand to be compensated for their risk will fluctuate. It may also be interesting to consider modelling volatility risk premiums using stochastic differential equations, however this would add a level of complexity to the option pricing problem from an analysis standpoint.

Although work has been done to show that volatility risk premiums are negative within equity markets, it would be interesting to fit our regime-switching framework to observed options price data. The focus would be to try and estimate the magnitude and sign of constant state-dependent MPVR using empirical data, in support of the mathematical results presented in these thesis.

Furthermore, the scope of research with respect to event-driven deterministic Poisson intensities can easily be broadened. As we showed using empirical data, there is an observable impact on trading volume due to the uncertainty surrounding an upcoming financial event. Our framework could be modified to model the evolution of trading volume of a publicly traded company. Similarly, deterministic Poisson intensities can be used to model changes in credit ratings due to their relationship with volatility regime shifts and with earnings surprises.

Bibliography

[1] Apple Inc. *Apple Reports Record Results*. Retrieved March 25, 2014 from http://www.apple.com/pr/library/2013/01/23Apple-Reports-Record-Results.html

[2] Apple Inc. *Apple Reports Second Quarter Results*. Retrieved March 25, 2014 from http://www.apple.com/pr/library/2013/04/23Apple-Reports-Second-Quarter-Results.html

[3] Apple Inc. *Apple Reports Third Quarter Results*. Retrieved March 25, 2014 from http://www.apple.com/pr/library/2013/07/23Apple-Reports-Third-Quarter-Results.html

[4] Apple Inc. *Apple Reports Fourth Quarter Results*. Retrieved March 25, 2014 from http://www.apple.com/pr/library/2013/10/28Apple-Reports-Fourth-Quarter-Results.html

[5] G. Bakshi and N. Kapadia. Delta-Hedged Gains and the Negative Market Volatility Risk Premium. *The Review of Financial Studies*, 16, 527–566, 2003.

[6] F. Black and M. Scholes. The Pricing of Options and Corporate Liabilities. *Journal of Political Economy*, 81, 637–654, 1973.

[7] N.P.B. Bollen. Valuing Options in Regime-Switching Models. *Journal of Derivatives*, 6, 38–49, 1998.

[8] H.P. Boswick. Volatility Mean Reversion and the Market Price of Volatility Risk. *Proceedings of the International Conference on Modelling and Forecasting Financial Volatility*, 159–170, 2001.

[9] P. Boyle and T. Draviam. Pricing Exotic Options under Regime-Switching. *Insurance: Mathematics and Economics*, 40, 267–282, 2007.

[10] B. Bradie. *A Friendly Introduction to Numerical Analysis*, Pearson Prentice Hall, New Jersey, 2006.

[11] J. Buffington and R.J. Elliott. Regime Switching and European Options. *Stochastic Theory and Control*, LNCIS 280, 73–82, 2002.

[12] P. Carr and L. Wu. Variance Risk Premiums. *Review of Financial Studies*, 22(3), 1311–1341, 2009.

[13] J.D. Coval and T. Shumway. Expected Option Returns. *The Journal of Finance*, 56(3), 983–1009, 2001.

[14] Z. Da and E. Schaumburg. The Pricing of Volatility Risk across Asset Classes. *Working Paper*, 2011.

[15] G.B. Di Masi, Y.M. Kabanov and W.J. Runggaldier. Mean-Variance Hedging of Options on Stocks with Markov Volatilities. *Theory of Probability and its Applications*, 39, 172–182, 1994.

[16] J.S. Doran and E.I. Ronn. Computing the Market Price of Volatility Risk in the Energy Commodity Markets. *Journal of Banking and Finance*, 32(12), 2541–2552, 2008.

[17] J. Duarte and C.S. Jones. The Price of Market Volatility risk. *Working Paper*, 2007.

[18] L.H. Ederington and J.H. Lee. How Markets Process Information: New Releases and Volatility. *The Journal of Finance*, 48(4), 1161–1191, 1993.

[19] A.J. Filardo. Business-Cycle Phases and Their Transitional Dynamics. *Journal of Business and Economic Statistics*, 12(3), 299–308, 1994.

[20] G. B. Folland. *Introduction to Partial Differential Equations*, Princeton University Press, New Jersey, 1995.

[21] K.R. French and R. Roll. Stock Return Variances: The Arrival of Information and the Reaction of Traders. *Journal of Financial Economics*, 17(1), 5–26, 1986.

[22] J.D. Hamilton. A New Approach to the Economic Analysis of Nonstationary Time Series and the Business Cycle, *Econometrica*, 57(2), 357–384, 1989.

[23] J.D. Hamilton. Analysis of Times Series Subject to Changes in Regime, *Journal of Econometrics*, 45, 39–70, 1990.

[24] P.R. Hansen and A. Lunde. A Forecast Comparison of Volatility Models: Does Anything Beat a GARCH(1,1)?, *Journal of Applied Econometrics*, 20, 873–889, 2005.

[25] M.R. Hardy. A Regime Switching Model of Long-Term Stock Returns. *North American Actuarial Journal*, 3, 41–53, 2001.

[26] C.R. Harvey and R.D. Huang. Public Information and Fixed Income Volatility. *Working Paper*, 1993.

[27] S.L. Heston. A Closed-Form Solution for Options with Stochastic Volatility with Applications to Bond and Currency Options. *The Review of Financial Studies*, 6, 327–343, 1993.

[28] J.C. Hull. *Options, Futures and Other Derivatives, Seventh Edition*, Pearson, New Jersey, 2008.

[29] J.C. Jackwerth and M. Rubinstein. Recovering Probability Distributions from Option Prices. *The Journal of Finance*, 51(5), 1611–1631, 1996.

[30] R. Jennings and L. Starks. Information Content and the Speed of Stock Price Adjustment. *Journal of Accounting Research*, 23(1), 336–350, 1985.

[31] R.S. Mamon and M.R. Rodrigo. Explicit Solutions to European Options in a Regime-Switching Economy. *Operations Research Letters*, 33, 581–586, 2005.

[32] R.C. Merton. Option Pricing when Underlying Stock Returns are Discontinuous. *Journal of Financial Economics*, 3, 125–144, 1975.

[33] M. Mielkie and M. Davison. A New Analytic Approximation Technique for Pricing Options in a Regime-Switching Market. Working Paper, 2014.

[34] M. Mielkie and M. Davison. Investigating the Market Price of Volatility Risk for Options in a Regime-Switching Market. To appear in *New Perspectives on Stochastic Modeling and Data Analysis*, Bozeman, J., Girardin, V., and Skiadas, C.H. (eds.), 2014.

[35] V. Naik. Option Valuation and Hedging Strategies with Jumps in the Volatility of Asset Returns. *The Journal of Finance*, 48, 1969–1984, 1993.

[36] P.V. O'Neil. *Beginning Partial Differential Equations*, Wiley, New York, 1999

[37] J.M. Patell and M.A. Wolfson. The Intraday Speed of Adjustment of Stock Prices to Earnings and Dividend Announcements. *Journal of Financial Economics*, 13(2), 223–252, 1984.

[38] T. Sauer. *Numerical Analysis*, Pearson Addison Wesley, Boston, 2006.

[39] S. Shreve. *Stochastic Calculus for Finance II: Continuous-Time Models*, Springer, New York, 2008.

[40] D.J. Skinner. Options Markets and the Information Content of Accounting Earnings Releases. *Journal of Accounting and Economics*, 13(3), 191–211, 1990.

[41] J. Stewart. *Early Transcendentals Single Variable Calculus, 5th Edition*, Thomson, California, 2003.

[42] TD Bank Group. *TD Bank Group Reports First Quarter 2013 Results*. Retrieved March 25, 2014 from http://www.td.com/document/PDF/investor/2013/Q1%202013%20Earnings%20News%20Release_E.pdf

[43] TD Bank Group. *TD Bank Group Reports Second Quarter 2013 Results*. Retrieved March 25, 2014 from http://www.td.com/document/PDF/investor/2013/2013-Q2_Earnings_News_Release_F_EN.pdf

[44] TD Bank Group. *TD Bank Group Reports Third Quarter 2013 Results*. Retrieved March 25, 2014 from http://www.td.com/document/PDF/investor/2013/2013-Q3_Earnings_News_Release_F_EN.pdf

[45] TD Bank Group. *TD Bank Group Reports Fourth Quarter and Fiscal 2013 Results*. Retrieved March 25, 2014 from http://www.td.com/document/PDF/investor/2013/2013-Q4_Earning_News_Release_F_EN.pdf

[46] The Options Clearing Corporation. *Understanding Options*, 1994. Retrieved April 9, 2014 from http://www.cboe.com/learncenter/pdf/understanding.pdf

[47] J.W. Thomas. *Numerical Partial Differential Equations: Finite Difference Methods*, Springer, New York, 1995.

[48] G. Waymire. Earnings Volatility and Voluntary Management Forecast Disclosure. *Journal of Accounting Research*, 23(1), 268–295, 1985

[49] P. Wilmott. *Paul Wilmott on Quantitative Finance, Second Edition*, Wiley, England, 2006.

[50] Yahoo Canada Finance. *Apple Inc. Historical Prices 1984-2014*. Retrieved March 25, 2014 from http://ca.finance.yahoo.com/q/hp?s=AAPL

[51] Yahoo Canada Finance. *S&P/TSX Composite Index Historical Prices 1984-2014*. Retrieved March 25, 2014 from http://ca.finance.yahoo.com/q/hp?s=%5EGSPTSE

[52] Yahoo Canada Finance. *Toronto-Dominion Bank Historical Prices 1995-2014*. Retrieved March 25, 2014 from http://ca.finance.yahoo.com/q/hp?s=TD.TO

[53] X. Xi and R.S. Mamon. Parameter Estimation of an Asset Price Model Driven by a Weak Hidden Markov Chain. *Economic Modelling*, 28, 26–46, 2011.

[54] X. Xi, M. Rodrigo, and R.S. Mamon. Parameter Estimation of a Regime-Switching Model Using an Inverse Stieltjes Moment Approach. *Advances in Statistics, Probability and Actuarial Science: Stochastic Processes, Finance and Control (Festschrift in Honour of Robert Elliott's 70th Birthday), Volume I*, Cohen, S., Madan, D., Siu, T., and Yang, H. (eds.), World Scientific, 549–569, 2012.

[55] X. Xi and R.S. Mamon. Parameter Estimation in a WHMM Setting with Independent and Volatility Components. To appear in *Hidden Markov Models in Finance: Volume II (Further Developments and Applications)*, Mamon, R.S., and Elliott, R. (eds.), 2014.

[56] D.D. Yao, Q. Zhang and X.Y. Zhou. A Regime-Switching Model for European Options. *Stochastic Processes, Optimization, and Control Theory: Applications in Financial Engineering, Queueing Networks, and Manufacturing Systems - International Series in Operations Research & Management Science*, 94, 281–300, 2006.

Appendix A

Additional Deterministic Intensity Analysis

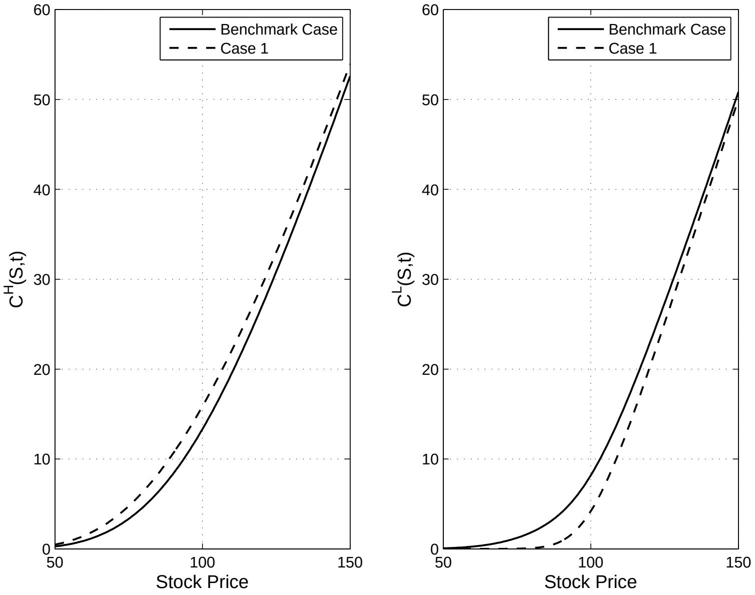

Figure A.1: Comparison of benchmark case and Case 1 numerical regime-switching option prices, zoomed about the strike $K = \$100$. Parameters as given in Table 7.4. Original plot depicted in Figure 7.12.

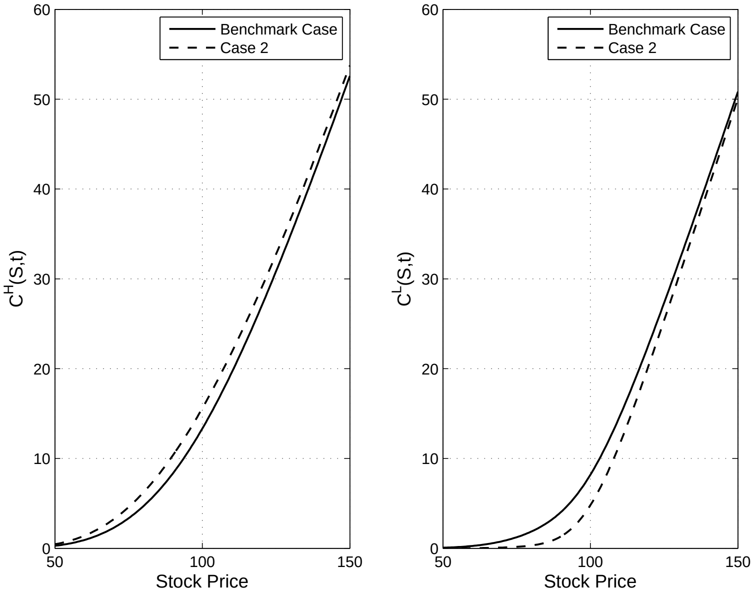

Figure A.2: Comparison of benchmark case and Case 2 numerical regime-switching option prices, zoomed about the strike $K = \$100$. Parameters as given in Table 7.4. Figure 7.15 depicts original, non-zoomed plot.

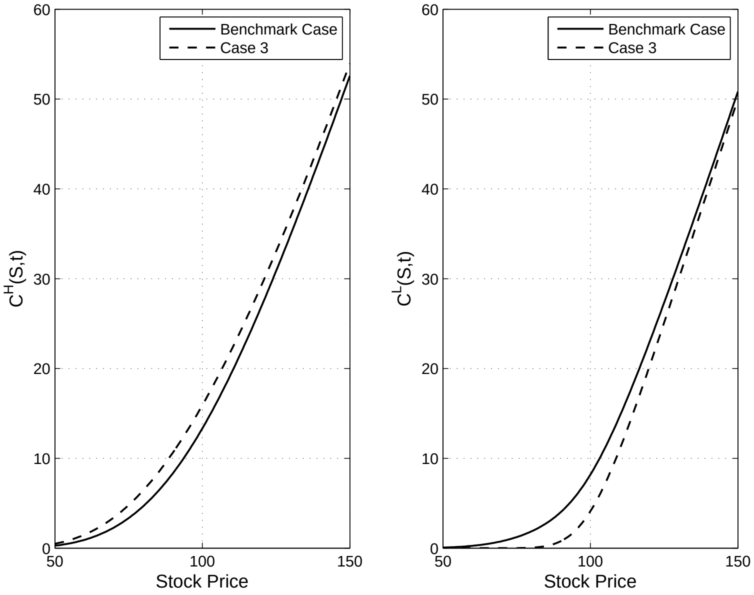

Figure A.3: Comparison of benchmark case and Case 3 numerical regime-switching option prices, zoomed about the strike $K = \$100$. Parameters as given in Table 7.4. Figure 7.18 depicts original, non-zoomed plot.

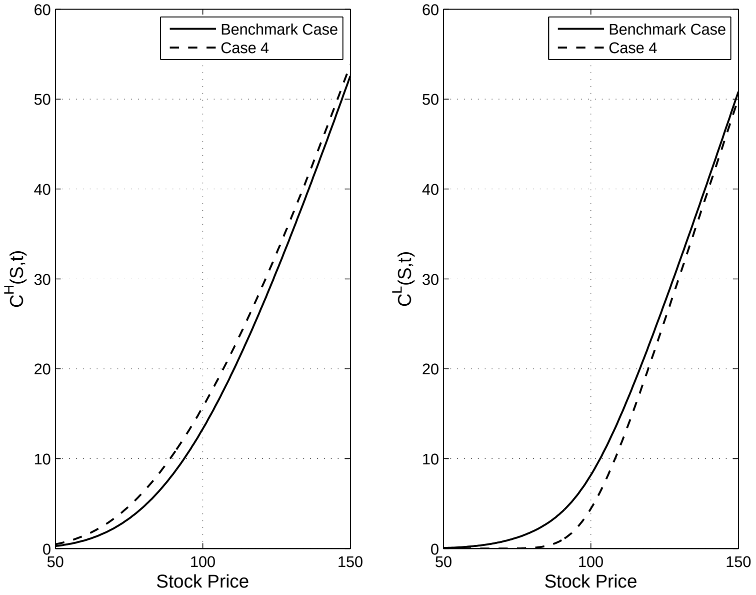

Figure A.4: Comparison of benchmark case and Case 4 numerical regime-switching option prices, zoomed about the strike $K = \$100$. Parameters as given in Table 7.4. Figure 7.21 depicts original, non-zoomed plot.

Curriculum Vitae

Name:	Melissa Anne Mielkie
Post-Secondary Education and Degrees:	The University of Western Ontario London, Ontario, Canada 2010–2014 Ph.D.
	The University of Western Ontario London, Ontario, Canada 2009–2010 M.Sc.
	The University of Western Ontario London, Ontario, Canada 2004–2009 Honours B.Sc.
Honours and Awards:	Western University Ontario Graduate Scholarship 2013–2014
	Western Graduate Research Scholarship 2009–2014
	University Students' Council Teaching Honour Roll 2012–2013
	Western Science Graduate Student Teaching Award 2012
Related Work Experience:	Graduate Teaching Assistant The University of Western Ontario 2009–2013
	Lecturer The University of Western Ontario 2013
	Research Assistant, NSERC Engage Grant The University of Western Ontario 2011

Related Work Experience: (cont'd)	Financial Risk Management Intern Manulife Financial, Toronto 2010

Publications:

Accepted Papers

(1) Mielkie, M. & Davison, M. Investigating the Market Price of Volatility Risk for Options in a Regime-Switching Market. To appear in New Perspectives on Stochastic Modeling and Data Analysis, Bozeman, J., Girardin, V., & Skiadas, C.H. (eds.)

Working Papers

(1) Mielkie, M. & Davison, M. A New Analytic Approximation Technique for Pricing Options in a Regime-Switching Market. Available at SSRN: http://ssrn.com/abstract=2167394 or http://dx.doi.org/10.2139/ssrn.2167394

Presentations:

(1) Mielkie, M. & Davison, M. Investigating the Market Price of Volatility Risk for Options in a Regime-Switching Market. The International Conference on Applied Mathematics, Modeling and Computational Science, August 26–30, 2013, Waterloo, Canada

(2) Mielkie, M. & Davison, M. Investigating the Market Price of Volatility Risk for Options in a Regime-Switching Market. 10th International Conference on Computational Management Science, May 1–3, 2013, Montreal, Canada

(3) Mielkie, M. & Davison, M. Investigating the Market Price of Volatility Risk for Options in a Regime-Switching Market. Bachelier Finance Society 7th World Congress, June 19–22, 2012, Sydney, Australia (Accepted on a Refereed Basis)

(4) Davison, M., Lu, B., Mielkie, M., & Moosavi, H. Understanding Negative Power Prices in the Ontario Market. 54th Annual Conference of the Canadian Operational Research Society, June 11–13, 2012, Niagara Falls, Canada (Presented by Coauthors)

(5) Mielkie, M. & Davison, M. Dynamic Hedging in a Market Driven by Regime-Switching Volatility. 3-C Risk Forum & 2011 International Conference on Engineering and Risk Management, October 28–30, 2011, Toronto, Canada